Papers presented to the

47th ANNUAL METEORITICAL SOCIETY MEETING

CO-SPONSORED BY

University of New Mexico

Lunar and Planetary Institute

WITH ADDITIONAL SUPPORT FROM

Los Alamos National Laboratory

HOSTED BY

Institute of Meteoritics and

Department of Geology University of New Mexico

ALBUQUERQUE, NEW MEXICO

JULY 30 - AUGUST 2, 1984

Abstracts and Program for the

47th Annual Meeting of the Meteoritical Society

Co-sponsored by: University of New Mexico
Lunar and Planetary Institute

With additional support from Los Alamos National Laboratory

Hosted by

Institute of Meteoritics and

Department of Geology, University of New Mexico

Albuquerque, New Mexico

July 30 - August 2, 1984

Compiled by

Lunar and Planetary Institute

3303 NASA Road One

Houston, Texas 77058

LPI Contribution 537

Compiled in 1984

by

Lunar and Planetary Institute

PREFACE

This volume contains abstracts that have been accepted by the Program Committee for oral presentation at the 47th Annual Meteoritical Society Meeting. Revised abstracts will be published in an issue of Meteoritics.

The Program Committee included Edward Scott (Chair), Cyrena Goodrich, Klaus Keil, and Jeffrey Taylor (University of New Mexico), Richard Bild (Sandia National Laboratories), David Curtis and Robert Reedy (Los Alamos National Laboratory), and Pamela Jones (Lunar and Planetary Institute). The Organizing Committee included Klaus Keil (Chair), Jeffrey Taylor, and Edward Scott, all of the University of New Mexico; Field Trip planners were Harry Planner, Klaus Keil, Fraser Goff, and Scott Baldridge.

Technical assistance was provided by: Michael Bersch, John Calhoun, George Carnako, Jim Connolly, George Conrad, Tammy Dickinson, Amy Dixon, Art Ehlmann, Elaine Faust, Mary Fillmon, Cyrena Goodrich, Michael Jercinovic, David Lusby, Margaret Recca, Steve Recca, Tom Servilla, Mimi Swanson, and Cecelia Williams.

Logistic and administrative support was provided by Pamela Jones and LeBecca Turner; this abstract volume was prepared by Tracy McCasey, with assistance from Lisa Bowman, Renee Dotson, and Karen Hrametz (all from the Lunar and Planetary Institute).

The Lunar and Planetary Institute is operated by the Universities Space Research Association under contract No. NASW-3389 with the National Aeronautics and Space Administration.

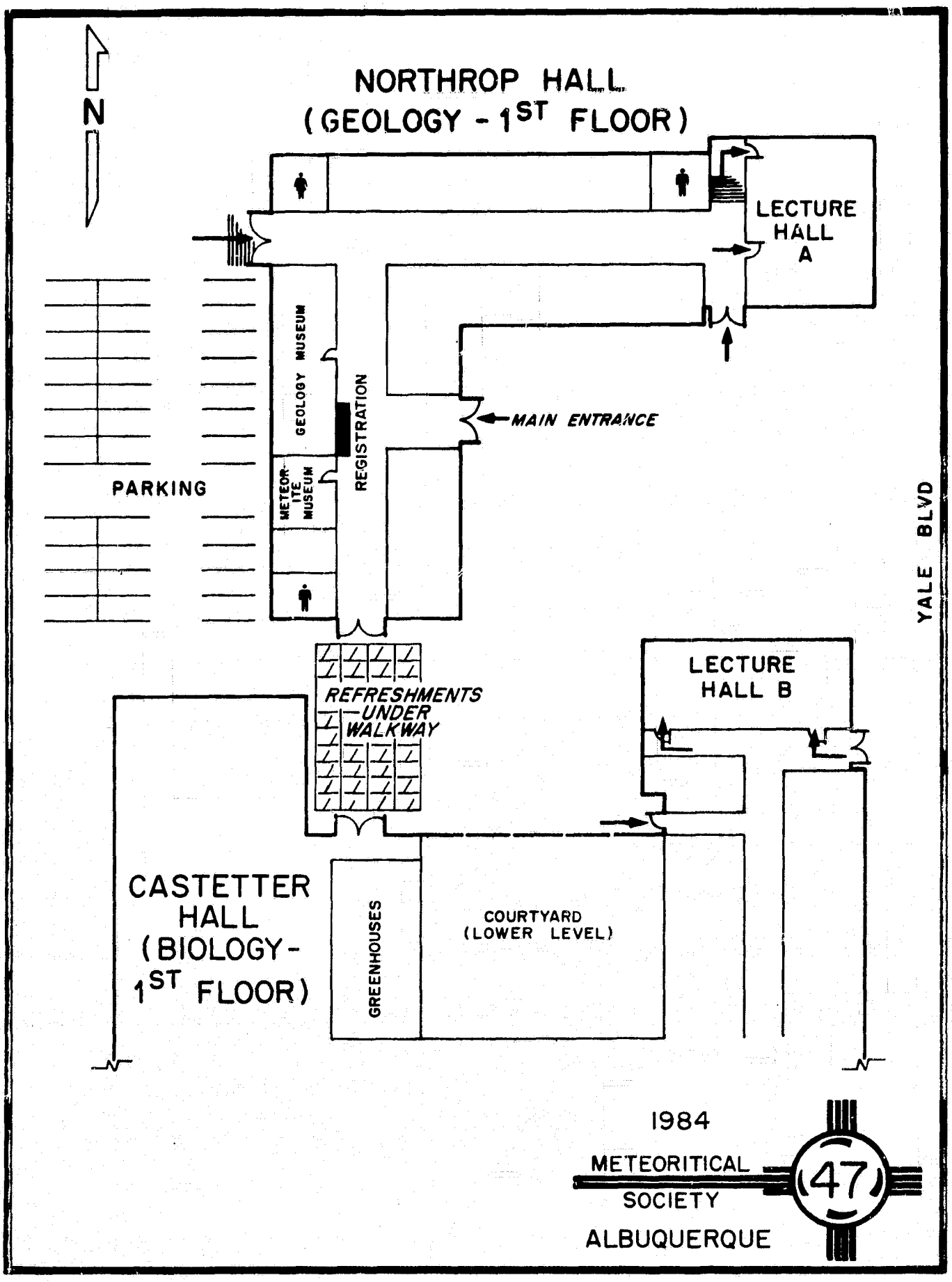
NORTHROP HALL
(GEOLOGY - 1ST FLOOR)
N
LECTURE HALL A
GEOLOGY MUSEUM
REGISTRATION
MAIN ENTRANCE
PARKING
METEORITE MUSEUM
YALE BLVD
REFRESHMENTS UNDER WALKWAY
LECTURE HALL B
CASTETTER HALL (BIOLOGY - 1ST FLOOR)
GREENHOUSES
COURTYARD (LOWER LEVEL)
1984
METEORITICAL SOCIETY
ALBUQUERQUE
47

MEETING CALENDAR

Sunday, July 29

PM		
4:00 - 9:00	Registration	Hilton Inn
7:00 - 10:00	Welcome to the Land of Enchantment	Hilton Inn
2:00 - 6:00	Lunar Science Council Meeting	Lobo Room #2 Hilton Inn
7:30 - 10:00	Meteoritical Society Council Meeting	Lobo Room #2 Hilton Inn

Monday, July 30

AM		
9:00 - 9:15	Welcome to the University of New Mexico President John Perovich	Room A
9:15 - 9:45	Address by Dr. George W. Wetherill President of the Meteoritical Society	Room A
10:00 - 11:45	Chondrules and Matrices of Chondrites	Room B
10:00 - 12:00	Cosmic Spherules	Room B
PM		
12:00 - 1:30	Nomenclautre Committee of Meteoritical Society	Lobo Room #2 Hilton Inn
1:30 - 4:45	Carbonaceous Chondrites	Room A
1:30 - 5:00	Iron Meteorites	Room B
6:00	Optional Trip up Sandia Mountain for Dinner	Depart from Hilton Inn
8:00 - 10:00	X-ray Microprobe Group	Civic Room Hilton Inn

Tuesday, July 31

AM		
8:30 - 12:00	Nebular Processes and Refractory Inclusions	Room A
8:30 - 11:45	Irradiation Effects	Room B
PM		
1:30 - 5:00	Achondrites	Room A
1:30 - 4:30	Asteriod Surfaces - Remote Sensing and Rocks	Room B
6:00	Optional Trip up Sandia Mountain for Dinner	Depart from Hilton Inn

Wednesday, August 1

AM		
8:30 - 11:30	SNC Meteorites	Room A
9:00 - 11:00	Thermal History of Chondrites	Room B
11:30 - 12:00	Business Meeting of Meteoritical Society	Room A
PM		
1:30 - 3:45	Isotopic Anomalies	Room A
3:45 - 5:00	Cosmochemistry	Room A
1:30 - 4:00	Enstatite Chondrites and Achondrites	Room B
4:00 - 5:00	Tektites	Room B
6:00 - 7:00	Cocktail Party	Hilton Inn
7:00	Banquet - Presentation of Leonard Medal to B. Y. Levin and Barringer Medal to E. M. Shoemaker.	Ballroom Hilton Inn

Thursday, August 2

AM		
8:30 - 10:00	Ordinary Chondrites	Room A
10:15 - 12:00	Antarctic Meteorites	Room A
8:30 - 11:30	Terrestrial and Lunar Impacts	Room B
PM		
1:30 - 4:30	Cosmic Dust, Comets and Cometary Missions	Room A
1:30 - 3:45	Early Solar System Chronology	Room B
4:30 - 7:30	Farewell Party	Hilton Inn

Friday, August 3

AM		
6:30	Two-day Field Trip to Canyon de Chelly and Chaco Canyon	Depart from Hilton Inn
7:30	Field Trip to Valles Caldera - Los Alamos	Depart from Hilton Inn

PRELIMINARY PROGRAM

47th METEORITICAL SOCIETY MEETING
July 30 - August 3, 1984
Albuquerque, New Mexico

Monday, July 30, 1984

SESSION A OPENING
9:00 a.m. Room A - UNM

9:00 John Perovich, President of the University of New Mexico
Welcome to the University of New Mexico

A-1 9:15 George W. Wetherill, President of the Meteoritical Society
The asteroidal source region of ordinary chondrites.

SESSION B - CHONDRULES AND MATRICES OF CHONDRITES
10:00 - 11:45 a.m. Room A - UNM

B-1 10:00 McSween H. Y., Jr.
Oxygen isotopes and ferromagnesian chondrule populations in carbonaceous chondrites.

B-2 10:15 Bischoff A.
Bulk compositions of Al-rich chondrules in ordinary and carbonaceous chondrites: Variations and similarities.

B-3 10:30 Ikeda Y.
Major element chemical compositions of chondrules in unequilibrated chondrites.

B-4 10:45 Recca S. I. Scott E. R. D. Taylor G. J. Keil K.
Fine-grained millimeter-sized objects in type 3 ordinary chondrites and their relation to chondrules and matrix.

B-5 11:00 Alexander C. Hutchison R. Barber D.
Chondrule rims and interchondrule matrix in U.O.C's

B-6 11:15 Hutchison R. Alexander C. Barber D. J.
Chondrules in the Bishunpur LL3 chondrite.

B-7 11:30 Goswami J. N.
Size dependence of chondrule textural types.

Monday, July 30, 1984

SESSION C - COSMIC SPHERULES
10:00 a.m. - 12:00 noon Room B-UNM

C-1 10:00 Jha R.
Atmospheric heating of meteorites: Results from nuclear track studies.

C-2 10:15 Millard H. T., Jr. Englert P.
Neutron activation analysis of stoney spherules from a marine sediment sample.

C-3 10:30 Mayeda T. K. Clayton R. N. Brownlee D. E.
Oxygen isotopes in deep sea spherules.

C-4 10:45 Smith J. V. Steele I. M.
Minor elements in relict olivine grains of deep-sea spheres: Match with Mg-rich olivines from C2 meteorites.

C-5 11:00 Brownlee D. E. Bates B. A. Wheelock M. M.
Platinum group nuggets in deep sea sediments.

C-6 11:15 Tazawa Y. Fujii Y.
Peculiar spherules from Antarctica and their origin.

C-7 11:30 Czajkowski J. Englert P.
Fractionation of siderophiles in cosmic spherules and its implications.

C-8 11:45 Budka P. Z.
The influence of gravitational body force in meteoritic chondrule and lunar glass formation.

12:00 - 1:30 Nomenclature Committee of Meteoritical Society Hilton Inn

Monday, July 30, 1984

SESSION D - CARBONACEOUS CHONDIRTES
1:30 - 4:45 p.m. Room A - UNM

D-1 1:30 Kerridge J. F. Macdougall J. D.
Evolutionary history of CI and CM chondrites.
(Invited speaker)

D-2 2:00 Rowe M. W. Hyman M. Ledger E. B.
Magnetite in the Essebi and Haripura CM chondrites.

D-3 2:15 Zolensky M. E.
Hydrothermal alteration of CM carbonaceous chondrites; implications of the identification of tochilinite as one type of meteoritic PCP.

D-4 2:30 Gooding J. L.
Aqueous alteration on meteorite parent bodies: Possible role of "unfrozen" water and the Antarctic meteorite analogy.

D-5 2:45 Housley R. M.
An SEM study of preterrestrial alteration effects in ALHA 77003.

D-6 3:00 Wark D. A.
Unexplained Fe, Ni, and S anomalies in CV chondrite components.

D-7 3:15 Steele I. M. Skirius C. M. Smith J. V.
Minor elements and cathodoluminescence of Mg-rich olivines from Murchison and Allende carbonaceous meteorites.

D-8 3:30 Cain P. M. McSween H. Y., Jr.
Strain analysis of the Leoville chondrite and conditions in asteroidal interiors.

D-9 4:00 Rubin A. E. James J. A. Keck B. D. Weeks K. S.
Sears D. W. G. Jarosewich E.
The Colony meteorite and the possible existence of a new chemical subgroup of CO3 chondrites.

D-10 4:15 Goswami J. N. Nishiizumi K.
Exposure history and compaction age of the Banten CM chondrite.

D-11 4:30 Heymann D. Smith M. J. Anderson J. B.
X-radiography of slices of the Allende meteorite.

Monday, July 30, 1984

SESSION E - IRON METEORITES
1:30 - 5:15 p.m. Room B - UNM

E-1 1:30 Reuter K. B. Goldstein J. I. Williams D. B. Butler E. P.
A study of tetrataenite.

E-2 1:45 Larsen L. Jensen G. B. Knudsen J. M. Roy-Poulsen H.
Roy-Poulsen N. O. Vistisen L.
Investigations of taenite from iron meteorites and chondrites.

E-3 2:00 Roy-Poulsen H. Clarke R. S., Jr. Jensen G. B. Knudsen J. M.
Roy-Poulsen N. O. Vistisen L.
Mössbauer spectroscopy and x-ray diffraction of samples from the Santa Catharina iron meteorite.

E-4 2:15 Clarke R. S., Jr.
Structural development in the Santa Catharina meteorite.

E-5 2:30 Dean D. C. Goldstein J. I.
Low temperature diffusion coefficients in the Fe-Ni and FeNiP systems--application to meteorite cooling rates.

E-6 2:45 Benkheiri Y.
^{244}Pu fission track and metallographic cooling rates of Toluca and Copiapo iron (IA) meteorites.

3:00 COFFEE BREAK

E-7 3:30 Jones J. H. Hart S. R.
Extreme incompatibility of Pb during the crystallization of magmatic iron meteorites.

E-8 3:45 Sellamuthu R. Goldstein J. I.
Experimental and theoretical study of the formation of the IIAB, IIIAB and IVA iron meteorite chemical groups from the parent liquid.

E-9 4:00 Malvin D. J. Jones J. H. Drake M. J.
Investigations concerning the magmatic iron meteorites: Static vs. dynamic experiments.

E-10 4:15 Clarke R. S., Jr. Sellamuthu R. Goldstein J. I.
Massive schreibersite in the Bellsbank and Santa Luzia meteorites.

E-11 4:30 Kracher A.
Inclusions in IAB irons: Is the partial differentiation model compatible with barometry and chronometry?

E-12 4:45 Prinz M. Nehru C. E. Delaney J. S. Fredriksson K. Palme H.
Silicate inclusions in IVA iron meteorites.

E-13 5:00 Zong P. Rubin A. E. Wasson J. T. Westcott J.
Guin: An ungrouped iron with silicate inclusions.

6:00 Optional trip up Sandia Mountain for dinner — Depart from Hilton Inn

8:00 - 10:00 X-ray Microprobe Group — Hilton Inn- Civic Room

Tuesday, July 31, 1984

SESSION F - NEBULAR PROCESSES AND REFRACTORY INCLUSIONS
8:30 a.m. - 12:00 noon Room A - UNM

F-1 8:30 Wood J. A.
Meteoritic constraints on processes in the solar nebula. (Invited speaker)

F-2 9:00 Trivedi B. M. P.
Chemical evolution of the solar nebula: A new model.

F-3 9:15 Stephens J. R.
Homogeneous condensation of gaseous mixtures of Si, Fe, O, N, and C in relative cosmic abundance and implications for astronomical condensation.

F-4 9:30 Bunch T. E. Chang S. Cassen P. Hollenbach D.
Dynamic thermal episodes in the protosolar nebula: Development of models from observations on CAI's.

9:45 COFFEE BREAK

F-5 10:00 Boynton W. V. Wark D. A.
Trace element abundances in rim layers of an Allende type A coarse-grained Ca,Al-rich inclusion.

F-6 10:15 Armstrong J. T. Hutcheon I. D. Wasserburg G. J.
Fremdlinge in Leoville and Allende CAI: Clues to post-formation cooling and alteration.

F-7 10:30 Hashimoto A. Grossman L.
Refractory inclusions in amoeboid olivine aggregates in Allende.

F-8 10:45 Fegley B. Palme H.
The chemistry and origin of refractory metal particles from Ca, Al-rich inclusions in carbonaceous chondrites.

F-9 11:00 Davis A. M.
A scandalously refractory inclusion in Ornans.

F-10 11:15 MacPherson G. J.
Refractory inclusions in the Mighei C2 meteorite.

F-11 11:30 Ekambaram V. Sluk S. M. Grossman L.
Trace elements in high-temperature inclusions from Murchison.

F-12 11:45 Kornacki A. S. Wood J. A.
The identification of group II inclusions by electron microprobe analysis of perovskite.

Tuesday, July 31, 1984

SESSION G - IRRADIATION EFFECTS
8:30 - 11:30 a.m. Room B-UNM

G-1 8:30 Regnier S. Lavielle B. Marti K. Simonoff G. N.
On the record of galactic cosmic ray flux and traffic break-ups in iron meteorites.

G-2 8:45 Murty S. V. S. Marti K.
The low-energy secondary cosmic ray flux: Detectors in iron meteorites.

G-3 9:00 Nishiizumi K. Elmore D. Arnold J. R.
Cosmogenic nuclides in peculiar meteorites.

G-4 9:15 Herpers U. Englert P.
^{22}Na, ^{60}Co and long-lived cosmogenic radionuclides in meteorite falls.

G-5 9:30 Heusser G. Ouyang Z. Pernicka E. Yi W. Hampel W. Kirsten T.
^{26}Al, ^{60}Co, ^{53}Mn, and ^{22}Na profiles in the Jilin drill cores.

9:45 COFFEE BREAK

G-6 10:00 Goswami J. N. Nishiizumi K. Arnold J. R.
Cosmogenic records in Antarctic meteorites-II.

G-7 10:15 Englert P. Sarafin R.
^{53}Mn in main fragments of the Norton County meteorite.

G-8 10:30 Wieler R. Signer P. Herpers U. Sarafin R. Bonani G. Hofmann H. J. Morenzoni E. Nessi M. Suter M. Wölfli W.
Cosmogenic nuclides in a cross section of the 300 kg Knyahinya chondrite.

G-9 10:45 Padia J. T. Rao M. N. Goswami J. N. Englert P. Herpers U.
The irradiation history of Dhurmsala meteorite.

G-10 11:00 Nautiyal C.M. Rao M.N.
Solar cosmic ray produced neon in lunar soils and their implication for the gas-rich meteorite studies.

G-11 11:15 Rocard F. Bénit J. Bibring J-P. Meunier R. Vassent B.
Solar wind and cosmic ray irradiation of grains and ices--application to erosion and synthesis of organic compounds in the solar system.

Tuesday, July 31, 1984

SESSION H - ACHONDRITES
1:30 - 5:00 p.m. Room A - UNM

H-1 1:30 Reid A. M. le Roex A. P.
Compositions of 7 Allan Hills polymict eucrites and one diogenite.

H-2 1:45 Fukuoka T.
Comparison of chemical compositions of Yamato polymict eucrites.

H-3 2:00 Treiman A. H.
Polymict eucrite ALHA 81011: Equilibrated clasts in a glassy matrix.

H-4 2:15 Dickinson T. Keil K. LaPaz L. Schmitt R. A. Smith M. R. Rhodes M.
Petrology of the Palo Blanco Creek eucrite.

H-5 2:30 Takeda H. Mori H. Ikeda Y.
Ordinary eucrites with slowly cooled textures and their crystallization history.

H-6 2:45 Delaney J. S.
The significance of two pyroxene mafic clasts in basaltic achondrites.

H-7 3:00 Warren P. H.
Origin of howardites, diogenites, and eucrites: A mass balance constraint.

3:15 COFFEE BREAK

H-8 3:30 Newsom H. E.
Evidence for the formation and the size of a metal core in the eucrite parent body.

H-9 3:45 Schmitt W. Weckwerth G. Wänke H.
The fractionation of siderophile and volatile elements on the eucrite parent body (EPB).

H-10 4:00 Ott U. Löhr H. P. Begemann F.
Ureilites: The case of missing diamonds and a new neon component.

H-11 4:15 Wacker J. F.
Noble gases in the unshocked ureilite Allan Hills 78019.

H-12 4:30 Goodrich C. A.
Ureilite petrogenesis: Clues from a graphite and metal-bearing intrusive complex, Disko Island, Greenland.

H-13 4:45 Klöck W. Palme H. Tobschall H. J.
Trace elements in native iron from Disko Island, West Greenland.

Tuesday, July 31, 1984

SESSION I - ASTEROID SURFACES - REMOTE SENSING AND ROCKS
1:30 - 4:30 p.m. Room B - UNM

I-1 1:30 Hörz F. Cintala M. See T.
Grainsize evolution and differential comminution in an experimental regolith.

I-2 1:45 Hawke B. R. Lucey P. Bell J. F. Spudis P. D.
Spectral reflectance studies of the Orientale region of the moon.

I-3 2:00 Pieters C. M.
Asteroid-meteorite connection: Regolith effects implied by lunar reflectance spectra.

I-4 2:15 King T. V. V. Gaffey M. J. McFadden L. A.
Spectroscopic evidence of regolith maturation.

I-5 2:30 Bell J. F. Gaffey M. J. Hawke B. R.
Spectroscopic identification of probable pallasite parent bodies.

I-6 2:45 Ostro S. J.
Radar investigation of asteroids.

3:00 COFFEE BREAK

I-7 3:15 Brückner J. Englert P. Reedy R. C. Wänke H.
High-energy neutron induced promt gamma-rays: Chemical remote sensing of planetary surfaces.

I-8 3:30 Wilkening L. L. Jensen S. E. Schaudt K.
Clastic texture of meteorites.

I-9 3:45 Ehlmann A. J. Keil K. Scott E. R. D. Weber H. W. Schultz L.
The Kendleton L4 fragmental breccia: Parent body surface history.

I-10 4:00 Williams C. V. Rubin A. E. Keil K. San Miguel A.
Petrology of some ordinary chondrite regolith breccias: Implications for parent body history.

I-11 4:15 Caffee M. W. Hohenberg C. M. Swindle T. D. Goswami J. N.
Confirmation of cosmogenic neon from precompaction irradiation of Kapoeta and Murchison.

6:00 Optional trip up Sandia Mountain for dinner Depart from Hilton Inn

Wednesday, August 1, 1984

SESSION J - SNC METEORITES
8:30 - 11:30 a.m. Room A - UNM

J-1 8:30 Reedy R. C.
Cosmogenic radionuclides and the exposure histories of SNC meteorites.

J-2 8:45 Sarafin R. Herpers U. Wieler R. Signer P.
Cosmogenic nuclides in Antarctic achondrites and chondrites.

J-3 9:00 Rajan R. S. Tamhane A. S. Poupeau G. Swindle T. D. Caffee M. Hohenberg C. M.
Evidence for ages older than 1.3 gyr in the Elephant Morraine shergottite.

J-4 9:15 Swindle T. D. Caffee M. W. Hohenberg C. M. Hudson G. B.
Noble gases in SNC meteorites.

J-5 9:30 Bogard D.
On the origin of excess ^{40}Ar in the four shergottite-achondrites.

J-6 9:45 Wiens R. C. Becker R. H. Pepin R. O.
Remeasurement of nitrogen in EETA 79001 glass.

J-7 10:00 Carr R. H. Wright I. P. Pillinger C. T.
Martian atmospheric CO_2 in an Antarctic meteorite?

10:15 COFFEE BREAK

J-8 10:30 Mori H. Takeda H.
Shock deformation texture of olivine crystals of the EETA 79001 shergottite.

J-9 10:45 Nyquist L. Wooden J. Bansal B. Wiesmann H. Shih C.-Y.
Sr and Nd isotopic systematic of EETA 79001.

J-10 11:00 Treiman A. H. Drake M. J.
Core formation in the Shergottite parent body (SPB).

J-11 11:15 Weckwerth G. Wänke H.
Chemical relationships among shergottites, nakhlites, and Chassigny.

Wednesday, August 1, 1984

SESSION K - THERMAL HISTORY OF CHONDRITES
8:30 - 11:00 a.m. Room B - UNM

K-1 8:30 Guimon R. K. Weeks K. S. Keck B. D. Sears D. W. G.
Thermoluminescence as a palaeothermometer?

K-2 8:45 Taylor G. J. Scott E. R. D.
A quantitative look at chondrite metamorphism.

K-3 9:00 Scott E. R. D. Taylor G. J.
Metamorphism of type 3 carbonaceous and ordinary chondrites.

K-4 9:15 Miyamoto M. McKay D. S. McKay G. A. Duke M. B.
Chemical zoning and homogenization of olivines in ordinary chondrites.

K-5 9:30 Bernatowicz T. Honda M. Podosek F.
Noble gas chronology of LL chondrites.

9:45 COFFEE BREAK

K-6 10:00 McConville P. Turner G.
Thermal history of the Peace River L6 chondrite based on 40Ar-39Ar measurements.

K-7 10:15 Wasson J. T. Kallemeyn G. W.
Cumberland falls (chondrite), Suwahib (Buwah) and other ordinary chondrites showing evidence of postaccretional reduction.

K-8 10:30 Jovanovic S. Reed G. W., Jr.
Meteorite Hg diffusion studies.

K-9 10:45 Lingner D. W. Huston T. J. Lipschutz M. E.
Mobile trace elements and thermal histories of H4-6 chondrites comparison with L4-6 chondrites.

Wednesday, August 1, 1984

SESSION L - ISOTOPIC ANOMALIES
1:30 - 3:45 p.m. Room A - UNM

L-1 1:30 Manuel O. K. Ramaduri R. Ramaduri S.
Heavy noble gases associated with Neon-E.

L-2 1:45 Zadnik M. G.
Noble gases in the Bells (C2) and Sharps (H3) meteorites.

L-3 2:00 Clayton D. D.
s-Process Nd in Allende residues.

L-4 2:15 Birck J. L. Allegre C. J.
Anomalous isotopic composition of chromium in Allende inclusions.

L-5 2:30 Molini-Velsko C. Mayeda T. K. Clayton R. N.
Correlated isotopic anomalies in the elements silicon and magnesium from Allende inclusions.

L-6 2:45 Zinner E. Fahey A. McKeegan K. D.
Magnesium and silicon isotopic composition of interplanetary dust particles.

3:00 COFFEE BREAK

L-7 3:15 Yang J. Epstein S.
Search for isotopic anomalies in Odessa (IA), Ochansk (H4), Plainview (H5), and Gladstone (H6).

L-8 3:30 Lewis R. S. Ohtsuki M.
Interstellar carbon grains from the Murchison meteorite: Electron microscopy.

Wednesday, August 1, 1984

SESSION M - COSMOCHEMISTRY
3:45 - 5:00 p.m. Room A - UNM

M-1 3:45 Wacker J. F. Anders E.
Where is the earth's missing xenon?

M-2 4:00 Curtis D. B. Gladney E. S.
Boron cosmochemistry.

M-3 4:15 Murrell M. T. Burnett D. S.
Actinide chemistry of Allende components.

M-4 4:30 de Chazal S. Crozaz G. Bourot-Denise M. Pellas P.
Plutonium and uranium in individual crystals of merrillite and apatite of St. Severin.

M-5 4:45 Crozaz G. Zinner E.
Ion probe determinations of the REE contents of individual meteoritic phosphate grains.

Wednesday, August 1, 1984

SESSION N - ENSTATITE CHONDRITES AND ACHONDRITES
1:30 - 4:00 p.m. Room B - UNM

N-1 1:30 Larimer J. W. Bartholomay H. A. Fegley B.
The chemistry of rare earth elements in the solar nebula.

N-2 1:45 Grossman J. N. Rubin A. E. Rambaldi E. R. Rajan R. S. Wasson J. T.
Chemical variations among chondrules from Qingzhen (EH3).

N-3 2:00 Weeks K. S. Sears D. W. G.
A new class of enstatite chondrite?

N-4 2:15 Kallemeyn G. W. Wasson J. T.
The composition of enstatite chondrites.

N-5 2:30 Nagahara H.
Silica-niningerite-enstatite clasts in the primitive enstatite chondrites.

N-6 2:45 Rambaldi E. R. Murrell M. T. Rajan R. S. Burnett D. S.
Coexisting chalcophile and lithophile uranium in Qingzhen (EH3) chondrite.

3:00 COFFEE BREAK

N-7 3:15 Cassidy W. A.
High temperature phase equilibria in the enstatite chondrite system.

N-8 3:30 Okada A. Keil K. Leonard B. F. Hutcheon I. D.
$Na_{0.3}(H2O)_1 CrS_2$, A new mineral in the Norton County enstatite chondrite.

N-9 3:45 Nininger H. H.
Bishopville: The importance of a field search.

Wednesday, August 1, 1984

SESSION O - TEKTITES
4:00 - 5:00 p.m. Room B-UNM

O-1 4:00 Glass B. P. Sanfilippo A. Burns C. A. Lerner D. H.
North American tektites and microtektites from Barbados, West Indies.

O-2 4:15 Fudali R. F. Ross D. Appleman D. E.
Relict minerals in a Muong Nong tektite.

O-3 4:30 Koeberl C. Kluger F. Kiesl W.
Geochemistry of Muong-Nong type tektites V: Unusual ferric/ferrous ratios.

O-4 4:45 Weinke H. H. Koeberl C.
Geochemistry of Muong-Nong type tektites VI: Major element determinations and inhomogenities.

6:00 - 7:00 Cocktail Party Hilton Inn

7:00 - Banquet - Presentation of Leonard Medal to B. Y. Levin and Barringer Medal to E. M. Shoemaker Ballroom

Thursday, August 2, 1984

SESSION P - ORDINARY CHONDRITES
8:30 - 10:00 a.m. Room A - UNM

P-1 8:30 Fredriksson K. Clarke R.S., Jr. Pugh R.
A new H-3 chondrite from Study Butte, Texas

P-2 8:45 Sipiera P. P.
Three new chondrite finds from Roosevelt County, New Mexico.

P-3 9:00 Pugh R. N.
Salem meteorite.

P-4 9:15 Okada A. Shima M. Takaoka N. Murayama S.
The chondrite Higashi-koen.

P-5 9:30 Nakamura N. Yanai K. Matsumoto Y.
Unique clasts with V-shaped REE pattern in L6 chondrites.

P-6 9:45 Prinz M. Nehru C. E. Weisberg M. K. Delaney J. S. Yanai K. Kojima H.
H chondritic clasts in a Yamato L6 chondrite: Implications for metamorphism.

10:00 COFFEE BREAK

SESSION Q - ANTARCTIC METEORITE STUDIES
10:15 a.m. - 12:00 noon Room A - UNM

Q-1 10:15 Annexstad J. O.
Meteorite concentrations in Antarctica--how complete is the picture?

Q-2 10:30 Hewins R. H.
Pairing in Antarctic mesosiderites.

Q-3 10:45 Marvin U. B.
An approach to the meteorite pairing problem at the Allan Hills, Antarctica.

Q-4 11:00 Schultz L. Freundel M.
Terrestrial ages of Antarctic meteorites.

Q-5 11:15 Dennison J. E. Lingner D. W. Lipschutz M. E.
Trace elements in Antarctic H5 chondrites: Weathering effects and comparison with non-Antarctic falls.

Q-6 11:30 Yanai K. Kojima H. Katsushima T.
Lunar meteorites in Japanese collection of the Yamato meteorites. (Invited Speaker)

Thursday, August 2, 1984

SESSION R - TERRESTRIAL AND LUNAR IMPACTS
8:30 - 11:30 a.m. Room B - UNM

R-1 8:30 Shoemaker E. M. Wolfe R. F.
Crater ages, comet showers, and the putative "death star." (Invited Speaker)

R-2 9:00 Kyte F. T.
Iridium sedimentation in the Cenozoic; no evidence for a death star.

R-3 9:15 Hildebrand, A. R. Boynton W. V. Zoller W. H.
Kilauea volcano aerosols. Evidence in siderophile element abundances for impact-induced oceanic volcanism at the K/T boundary.

R-4 9:30 Newsom H. E. Graup G.
Hydrothermal alteration of suevite impact ejecta at the Ries meteorite crater, F. R. Germany.

R-5 9:45 Wood C. A. Dailey C. Daley W. Wells G.
Searching for impact craters using space shuttle photography.

R-6 10:00 Dietz R. S. McHone J. F.
Shatter cones: Definitive criterion for meteorite impact.

10:15 COFFEE BREAK

R-7 10:30 McHone J. F. Emilsson T. I. Yang W-H. Kirkpatrick R. J. Vergo N. Oldfield E.
Coesite and stishovite detected in natural concentrations by solid-state silicone-29 nuclear magnetic resonance.

R-8 10:45 Sutton S. R.
Thermoluminescence age of Meteor Crater, Arizona.

R-9 11:00 Read W. F.
The circular structure at Glover Bluff: What and where it is.

R-10 11:15 Runcorn S. K.
Lunar palaeomagnetism, polar wandering and the existence of primeval lunar satellites.

Thursday, August 2, 1984

SESSION S - COSMIC DUST, COMETS AND COMETARY MISSIONS
1:30 - 4:30 p.m. Room A - UNM

S-1 1:30 Tomeoka K. Buseck P. R.
A hydrated interplanetary dust particle containing calcium- and aluminum-rich refractory mineral: Possible relations to carbonaceous chondrites.

S-2 1:45 Rietmeijer F. J. M. Mackinnon I. D. R.
Diagenesis in interplanetary dust: Chondritic porous aggregate W7029*A.

S-3 2:00 Sandford S. A. Walker R. M.
Links between astronomical observations of protostellar clouds and laboratory measurements of interplanetary dust: The 6.8 carbonate band.

S-4 2:15 McKeegan K. D. Sandford S. A. Walker R. M. Wopenka B. Zinner E.
D/H ratios in interplanetary dust and their relationship to IR, Raman, and EDX observations.

S-5 2:30 Wopenka B. Sandford S. A.
Laser Raman Microprobe study of mineral phases in meteorites.

S-6 2:45 Bild R. W. Tallant D. R.
Raman Microscopy study of the Lodran meteorite.

3:00 COFFEE BREAK

S-7 3:15 Russell J. A.
The Perseids and comet Swift-Tuttle 1862 III.

S-8 3:30 Johnstone A. D. Reinhard R.
The Giotto mission to Halley's comet. (Invited Speaker)

S-9 3:45 Swenson B. L. Tsou P. Friedlander A. Mascy A. C.
A proposed Giotto/comet coma sample return mission. (Invited Speaker)

S-10 4:00 Brownlee D. E.
Sample return from a comet flyby. (Invited Speaker)

4:15 Discussion of papers S 8-10

THURSDAY, AUGUST 2, 1984

SESSION T - EARLY SOLAR SYSTEM CHRONOLOGY
1:30 - 3:45 p.m. Room B-UNM

T-1 1:30 Brigham C. A. Papanastassiou D. A. Wasserburg G. J.
Mg isotopic measurements in fine-grained Ca-Al-rich inclusions.

T-2 1:45 Hutcheon I. D. Armstrong J. T. Wasserburg G. J.
Excess ^{41}K in Allende CAI: A hint re-examined.

T-3 2:00 Hinton R. W. MacPherson G. J. Grossman L.
Magnesium isotopic analysis of Gr-1--A second corundum-rich Murchison inclusion.

T-4 2:15 Hutcheon I. D. Armstrong J. T. Wasserburg G. J.
Mg isotopic studies of Leoville "compact" type A CAI.

2:30 COFFEE BREAK

T-5 2:45 Papanastassiou D. A. Wasserburg G. J. Marvin U. B.
Absence of excess ^{26}Mg in anorthite from the Vaca Muerta mesosiderite.

T-6 3:00 De Laeter J. R. Rosman K. J. R.
A possible ^{126}Sn chronometer for the early solar system.

T-7 3:15 Chen J. H. Wasserburg G. J.
Anomalous silver in sulfide nodules.

T-8 3:30 Teshima J. M. Wasserburg G. J. El Goresy A.
Petrography of Cape York and Grant: Irons with simple Pd-Ag systematics.

4:30 - 7:30 FAREWELL PARTY Hilton Inn

SESSION U - PAPERS PRESENTED BY ABSTRACT ONLY

U-1 Bradley J. P. Brownlee D. C.
Discovery of nuclear tracks in interplanetary dust.

U-2 Budka P. Z. Milillo F. F.
Speculations on the formation of metallic meteorite phases.

U-3 Levi-Donati G. R. Brandstätter F. Kurat G.
Barntrup: LL-4 chondrite.

U-4 Ulff-Møller F.
On the potential importance of carbon during metal core segregation in planetoids.

Friday, August 3, 1984

FIELD TRIPS

6:30 a.m.	Two-day field trip to Canyon de Chelly and Chaco Canyon	Depart from Hilton Inn
7:30 a.m.	Field trip to Valles Caldera - Los Alamos	Depart from Hilton Inn

THE ASTEROIDAL SOURCE REGION OF ORDINARY CHONDRITES; George W. Wetherill, DTM, Carnegie Institution of Washington, Washington, D.C. 20015.

The final, Earth-impacting orbits of ordinary chondritic meteorites have a very special distribution. By use of visual radiant and time of fall data, as well as photographic fireball orbits (1) it is inferred that chondrite perihelia are concentrated near 1 A.U., eccentricities are usually rather high ($\sim$0.5), and inclinations are low ($\sim 10^{o}$). Velocity selection resulting from atmospheric ablation plays a significant role in determining this orbital distribution, but by no means suffices to explain it. The observed distribution is a fragile one, and can easily be destroyed by Earth and Venus perturbations. This places severe constraints on the location of the original source bodies, of which these meteorites are fragments.

New calculations have been made of the expected distribution of final orbits from a range of initial sources, taking into consideration close encounter planetary perturbations, secular resonance, destruction by collision in space, and atmospheric ablation.

It is found that the observed distribution can be produced only by fragments gravitationally accelerated by resonance at the 3:1 Kirkwood gap (a = 2.50 A.U.) into marginally Earth-crossing orbits, presumably by the mechanism described by Wisdom (2). Furthermore, the population of asteroidal collision fragments injected into the resonant region must be strongly biased to favor smaller ($\lesssim$10m) bodies, rather than being accompanied by the usual proportion of larger ejected objects. Other sources (other Kirkwood gaps, Flora region of the asteroid belt, Apollo-Amor objects, cometary orbits) fail for one reason or another. Meteorites, as well as non-cometary Apollo-Amor objects, are likely to be produced in these other asteroidal source regions, but their number appears to be insufficient for their fragments to dominate the flux of ordinary chondrites.

Larger asteroids, as well as their retinue of smaller bodies resulting from collisions, with semi-major axes of 2.44 to 2.48 A.U. and 2.52 to 2.56 A.U. should therefore be the dominant sources of ordinary chondrites. No compelling arguments can be given to explain possible discrepancies between the reflectance spectra of S-asteroids in this region and recovered ordinary chondrites, or the small variety of ordinary chondrite types. Several possible explanations can be given, however.

(1) Wetherill, G. W. and ReVelle, D. O. (1981) Which fireballs are meteorites? A study of the Prairie Network photographic meteor data. Icarus 48, 308-328.

(2) Wisdom, J. (1983) Chaotic behavior and the origin of the 3:1 Kirkwood gap. Icarus 56, 51-74.

OXYGEN ISOTOPES AND FERROMAGNESIAN CHONDRULE POPULATIONS IN CARBONACEOUS CHONDRITES. Harry Y. McSween, Jr., Department of Geological Sciences, University of Tennessee, Knoxville, TN 37996.

Studies of porphyritic chondrules in carbonaceous chondrites (1,2,3) have recognized the existence of two populations (termed I and II) that are distinct in bulk composition, mineral chemistry, oxidation state, and texture. Population I chondrules are the major constituents of carbonaceous chondrites; only a few percent of chondrules are II. Recent oxygen isotopic analyses of individual chondrules in Allende (4) defined an apparent mixing line (presumably between ^{17}O-enriched solid and ^{17}O- and ^{18}O-enriched gas) that is different from that for chondrules in ordinary chondrites. Given the other variations between population I and II chondrules, it seems prudent to determine if they are distinct in their isotopic compositions as well. These isotopically analyzed chondrules have now been characterized in terms of petrography and chemistry with the intention of resolving possible isotopic differences between populations. Unfortunately, among the 22 ferromagnesian chondrules analyzed, none possess all the properties used to define population II chondrules. However, barred olivine chondrules can be of either compositional type (3), and 6 of these may be assigned to II based on mineral chemistry and statistical analysis of their bulk compositions. These chondrules cluster as one extreme end of the spectrum of isotopic compositions defined by the Allende chondrule data.

Formation of the two chondrule populations required different precursor materials and presumably occurred at different locations, as multiple chondrules are always of the same population. The suggestion has been previously made (2) that the two populations may have equilibrated with different nebular gas compositions. However, isotopic data for I and II chondrules lie along the same linear regression line ($r = 0.975$). Thus this hypothesis is unlikely because the population II chondrules appear to be distinct from I only in degree of equilibration, and not in the composition with which they equilibrated. A more plausible model (4) is that chondrules which were relatively small and had melted completely exchanged oxygen more readily than larger or incompletely melted chondrules. Population II chondrules have lower liquidus temperatures than I, and consequently would have been more easily melted and may have remained liquid for longer times in a cooling nebula. This idea is consistent with the observations that barred (i.e. completely molten) chondrules of both populations appear to have exchanged the most oxygen, that barred II chondrules have exchanged more than barred I, and that larger barred chondrules have exchanged less than smaller ones. Barred chondrules in ordinary chondrites appear to exhibit a similar effect, though their solid precursors had a different initial isotopic composition.

References

(1) McSween, H. Y. (1977) Geochim. Cosmochim. Acta 41, 1777-1790.
(2) McSween, H. Y. et al. (1983) Proc. Conf. Chondrules and Their Origins, 195-210.
(3) Scott, E. R. D. and G. J. Taylor (1983) J. Geophys. Res. 88, B275-286.
(4) Clayton, R. N. et al. (1983) Proc. Conf. Chondrules and Their Origins, 37-43.

B-2

N85 15601

BULK COMPOSITIONS OF AL-RICH CHONDRULES IN ORDINARY AND CARBONACEOUS CHONDRITES: VARIATIONS AND SIMILARITIES. A. Bischoff, Institute of Mineralogy, Corrensstr. 24, 4400 Münster, F.R.G.

Al-rich chondrules are wide-spread constituents of ordinary chondrites (1-3). Their bulk compositions are transitional between the various subgroups of Al-rich chondrules (2,3).

Chondrules in ordinary chondrites. An extended study of ordinary chondrites revealed that chondrules exist which are transitional in composition between Al-rich and Mg-Fe-rich types in contrast to the finding of Wlotzka (4) who inferred a gap in compositions between the Ca-Al-rich and Mg-Fe-rich chondrules. In Fig. 1 own and literature data (5-7) of transitional chondrule bulk compositions are plotted. They show that no compositional gap exists between the Mg-Fe-rich and Al-rich chondrules. Chondrules with Na_2O-contents > 3.0 wt.% are indicated by crosses. Variable CaO/Na_2O-ratios for chondrule bulk compositions exist, similar to what has been described for the subgroups of Al-rich chondrules (2,3).

Chondrules in carbonaceous chondrites. Al-rich and transitional chondrules similar to those described above have been found also in carbonaceous chondrites. So far 39 chondrules from the carbonaceous chondrites Leoville, Allende, Vigarano and Colony have been investigated. Their bulk compositions in terms of Al_2O_3 vs. CaO are plotted in Fig. 2. Some chondrules contain relatively high Na_2O-contents (indicated by the wt.% values in Fig. 2). Not only are the bulk compositions of Al-rich and transitional chondrules very similar to the respective chondrules in ordinary chondrites, even their textures are sometimes almost identical. The occurrence of chemically and texturally similar chondrules in ordinary and carbonaceous chondrites provides additional evidence that carbonaceous and ordinary chondrites and their constituents formed by related processes.

References: (1) Bischoff A. and Keil K. (1983a): Nature 303, 588-592. (2) Bischoff A. and Keil K. (1983b): Spec. Publ. No. 22. Univ. of New Mexico, Institute of Meteoritics, 1-33. (3) Bischoff A. and Keil K. (1984): Geochim. Cosmochim. Acta (in press). (4) Wlotzka F. (1982): In Conf. on Chondrules and their Origins, Contrib. 493, 61. (5) Gooding J.L. (1979): Ph.D. Dissertation, Univ. of New Mexico, 392pp. (6) Lux G. et al.,(1980): Geochim. Cosmochim. Acta 44, 841-855. (7) McSween H.Y. JR. (1977): Geochim. Cosmochim. Acta 41, 1843-1860.

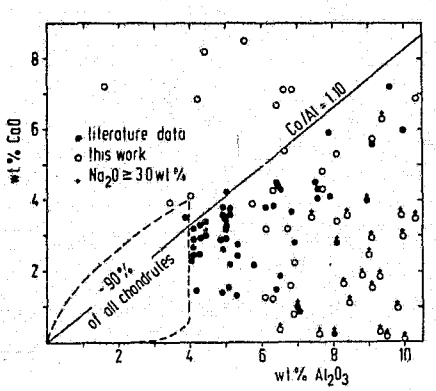

Fig. 1

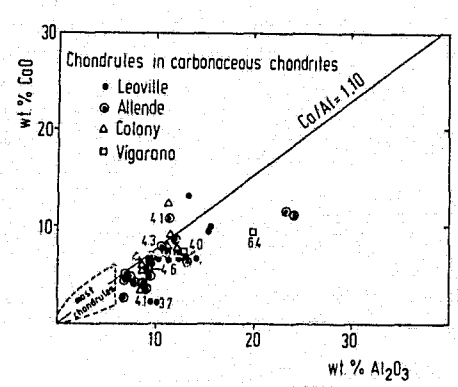

Fig. 2

MAJOR ELEMENT CHEMICAL COMPOSITIONS OF CHONDRULES IN UNEQUILIBRATED CHONDRITES; Y. Ikeda, Dept. Earth Sciences, Ibaraki Univ., Mito 310, Japan.

The chemical compositions (except for metals and sulfides in chondrules) of more than 500 chondrules from unequilibrated E, H, L, LL, and C chondrites were measured using a broad beam of an electron-probe microanalyser.

The compositions of chondrules can be represented by various mixtures of normative compositions of olivine, low-Ca pyroxene, plagioclase, and high-Ca pyroxene with minor amounts of spinel, feldspathoid, SiO_2-minerals, etc., indicating that the chondrule precursor materials consisted of aggregates of these minerals.

The Al, Na, and K contents of most chondrules reflect the compositions of the ternary feldspar (An-Ab-Kf) of the chondrule precursor materials, and chemical types of chondrules (KF, SP, IP, and CP) are defined on the basis of the atomic proportion of Al, Na, and K. The KF chondrule type (K/Na+K > 0.5) is restricted to brecciated LL chondrites. The CP type (Al/Al+Na+K > 0.95) is rare and occurs mainly in carbonaceous chondrites. The IP type (0.65 < Al/Al+Na+K < 0.95) and the SP type (Al/Al+Na+K < 0.65, and K/Na+K < 0.5) are most abundant in all chondrites: the relative frequency of IP and SP types differes among brecciated LL type chondrites, ordinary chondrites (except for the brecciated LL type), and carbonaceous chondrites.

The frequency of Al/Al+Na+K atomic ratios of IP and SP chonrules in ordinary chondrites is bimodal: IP chondrules show broad peak or plateau in the range of 0.65 to 0.95, and SP chondrules show a sharp peak at the ratios of 0.50 to 0.55. The IP type is magnesian and SiO_2-poor as a whole in comparison with the SP type. The Na/Al ratios of pyroxenes in IP chondrules tend to be lower than those in SP chondrules. Spinels in IP chondrules seem to be richer in Al contents than those in SP type which are richer in Cr contents (Kimura, personal communication). The IP type lacks radial-pyroxene chondrules whereas the SP type includes them commonly. The former shows higher crystallinity as a whole and includes sometimes relic minerals whereas the latter includes abundant glassy groundmasses and is free from relic minerals. The precursor materials of SP chondrules are considered to comprize low-temperature condensates more than those of IP chondrules.

B-4

FINE-GRAINED MILLIMETER-SIZED OBJECTS IN TYPE 3 ORDINARY CHONDRITES AND THEIR RELATION TO CHONDRULES AND MATRIX, S.I. Recca, E.R.D. Scott, G.J. Taylor, and K. Keil, Institute of Meteoritics, Department of Geology, University of New Mexico, Albuquerque, NM 87131

Fine-grained, opaque, silicate-rich matrix material, occurring as rims on chondrules and clasts, discrete clasts, and between chondrule and mineral fragments is a primitive component of chondrites and may resemble the material from which chondrules formed (1,2). To elucidate the relationship between chondrules and matrix and to help identify chondrule precursor material, we studied the mineralogy and bulk compositions of 30 mm-sized, fine-grained objects in Tieschitz (H3.6), Sharps (H3.4), Allan Hills A77299 (H3.7), Yamato 74191 (L3.6), Semarkona (LL3.0), and St. Mary's Co. (LL3.3). All are composed of submicron to micron sized material and may contain larger mineral fragments. Some of these objects may have been considered chondrules by other authors; some have been described as matrix lumps. Three texturally and mineralogically distinct types of objects have been identified; all are minor components of the chondrites studied (<1% except Sharps where melt-breccia-textured objects are ~1%).

A) Network-textured objects (0.3 - >1mm) have matrix like compositions, contain $\lesssim$30 vol.% unzoned mineral fragments (Fa <1 - Fa 50; En 2 - 40, Wo 0.1 - 45) in a network-textured groundmass composed of amoeboidal patches and stringers of olivine (~Fa 50 ± 10) and pyroxene (~En 2 - 10), with an average grain size of $\lesssim$1μm. Many mineral fragments are in extreme disequilibrium with the ground mass, e.g. Fa 3.5 in contact with Fa 50, with no diffusion between the phases. These objects usually have finer-grained (<<1μm), network-textured opaque rims 10 - 50μm thick. The rims are similar in composition to the objects they enclose, but are devoid of mineral fragments and in all but one case are higher in feldspathic components.

B) Melt-breccia-textured objects contain 10 - 50 vol.% mineral fragments in a fine grained igneous groundmass and generally are not rimmed. They may contain patches of network-textured material and areas which may be recrystallized network-textured material. Mineral fragments are often zoned, e.g. Fa <1 - 30, with CaO anticorrelating with FeO, indicative of metamorphism. In some cases network textured areas grade through recrystallized material and into igneous textured material without perceptible boundaries.

C) One clastic-textured object has been observed (in Yamato 74191). This object consists of fine grained (<0.1 - >10μm) mineral and chondrule fragments, contains little interstitial glass, is devoid of network-textured groundmass, and has a fine-grained, opaque rim. The relationship of this object to the others described is unclear.

Network-textured objects are texturally and chemically similar to matrix, but patches of network textured material in matrix are small (<50μm), irregularly shaped, and often closely associated with chondrule fragments. Network-textured objects are much larger ($\geq$0.3mm), spherical to subspherical, generally rimmed by finer-grained material, contain no obvious chondrule fragments, and show no evidence of having been previously incorporated into another object. These observations suggest that network textured matrix areas may be fragments of network-textured objects.

Bulk compositions of network and melt-breccia-textured objects define a rather narrow trend on a plot of Si/Al vs. Mg/Al, emphasizing a possible genetic relationship. These data show that Si/Mg is higher for network and melt-breccia-textured objects than for porphyritic and barred olivine chondrules. Melting in vaccuo of network-textured objects would cause a loss of Si relative to Mg (3), suggesting that material compositionally similar to fine grained objects could have been precursors to some chondrules.

Huss G.R. et al. (1981) Geochim. Cosmochim. Acta, 45, 33-51.
Scott E.R.D. et al. (1984) Geochim. Cosmochim. Acta, in press.
Hashimoto A. (1983) Geochem. Jour., 17, 111-145.

CHONDRULE RIMS AND INTERCHONDRULE MATRIX IN U.O.C's:C.Alexander*, R.Hutchison**,D.Barber*.* Essex Univ. U.K. ** Brit.Mus.Nat.Hist.London U.K

In this study opaque rims around chondrules and clasts have been distinguished from opaque,interchondrule matrix apparently unrelated spatially to chondrules and clasts.Microprobe,SEM,and ATEM techniques were used in this study of Bishunpur(LL3),Tieschitz(H3) and other U.O.C's.

The mean chemical composition for dark rim and matrix in Bishunpur and Tieschitz are similar to the 'opaque matrix' of Huss et al(1).However,the mean dark rim compositions in Bishunpur have significantly higher Fe,and lower Na,K,Al and Si than opaque interchondrule matrix.The 'opaque matrix' of Huss et al(1) essentially lies between these compositions.In Tieschitz only rim material was observed.

Several components in Bishunpur opaque material have been identified by microprobe and ATEM.The interchondrule matrix is dominated by opx(~En60) and olivine(~Fo60),similar to the mean matrix olivine compositions of Huss et al(1).However,the olivine component in dark rims is in general Fa-rich(~Fo30) explaining the Fe enrichment described above fig(1).In addition there is an Na,K,AL,Si-rich interstitial glass of near albitic composition that is common to both rim and matrix.The Na/K ratio in this phase is very similar to those in clast and chondrule mesostases fig(2).However,in some chondrules and clasts plots of Na,K vs Al show parallel trends to rim and matrix but displaced towards higher Al suggesting vapour fractionation may have operated.

In Bishunpur rims as well as the silicate-FeS,FeNi layering described by Allen et al(2) we have observed discontinuous layering within the silicate portion.This is apparently due to variations in the proportions of the components described above,particularly the glassy phase.

In Tieschitz the rims are Si-poor and dominated by normative olivine(Fo50).Again there is an Na,K,Al component but is often nepheline normative rather than albitic.It too is probably present asglass,Ashworth(pers.comm.)

Thus in Bishunpur atleast there is a strong genetic link between matrix and rims although rims seem to have formed under different possibly more oxidising conditions.Also the presence of the same component in rims,matrix chondrules and clasts suggests a common source. (1)Huss et al G.C.A. 45,33,1981. (2)Allen et al G.C.A. 44,1161,1981.

Fig. 1

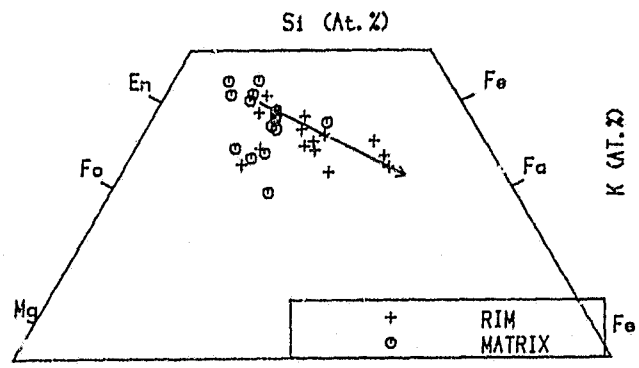

Fig. 2

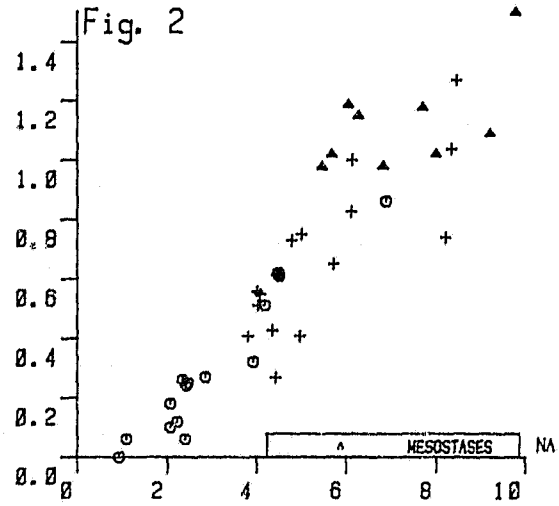

CHONDRULES IN THE BISHUNPUR LL3 CHONDRITE:

R. Hutchison,* C. Alexander** and D.J. Barber** . *Mineralogy Department, British Museum (Natural History), London SW7 5BD, ** Physics Department, University of Essex, Colchester CO4 3SQ, U.K.

Twenty-six chondrules, chondrule fragments or clasts were analysed by microprobe. An automated wavelength dispersive instrument with a 20 μm beam integrated a series of analyses in traverses across each object. Depending on the size of the cross-sectional area, from 1 to 24 analyses were performed for each bulk analysis. Si,Ti,Al,Cr,Fe,Ni,Mn,Mg,Ca,Na,K and S were determined, and an analysed augite was used as a secondary standard before and after each set of analyses. The work is part of a study of chondrule rims, interchondrule matrix, chondrules and clasts in unequilibrated ordinary chondrites.

Only two of the twenty-six objects analysed have Ca/Al atomic ratios greater than the ordinary chondritic average of 0.74; this is true for three of nineteen chondrules analysed by McSween (1). The bulk meteorite has a normal Ca/Al ratio (from 2), so presumably a Ca-rich, Al-poor component must be present to compensate for chondrules and clasts (Fig. 1). This component is unlikely to be rim or matrix (3), but may be phosphate associated with metal or sulphide. Na/Al ratios range from 1 to almost zero, but there is no hiatus as in a suite of Manych chondrules and glasses (3). Representatives of a noritic suite of chondrules and clasts (3) are probably present in Bishunpur, but here they grade towards others with normal ordinary chondritic normative feldspar.

(1) McSween H. Y. (1977) Unpublished preprint, Center for Astrophys., Cambridge, Mass 02138.
(2) Dodd, R.T. Van Schmus, W.R. and Koffman D.M.(1967) Geochim. Cosmochim. Acta 31, p.921-951.
(3) Hutchison, R. and Bevan A.W.R. (1983) In Chondrules and their Origins Houston, lunar and Planetary Inst. p.162-179.

Fig. 1. Ca/Al (atomic) ratio vs Na_2O (wt%) and Na/Al (atomic) vs CaO (wt%) in 26 objects in Bishunpur (Analyst: R. Hutchison). The horizontal line represnts the ordinary chondritic Ca/Al ratio. Squares: bulk meteorite(3).

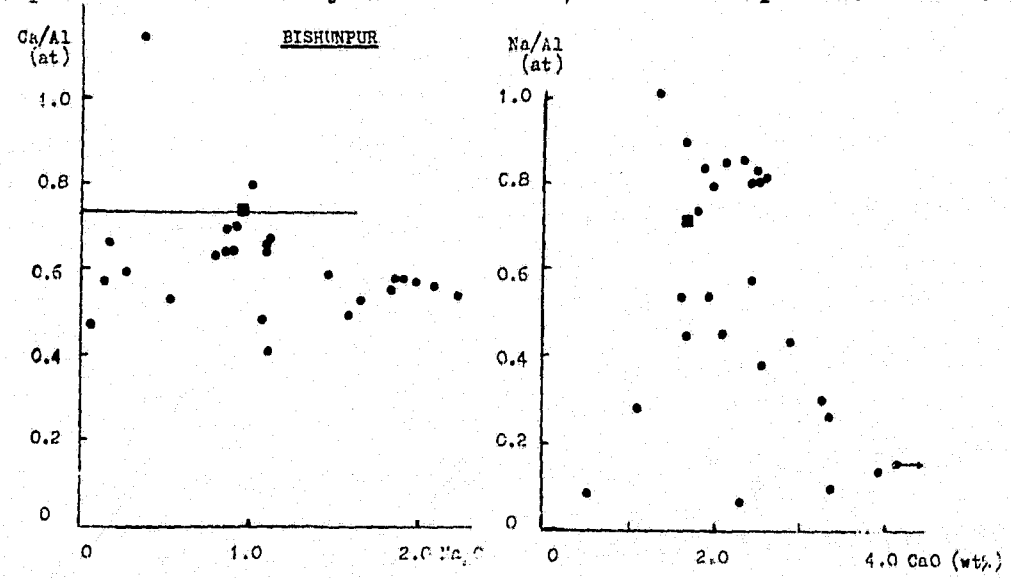

SIZE DEPENDENCE OF CHONDRULE TEXTURAL TYPES, J.N. Goswami, Physical Research Laboratory, Ahmedabad 380009, India.

Chondrule textural types were studied for size-sorted chondrules from the ordinary chondrites Dhajala (H 3-4), Weston (H4) and Chainpur (LL3) and the CM chondrite Murchison. Aliquot samples from size-sorted Dhajala chondrules were studied earlier for their oxygen isotopic composition (1). Chondrules from Weston were studied for their precompaction irradiation records using the nuclear track technique. Chondrule characterization was primarily intended for identifying any correlation that may exist between chondrule textural types and oxygen isotope or track data. Although no such correlation was found, a distinct dependence of chondrule textural type on chondrule size was evident in the data for both Dhajala and Weston chondrules. The percentage of non-porphyritic chondrules increases from $\sim$ 20 %, for chondrules in the size-range 200-800 micron, to $\sim$ 40 % for chondrules in the 100-200 micron size-range. Exclusion of metallic chondrules from the data does not alter this trend. No significant deviation was noticed in the abundance pattern of non-porphyritic chondrules within individual size fractions (200-300; 300-530 and 530-820 micron) in the 200-800 micron size interval. The abundance of non-porphyritic chondrules in this size-range is similar to those reported by Gooding and Keil (2) for chondrules (> 400 micron) in these two meteorites. To check whether the observedtrend is common to all meteorite types, we have studied size-sorted chondrules from the LL3 chondrite Chainpur and CM chondrite Murchison in the size-range 0.1-2.0 mm and 0.1-0.4 mm respectively. While there is a definite overabundance of non-porphyritic chondrules in the 100-200 micron size-fraction of Murchison chondrules, the trend is not as distinct inthe case of Chainpur chondrules. The overall data for the four meteorites seem to suggest 200 micron as the cut-off size below which radiative cooling was extremely efficient during the chondrule forming process. This offers us the possibility of using physical and chemical characteristics of small (< 200 micron) chondrules to constrain the temperature history during the chondrule formation process.

1. Clayton R.N. et al., (1983), Meteoritics 18, 282,.2
2. Gooding J.L. and Keil K., (1981), Meteoritics 16, 17.

ATMOSPHERIC HEATING OF METEORITES: RESULTS FROM NUCLEAR TRACK STUDIES. R. Jha, Physical Research Laboratory, Ahmedabad, 380 009, India.

A quantitative model has recently been proposed for estimating the degree of annealing of nuclear tracks in mineral grains subjected to a variable temperature history (1,2). Here we apply this model to study the track annealing records in different meteorites resulting from their atmospheric heating. We have measured scale lengths of complete and partial track annealing, ΔX_1 and ΔX_2 respectively, in mineral grains close to fusion crust in about a dozen meteorites (3). Values of ΔX_1 and ΔX_2 depend on extent and duration of heating during atmospheric transit and hence on meteorite entry parameters, e.g. mass, velocity and angle of entry. To estimate ΔX_1 and ΔX_2 analytically, we first obtain the temperature history during atmospheric heating at different distances from the crusted surface of the meteorite by solving heat conduction equation in conjunction with meteorite entry model (4) of Revelle (1979), and then use our annealing model (2) to evaluate the degree of annealing of tracks. In Table 1 we show that the measured values of ΔX_1 and ΔX_2 in three of the meteorites studied are consistent with analytically obtained values using pre-atmospheric mass (m_E), entry velocity (v_E) and entry angle (θ_E) of these meteorites as reported in literature.

The present work is in its initial stages with respect to modeling the annealing during ablation. With improvements, it promises to provide valuable constraints on the ablation history.

REFERENCES: (1) Goswami et al., 1983, Meteoritics 18, 304. (2) Goswami et al., 1984, Earth Planet. Sci. Lett. (in press). (3) Jha, R. and Lal, D. (in preparation). (4) Revelle, D. O., 1979, J. Atmos. Terres. Phys. 41, 453-473.

TABLE 1. Entry parameters and the estimated and measured values of ΔX_1 and ΔX_2.

Meteorite	m_E(kg)	v_E(km/s)	θ_E^o	Scale Lengths(mm)* ΔX_1	ΔX_2
Norton County	3600[a]	(16±2);14[+]	15[c]	0.8(0.8)	1.5(1.2)
Peace River	360[++]	(20±4);17[+]	15-45[d];25[+]	1.0(1.0)	0.5(0.5)
Barwell	85[e]	(<15)[e];12[+]	20±2[f]	0.7(0.7)	0.4(0.5)

[+]Adopted values. [++]Assumed m_E which gives correct terminal mass of 50 kg.
*Numbers within parentheses are measured values.

(a) Bhandari et al., 1980, Nucl. Tracks 4, 213. (b) Millman, P. M., 1969, Meteorite Research, 541. (c) Beck, C. W. and LaPaz, L., 1951, Amer. Mineral. 35, 45. (d) Folinsbee, R. E. and Bayrock, L. A., 1964, R.A.S.C. 58, 109. (e) Bagolia et al., 1978, Nucl. Tracks 2, 29. (f) Miles, H. G. and Meadows, A. J., 1966, Nature 210, 983.

NEUTRON ACTIVATION ANALYSIS OF STONEY SPHERULES FROM A MARINE SEDIMENT SAMPLE

H.T.Millard,Jr.,U.S.Geological Survey,MS424,Denver Fed.Cen.,Denver CO 80225
P.Englert,Institut fur Kernchemie der Universitat zu Koln,D5000,Koln-1(FRG)

The identification of extra-terrestrial material in samples collected at the surface of the earth is a difficult problem. Criteria were established for black magnetic spherules (Millard and Finkelman,1970 and Brownlee,1978) which involve the presence of: Fe, Ni, and Co in iron meteoritic ratios, wustite, and Fe-Ni metal. Similar reliable criteria for stoney spherules are not well established. In the present study, neutron activation analysis was performed on eight stoney spherules separated from the same marine sediment used by Millard and Finkelman(1970). Following short and long neutron irradiations, 22 elements were determined with the aid of Compton-suppression and triple-coincidence gamma counting (Millard, et al.,1984). Of these elements, Fe, Mg, Al, Ni, Cr, Co, Ir, and Sc are the best discriminators between chondritic and terrestrial compositions. Three of the spherules have compositions very close to chondrites and of these, two contain 0.5 and 0.25 ppm Ir. The other five spherules contain much less than chondritic concentrations of Ni but this element may be segregated and lost during ablation of the parent meteorite. One of these five low-Ni spherules contains 2.9 ppm Ir while the other four contain less than 0.05 ppm Ir.

Millard,H.T.,Jr. and R.B.Finkelman,1970,J.Geophys.Res. 75,2125-2134.
Brownlee,D.E.,1978,in Cosmic Dust,J.A.M.Mcdonnell,ed.,p.323-327.
Millard,H.T.,Jr.,P.Englert and U.Herpers,1984,abstract for Instrumental Multielement Analysis Conference,Julich.

OXYGEN ISOTOPES IN DEEP SEA SPHERULES. Toshiko K. Mayeda and Robert N. Clayton, University of Chicago, Chicago, IL 60637, and Donald E. Brownlee, University of Washington, Seattle, WA 98195.

It is important to determine the genetic relationships between the dust and small particles in the solar system on the one hand, and the meteorites and larger bodies on the other. Oxygen isotopes have proved useful in identifying such relationships between one meteorite group and another. Of the various samples of sub-millimeter extraterrestrial particles available for laboratory study, only the deep-sea spherules (Brownlee, 1981) are abundant enough for precise oxygen isotope analysis using existing techniques. Preliminary results were presented by Mayeda et al. (1983). Complications arise in interpretation of the isotopic data, since these particles have been melted during passage through the Earth's atmosphere, and have been in contact with seawater for prolonged periods. We use a comparison between spherules that were originally silicates and those that were originally metallic to deduce their pre-terrestrial isotopic compositions.

The type I spherules, which enter the atmosphere as metallic particles, contain only atmospheric oxygen. The type S spherules contain a mixture of atmospheric oxygen and their original extraterrestrial oxygen. The measured isotopic compositions of seven size-sorted composite samples (containing 40 to >500 individual spherules) define a mixing line on the oxygen three-isotope graph with the equation: $\delta^{17}O = 0.603\delta^{18}O - 4.07$. This line intersects the terrestrial fractionation line at $\delta^{18}O = +47.3‰$, $\delta^{17}O = +24.6‰$, which also corresponds to the measured composition of the largest-sized type I spherules. This oxygen is much heavier than that of the troposphere ($\delta^{18}O = 23.6$, $\delta^{17}O = 12.3$) or that of the fusion crust of macro-meteorites ($\delta^{18}O = 15.0$, $\delta^{17}O = 7.6$ for Treysa). It is likely that the Earth's mesosphere is strongly enriched in heavy isotopes of oxygen at altitudes near 90 km at which the iron particles were oxidized. Fractionation due to the combined diffusion of O atoms and O_2 molecules may be responsible.

Type S spherules have isotopic compositions which do not correspond to any known meteorite ($\delta^{18}O$ 22 to 25, $\delta^{17}O$ 9.5 to 11). From their Fe^{3+} content, it can be calculated that at least 10% of their oxygen is of atmospheric origin. If the mixing line is extrapolated until it reaches the composition of known meteorites, the only candidates for the extraterrestrial end-member are C3 chondrites or the anhydrous component of C2 chondrites. Ordinary chondrites and C1 and C2 phyllosilicates are ruled out. The observed isotopic compositions of S-type spherules can be made by a 50:50 mixture of C3 oxygen and mesospheric oxygen.

References: D. E. Brownlee (1981) in The Sea, vol. 7, p. 733-762.

T. K. Mayeda, R. N. Clayton, and D. E. Brownlee (1983) Meteoritics, 18, 349-350.

C-4 N85 15610

MINOR ELEMENTS IN RELICT OLIVINE GRAINS OF DEEP-SEA SPHERES: MATCH WITH MG-RICH OLIVINES FROM C2 METEORITES; J.V. Smith, I.M. Steele, Geophysical Sciences, University of Chicago, Chicago, IL 60637, and D.E. Brownlee, Astronomy, FM20, University of Washington, Seattle, WA 98195.

The bulk composition and relict minerals of meteoroid ablation spheres from deep-sea sediments (1) should be relatable to the parental material, and indeed bulk compositions and elemental ratios favor a CI/CM affinity for most spheres (2). Although largely melted, some Deep Sea Spheres (DSS) have retained rare grains (mainly olivine and pyroxene) apparently unmodified chemically by ablation heating or seawater alteration. We made high-precision electron microprobe analyses of minor elements in relict olivines for comparison with compositions of olivines in known meteorites [Belgica, C2 (3); Murchison, C2, and Allende, C3, (4); achondrites (5); Bells, C2 (6)].

All relict olivines are very Mg-rich ($Fo_{99.5-98}$; FeO 0.5-2 wt.%) with a characteristic pattern of minor elements: (a) MnO ranges from 0.0 to 0.3 wt.% with a near-linear positive correlation with FeO, (b) CaO ranges from 0.4 to 0.05 wt.%, with a weak nonlinear correlation with FeO; (c) Cr (wt.% metal; unknown oxidation state) ranges from 0.1 to 0.4 wt.% with a weak positive correlation with FeO; (d) TiO_2 ranges from 0 to 450 ppmw with a weak negative correlation with FeO; (e) Al_2O_3 ranges from 100-1500 ppmw.

No terrestrial olivines can match all these chemical features, thus reinforcing other evidence for an extraterrestrial origin. There is no match with achondritic olivines (5). Mg-rich olivines occur in all types of carbonaceous meteorites, but the minor elements of most DSS olivines do not match with those for Allende (C3) olivines, and fit poorly with those of Murchison (C2) olivines. There is a good fit for Fe and Cr with those of the olivines in the unusual Belgica 7904 (C2) meteorite (3).

Final interpretation must await a thorough examination of olivines in a range of C2 meteorites. However, it seems likely that the relict olivines of at least many deep-sea spheres are chemically related to olivines in at least one C2 meteorite. Further study is needed of deep-sea spheres to determine whether other types of meteoritic olivine can be matched by relict olivines. NASA NAG 9-47 and NSG 9052.

1. Blanchard, M.B., Brownlee, D.E., Bunch, T.E., Hodge, P.W., and Kyte, F.T. (1980) EPSL 46, 178. 2. Bates, R.A. and Brownlee, D.E. (1984) Lunar Planetary Sci. XV, 40. 3. Steele, I.M., Cox, R.T. Jr., and Smith, J.V. (1984) Lunar Planetary Sci XV, 820. 4. Steele, I.M., Skirius, C.M., and Smith, J.V. (1984), abstract for this meeting. 5. Smith, J.V., Steele, I. M. and Leitch, C.A. (1983) Proc. Lunar Planet Sci Conf 14th, in JGR 88 Suppl, B229. 6. Davis, A.M. and Olsen E. (1984) Lunar Planetary Sci XV, 190.

PLATINUM GROUP NUGGETS IN DEEP SEA SEDIMENTS

D.E. Brownlee, B.A. Bates, and M.M. Wheelock, Dept. of Astronomy, Univ. of Washington

The existence of "iron" meteor ablation spheres in deep sea sediments has been known for over a century. These spheres have generally been believed to be composed either of pure magnetite and wustite or an oxide shell surrounding a NiFe metal core, usually smaller than half the size of the sphere. In a study of a large number of 300μm-600μm spheres we found that the "pure oxide spheres", the most common in sediments, usually contain a solitary <10μm platinum group nugget (PGN) composed almost entirely of group VIII noble metals. A PGN is never found in a sphere that contains a NiFe core. The amount of Pt group elements in the nuggets is consistent with formation by concentration of all noble metals from a chondritic metal particle the size of the host sphere. We believe that this concentration by a factor of 10^5 occurs by nearly total oxidation of molten meteoritic metal where the noble metals survive as the only metallic phase. The possibility that the PGNs are relict grains is not likely because, while they are very common in iron spheres, they have not been observed in stony (chondritic composition) spheres. Twelve PGNs were analyzed and most had chondritic abundances with some depletions taht correlate with element volatility. Seven of the PGNs have chondritic abundances of Os, Ir, Ru, Pt and Rh. One of these also has a chondritic abundance for Pd but for the others Pd is depleted, presumably because of its comparatively high volatility. Three nuggets have a chondritic Os/IR ratio, but large depletions in the other more volatile elements. The most extreme case is a PGN composed of 41 wt% Os, 35% Ir, and 15% Ru. All of the other noble metals are depleted by more than a factor of 10. One unusual nugget has Ru, Pt and Rh abundances 2-3 times chondritic, indicating origin from a nonchondritic source, possibly a IIIAB iron.

PGN formation by oxidation of a molten metal sphere entering the atmosphere cannot occur if the oxygen abundance in the atmosphere is less than half of its present value. The first appearance of PGNs in the geological record should mark when, in the Earth's history, oxygen rose to this level.

C-6 N85 15612

PECULIAR SPHERULES FROM ANTARCTICA AND THEIR ORIGIN;
Yuji Tazawa(1) and Yoshiyuki Fujii(2), Department of Physics, Kyoto University, Kyoto 606(1), National Institute of Polar Research, Tokyo 173(2).

Previously(1,2), it had been obtained that two calcium-titanium-oxide (perovskite-like) spherules (CTS) and an iron-chromium-nickel-oxide one (FCN) from a segment (ranged between 32m and 33.5m in depth) of an ice-core collected at Mizuho Station, East Antarctica (70°42'S, 44°20'E)(3). They showed an anomalous REE abundance pattern enriched in Sm by a factor of about 10 relative to the typical pattern of terrestrial perovskites(4,5).

Subsequently, more than forty spherules from ten other depth ranges of the ice-core have been analyzed by means of INAA, SEM/EDS, XDP, etc., and curious results have been obtained: (a) Both CTS and FCN occur in every depth range. (b) CTS, FCN and others are in the ratio about 2:2:1 among all the analyzed spherules. (c) All of CTS show the same chemical and mineralogical characteristics as those previously obtained. (d) It is not a few case that CTS contains some amounts of Cr and Fe, and/or FCN contains Ca and Ti. (e) There are two composite particles among all the spherules, the one is two small CTS stick onto a large zircon ($ZrSiO_4$) spherule, and the other is a large FCN and a small CTS stick together.

These results seem to be strongly implying that CTS and FCN had originated in a common natural material and from a common natural process.

When, where, and what kinds of material and process had these strange spherules formed, and how had they been brought and stored in the Mizuho ice-core? We examine several likelier candidates for this subject on their aptitudes.

References:

(1) Tazawa Y. and Fujii Y. (1983) Proc. 5th Symp. Polar Meteorol. Glaciol., in Mem. Natl. Inst. Polar Res. Spec. Issue, 29, p.220.(abstract)
(2) Tazawa Y. and Fujii Y. (1984)(to be submit)
(3) Suzuki Y. and Takizawa T. (1978) Mem. Natl. Inst. Polar Res. Spec. Issue, 10, p.1-24.
(4) Eby G.N. (1975) Geochim. Cosmochim. Acta, 39, p.597-620.
(5) Onuma N., Ninomiya S. and Nagasawa H. (1981) Geochemical Journal, 15, p.221-228.

FRACTIONATION OF SIDEROPHILES IN COSMIC SPHERULES AND ITS IMPLICATIONS.

J.Czajkowski, Univ. of Calif.,San Diego, Dept.of Chem.,B-017,La Jolla,CA 92093,
P.Englert,Institut für Kernchemie der Universität zu Köln, D5000 Köln 1, FRG.

Fractionation of siderophiles bewtween metal and silicate phases at different oxygen fugacities has been extensively studied(1). Such data could be applied to a study of fractionation during formation of stony or iron spherules. However there also exists another kind of fractionation which takes place within the spherules as they are molten and oxidized in the Earth's atmosphere. During this process two phases develop,one oxidized,the other not. Unoxidized phase is the globule described as to its shape and high Fe and Ni contents as far back as '64(2),and as recently as '83(3).The process of atmospheric melting is dependent on many factors,one of them being the density of atmosphere(3).It may be safe to assume that the density profile of atmosphere has remained constant with time, whereas its composition has not.Thus in the Pre-Cambrian when the atmosphere is believed to have been reducing,the infalling materials might have been melting at the same altitude as the contemporary ones but at different oxidizing conditions.In consequence,spherules formed then might be unoxidized,and contain no globules.Based on fractionation of siderophiles between the globule and the oxidized matrix, in principle it should be possible to tell something about the oxygen content of the atmosphere with time.Previous analytical work dealing with sectioning of spherules(4) has demonstrated uneven distributions of siderophiles between parts of the same spherule which would be expected if indeed the analyzed spherules contained different phases, one being the metal globule. This study has also been initiated in order to make quantitative explanations (e.g.3&5), of depletions or absence of siderophiles in spherules.Thus two questions were posed: how much of the siderophiles are lost with globule,and can the measured fractionation be used in any way to estimate oxygen content of the atmosphere with time. In attempt to answer the first question and shed some light on the other, the following experiment has been done. Eighteen iron spherules were taken from Millard collection, SEM photographed,weighed,and then gently crushed.Three largest pieces of crushed magnetite matrix were selected, weighed, and analyzed for Ir, Au, Fe, Co, and Ni using INAA. Similarly isolated globules were photographed, weighed and analyzed.To minimize losses special irradiation holders were developed,similar in concept to the one used by(5).The holders consisted of two 1x10x20 mm quartz plates, one having 24 holes drilled into it, the other serving as a cover. To hold the plates together special clamps were made out of Al with a capacity of 2 sets of plates per clamp.Into each plate samples and 3 Fe-meteorite (Carbo) standards were loaded. Carbo was previously homogenized on a gram size basis in a RF oven. Small flakes were cut off with a steel blade and weighed as the rest of samples on an ultramicrobalance. Larger samples (>2µg) were irradiated at a flux= ~7*10^13n/cm^2sec for ~48hrs, and the smaller ones at a similar flux for~113hrs.After decay of ~3-5 days samples were transferred to clean vials and counted using Ge(Li) detectors. Exemplary calculation for a globule gives: 152±9ppm Ir,94±8% Ni,14±1% Fe,and 0.57±0.03% Co,and for one complementary matrix fragment:5.9±0.4% Ni,71±4% Fe,0.37±0.01% Co,(Ir undetected), which translates to a fractionation (globule/matrix) of >150 for Ir, 16 Ni, 0.2 Fe, and 1.5 for Co.

Acknowledgements.We wish to thank: Mr.R.Berndt and Ms.V.Zschau for their contribution to this project,(both at the University of Cologne, FRG).

(1).Rammensee,W.,H.Palme,H.Wanke,Lunar Planet. Sci. XIV(1983)628.(abstract)
(2).Fechtig,H.,K.Utech,Ann.New York Acad.Sci.119(1964)243-49.
(3).Brownlee,D.E.,B.Bates,R.H.Beauchamp,in Chondrules and their Origins(1983)10.
(4).Czajkowski,J.,P.A.Farnsworth, Meteoritics 18(1983)287.(abstract)
(5).Ganapathy,R. and D.E.Brownlee, Science 206(1979)1075-77.

C-8

N85 15614

THE INFLUENCE OF GRAVITATIONAL BODY FORCE IN METEORITIC CHONDRULE AND LUNAR GLASS FORMATION

P.Z. Budka, Dept. of Mechanical Engineering, Union College, Schenectady, New York 12308.

The effects of gravitational body force must be considered in the formation of extraterrestrial materials such as meteoritic chondrules and lunar glasses. Solidification experiments conducted in microgravity as well as at g values greater than earth's gravitational force have demonstrated that gravitational force can have profound and sometimes unexpected effects upon the way materials solidify and, therefore, upon their physical and mechanical properties. Solutal, thermal and sedimentation effects differ from those experienced on earth. Because buoyancy forces are reduced, materials of different densities may remain in close proximity.

The spherical morphology of chondrules and many lunar glasses may reflect the tendency for free-floating liquids to form spherical droplets in a microgravity environment, a form which minimizes surface energy. Under these conditions, surface energy forces dominate gravity forces. The formation of two common chondrule textures, barred and radiating chondrules, can be explained using observations from glass science. Similar textures occur in silicate melts. For example, barium disilicate spherulites (similar to radiating chondrules) may break up into a lathlike (barred) structure upon aging. Nucleating agents, such as P_2O_5, present during chondrule formation, may determine whether local solidification occurs as glass, crystal, or a mixture of the two.

The inhomogeneity of lunar glasses can be compared with the lack of mixing observed during Skylab fluid mechanics experiments. In microgravity, droplets of different compositions may meet and coalesce, but mixing does not occur immediately. Many lunar glasses solidified before diffusion could homogenize the composition.

The Materials Processing in Space Program has demonstrated that gravitational force can have a significant and complex influence on solidification. Given the wide variety of cosmic bodies and the complexity of cosmic processes still being discovered, there is no reason to assume that extraterrestrial materials have experienced the same gravitational force that exists on earth.

EVOLUTIONARY HISTORY OF CI AND CM CHONDRITES

J.F.Kerridge, Institute of Geophysics, UCLA, Los Angeles, Ca 90024, and
J.D.Macdougall, Scripps Institution of Oceanography, UCSD, La Jolla, Ca 92093

It is now clear that several different processes have acted upon various components of carbonaceous chondrites, and that at least some of those processes occurred very early in solar system history. Because these meteorites are breccias, petrographic relationships are seldom informative about the order in which those processes took place. Nonetheless, information about such an evolutionary sequence would be of potential value in defining the nature of the source region for these meteorites, so we report here an initial attempt at establishing the course of events during evolution of CI and CM chondrites.

Implantation of solar wind-derived noble gases into CI magnetite [1] apparently postdated the period of aqueous activity believed to have been responsible for magnetite production [2]. The actual time of that mineralisation event may be constrained by $^{129}I/^{127}I$ of the magnetite [3] and $^{87}Sr/^{86}Sr$ of the, apparently contemporaneous, carbonates [4]. Carbonate crystallisation roughly coincided with one or more episodes of impact-driven brecciation [5].

Track distributions in some CM chondrules show that one or more chondrule-forming events predated an epoch of solar flare irradiation [6]. Isolated olivines in CI and CM chondrites presumably acquired their solar flare-track records during the same epoch [6]. If those olivines originated in chondrules [7], at least some of them were liberated from their parental chondrules prior to the irradiation [6]. If they did not originate in chondrules [8], and even possibly if they did, a secondary metasomatic event intervened between crystallisation of the olivines and their irradiation [9] which, at least for CI olivines, presumably coincided with the solar wind irradiation of magnetite, discussed above. Compaction of CI and CM olivines into the matrix apparently took place 4.2 to 4.4 Gy ago [10,11].

[1] Jeffery P.M. & Anders E. (1970) Geochim.Cosmochim.Acta 34,1175-1198.
[2] Kerridge J.F., Mackay A.L. & Boynton W.V. (1979) Science 205,395-397.
[3] Lewis R.S. & Anders E. (1975) Proc.Nat.Acad.Sci.USA 72,268-273.
[4] Macdougall J.D., Lugmair G.W. & Kerridge J.F. (1984) Nature 307,249-251.
[5] Richardson S.M. (1978) Meteoritics 13,141-159.
[6] Goswami J.N. & Macdougall J.D. (1983) J.Geophys.Res. 88,A755-A764.
[7] Richardson S.M. & McSween H.Y. (1978) Earth Plan.Sci.Lett. 37,485-491.
[8] Olsen E. & Grossman L. (1978) Earth Plan.Sci.Lett. 41,111-127.
[9] Kerridge J.F. & Macdougall J.D. (1976) Earth Plan.Sci.Lett. 29,341-348.
[10] Macdougall J.D. & Kothari B.K. (1976) Earth Plan.Sci.Lett. 33,36-44.
[11] Macdougall J.D. (1977) Meteoritics 12,301-302.

MAGNETITE IN THE ESSEBI AND HARIPURA CM CHONDRITES; M. W. Rowe and M. Hyman, Department of Chemistry, Texas A&M University, College Station, Texas 77843, and E. B. Ledger, Department of Geology, Stephen F. Austin State University, Nacogdoches, Texas 75962.

The unusual microscopic magnetite morphologies previously thought to occur only in the CI chondrites were recently reported in two CM chondrites as well — Essebi and Haripura. These include: grainy spheroids, probably spherulites, found both singly and in groups of up to a dozen and ranging in size from ∿4-10 μm in diameter; collections of microcrystals varying from ∿0.3 to 6 μm in diameter; layered, nearly circular plates forming a spheroidal plaquette ∿7.5 μm in diameter; clusters of variable sized nodules ∿0.3 to 6 μm, with concave features; framboidal magnetite; and finally collections of less distinct globules. All of these forms were sent <u>in situ</u> in small multiple pieces, ∿1-5 mg each. No pre-treatment or processing was done except that the samples were coated with ∿50 Å of Au-Pd to prevent charge build-up during electron microscopy.

In this presentation, we will discuss electron microprobe analysis of some of these features and the surrounding materials. The results will be discussed with regard to the possible chemical precursors for magnetite production in carbonaceous chondrites.

HYDROTHERMAL ALTERATION OF CM CARBONACEOUS CHONDRITES; IMPLICATIONS OF THE IDENTIFICATION OF TOCHILINITE AS ONE TYPE OF METEORITIC PCP

Michael E. Zolensky, SN4, NASA Johnson Space Center, Houston, TX. 77058.

Poorly characterized phases (PCP's) constitute up to 30 volume percent of some CM carbonaceous chondrites [1], and are therefore an important key to an understanding of the physico-chemical conditions attending matrix evolution. An iron-rich form of the terrestrial phase tochilinite has recently been identified as a common type of PCP [2]. Tochilinite has the general formula $6Fe_{0.9}S \cdot 5(Mg,Fe)(OH)_2$ and consists of alternating mackinawite (FeS) and brucite ($(Mg,Fe)(OH)_2$) sheets, with iron vacancies in the sulfide sheets. In iron-rich tochilinite, ferrous hydroxide, called amakinite, replaces brucite.

On earth the occurrence of tochilinite is limited to hydrothermally altered ultramafic rocks, where it mantles sulfide grains and fills cavities in serpentine [3]. The mineral associations of PCP in CM carbonaceous chondrites [1] is essentially identical to those for tochilinite in terrestrial rocks [2]. Assuming that the similarity of these parageneses in both terrestrial and meteoritic materials is not simply fortuitous, we may make some comments regarding the nature of the hydrothermal fluids responsible for the alteration of CM carbonaceous chondrite matrix material. As little is presently known regarding the stability of tochilinite this will be an indirect process.

Brucite forms from the breakdown of forsterite, as can be illustrated by the reaction: forsterite = brucite + chrysotile ± magnetite. Various studies have placed the temperature of this reaction at 350 to 450°C, in the pressure range below 20 kbars [4]. At the oxygen fugacities defined by the iron/magnetite or iron/awaruite (Ni_2Fe) buffers, the iron content of brucite indicates the temperature of the above reaction below the stability curve. The assemblage magnetite + brucite forms at the expense of amakinite (iron-rich brucite) at the high temperature end of the brucite stability field, with amakinite forming as temperature decreases, probably according to the reaction: $3Fe(OH)_2 = Fe_3O_4 + 2H_2O + H_2$ [4]. At oxygen fugacities higher than the iron/magnetite or iron/awaruite buffers, with temperature and pressure being constant, magnetite forms at the expense of amakinite. Therefore amakinite is most stable at temperatures well below 350°C, and at low fO_2. The pH of solutions in equilibrium with brucite-containing serpentinites is generally 10 to 12, in the temperature range 10 to 330°C, and the pressure range 1 to 1500 bars [4,5].

In altered ultramafic bodies mackinawite can form by the breakdown of pyrrhotite under coditions of decreasing temperature (below 170°C) and increasing sulfur fugacity [6]. Mackinawite also forms as the first corrosion product of iron at low temperatures in H_2S saturated solutions [7]. Both pyrrhotite and iron metal are reported from CM carbonaceous chondrite matrices, with the former being far more common.

In summary, if CM carbonaceous chondrites have undergone hydrothermal alteration, iron-rich tochilinite, at least, probably grew from aqueous solutions characterized by low fO_2, high fS_2, pH 10 to 12, and at a temperature at or below 170°C.

References: 1. Bunch, T.E. and Chang, S., GCA, 44, 1543-1577, 1980; 2. Mackinnon, I.D.R. and Zolensky, M.E., Nature, in press; 3. Jambor, J.L., Geol. Surv. Can., Paper 76-1B, 1976; 4. Moody, J.B., Lithos, 9, 125-138, 1976; 5. Barnes, I., et al., Contr. Mineral. Petrol., 35, 263-276, 1972; 6. Zoka, H., et al., J. Sci. Hiroshima Univ., 7, 37-53, 1973; 7. Shoesmith, D.W., et al., J. Electrochem. Soc., 127, 1007-1015, 1980.

AQUEOUS ALTERATION ON METEORITE PARENT BODIES: POSSIBLE ROLE OF "UNFROZEN" WATER AND THE ANTARCTIC METEORITE ANALOGY. J. L. Gooding, Planetary Materials Branch, NASA/Johnson Space Center, Houston, TX 77058.

Clayton and Mayeda (1) made a stimulating argument, based on oxygen isotopy, that alteration of CM2 chondrites occurred at or near 0 C (273 K). Such a scenario can be understood if C-chondrite parent bodies evolved as rock/ice mixtures that contained "unfrozen" (mobile or "quasi-liquid" below 273 K) pore water, a well-known phenomenon in cold-region soils on Earth (2). The importance of unfrozen-water diagenesis in C-chondrite history can be tested by a combined program of experimental simulations and petrologic study of analogous features developed by weathering of meteorites in or on Antarctic ice (3). In each of several experiments, an homogenized mineral (or rock) powder was mixed with distilled water and the resulting slurry cooled at 5 K/min to 200 K under flow of carbon dioxide in a differential scanning calorimeter. During subsequent heating, the dynamic melting interval of ice was determined from the corresponding endoenthalpic peak. As expected, formation of unfrozen water was found to depend on substrate mineralogy, with phyllosilicates producing the most profound effects (Fig. 1). However, unfrozen water also formed in slurries of the CV3 chondrite Allende, suggesting that unfrozen water could have been important even in rock/ice bodies involving mostly anhydrous igneous substrates although traces of carbonaceous matter might have further enhanced the effect. Conceivably, slow diagenetic production of trace phyllosilicates and salts by the initial unfrozen water component might have started a positive-feedback loop that would have facilitated continued aqueous alteration until either diagenetic "equilibrium" was attained or the environment was disrupted. Even so, quantitative application of these ideas will require identification of the temperature/composition/pore-structure combinations that would nurture thermodynamically "liquid" layers capable of leaching primary minerals and precipitating secondary minerals to the extent found in C-chondrites. As possible sources of mechanism and rate information, interesting analog cases among Antarctic meteorites include PCA82500, a badly corroded C4(?) chondrite, and ALH82102, an H chondrite that was found solidly frozen in glacial ice but which was still substantially oxidized throughout.

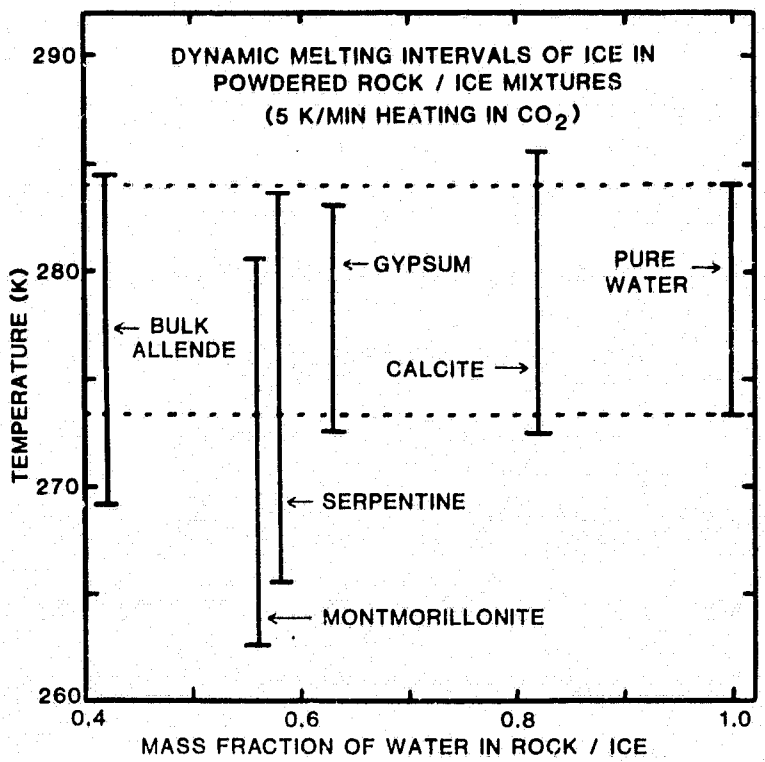

References: (1) R. N. Clayton and T. K. Mayeda (1984) Earth Planet. Sci. Lett., 67, 151. (2) D. M. Anderson (1966) Soil Sci. Soc. Amer. Proc., 30, 670. (3) J. L. Gooding (1984) Lunar Planet. Sci. XV, 308, LPI, Houston.

AN SEM STUDY OF PRETERRESTRIAL ALTERATION EFFECTS IN ALHA 77003. R. M. Housley, Rockwell International Science Center, Thousand Oaks, CA 91360.

All unequilibrated meteorites which we have examined in our on-going SEM studies show abundant evidence of alteration of chondrule minerals and fragments to fine grained material resembling some components of the matrices. In Bishunpur L3, Semarkona LL3, and Vigarano CV3 the matrices themselves are very complex and highly variable in both composition and texture. In them glass near the edges of some chondrules has altered to a texture and composition indistinguishable from the adjacent matrix. If glass of variable composition was initially much more abundant it seems reasonable that a large fraction of these matrices could have formed from its alteration. There are no evident criteria that suggest that any component of these matrices be identified as a primative nebular condensate.

In the Allende CV3 meteorite the matrix is fairly uniform and dominated by iron-rich olivine. We have found compelling evidence [1] that this matrix has been largely produced from previously more abundant clinoenstatite and iron metal by a reaction such as

$$Fe + \tfrac{1}{2}\, O_2 + Mg\, Si\, O_3 \rightarrow [Mg,Fe]_2\, SiO_4. \qquad (1)$$

For this to work there must be an efficient mechanism for transporting the iron. Allende chondrules contain many spherical cavities partly filled with chromite and peniandite crystals providing evidence the iron indeed was oxidized and transported although the mechanism remains unknown.

ALHA77003 resembles Allende in several ways. The matrix is dominated by iron-rich olivine and chondrules frequently contain spherical cavities with chromite crystals. Pyroxenes generally show evidence that reaction (1) has taken place to a limited extent around their edges and along internal fractures.

However, here the similarity ends. ALHA77003 is much less oxidized than Allende and contains a considerably smaller fraction of matrix. It contains abundant low nickel kamacite and clinoenstatite, frequently in direct contact. Clearly not enough oxygen was available for reaction (1) to proceed.

On the other hand every forsteritic olivine crystal except some in the centers of chondrules, has been altered to iron-rich olivine along all borders and internal fractures. Occasionally fine-grained porous textures resembling the matrix have developed. The coexisting pyroxenes, feldspars and in some cases glassy mesostaces seem to have been little affected.

It seems natural to infer that significant alteration took place in an environment that was not oxidizing but which provided for efficient iron and magnesium transport.

[1] Housley, R. M. and Cirlin, E. H. (1983) On the alteration of Allende chondrules and the formation of matrix. Proc. Conf. Chondrules and Their Origins, p. 145-161.

UNEXPLAINED FE, NI AND S ANOMALIES IN CV CHONDRITE COMPONENTS;
D. A. Wark, Lunar and Planetary Lab., Univ. of Arizona, Tucson, 85721.

Large negative anomalies in Fe, Co, Ni, S and Se are present in Allende Type B Ca-Al-rich inclusions (CAI's), as shown in Fig. 1. Similar plots (not shown here), based on compilations of all the known published analyses, indicate that Allende chondrules, aggregates and other types of CAI's also display these anomalies [1].

These observations show that: (1) Since Fe, Co, Ni, S and Se are more depleted than elements bracketing them in volatility (such as Pt and Au, and Sn and Cd), the anomalies were not produced during the volatility-dependent, high temperature CAI-forming processes. (2) Since Pt, Au, Ge and other siderophiles are not as depleted as Fe, Co and Ni, the anomalies are not due to a metal/silicate fractionation. (3) The association of Fe, Co, and Ni anomalies with S and Se anomalies suggests that the anomalies are due to the removal of FeNi sulfide. (4) Since these anomalies occur in all types of Allende inclusions, aggregates and chondrules, the Allende parental material must have undergone sulfide loss before the formation of these components.

For reasons presented in [1,2], it is argued that primordial sulfide-rich grains (plus some silicate and metal grains) clumped together and were gravitationally removed as a part of the protosolar nebula first heated up. Continued heating of the sulfide-depleted dust then gave rise to the CAI's, aggregates and chondrules of CV chondrites. The composition of the removed sulfide-rich dust (calculated [3] by subtracting the compositions of Allende components from primordial CI matter) is very similar to that of the EH chondrites, suggesting a complementary relationship between CV and EH chondrites. Other recent evidence also supports this possibility: - (a) Volatilization of sulfide-rich, silicate- (and oxygen-) poor dust would create a highly reducing environment favorable to E chondrite formation [4]; (b) the Qingzhen E3 chondrite contains some fragments formed in an oxidized (and presumably adjacent) region [5]; and (c) peculiar CCFXe and isotopically light N components are found only in the C and E chondrites [6].

References: [1] Wark (1984), Ph.D. thesis, Melbourne Univ. [2] Wark (1983), LPS XIV, 820-821 and 824-825. [3] Wark (1984), Submitted to GCA. [4] Larimer and Bartholomay (1983), LPS XIV, 423; Rubin (1984), EPSL (in press). [5] Housley et al. (1983) Meteoritics 18, 317-318; Rambaldi et al. (1984) LPS XV, 661-662. [6] Hertogen et al. (1983) GCA 47, 2241-2255.

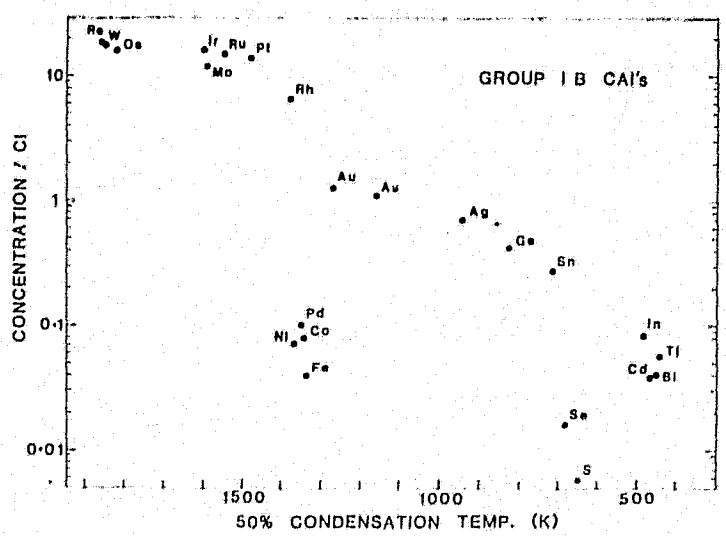

MINOR ELEMENTS AND CATHODOLUMINESCENCE OF MG-RICH OLIVINES FROM MURCHISON AND ALLENDE CARBONACEOUS METEORITES; I.M. Steele, C.M. Skirius, J. V. Smith, Geophysical Sciences, University of Chicago, Chicago, IL 60637.

The morphology and inclusions of individual Mg-rich olivine grains from C2 chondrites provide disputed evidence for origin either from a liquid or a vapor (1-5). We examined olivine grains from Murchison (C2) and Allende (C3) meteorites, to extend data (6) on Belgica 7904 (C2). Cathodoluminescence revealed the relation of chemical zoning to external shape and inclusions. High precision electron-probe analyses of selected spots for Na, Al, P, Ca, Ti, Cr and Mn provided chemical constraints on the source material.

Cathodoluminescence. Most Mg-rich olivines in both Murchison and Allende show outward zoning from a blue core to a red or dark rim. Variations include: lack of dark rim; dark core and blue rim; no blue core. A blue core is generally euhedral with extremely sharp boundaries, but some boundaries are gradational. Most blue regions lack silicate, metal and glass inclusions, whereas red regions generally contain inclusions. Each red or dark rim is continuous, but its width may vary. Channels and networks through blue regions are filled with red or dark olivine, or another type of blue. Although most zoned grains are isolated in matrix, doublets are common, and porphyritic aggregates may surround a near-central blue grain.

Chemical Features. Step scans were made radially across blue-red/black boundaries, in addition to many point analyses. Precision for minor elements is 50-100 ppmw (2σ); any fluorescence error is small, and does not affect conclusions. Data for Allende are superior to those from Murchison because of larger number and size of grains. Approximate ranges are:

		Allende		Murchison	
		blue	red	blue	red
Mg/(Mg + Fe)	mol %	99.5	<99.5	99.6	<99.5
Al_2O_3	wt.%	0.4-0.5	<0.1	0.15	<0.15
CaO	wt.%	0.45-0.75	<0.15	0.25-0.7	<0.2
TiO_2	ppmw	400-1000	100-200	>150	<150
Cr_2O_3	wt.%	0.1-0.15	>0.15	0.2	>0.2
MnO	ppmw	<150	>150	<100	>100

The unusually high Al, Ti and Ca of the blue cores suggest crystallization at high temperature (cf. 7,8) from a source enriched in refractory elements (V is also detected). The lower values in the rim suggest crystallization from an unenriched source. The sharp chemical discontinuity rules out extensive diffusion and prolonged metamorphism.

Proposed explanation. From several possible explanations we tentatively suggest at least two stages: (a) growth of the blue core from a vapor enriched in refractory elements (hence lack of inclusions); (b) growth of red/dark rim from an unenriched liquid which entrapped the blue core. Mechanical transfer may be involved. The channels and networks are puzzling at this time. Whatever the true explanation, a complex history is needed for a simple mineral, and further study should provide additional restraints on formation of carbonaceous meteorites. NASA NAG 9-47. 1. Desnoyers C. (1980) EPSL 47, 223. 2. McSween, H.Y. Jr. (1977) GCA 41, 411. 3. Olsen E., Grossman L. (1978) EPSL 41, 111. 4. Richardson, S.M., McSween, H.Y. Jr. (1978) EPSL 37, 485. 5. Roedder, E. (1981) Bull. Min. 104, 339. 6. Steele, I.M., Cox, R.T. Jr., Smith, J.V. (1984) Lunar Planet Sc. XV, 820. 7.Simkin, T., Smith J.V. (1970) J. Geol. 78, 304. 8. Dawson, J.B., Hervig, R.L., Smith, J.V.(1981) Fortschr. Min. 59, 303.

N85 15620

STRAIN ANALYSIS OF THE LEOVILLE CHONDRITE AND CONDITIONS IN ASTEROIDAL INTERIORS. Parham M. Cain and Harry Y. McSween, Jr., Department of Geological Sciences, University of Tennessee, Knoxville, TN 37996.

Deformed chondrules in the Leoville carbonaceous chondrite define a preferred orientation (1), also recognized previously in other CV3 chondrites (2). Strain analysis of Leoville by the method of (3) indicates an apparent strain ellipse axial ratio for the whole rock of 2.0:1, whereas the technique of (4) gives an axial ratio of 1.9:1 for the chondrules only. Total uniaxial shortening of Leoville falls in the range of 28-34%. We consider this to be the result of compaction due to overburden.

Identifying the strain mechanism is necessary for understanding the conditions which caused this compressional shortening. Very little is known about strain mechanisms in chondrites. Luckily, the major mineralogical constituent of CV3 meteorites is olivine, for which experimental data on strain mechanisms exist. The conditions that caused strain in the olivine were obviously applicable to the whole meteorite. Possible mechanisms of olivine deformation are cataclasis, low-temperature plasticity, power-law creep, and diffusional flow, each of which occurs under different combinations of temperature and deviatoric stress (5) (refer to figure). Cataclasis can be ruled out on the basis of its high deviatoric stress requirement; some fractures occur in chondrule olivines, but these may have formed during excavation or impact. Low-temperature plasticity and power-law creep occur by means of various types of lattice dislocations. However, methods of thermal decoration (6) and chemical etching (7) of dislocations failed to indicate evidence for either mechanism. Thus, the inference is that diffusional flow, characteristic of low- to moderately high-temperatures and low deviatoric stress, was the major deformation mechanism.

The calculated deviatoric stresses at the centers of typical asteroidal bodies of 150-300 km radii are less than 0.86 kb. These values are appropriate for diffusional flow in olivine at less than 1000°C. At reasonable geologic strain rates (8), the apparent uniaxial shortening in Leoville would require on the order of 10^5 - 10^7 years for development. However, diffusional flow in olivine at these strain rates necessitates temperatures of ∿ 700-1000°C (see figure), significantly higher than those previously accepted for CV3 chondrites. Thermal constraints from mineralogic, isotopic, and magnetic data suggest maximum temperatures of 500-585°C for these meteorites. The high temperatures seemingly required for chondrule deformation remain an unsolved problem, but the strain imposed on Leoville is broadly consistent with that resulting from accretionary overburden in the interior of an asteroidal body. Given that such strain can occur in asteroids, a perplexing question is therefore: why does it not occur in most chondrites?

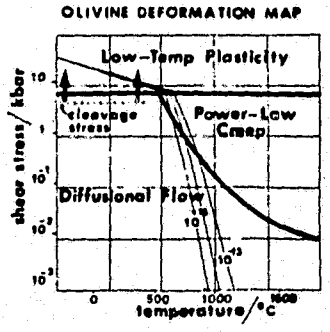

References

(1) Cain P. M. and McSween H. Y. (1984) Lunar Planet. Sci. XV, 116-117.
(2) Martin P. M. and Mills A. A. (1980) EPSL 51, 18-25.
(3) Fry N. (1979) Tectonphys. 60, 89-105.
(4) Dunnet D. (1969) Tectonophys. 7, 117-136.
(5) Ashby M. and Verrall R. A. (1977) Phil. Trans. Roval Soc. London 288, 59-95.
(6) Kohlstedt D. L. and Geotze C. (1974) J. Geophys. Res. 79, 2045-2051.
(7) Wegner M. W. and Christie J. M. (1974) Contrib. Min. Pet. 43, 195-212.
(8) Pfiffner W. A. and Ramsay J. G. (1982) J. Geophys. Res. 87, 311-321.

THE COLONY METEORITE AND THE POSSIBLE EXISTENCE OF A NEW CHEMICAL SUBGROUP OF CO3 CHONDRITES; A.E. Rubin, Inst. of Geophys. Planet. Phys., Univ. California, Los Angeles, CA 90024; and J.A. James, B.D. Keck, K.S Weeks and D.W.G. Sears, Dept. of Chemistry, Univ. Arkansas, Fayetteville, AR 72701; and E. Jarosewich, Dept. of Mineral Sciences, Smithsonian Institution, Washington, D.C. 20560

The Colony meteorite, found in Oklahoma around 1975, has an unrecrystallized texture and contains heterogeneous olivine and low-Ca pyroxene, kamacite with low Ni and Co and high Cr, amoeboid inclusions with low FeO and MnO, and numerous small chondrules with clear pink glass. These characteristics are shared by members of the least metamorphosed subgroup of CO3 chondrites. Colony contains a fine-grained matrix that has higher FeO (46.0 wt.%) and K2O (0.14 wt.%) and lower MgO (11.6 wt.%) and Na2O (0.13 wt.%) than normal CO3 matrices. Allan Hills A77307 (A77307) is another unmetamorphosed meteorite that has many petrologic similarities to normal CO chondrites, including matrix abundance, mineral compositions and chondrule size. However, it differs from them in its abundance of magnetite and presence of iron carbides. The olivine and low-Ca pyroxene compositional distributions of Colony and A77307 are very similar.

Colony is a breccia; it contains a centimeter-sized CO3-like clast possessing a fine-grained matrix richer in MgO and Cr2O3 and poorer in Na2O, K2O, CaO and SO3 than matrix material in the host. The clast/host boundary is very sharp and well-defined. Silicates in the clast have more pronounced undulose extinction, attesting to a somewhat more violent shock history. Chondrites such as Colony, Piancaldoli (LL3) and Leoville (CV3) are composed of clasts with similar lithologies to those of their hosts; they may all be accretionary breccias.

The composition of Colony was determined by INAA and wet chemistry: Al, Sc, V, Cr, Ir, Fe, Au and Ga are in the CO range, but some lithophiles (Ca, Mg, Mn), siderophiles (Ni, Co) and chalcophiles (S, Se, Zn) are depleted by factors of 10-40%. A77307 also has unusual characteristics. Like Colony, it has low Ca, Mg, Mn, Ni and (possibly) Co, but CO-CV levels of Se and Zn. A77307 also contains very high Cd, but this element has not yet been measured in Colony. The shapes of the thermoluminescence glow curves of Colony and A77307 are very similar (having peaks at 170 and 250 C), but differ significantly from those of normal CO chondrites (which have peaks at 90-110 and 190-210 C).

It is difficult to explain the compositional differences between Colony and A77307 and other CO chondrites by terrestrial weathering. These differences are somewhat similar to those between L and H ordinary chondrites and EL and EH enstatite chondrites. We suggest that Colony and A77307 represent a distinct chemical subgroup of CO3 chondrites, characterized by low Ni, Co, S, Ca, Mg, Mn and, possibly, high Cd.

We have found that the modal abundance of amoeboid inclusions in CO3 chondrites is inversely correlated with olivine heterogeneity. This indicates that the least metamorphosed CO3 chondrites tend to have the fewest amoeboid inclusions. Colony and A77307 follow this trend and thus appear to share the same general evolutionary history as the other CO3 chondrites. The more metamorphosed CO3 chondrites may have agglomerated at a different time than the others, during a period when the nebular supply of amoeboid inclusions was ample. These objects must then have been preferentially metamorphosed at their particular locations in the CO parent body.

EXPOSURE HISTORY AND COMPACTION AGE OF BANTEN CM CHONDRITE,

J.N. Goswami[1] and K. Nishiizumi[2], [1]Physical Research Laboratory, Ahmedabad 380 009, India, [2]Dept. of Chemistry, Univ. of California, San Diego, California 92093.

Records of nuclear tracks produced by solar flare and galactic cosmic ray heavy nuclei and cosmogenic ^{53}Mn activity in the Banten meteorite, the latest addition to the Non-Antarctic CM group of chondrites (1), have been studied to obtain information on its cosmic ray exposure history. The compaction dating method (2) was used to estimate the compaction age of this chondrite. The average background track density in olivine grains, obtained from a near-crust fragment, is $\sim 10^5$ cm-2. The measured ^{53}Mn activity of 237 $\pm$ 10 dpm/Kg (Fe + 1/3 Ni), indicates an exposure age of 4.5 m.y., which is towards the higher end of the exposure age distribution for CM chondrites. The shielding depth of the analysed sample within the preatmospheric meteorite is 12 cm. Determination of preatmospheric mass is made difficult as fragmentation must have occurred during the fall of the Banten meteorite (1). A lower limit of 75 kg can be assigned to the preatmospheric mass of this meteorite based on the limited data obtained in this work.

Precompaction solar flare heavy nuclei track irradiation records were found in several olivine grains. The fraction of such track-rich grains is $\sim$ 5%. Banten is thus one more addition to the group of gas-rich CM chondrites. Mass-spectrometric studies are currently in progress to study the light noble gas concentrations in this meteorite.

To obtain compaction age of this meteorite we have removed several euhedral olivine grains directly from the matrix and measured the track densities on the grain-surfaces in contact with the matrix. Each grain was then grinded down and etched to obtain the background track-density. While definite excess of track density on grain-surfaces have been found, the excess is very nominal unlike the case for other CM chondrites (2). Whether this is due to a lower average plutonium content in the Banten matrix can be ascertained only after completion of U-determination presently in progress.

1. Fredriksson K. et al. (1979), Meteorites 14, 400.
2. Macdougall J.D. and Kothari B.K. (1976), EPSL 33, 36.

X-RADIOGRAPHY OF SLICES OF THE ALLENDE METEORITE; D. Heymann, M. J. Smith, and J. B. Anderson, Department of Geology, Rice University, Houston, Texas 77001

A 2.2 kg fragment of the Allende Meteorite, on loan from the Houston Museum of Science, was derinded and sliced by bandsawing. Nice slices, 7-9 mm thick (average), and two buttends were generated. X-radiographs were made of all slices. The following features are resolved: grains of "blocky" troilite (bright spots), troilite-rimmed chondrules (bright halos), chondrules with central "vugs" (dim halos), white aggregates (dark patches), and dark inclusions (medium dark patches). The number of FeS grains larger than about 0.5 mm is one per 6 ± 1 gram of this fragment. Their "concentration" appears to be uniform at the 1 kg weight level, but is not uniform at the 100 g level. The number of FeS-rimmed chondrules is one per 10 ± 2 g. Their "concentration" is also non-uniform at the 100 g weight level. The number of white aggregates is roughly one per 20 g. These "disc-shaped" objects show a distinct preferred orientation of the axis orthogonal to the plane of the "disc". Chondrules with central vugs are numerous. Linear and curved arrays ("strings") of chondrules, up to a few cm long, are observed. Our interpretation of the observed features is: our fragment contains an internal "surface" which separates two regions with distinct differences in rock coherence, "concentrations" of FeS-grains, troilite-rimmed chondrules, and white aggregates. Whether this is a "depositional surface" we do not know. We think that the lineations are due to "mini slope-slides" with chondrules rolling farther downslope than angular grains do, but the directions of all such lineations present a rather complex picture. The preferred orientation of the white aggregates suggests a sequence of near-parallel depositional surfaces, with the "disc planes" parallel to these surfaces. We conclude that "slice" X-radiography can develop into a useful tool for studies of the sedimentary environment of the Allende meteorite and possibly of those other chondritic meteorites.

A STUDY OF TETRATAENITE; K. B. Reuter, J. I. Goldstein, and D. B. Williams, Department of Metallurgy and Materials Engineering, Lehigh University, Bethlehem, PA 18015 and E. P. Butler, Department of Metallurgy and Materials Science, Imperial College, London, England

Tetrataenite is the ordered FeNi phase observed in clear taenite (I); clear taenite (I) has the highest Ni content of the metallic phases of meteorites ranging from 48-57 wt% Ni (Albertsen et al., 1978; Scott and Clarke, 1979; Mehta et al., 1980). The tetrataenite in Dayton was examined using conventional transmission (TEM) and analytical electron microscopy (AEM). Tetrataenite was also simulated in terrestrial Fe-Ni alloys through electron irradiation of thin-foil specimens on the high voltage electron microscope (HVEM). The purpose of this work was to correlate the results of the TEM, AEM and HVEM studies on Dayton and on terrestrial iron-nickel alloys to the low temperature iron-nickel phase diagram (<400°C).

Thin-foil specimens of Dayton were prepared by jet-polishing 3 mm discs followed by 15 minutes of ion-beam cleaning. Thin-foil specimens were also prepared from homogeneous iron-nickel alloys in the composition range from 35 to 65 wt% Ni. After austenitizing, the 3 mm discs were jet-polished. Irradiation was done on the KRATOS AEI-EM7 HVEM in the temperature range 200-320°C.

Oxide forms spontaneously on the surfaces of thin-foil iron-nickel specimens. By determining the metal/oxide orientation relationships for $[001]_\gamma$, $[011]_\gamma$, $[\bar{1}11]_\gamma$ and $[013]_\gamma$, the reflections due to the oxide and the superlattice are distinguished. In Dayton, the clear taenite (I) is fully ordered until near the cloudy zone interface. The ordered domains ranged in size from 30-650 nm with the largest domains corresponding to the highest Ni content (51 wt% Ni) and the smallest domain size corresponding to the lowest Ni content (45 wt% Ni). In terrestrial alloys irradiated on the HVEM, the extent of electron irradiation induced ordering was determined as a function of temperature and composition. Ordering occurred in every specimen irradiated. At 200°C, the 35-65 wt% Ni specimens ordered; increasing the temperature to 280°C, the 40-65 wt% Ni specimens ordered. A 65 wt% Ni specimen irradiated at 300°C and a 60 wt% Ni specimen irradiated at 320°C also ordered. The superlattice domains ranged in size from 4-15 nm.

The above results from Dayton and the terrestrial alloys are correlated to an iron-nickel phase diagram with the following conclusions: 1) The general shape for the ordered phase field may look like that shown in Figure for γ'; 2) The ordered phase field may be located on the phase diagram to include 45 to 51 wt% Ni; 3) A wide two phase ordered plus disordered region should extend from 35-65 wt% at 200°C, decreasing in size as the temperature increases.

Although no boundaries on an Fe-Ni phase diagram can be clearly delineated from this work, the results are in approximate agreement with the phase diagram proposed by Goldstein and Williams (1982). Financial support for the work at Lehigh from NASA grant NAG9-45 is gratefully acknowledged.

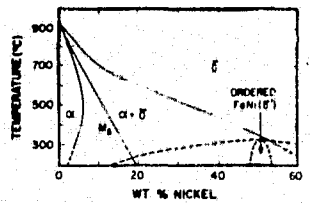

Fe-Ni phase diagram proposed by Goldstein and Williams (1982)

Albertsen, J.F., G.B. Jensen and J.M. Knudsen, 1978. Nature 273, 453-454.
Goldstein, J.I. and D.B. Williams, 1982. Proc. Inter. Conf. Solid-Solid Phase Transformations, Pittsburgh, PA, 715-719.
Mehta, S., P.M. Novotny, D.B. Williams and J.I. Goldstein, 1980. Nature 284 151-153.
Scott, E.R.D. and R.S. Clarke, Jr., 1979. Nature 281, 360-362.

INVESTIGATIONS OF TAENITE FROM IRON METEORITES AND CHONDRITES;

L. Larsen[+], G. B. Jensen[□], J. M. Knudsen[○], H. Roy-Poulsen[+], N. O. Roy-Poulsen[+], and L. Vistisen[+].
[+]Niels Bohr Institute, Blegdamsvej 17, DK-2100 Copenhagen Ø, Denmark.
[□]Department of Electrophysics, The Technical University of Denmark, DK-2800 Lyngby, Denmark.
[○]Physics Laboratory I, H. C. Ørsted Institute, Universitetsparken 5, DK-2100 Copenhagen Ø, Denmark.

Mössbauer spectroscopy of taenite from iron meteorites and chondrites shows in general the presence of two phases: a ferromagnetic, atomically ordered FeNi (∿50% Ni) phase, tetrataenite, and a paramagnetic, atomically disordered Fe-Ni (∿25% Ni) phase.

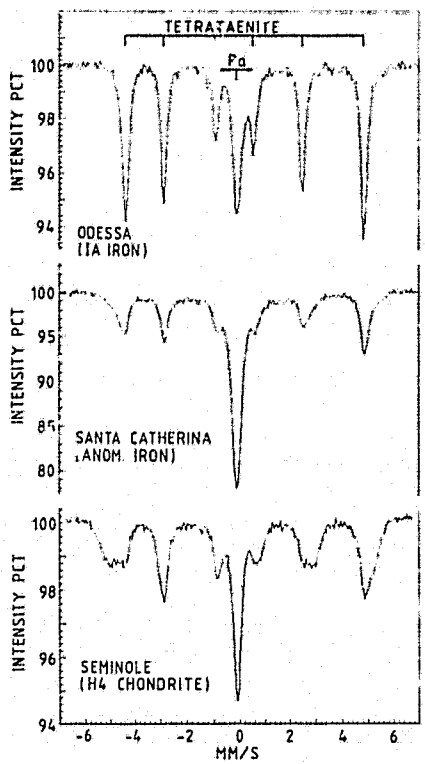

Fig. 1: Mössbauer spectra of taenite from different meteorites. (Pa: paramagnetic phase).

However, the spectral components interpreted as corresponding to tetrataenite are not all alike (Fig. 1). For some meteorites the spectra corresponding to tetrataenite show broad and asymmetric lines, giving rise to changes in the magnetic hyperfine field and the electric quadrupole shift. These effects have been interpreted as due to a variation in the degree of order of tetrataenite (1,2).

We have recently shown that for the chondrite Neenach the broadening of the lines may be ascribed to the presence of an atomically disordered FeNi (∿50% Ni) phase (3). It will be shown that also in other meteorites, both iron meteorites and chondrites, the broadening of the tetrataenite lines may be ascribed to the presence of the atomically disordered FeNi (∿50% Ni) phase.

Thus, the apparent variation in the degree of order of tetrataenite in meteorites may be due to a variation in the relative amounts of the ordered, respectively the disordered FeNi (∿50% Ni) phase. The results will be discussed on basis of the Fe-Ni phase diagram.

We note that, except for the superstructure reflections of tetrataenite, all the three phases mentioned above show identical X-ray diffraction patterns (i.e. f.c.c. structure with same lattice parameter), and therefore they cannot be distinguished by diffraction techniques alone.

(1) Albertsen, J. F. et al. (1980). Meteoritics 15, p. 258.
(2) Danon, J. et al. (1982). Meteoritics 17, p. 202.
(3) Larsen, L. et al. (1983). Meteoritics 18, p. 334.

MÖSSBAUER SPECTROSCOPY AND X-RAY DIFFRACTION OF SAMPLES FROM THE SANTA CATHARINA IRON METEORITE

H. Roy-Poulsen[+], R. S. Clarke, Jr.[x], G. B. Jensen[□], J. M. Knudsen[○], L. Larsen[+], N. O. Roy-Poulsen[+], and L. Vistisen[+].

[+]Niels Bohr Institute, Blegdamsvej 17, DK-2100 Copenhagen Ø, Denmark.

[x]Smithsonian Institution, Washington, DC 20560.

[□]Department of Electrophysics, The Technical University of Denmark, DK-2800 Lyngby, Denmark.

[○]Physics Laboratory I, H. C. Ørsted Institute, Universitetsparken 5, DK-2100 Copenhagen Ø, Denmark.

Conversion Electron Mössbauer Spectroscopy (CEMS) of samples from the Santa Catharina iron meteorite shows the presence of the ordered iron-nickel phase with ~50% Ni, tetrataenite, and of the paramagnetic iron-nickel phase with ~25% Ni. The FeNi phase with ~50% Ni amounts to ~70% of the iron-nickel alloys.

Furthermore, the CEM spectra show the presence of small peaks from one or more spinel compounds, most probably Fe_3O_4. These small peaks are more pronounced when regions near the rim of the samples are analyzed.

X-ray diffraction of different areas of the samples, both optically dark and optically light areas, shows the presence of a diffraction pattern from a single f.c.c. lattice with a lattice parameter of a≈3.58Å. This means that the two different Fe-Ni phases seen in the CEMS analysis occupy the same lattice. The X-ray photographs do also show the presence of superstructure reflections from the ordered FeNi phase, and that the orientation of the f.c.c. lattice is the same within the whole sample (surface area ~50 mm^2).

As in the CEMS analysis the X-ray diffraction analysis do also show the presence of more compounds. Some of the X-ray photographs (mostly from near-rim regions) show a weak diffraction pattern from a "powder compound" with f.c.c. structure and a lattice parameter of a≈8.4Å, and some show two weak reflections, which can be interpreted as coming from an epitaxially grown compound with f.c.c. structure and a lattice parameter of a≈8.4Å. These two diffraction patterns may belong to the same or to different compounds. The data obtained suggest that the most probable candidates are Fe_2NiO_4 and Fe_3O_4, and this interpretation is in accordance with the CEMS analysis.

E-4 N85 15625

STRUCTURAL DEVELOPMENT IN THE SANTA CATHARINA METEORITE

Roy S. Clarke, Jr., Division of Meteorites, National Museum of Natural History, Smithsonian Institution, Washington, D.C. 20560

The Santa Catharina, Brazil, meteorite is a deeply weathered, chemically anomalous ataxite with the third highest Ni value on record. Recently, physicists and metallurgists have found remnant Santa Catharina material to be of interest. Its composition is in the range of the technologically important Invar alloys, and Mössbauer and X-ray data have led to the suggestion that the meteorite transformed at very low temperatures to major amounts of the ordered NiFe mineral tetrataenite and a martensitic phase. This metallographic study was undertaken to seek support for the idea that Santa Catharina is really massive 'cloudy taenite'.

Available metal-rich nuggets of Santa Catharina appear to have been single crystals of taenite in the few centimeter size range, separated from each other by grain boundries occupied by troilite and schreibersite. Metallographic and electron microprobe data allow one to postulate the following cooling and structural development history: (1) single crystal taenite formed at high temperature, (2) phosphate formed within the taenite and grain boundary schreibersite formed at interfaces with troilite or with other taenite crystals, (3) schreibersite began to precipitate within taenite at about 650°C, (4) at about 450°C the meteorite entered the three phase field at which point kamacite precipitated and started growing, (5) kamacite/schreibersite interface measurements indicate that cooling continued down to about 350°C, with large Ni diffusion gradients developing within schreibersites.

Terrestrial weathering has destroyed much of the Santa Catharina mass and has severely modified all of the specimens available to me. Oxide formation along grain boundaries and cracks ranges from mild to severe. Oxidation within taenite crystals has penetrated along crystallographic planes into the deep interior. Areas of incipient corrosion within taenite typically contain from 4 to 6% O_2, about 0.1% Cl, and 42 to 48% Ni. Areas of more advanced oxide formation contain similar levels of Ni and Fe, slightly more O, and no detectable Cl. It is suspected that Cl plays a role in the corrosion process but is not retained in the fully developed corrosion product.

No evidence has been found to support the suggestion that tetrataenite is present in Santa Catharina. The techniques employed, however, may have been insufficiently sensitive for the task. It is also worth noting that a 34% Ni alloy transforming to tetrataenite and ~25% Ni martensite would only be expected to produce one-third tetrataenite. Much evidence has been found for deep penetration of weathering and the presence of unidentified weathering products.

The presence of Ni diffusion gradients in Santa Catharina schreibersite comparable to those previously observed in taenite lamellae is a new observation of some interest. These gradients offer the possibility to determine a cooling rate on a structurally unique meteorite.

LOW TEMPERATURE DIFFUSION COEFFICIENTS IN THE Fe-Ni AND FeNiP SYSTEMS--APPLICATION TO METEORITE COOLING RATES; D. C. Dean and J. I. Goldstein, Department of Metallurgy & Materials Engineering, Lehigh University, Bethlehem, PA 18015

The interdiffusion coefficient of FeNi in fcc taenite (gamma) of Fe-Ni and Fe-Ni-0.2 P alloys was measured as a function temperature between 600 and 900 degrees C. This temperature range is directly applicable to the nucleation and growth of the Widmanstätten pattern in iron meteorites and metal regions of stony and stony-iron meteorites. Diffusion couples were made from FeNi or FeNiP alloys which ensured that the couples were in the taenite phase at the diffusion temperature. The analytical electron microscope (AEM), with a chemical spatial resolution of approximately 0.025 microns, was used to measure the diffusion profiles. The diffusion profiles were often less than 2 microns in length. To ensure that lattice diffusion was controlling at these temperatures, a bonding practice was developed such that the grain size was at least 20 microns at the bond interface. The presence or absence of grain boundary diffusion was determined by measuring the Ni profile normal to the existing grain boundaries with the AEM.

Ignoring any variation of interdiffusion coefficient with composition, the measured data is plotted versus the reciprocal of the diffusion temperature in Figure 1. The FeNi data generally follow the extrapolated Goldstein, et al. (1965) data from high temperatures. The FeNiP data indicates that small additions of P (0.2 wt%) cause a 3 to 10 fold increase in the FeNi interdiffusion coefficient increasing with decreasing temperature. This increase is about the same as that predicted by Narayan and Goldstein (1983) at the Widmanstätten growth temperature, $\leq 700^{\circ}C$. The cooling rates of the iron meteorites should be the same as those given by Narayan and Goldstein (1984). Preliminary results for the diffusion of FeNi in the bcc kamacite (alpha) show a significant decrease when compared to available data.

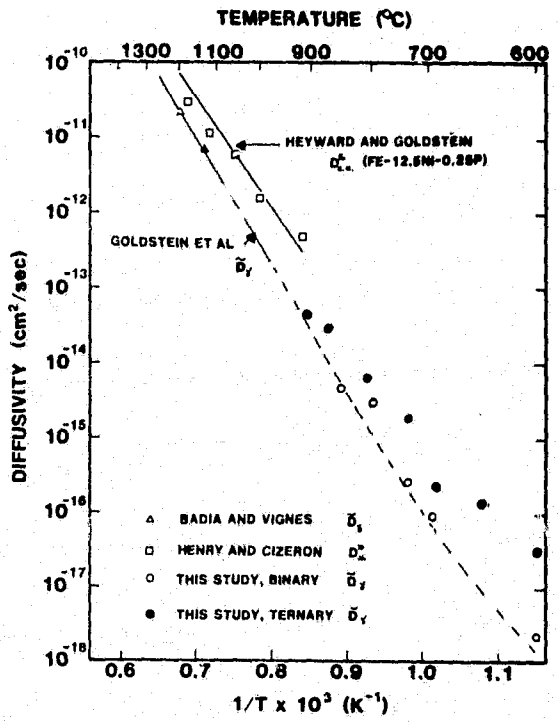

Fig. 1: Interdiffusion coefficient $\tilde{D}(cm^2/sec)$ of Fe-Ni and Fe-Ni-P versus inverse temperature (K^{-1}).

References:
Goldstein,J.I., R.E.Hanneman and R.E. Oglivie, 1965, Trans. TMS AIME 233, 812-20.
Heyward,T.R. and J.I.Goldstein, 1973 Metall. Trans., 4, 2335-42.
Badia,M. and A.Vignes, 1969, Acta Met., 17, 177-87.
Henry,G. and G.Cizeron, 1978, Ann. Chim. Fr., 3, 167-76.
Narayan,C. and J.I.Goldstein, 1983, Metall. Trans.A, 14A, 2437-39.
Narayan,C. and J.I.Goldstein, 1984, submitted to Geo. Chem. Abs.

^{244}Pu FISSION TRACK AND METALLOGRAPHIC COOLING RATES OF TOLUCA AND COPIAPO IRON (IA) METEORITES. Y. Benkheiri, Laboratoire de Minéralogie, Muséum National d'Histoire Naturelle, 61 rue Buffon 75005 PARIS.

The cooling rate of one silicate inclusion from Toluca (Iron IA) was determined by means of the multiple fission track ^{244}Pu detector method (1). The value was found to be $\sim$ 3.7 and $\sim$ 4.3°C/Myr for apatite and merrillite crystals respectively, adjacent to diopsides, i.e. between the temperature interval $\sim$500 - $\sim$ 100°C. This cooling rate is similar to those found for 2 silicate inclusions from Copiapo and Landes (2). Metallographic cooling rates were obtained for Copiapo, firstly in the case of the Widmandstätten pattern in the iron, and also on metallic grains included in the silicate portion, by using the previous methods (3, 4, 5, 6, 7). Taking into account the metal composition (P$\simeq$ 0.14 %, Ni $\simeq$ 7 %), an equilibrium nucleation temperature of $\sim$ 730°C is derived for kamacite, and a cooling rate of $\sim$1°C/Myr is found for the metal. For the metallic grains in the silicate portion, the metallographic cooling rate was found to be $\sim$10°C/Myr ($\pm$ 60%), in good agreement with the fission track data.

It should be noted that all these cooling rate values are more or less (within a factor of 2 to 3) in general agreement for the three irons.

On the other hand, these results are diametrically opposed to those recently presented by Narayan and Goldstein (1983) who found for IA irons cooling rates of 400-4000°C/Myr. At the present stage, there is no way to reconcile such contradictory results.

(1) Pellas P. and Storzer D. (1981) Proc. R. Soc. Lond. A 374, 253-270.
(2) Benkheiri Y. Pellas P. and Storzer D. (1979) Icarus 40, 497-501.
(3) Goldstein J.I. and Short J.M. (1967). Geochim. Cosmochim. Acta, 31,1001.
(4) Doan A.S. and Goldstein J.I. (1969). Meteorite Research (ed. P.M. Millman) 763-779.
(5) Goldstein J.I. and Doan A.S. (1972) Geochim. Cosmochim. Acta 36, 51-69.
(6) Moren A.E. and Goldstein J.I. (1978) E.P.S.L. 40, 151-161.
(7) Willis J. and Goldstein J.I. (1981) Proc. Lunar Pl. Sci. 1135.
(8) Narayan C. and Goldstein J.I. (1983) Geochim Cosmochim Acta

EXTREME INCOMPATIBILITY OF Pb DURING THE CRYSTALLIZATION OF MAGMATIC IRON METEORITES. J. H. Jones[1] and S. R. Hart[2]. [1]Lunar and Planetary Laboratory, University of Arizona, Tucson, AZ 85721; [2]Center for Geoalchemy, Department of Earth, Atmospheric and Planetary Sciences, M.I.T., Cambridge, MA 02139.

Recently Chen and Wasserburg [1] have presented lead concentration and isotopic data on coexisting iron metal and troilite, separated from two iron meteorites, Cape York and Mundrabilla. Lead was found to be concentrated in troilite by only a factor of 2-3X over Pb levels found in the metal phase. This was surprising since Pb is typically thought to be much more chalcophile than siderophile. For example, Jones and Drake [2] found the partition coefficient of Pb [D(Pb)] between iron-nickel metal and a sulfur-bearing metallic liquid to be $\geq$ 140 in favor of the liquid.

This two-order-of-magnitude discrepancy between the laboratory and natural samples has led us to investigate the partitioning behavior of Pb in the three-phase system metal-troilite-sulfide liquid. A sample whose bulk composition was similar to the eutectic composition of the Fe-FeS system was spiked with ~1% natural Pb metal and equilibrated at 970°C for three days. Microscopic examination and electron microprobe analysis of a polished section showed three phases--Fe metal, troilite and an Fe-S-Pb-O metallic liquid. The Pb concentration of the metallic liquid was ~1.4 wt.%; the Pb contents of both the troilite and the Fe metal were below the detection limit of the electron probe.

To better define the Pb concentrations of the solid phases, the same sample was analyzed for Pb and Fe using the M.I.T., Harvard and Brown ion microprobe. The Fe-54/Pb-208 ratio of the three phases was used to calculate approximate Pb concentrations of the troilite and metal, using the metallic liquid as a standard. Isobaric interferences were eliminated using modest energy filtering (25V). No matrix corrections were applied. Two troilite analyses yielded Pb concentrations of 76 and 88 ppm ($\pm$ 20%); a single metal analysis gave a Pb concentration of 9 $\pm$ 4 ppm. Lead isotopic ratios were constant for all phases and were in agreement with the isotopic composition of the dopant Pb. Extensive (1-1.5 hr) sputter-cleaning of the metal and troilite surfaces resulted in Fe/Pb ratios which did not change with time and were presumably not artifacts of surface contamination. If ion yields (M^+) from other systems (e.g., M, MS, MO, M_2SiO_4) may be used as analogs to evaluate the effects of the matrix on the measured Fe/Pb ratios, the concentrations given above are probably accurate to within a factor of 2-3. (For example, Pb is ionized about 2.7 times more efficiently from PbS than from Pb metal.) Appropriate standards are necessary to reduce this uncertainty.

Even at this level of precision, some conclusions and speculations are possible: (1) The D(Pb) (troilite/metallic liquid) is low (~.01-.001) and, contrary to expectation, troilite, like metal, excludes Pb very effectively during the crystallization of metallic liquids; (2) Pb in iron meteorites is conceivably concentrated in trace phases which are less susceptible to contamination than metal and troilite; and (3) taken at face value D(Pb)(metal/troilite) is ~0.1, but given the Pb and Fe ion yields from simple endmember phases (Fe, FeS, Pb, PbS), this D is more likely to be ~0.05-0.03. Thus it appears that disagreement still exists between the Pb partitioning data obtained on natural metal-sulfide assemblages and that measured from laboratory experiments, but only by a factor of 10 rather than a factor of 100.

[1]Lunar Planet.Sci. XIV, 103-104; [2] Lunar Planet. Sci. XIII, 369-370.

E-8 N85 15628

EXPERIMENTAL AND THEORETICAL STUDY OF THE FORMATION OF THE IIAB, IIIAB AND IVA IRON METEORITE CHEMICAL GROUPS FROM THE PARENT LIQUID:

R. Sellamuthu and J. I. Goldstein, Dept. of Metallurgy & Materials Engineering, Lehigh University, Bethlehem, PA 18015

Segregation of solute elements was measured in plane front solidified Fe-Ni-S-P alloys of meteoritic composition containing Ir, Ge and/or Cu. The Ni and P contents reach maximum values of 10.5 wt% and 1.1 wt%, respectively, in austenite (taenite) at the end of primary solidification. Distribution coefficients of Ni, P, Ir, Ge and Cu were determined from the solidified alloys. The distribution coefficients vary with the S and P content of the liquid. In addition the distribution coefficients of Ni, P, Ir and Ge increase and the distribution coefficient of Cu decreases with the S to P ratio (the S-P interaction effect). Equations that describe the concentration dependence of the distribution coefficients have been developed and used to calculate solute redistribution during the solidification of IIAB, IIIAB and IVA parent bodies. The calculated P vs Ni, Ir vs Ni and Ge vs Ni trends are in good agreement with the observed meteoritic data as shown in Figures 1 to 3.

Since the calculated value of the maximum solid solubility of P (1.1wt%) agrees well with the observed maximum P composition data for IIAB and IIIAB irons, we conclude that complete crystallization of the parent liquids of IIAB and IIIAB had occurred before any fragmentation of the solidified body. Therefore, IIAB iron meteorites such as Santa Luzia and Sao Juliao, and IIIAB iron meteorites such as Tieroco Creek, Sam's Valley and Narraburra must have formed at the very end of the austenite or taenite crystallization process. The IVA meteorites may contain too little bulk P to reach the maximum P solubility or may not have been completely solidified. Our calculations indicate only 95% crystallization.

Our calculations show that a well-recognizable match between the calculated solidification trend and the observed data can be obtained only when the parent liquid is considered homogeneous. The calculated bulk P and S contents for the parent liquids (wt%) are 0.27 and 10.0 for IIAB, 0.19 and 4.2 for IIIAB, and 0.05 and 1.8 for IVA, respectively. These bulk compositions fall within the homogeneous liquid region of the Fe-S-P phase diagram.

We therefore conclude that each of the three magmatic meteorite groups was originally a single, homogeneous molten pool in the parent body with significant S and P contents and that the liquid subsequently transformed to solid upon cooling before the fragmentation of the parent body. Solute partitioning which occurred during the crystallization of the parent liquid is responsible for the observed compositional trend within each group.

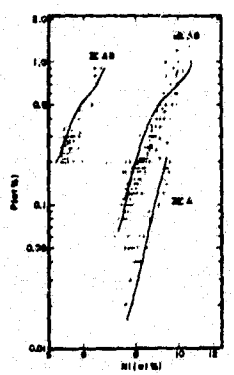

Fig.1.P-Ni trend

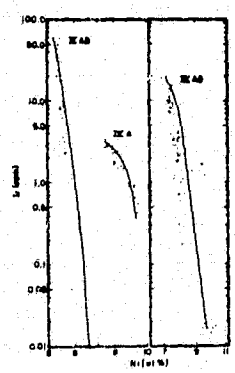

Fig.2.Ir-Ni trend

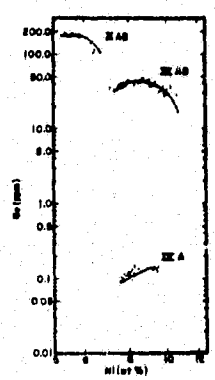

Fig.3.Ge-Ni trend

INVESTIGATIONS CONCERNING THE MAGMATIC IRON METEORITES: STATIC VS. DYNAMIC EXPERIMENTS. Daniel J. Malvin, John H. Jones, and Michael J. Drake, Lunar and Planetary Laboratory, University of Arizona, Tucson, AZ 85721.

It is now recognized that large concentrations of nonmetals (S,P,C) in metallic (Fe,Ni) systems can dramatically affect the partition coefficients [D (solid metal/liquid metal)] of many trace elements of cosmochemical interest [1,2,3]. Over the past three years there has been substantial agreement between the Lehigh and Arizona groups as to both the absolute D for a given trace element i [when the concentration of a nonmetal (N) is known] and the general functional form of $^{i}D(N)$ [2,3]. Although the exact experimental details between these two groups differed considerably, a common feature to both groups was that the experiments were static (constant temperature for the duration of the experiment) in an attempt to achieve equilibrium. More recently, the Lehigh group has undertaken an important series of dynamic experiments [4,5], where an experimental charge is slowly drawn from the furnace. The sample solidifies by fractional crystallization until the charge is completely solid and the zoning profile in the solid is used to reconstruct $^{i}D(N)$ [4].

These dynamic experiments have produced functional forms for $^{i}D(N)$ which are often radically different from those inferred from static experiments [3,5], which do not obey any recognized thermodynamic model for melt-component interactions, and which differ for each element i. The reasons for this disagreement with static experiments are unclear. Sometimes, as in the case of Ge, the dynamic and static experiments do not even agree as to whether the trace element should behave as a "compatible" or "incompatible" element. The complexity of the dynamic experiments makes it difficult to suggest specific experimental problems which could cause the discrepancy between the dynamic and static D's. Static experiments are more readily evaluated, and possible problems which have been proposed in discussions between Lehigh and Arizona are: (1) failure to quench rapidly enough to preserve the composition of the metallic liquid; (2) breakdown of Henry's Law behavior at experimental "trace element" concentrations of 1 wt. % or greater; and (3) very nonideal interactions between nonmetals, such that experiments in simple systems with one nonmetal cannot be used to extrapolate to more complex systems (i.e., those containing two or more nonmetals).

We have attempted to evaluate these potential problems by a series of metallic solid/metallic liquid partitioning experiments in the Fe-Ni-S-P system using Ge ($\sim$1 wt. %) as a tracer. The four experiments were isothermal ($\sim 1250^{\circ}C$), but the P/S ratio of the liquid was varied from 0.02 to 1.8. The charges were analyzed and the measured D's for Ge, P, and Ni were compared to the D's predicted by dynamic experiments [5] (which contained both P and S) and to the static experiments [3] (Table 1). In the case of the static experiments, the effects of the nonmetals on D were assumed to be additive. The measured D's were always less than 30% different from the predictions of the static experiments for P and always less than 10% for Ge, but commonly differed from the predictions of the dynamic experiments by $\sim$100%. One of these charge compositions, for which there was a large disagreement with the dynamic experiments for both ^{Ge}D and ^{P}D, was selected for a series of quenching and Henry's Law experiments. The S and P contents of the metallic liquid were within the concentration range for which the predictions of the dynamic experiments should be valid [4]. No significant change in ^{Ge}D or ^{P}D was observed as the Ge concentration of the liquid metal was varied from 0.08 to 0.7 wt. %. The variation in D's between the experiments quenched in water, liquid nitrogen, and air was also unimportant.

Thus, the major objections to static experiments appear to be unfounded. Our confidence in static experiments is strengthened by new partitioning experiments between immiscible metallic liquids which indicate that the additive equations from static experiments [3] will also predict ^{Au}D (S-rich liquid/P-rich liquid) to within acceptable accuracy ($\sim$25%). Although it is still unclear why the static and dynamic experiments differ, the static experiments appear to meet all criteria for equilibrium that have been proposed by either the Arizona or Lehigh group. We, therefore, regard the ability of $^{i}D(N)$'s generated by the dynamic experiments to reproduce iron meteorite compositional trends [5] as fortuitous. Differentiation of magmatic iron meteorites remains to be modelled successfully.

[1] NARAYAN AND GOLDSTEIN (1982) Geochim. Cosmochim. Acta 46, 259-268. [2] WILLIS AND GOLDSTEIN (1982) Proc. Lunar Planet. Sci. Conf. 13th, A435-A445. [3] JONES AND DRAKE (1983) Geochim. Cosmochim. Acta 47, 1199-1209. [4] SELLAMUTHU AND GOLDSTEIN (1983) Proc. Lunar Planet. Sci. Conf. 11th, B343-B352. [5] SELLAMUTHU AND GOLDSTEIN (1984) Lunar Planet. Sci. XV, 746-747.

TABLE 1

EXPERIMENT	$^{2S}_{L}$	$^{2P}_{L}$	MEASURED Ni_D	MEASURED P_D	MEASURED Ge_D	CALCULATED J6D* Ni_D	CALCULATED J6D* P_D	CALCULATED J6D* Ge_D	CALCULATED S&G** Ni_D	CALCULATED S&G** P_D	CALCULATED S&G** Ge_D
40-A	21.1	0.46	1.22	0.44	4.22	1.27	0.57	4.59	1.14	1.31	3.65
						Δ% 4.1	28.4	8.8	6.6	195	13.5
40-B	11.1	2.14	0.989	0.14	1.71	0.999	0.13	1.61	0.942	0.29	0.32
						Δ% 1.0	11.8	5.8	4.8	98	81
40-C	4.55	4.53	0.933	0.10	1.32	0.950	0.10	1.32	0.909	0.34	0.02
						Δ% 1.8	1.9	0	2.6	34	98
40-D	2.7	4.0	0.941	0.12	1.25	0.932	0.10	1.33	0.905	0.11	0.01
						Δ% 1.0	15	6.4	3.8	3.4	99

* Using the equations of Jones and Drake [3]
** Using the equations of Sellamuthu and Goldstein [5]

$$\Delta\% = \left| \frac{D_{calc} - D_{meas}}{D_{meas}} \right| \times 100$$

MASSIVE SCHREIBERSITE IN THE BELLSBANK AND SANTA LUZIA METEORITES

R.S. Clarke, Jr.,* R. Sellamuthu, ** and J.I. Goldstein**; *Division of Meteorites, Smithsonian Institution, Washington, D.C. 20560, ** Department of Metallurgy and Materials Engineering, Lehigh University, Bethlehem, PA 18015.

Massive schreibersite growth has been studied previously in several representative coarse-structured iron meteorites (1). The Fe-Ni-P equilibrium diagram combined with diffusion kinetics permits reconstruction in fair detail of the subsolidus cooling history and structural development process. Massive schreibersite growth may be viewed as localization of large amounts of P at high temperature, P that has diffused in the solid state over large distances. The coupled movement of Ni is much less dramatic. Our studies also apply constraints on the possibilities of structures surviving from high temperatures, the liquidus range.

Two of the meteorites we studied were Bellsbank (ungrouped) and Santa Luzia (IIB), and we concluded that their massive schreibersites grew in the solid state at temperatures below 900°C. Recently, other workers (2) have suggested that these same structures resulted from crystallization of P-rich liquid on the IIAB parent body. It seems likely that this structural development argument is incorrect and that Bellsbank is not from the IIAB parent body.

If residual liquid schreibersite did exist in meteorites of the Bellsbank and Santa Luzia compositions in the 1000°C temperature range, it would have been obliterated by dissolution in a short span of years. At this temperature, P solubility in kamacite is about 4 at. %, and in taenite about 2 at. %. The time required for P to diffuse 1 cm in kamacite is only 10 yrs at 1000°C or 60 yrs at 900°C. Ni diffusion is somewhat slower, as is diffusion in taenite. However, more than enough time must have been available for homogenization.

The liquid entrapment suggestion is also difficult to reconcile with recent experimental work that shows that a P-rich liquid is only possible at very high S contents. There is not sufficient S in these meteorites. Difficulty in matching P-Ni trends in the Bellsbank trio meteorites with IIAB trends suggests that they are not from the IIAB parent body.

1. R.S. Clarke, Jr. and J.I. Goldstein. 1978. Schreibersite Growth and Its Influence on the Metallography of Coarse-Structured Iron Meteorites. Smithsonian Contributions to the Earth Sciences, 21:80 pp.
2. D.J. Malvin, D. Wang, and J.T. Wasson. 1984. Chemical Classifcation of Iron Meteorites - X. Multi-element Studies of 43 Irons, Resolution of Group IIIE from IIIAB, and Evaluation of Cu as a Taxonomic Parameter. Geochimica et Cosmochimica Acta, 48:785 - 804.

INCLUSIONS IN IAB IRONS: IS THE PARTIAL DIFFERENTIATION MODEL COMPATIBLE WITH BAROMETRY AND CHRONOMETRY?

Alfred Kracher, Department of Earth Sciences, Iowa State University, Ames, IA 50011

Group IAB irons and winonaites probably formed on one or more parent bodies which were heated above the solidus of the metal/sulfide assemblage, but not high enough to cause substantial melting of silicates (1). If lodranites come from the same parent body (2), some parts of it reached higher temperatures. Many IAB irons are rich in carbon. Near 1400 K two carbon sinks become effective: dissolution in melt and reaction to CO/CO_2. The miscibility gap in the Fe-S-C system limits solution in the melt to below about 0.1 % by weight. The reduction of silicates depends on their FeO content and the confining pressure which limits CO/CO_2 escape (3). At the composition of IAB silicates and the temperatures recorded in them the graphite surface is around 20-50 bar. The present redox state of the silicates was probably established by graphite reduction. The presence of gas-rich, presumably "primordial" graphite (4) suggests that not all elemental carbon was consumed. This implies that the redox state of silicates reflects equilibration, perhaps incomplete, at the graphite surface. Confining pressures calculated from the $C-CO-CO_2$ equilibrium indicate burial depths greater than for ordinary chondrite metamorphism, in good agreement with more complete gas retention in winonaites than in metamorphosed ordinary chondrites (5). These pressures are about 100X lower than inferred by sphalerite barometry (6); there is no explanation for this discrepancy yet.

Silicate inclusions in IAB irons show a positive correlation of apparent I/Xe age with Ni content of the host metal (7). Although the partial differentiation model would allow for real age differences in a regularly layered parent body, an alternative explanation might be more plausible: during early partial differentiation, the S-rich melt dissolved a fraction of I which still contained live ^{129}I. During fractional crystallization, I was fractionated from Xe: I was incorporated in crystallizing troilite, Xe remained in the melt. Thus the residual melt became enriched in radiogenic Xe ($^{129}Xe_r$). When melt engulfed silicate fragments, both I and Xe associated with the melt were trapped at sites in the silicates. The "isochrons" result from mixing of silicate-derived "normal" I-Xe, and melt-derived I-Xe in similar proportions, the latter component containing increasing amounts of excess $^{129}Xe_r$ with increasing melt evolution. Mundrabilla, which consists largely of quenched melt (1) contains troilite with very high apparent I/Xe age (7), strongly supporting the suggestion of excess $^{129}Xe_r$ in the melt.

References: (1) Kracher A. (1982) GRL 9,412; (1983) LPS XIV, 403. (2) Prinz M. et al. (1983) LPS XIV,616. (3) Brett R. and Sato M. (1984) GCA 48,111. (4) Crabb J. (1983) LPS XIV,134; Meteoritics 18,283. (5) Schultz L. et al. (1982) EPSL 61,23. (6) Kissin S.A. and Schwarcz H.P. (1982) LPS XIII,393. (7) Niemeyer S. (1979) GCA 43,843.

SILICATE INCLUSIONS IN IVA IRON METEORITES; M. Prinz,[1] C.E. Nehru,[1,2] J.S. Delaney,[1] K. Fredriksson,[3] and H. Palme,[4] 1. Am. Mus. Nat. Hist., NY, NY 10024. 2. B'klyn Coll., B'klyn, NY 11210. 3. Smith. Inst., Wash. DC 20560. 4. MPI Chemie, Mainz, FRG.

IVA irons formed by magmatic processes but there has been much controversy as to their cooling rates (uniform or variable) and whether they represent cores or "raisins" in one or more parent bodies. A study of the silicates was undertaken to determine their implications for the IVA parent body history. Tridymite is found in Gibeon and Bishop Canyon, and silicate assemblages are found in Saõ Joaõ Nepomuceno ("Nepo") and the stony-iron (with IVA metal) Steinbach. Oxygen isotopes were found to be within the range of L or LL chondrites (Clayton et al., 1983). **Texture.** Inclusions in Steinbach and Nepo are large (up to 2 cm), have curved boundaries in sharp contact with the metal, make up about 50% of Steinbach and about 10% of Nepo, and are mainly low Ca pyroxene and tridymite, with minor chromite. Pyx and trid are large and clear, show no shock effects, are coarse grained (up to 5 mm) and intergrown, with sharp curved boundaries. They crystallized simultaneously, as they sometimes contain inclusions of each other, and the assemblage appears to be igneous. **Modes.** Steinbach and Nepo silicates contain, respectively: low Ca pyx (56.1, 84.5%), trid (43.3, 15.3%), and chromite (0.5, 0.2%). No plag or phosphate was found. Each contains two low Ca pyroxenes of similar composition (Wo_1En_{85}) although it is less common in Nepo; clinobronzite is included within clear orthobronzite. **Mineralogy.** Clinobronzite formed by inversion from protobronzite at about 1200°C at an fO_2 of 10^{-12}; silicates cooled rapidly in the 1200°-700°C range to preserve the unusual pyroxene assemblages. Nepo cooled more slowly than Steinbach. **Major and Trace Elements.** Calculated bulk analyses of both assemblages show high SiO2 (61-71%), 7-8% FeO, 21-29% MgO and no Na, K or P. Siderophile element data are consistent with IVA classification, but Steinbach has a much lower Ir/Au ratio than Nepo. The refractory metals Ir, Os, Re occur in chondritic proportions in both meteorites and Ga is higher in Steinbach. The most surprising result is that the REE in the pyroxene of both meteorites are extremely low, although Nepo is higher than Steinbach by about a factor of two. **Conclusions.** Application of partition coefficients shows that the parent magmas were close to that of chondritic composition for refractory elements. These IVA silicate assemblages appear to have been derived from a chondritic assemblage by almost total melting and fractionation but the low REE patterns of the pyroxene, high tridymite content, and lack of incompatible elements implies an extremely unusual process. A single stage cumulate theory would result in olivine enrichment, REE in residual pyx, and feldspathic components in addition to tridymite. Two hypotheses, high speculative, have been considered: (1) The original assemblage was an olivine cumulate, analogous to pallasite, initially in contact with Si-bearing metal. The metal was oxidized and a silica component reacted with olivine to produce low Ca pyroxene, and free silica. This hypothesis has problems. (2) The assemblage formed in a two-stage melting process. First, an olivine-pyroxene cumulate was derived from a molten chondritic parent. Next, a second melting event (possibly induced by bringing in hot metal from a deeper site as a result of planetary gravitational instability) results in progressive heating and migration of incompatible components, followed by eutectic melting in the system olivine-SiO_2, on the pyroxene+SiO_2 join, resulting in a liquid of eutectic composition. The combined Steinbach and Nepo assemblages come remarkably close to a eutectic mixture. Hypothesis (2) is preferred and is consistent with either the core or raisin hypotheses. The silicates represent achondritic assemblages accompanying the achondritic IVA metal.

GUIN: AN UNGROUPED IRON WITH SILICATE INCLUSIONS; Puhe Zong, Alan E. Rubin, and John T. Wasson, Institute of Geophysics and Planetary Physics, University of California, Los Angeles, CA 90024; and Jim Westcott, P.O. Box 327, Sedona, AZ 86336.

The Guin, Alabama iron meteorite was found in 1969 as a single 34.5 kg mass. It is a coarse octahedrite containing numerous silicate inclusions, silicate grain fragments and schreibersite-mantled troilite nodules. One 1.5x2.5 cm silicate inclusion, shaped like an ovoid droplet, was studied in detail; it is very similar to inclusions in IIE irons. Surrounding the inclusion is a mm-thick, discontinuous band of troilite and schreibersite (21 wt.% Ni). The inclusion contains large (3-9 mm) subhedral to euhedral grains of augite ($Fs_{10}Wo_{42}$) with deformation lamellae; bronzite ($Fs_{21}Wo_4$) occurs as an overgrowth on one large augite grain. The augite and bronzite grains are zoned (e.g., Fs9.5-13.2 in one augite). Surrounding the pyroxene grains is a dark, cryptocrystalline plagioclase-rich ($Ab_{87}Or_4$) matrix (possibly devitrified glass) containing very abundant 0.5-1.5 um opaque grains. Stoichiometric plagioclase ($Ab_{86}Or_3$) and minor bronzite, occurring as 150-600 um grains, comprise a ring between the matrix and metal host along one side of the inclusion. Merrillite occurs as a cluster of anhedral 80-620 um grains near one edge of the inclusion. The bulk composition of the inclusion, estimated from modal abundances of these minerals, is (in wt.%): 65.6% SiO_2, 0.77% TiO_2, 13.3% Al_2O_3, 0.29% Cr_2O_3, 2.7% FeO, 0.10% MnO, 4.9% MgO, 5.9% CaO, 6.6% Na_2O, 0.47% K_2O, 0.10% P_2O_5, and 0.02% S.

The size, shape, texture, mineralogy and mineral compositions of the silicate inclusion are very similar to those in IIE irons. However, preliminary INAA results on a 561 mg sample of Guin metal give the following composition: 10.6 ug/g Cr, 6.23 mg/g Co, 93.3 mg/g Ni, 198 ug/g Cu, 43.5 ug/g Ga, 15.0 ug/g As, 2140 ng/g W, 630 ng/g Re, 7.54 ug/g Ir, and 1.64 ug/g Au. Ga and Co are much too high for Guin to be a member of group IIE. Although these data are most consistent with a IIICD classification, Co, W and Ir are somehwat high and Ga somewhat low. Moreover, IIICD meteorites are generally fine or finest octahedrites or ataxites, unlike Guin. We designate Guin ungrouped pending acquisition of more data, especially Ge.

We propose the following speculative scenario for the origin of Guin and its silicate inclusion. The large euhedral 3x9 mm augite in the inclusion is normally zoned and unlikely to have grown from a shock melt. This suggests that the inclusion originally formed by an igneous process, possibly involving melting or partial melting of parental chondritic material with loss of olivine. The resultant assemblage may have consisted primarily of augite and oligoclase. A shock event melted the plagioclase in the assemblage, produced the rounded ovoid shape of the inclusion (due to surface tension) and formed the deformation lamellae in the augite. The outer layers of some augite grains were melted, enriching the melt in iron. Bronzite crystallized from this melt as an overgrowth on residual augite. Debris at the inclusion margin may have served as seed nuclei for the grains in the plagioclase ring.

The shock event injected the inclusion into a hot (possibly molten) metal segregation near the surface that may also have been produced by shock. Subsequently, the assemblage cooled slowly (but not necessarily monotonically), forming a coarse Widmanstatten structure in the metal. As the temperature fell below 500-600 C, schreibersite nucleated around the inclusion and troilite nodules. Our model for Guin is similar to the shock model proposed by Wasson et al. (1980) for the IAB and IIICD irons.

METEORITIC CONSTRAINTS ON PROCESSES IN THE SOLAR NEBULA

John A. Wood, Harvard-Smithsonian Center for Astrophysics,
60 Garden Street, Cambridge Massachusetts 02138

High-temperature events or processes in the solar nebula were required to form the chondrules and CAI's that make up the bulk of the substance of most chondrites. There is no consensus in the meteoritical community as to the nature of these high-temperature events or processes. In spite of this major area of uncertainty, however, several broad conclusions can be reached about properties of the nebula.

(1) The chondrules and CAI's were formed in regions where the dust/gas ratio was orders of magnitude above the cosmic value. This follows from the relatively high Fe^{2+} content of minerals in the chondrules and CAI's, which requires formation of these objects in an environment with O/H orders of magnitude greater than cosmic. The only way to pump up O/H to these levels is to fractionate dust from gas, then partially vaporize the dust in dust-rich zones. Oxygen released by the vaporizing (oxide) dust would temporarily increase the local O/H.

(2) After these high-temperature objects were formed, they began to accrete very promptly (a time scale of hours, probably). The texturally distinct subtypes of chondrites must reflect minor variations in the chondrule-forming and CAI-forming process. If the chondrules and CAI's, and also matrix dust, had orbited for thousands of years in the nebula before accretion, they would have mingled and the chemical and textural distinctions between subtypes would be lost. In some cases, a chemical argument can be made for rapid accretion. In C2 chondrites Fe/Si in chondrules is less than the cosmic value, and Fe/Si in matrix material is greater than cosmic, yet Fe/Si for the bulk chondrite is close to cosmic. Clearly the chondrule-forming event depleted the chondrules in Fe, but the Fe lost from them ended up in the matrix material, and the chondrules and matrix dust involved in this exchange were comprehensively accreted to restore the original cosmic abundances. This would be impossible if the chondrules and dust, which have very different physical properties, remained dispersed in the nebula for any appreciable period of time.

(3) Formation and aggregation of the chondrite components happened at the same radial distance in the nebula where chondrites reside today (the asteroid belt, ~2 AU). This follows from (2). If accretion happened rapidly, the chondrite components would not exist long enough as small particles to be moved great distances in the nebula by gas dynamic effects (e.g., from inside the present orbit of Mercury to the present asteroid belt).

(4) The ambient temperature of the nebula at that time and place was relatively low (<700 K), and was not responsible for the thermal processing of the chondrules and CAI's. Some other, transient, high-energy events or processes formed them. The C2 chondrites, once accreted, had to be stored in a relatively cool place to preserve their low-temperature matrix mineralogy. If the C2 parent bodies had spent all or part of their time near the midplane of a hot nebula, they would have been metamorphosed to anhydrous assemblages.

F-2

N85 15631

CHEMICAL EVOLUTION OF THE SOLAR NEBULA : A NEW MODEL; B.M.P. Trivedi, Arizona State University, Tempe, AZ 85287.

The common notion among cosmochemists of a hot solar nebula from which meteoritic minerals condensed is not supported by theories of star formation. A model is developed which can give the same sequence of condensation without recourse to hot solar nebula. In this model, the solar nebula was formed from the matter ejected by the Sun during its T Tauri phase(1) and the chemical condensation took place in this outflowing matter. Isotopic anomalies and the unique minerals found in meteorites may be explained by this model.

If the solar nebula formed from the mass lost by the proto-Sun, then its chemical evolution would depend on the nature of the material flow, the rate of mass flow and the intensity of the emitted radiation(UV, X-rays, proton flux etc.). Observation of T Tauri stars give the following information, which could be applicable to the proto-Sun. 1) phospheric temperature is 3500K and falls as $r^{-0.5}$ along radial direction, 2) the mass flow rate is 10^{-6} - 10^{-7} M_0 per year and is mostly in the equatorial plane, 3) the intensity of X-rays, UV and proton flux are several orders of magnitude higher than those from the present Sun. In order to calculate the condensation sequence, we need temperature and pressure at a given radial distance in the outflowing matter. The temperature would be given by $T = 3500(3.5 \times 10^{11}/r)^{1/2}$ where $3.5 \times 10^{11} = 5\ r_0$ is taken as the radius of the proto-Sun. To calculate pressure, let us assume the mass loss rate 10^{-7} M_0 per year, the expansion velocity in the neighbourhood of the Sun as 2×10^7 cm s^{-1}, the thickness of the nebular flow as 7×10^{10} cm. Using the polytropic relation we can calculate the pressure. At a distance of 2×10^{12} cm. where T = 1450 K, the pressure $p \sim 2 \times 10^{-8}$ atm and we expect Al_2O_3 to condense. As the gas expands and cools the remaining elements would condense. At $r = 3.5 \times 10^{12}$ cm , T = 1100 K and $p \sim 10^{-8}$ atm., Fe would condense. Thus all the refractory minerals would condense within the orbit of Mercury, 5.8×10^{12} cm. By the time, the outflowing matter reaches the asteroid region, the temperature would drop to 300 K and one would expect complete condensation, including volatiles. Highly reduced atmosphere could be generated near the Sun where the minerals in enstatite chondrites could form. The Ca-Al rich inclusions carrying isotopic anomalies could also be produced close to the Sun probably in the general condensation sequence after Al_2O_3. Chondrule formation requires fast heating and cooling of matter. This could be achieved through shock wave heating.

Finally there is a good possibility that the isotopic anomalies were generated during the T Tauri phase by irradiation of the outflowing matter by different kinds of radiation. The effect of UV radiation in producing oxygen anomaly has already been demonstrated by Thiemens and Heidenreich(2) and Worden et al.(3) have found that flare events during T Tauri phase produce proton flux large enough to produce anomalies like Al^{26}. It will be interesting to explore the role of radiation in producing other anomalies.

REFERENCES:

1). Trivedi, B.M.P.(1984), Ap. J., 281, 000.
2). Thiemens, M.H. and Heidenreich, J.E. (1983), Science, 219, 1073.
3). Worden, S.P., Schneeberger, T.J., Kuhn, J.R. and Africano, J.L., Ap. J., 244, 520.

HOMOGENEOUS CONDENSATION OF GASEOUS MIXTURES OF Si, Fe, O, N, and C IN RELATIVE COSMIC ABUNDANCE AND IMPLICATIONS FOR ASTRONOMICAL CONDENSATION:

J. R. Stephens, Los Alamos National Laboratory

The pressure versus temperature curves for homogeneous nucleation and condensation of two gaseous mixtures with nearly relative solar abundance of Si, Fe, O, N, and C in an excess of H have been experimentally determined. The experiments were carried out by heating mixtures of CO, $Fe(CO)_5$, H_2, SiH_4, and N_2O in Ar behind reflected shocks in a shock tube. The nucleation and condensation, which took place in the subsequent gas-dynamic expansion (cooling phase), was monitored by light scattering and turbidity, similar to Frurip and Bauer(1977), with improvements by Stephens and Bauer(1981a). Grain morphologies and crystalline phases present in the condensates were determined by electron microscopy. The elemental abundance ratios relative to Si are:

	H/C/N/O/Si/Fe/Ar
Low Fe mixture	14.5/10.0/2.8/17.5/1.0/0.79/55.5
High Fe mixture	25.0/11.7/13.8/21.4/1.0/1.8/109

The condensation temperatures for the two mixtures were similar, ranging from 4000 K at 100 torr calculated SiO pressure to 1900 K at 4 torr SiO pressure. The data fall on the same line as SiO_x condensation temperatures and are distinctly different fom condensation temperatures of Fe and Si metals reported earlier by Stephens and Bauer (1981b). The condensation curves show substantial supersaturation, well away from the "equilibrium condensation" curves calculated for these mixtures, and also are disparate from extrapolations of the condensation curves for a cosmic mixture calculated by Blander and Katz (1967) using classical nucleation theory. The condensation data reported here extrapolate well to the condensation data on SiO_x and $Mg+SiO_x$ of Nuth and Donn (1983) taken at pressures from 10^{-2} and 10^{-3} torr and temperatures below 1100 K.

These data cast doubt on the validity of both "equilibrium" and classical nucleation theoretical approaches to predict homogeneous condensation in a solar nebula or stellar atmosphere. Such approaches are not good descriptions of condensation of complex vapors under the high pressure conditions present in our experiments. The assumptions underlying the classical and "equilibrium" descriptions are less valid under astronomical conditions, as has been pointed out by Donn (1979). Other theoretical descriptions of complex gas condensation need to be formulated which more closely match the actual processes in the astronomical environments.

Blander, M. and J. L. Katz, 1967. Geochimica et Cosmochimica Acta 31, 1025
Donn, B., 1979. Astrophys. Space Sci. 65, 167
Frurip, D. J. and S. H. Bauer, 1977. J. Phys. Chem. 81, 1001
Nuth, J. A. and B. Donn, 1983. J. Chem. Phys. 78, 1618
Stephens, J. R. and S. H. Bauer, 1981a. Proceedings of the 13th International Symposium on Shock Tubes and Waves, The Niagara Frontier NY, July 6-9, 1981
Stephens, J. R. and S. H. Bauer, 1981b. Meteoritics 16, 388

N85 15633

DYNAMIC THERMAL EPISODES IN THE PROTOSOLAR NEBULA: DEVELOPMENT OF MODELS FROM OBSERVATIONS ON CAI'S; T.E. Bunch, and S. Chang, Extraterrestrial Research Division; P. Cassen and D. Hollenbach, Space Sciences Division; NASA-Ames Research Center, Moffett Field, CA 94035.

Evaluation of earlier observations (1) indicated that "layered" rims on coarse-grained Allende CAI's were possibly the result of partial melting by ablation/drag-heating and reaction of CAI exteriors with a gas or gases of non-solar composition. Bunch and Chang (2) reported the common occurrence of thin, fine-grained, matrix-like bands that at least partially surround rims of CAI's. Although material in these bands in general appear to be similar to matrix, SEM observations show them to be dissimilar in volatile element content, mineral composition and grain morphology. Moreover, they appear to be related in time of formation with rim development and Na-metasomatism of CAI's. Our observations implicate a short-lived but intense heating episode followed by rapid cooling as the mechanism responsible for these CAI features.

The fact that the sizes of CAI's seem rarely to exceed 1 cm or so in diameter makes it unlikely that more than a cm of material was typically lost during the heating event that appears to have partially melted the exteriors and produced the rims. This inference, plus the fact that the interiors of most inclusions were largely unaffected by this heat pulse, puts a strong contraint on the duration, t, of the event: $t = r^2/k < 100$ s (for r = depth of penetration of the heat pulse < 1 cm, k = thermal diffusivity = 10^{-2} cm^2/s). Relative velocities of more than several km/s are required to raise the temperature of the exterior of an inclusion to melting. The deceleration time must be no longer than 100 s to meet the constraint on the duration of the heat pulse; this requires that the inclusions encountered gas densities of about 10^{16} molecules/cm^3. Such densities are within the range likely for the solar nebula. Shorter heat pulses would require correspondingly higher densities, as might be encountered in a protoplanetary atmosphere.

It seems improbable that CAI's up to a cm in size could be transported from one thermal regime to another in the nebula rapidly enough to satisfy the constraint on t, unless very strong gradients - essentially discontinuties - were encountered. One possibility is that CAI's were decelerated by shocks either upon entry by already formed inclusions into the nebula (as proposed by Wood (3) for chondrule formation), or by passage of the inclusions through shocked regions within the nebula. Another possibility is that the inclusions were heated during deceleration into a protoplanetary atmosphere, but somehow failed to be incorporated in the protoplanet itself. In any of these schemes, apparently, the primary heating must be that associated with deceleration of the inclusions in the ambient gas. (1) T.E. Bunch and S. Chang, 1980. Meteoritics 15, 270. (2) T.E. Bunch and S. Chang, 1984. LPS XV, 100. (3) J.A. Wood, 1983. Meteoritics 18, 424.

TRACE ELEMENT ABUNDANCES IN RIM LAYERS OF AN ALLENDE TYPE A COARSE-GRAINED CA,AL-RICH INCLUSION. W. V. Boynton and D. A. Wark, Lunar & Planetary Laboratory, University of Arizona, Tucson AZ 85721.

We have measured trace element abundances in rim samples of an Allende Type A Ca,Al-rich inclusion (CAI) and find that the rim is much more refractory than the interior. This result is difficult to reconcile with some existing models for rim formation based on mineralogical data.

The rims on Type A CAI's are composed of thin layers (ranging outward) of: spinel and perovskite, melilite (often altered to nepheline and sodalite), Ti-pyroxene, diopside, hedenbergite, and andradite [1]. These rim layers are the same as those in the individual microscopic bodies making up fine-grained Group II aggregates, which were therefore suggested to be pure rim material [1]. Various origins have been proposed for these rims. Wark and Lovering [1] suggested that they were layers formed in different episodes of condensation; Bunch and Chang [2] and Wark [3] later proposed that they crystallized from a thin melt on the surface, but Wark [4] now favors an origin as non-equilibrium condensates. MacPherson et al. [5] proposed that rims formed as by-products of CAI alteration.

In addition to analyzing a pure intact rim fragment, we also generated separates of individual layers in the rim. We found the REE pattern of the interior of the CAI to be flat except for positive Eu and Yb anomalies (Fig. 1). Except for the Yb anomaly, this pattern is typical of those in Group I Type A CAI's. The rim sample also has a nearly flat REE pattern but is enriched to about 5 times the level in the interior. The rim sample, however, has negative Eu and Yb anomalies. A pyroxene separate of the rim has a REE pattern nearly identical to the bulk rim; there is thus no evidence of heavy REE enrichment, as expected for pyroxene crystal-chemical control of REE abundances. The depletion of the two most volatile REE, Eu and Yb, as well as the factor of five enrichment of the other REE, indicates that the rim is far more refractory than the interior. The rim therefore cannot have been made as a by-product of alteration, nor can it have formed as a thin surface melt.

The rim might, however, have formed as a completely independent condensate, or as a flash heating residue of the interior. We expect to be able to test these speculations more rigorously when these analyses are complete. In any event, rims appear to have had very complex origins, in agreement with previous suggestions of a very chaotic solar nebula [6].

[1] Wark D. A. and Lovering, J. F. (1977) Proc. LSC 8th, 95. [2] Bunch T. E. and Chang S. (1980) Meteoritics 15, 270. [3] Wark D. A. (1981) LPSXII, 1145. [4] Wark D. A. (1984) Chap. 8, Ph.D. thesis, Melbourne Univ. [5] MacPherson et al. (1981) Proc. LPSC 12B, 1079. [6] Boynton W. V. (1978), in Protostars and Planets, Univ. of Arizona Press.

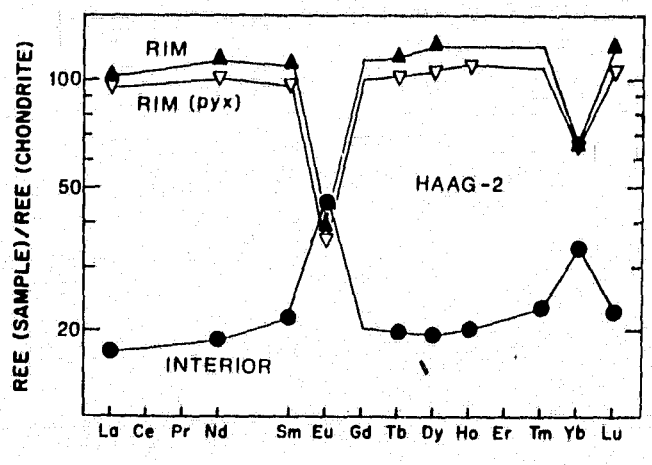

Fig. 1. REE pattern of samples from a Type A CAI. The rim is more enriched in REE and hence more refractory than the interior.

FREMDLINGE IN LEOVILLE AND ALLENDE CAI: CLUES TO POST-FORMATION COOLING AND ALTERATION; J.T. Armstrong, I.D. Hutcheon and G.J. Wasserburg, The Lunatic Asylum, Div. of Geol. & Planet. Sci., California Institute of Technology, Pasadena, CA 91125.

Fremdlinge are perhaps the most exotic and least understood objects in CAI and their very existence places severe constraints regarding formation and cooling histories of the host CAI. Following the discovery and description of Willy[1], which appears to be an "Ur-Fremdling" or prototype for smaller Fremdlinge in CAI, we have begun a systematic study of CAI of different petrographic types to see if the Fremdlinge are consistent with a common mode of formation and differing degrees of reprocessing. Fifteen type B1, B2, and compact A CAI from Allende and Leoville were selected. The relative abundance of Fremdlinge varies dramatically among CAI, however some CAI of each type and from each meteorite contain abundant Fremdlinge. The range of phase assemblages and mineral chemistries of Fremdlinge from Allende and Leoville is very similar suggesting that the parent sources for Fremdlinge were quite similar. Chemically and texturally, Fremdlinge grade continuously from complex, heterogeneous Willy-like objects to altered, homogeneous metal nuggets. Some complex Fremdlinge like Willy were found in B1 CAI; none were observed in B2 CAI.

Heterogeneous Fremdlinge, such as Willy, are comprised predominantly of euhedral crystals of V-rich magnetite (V-mt) and metal and are surrounded with well developed rims of V-rich fassaite (V-fas). The metal is Ni-rich (~ 60 wt.%) and contains Co/Ni in cosmic abundance. Minor amounts of Pt and Ir are dissolved in the metal, while Os and Ru are present in discrete domains or nuggets which are also rich in Fe and Co. Minor phases include Fe, Ni-sulfide, apatite, and W and Mo-rich oxides and sulfides. The sulfide is not in equilibrium with the metal, having different Co/Ni, Cr/Ni, and V/Ni.

Less heterogeneous Fremdlinge are composed predominantly of metal and sulfide with minor Ca-phosphate. They contain significantly less V-mt than Willy-like Fremdlinge, but typically have at least a partial, apparently residual, V-fas rim. The Ni content of the metal is variable. Metal partially formed by secondary reduction of pre-existing V-mt is depleted in Ni, Co and Pt. The sulfide appears to be in equilibrium with the metal, having the same Co/Ni, Cr/Ni, and V/Ni. The Pt content of metal appearing to be partially replaced by sulfide is higher than in Willy-like Fremdlinge. In extreme cases the Pt is exsolved into discrete Pt-Ir blebs. Os-Ru rich blebs of variable composition are also found. In some cases Fremdlinge are composed entirely of Fe-poor or Fe-absent Ni-Co-Pt metal and sulfide and may be residues of extreme oxidation or sulfidization of preexisting Ni-Fe.

In the least heterogeneous Fremdlinge the major phase is metal with minor Ca-phosphate. Fas rims and Mt are very rare and low in V. Sulfide may be present as a minor phase. The metal within individual Fremdlinge is homogeneous in composition with the refractory siderophiles dissolved in the Ni-Fe instead of present in discrete nuggets. In some CAI's these Fremdlinge occur with metal veins of similar composition radiating away from them suggesting that the metal was completely molten at one time.

All of the Fremdlinge have significant similarities suggesting common sources and formation mechanisms. Striking textural and compositional variations are, however, also readily apparent. We believe that these differences reflect the degree of reprocessing after incorporation into CAI of primary Fremdlinge typified by Willy. The basic question remains the conditions of formation of primary Fremdlinge, but it appears that textures and compositions of Fremdlinge may also help elucidate the cooling and metamorphic histories of CAI. Ref.: (1) LPSC XV, 13-14, 1984.

REFRACTORY INCLUSIONS IN AMOEBOID OLIVINE AGGREGATES IN ALLENDE; A. Hashimoto & L. Grossman, Dept. Geophysical Sci., Univ. Chicago, Chicago IL 60637.

Amoeboid olivine aggregates (AOA) are irregularly-shaped objects made mostly of olivine (Ol) with lesser pyroxene (Cpx) and feldspathoids (Fsp) (1). SEM studies (2) show aggregate textures: equant Ol crystals and clumps of crystals are enclosed by finer-grained, loosely-packed matrices of Ol plates, Cpx crystals and Fsp. Rare perovskite (Pv) + spinel (Sp) (1) were found in cores of Ol clumps (2) and were suggested (1,2) as refractory trace element carriers (3). We present more detailed SEM work on these refractory inclusions within AOA.

Although systematic searches were not conducted, ~30 refractory inclusions were examined in one AOA, TS55F1 (13mm in length), and ~10 in another, TS51F1 (7mm). The former is of special interest, as it contains the two largest inclusions seen to date. One of these, 102, is ~300μm in diameter and contains an elliptical core (~200μm in length) consisting mostly of Sp which encloses wormy melilite (Mel; Ge~90; ≤30μm) and minor Pv. Cavities tend to be associated with Mel. The Mel texture resembles that in blue spherules in Murchison (4) but the latter contain hibonite and less Mel. Surrounding the core is a 20μm-thick zone consisting of a cavity-riddled, fine-grained mixture of anorthite (An97), Sp (5%FeO), nepheline (Nep), ilmenite (Ilm) and grossular (Gr), which embays and veins the core, preferentially attacking Mel. Outside this zone is a 2μm-thick band of Fas, then a 15μm-thick band of aluminous diopside (Di). Around the entire structure and attached to it is a 30μm-thick mantle of Ol grains (≤15μm) which are zoned from Fo96 outward to Fo84. Outside of this is a narrow (5μm), discontinuous rind of hedenbergite (Hd) which separates the inclusion from the matrix.

The other large (300μm) inclusion, 101, has a core made mostly of Mel (Ge~90) enclosing odd skeletal Sp crystals (≤20μm) and rare Pv. The core is rimmed by a spherically concentric set of cavity-riddled layers that is almost identical to that in 102. Sp crystals in the first layer have the peculiar, elongated shape of those in the core but contain FeO, are rimmed by Fas and separated by Nep, An and Gr, suggesting that this layer is an alteration product of the core in which Mel was preferentially replaced by the latter phases.

Almost all other refractory inclusions studied in both AOA are much smaller than these, 50-150μm. Mel is absent from all of these, cavities tend to be more abundant and Sp more FeO-rich (≤ 12%) than in the cores of 101 and 102. Those with the least volume of cavities in the core have Fas ± Nep associated with the cavities. As the proportion of cavities in the core increases, amounts of Sp, Fas, Gr, An and Pv decrease and amounts of Ol, Nep ± Ilm increase. In the most cavity-rich, the only remaining features reminiscent of those in 101 and 102 are the outer layers of Di, Ol and Hd. In these, the cores are porous, fine-grained mixtures of Nep, Ol (Fo~90) and Ilm.

The sequence of rim layers around cores of refractory inclusions in AOA is very similar, but for the Ol layer, to that on many Allende coarse-grained inclusions. In (5), the latter were attributed to reaction of primary Mel in inclusion interiors with the nebular gas. In large refractory inclusions in AOA, we see clear evidence for formation of the first rim layer by replacement of interior Mel. Small refractory inclusions in AOA are more altered than large ones and record a range of alteration intensity. Rim layers occur on inclusions lacking Mel in their cores, but textural similarity of remaining phases to those in Mel-bearing inclusions and the presence of cavities suggest its former presence.

Refs: (1) Grossman, L. and Steele, I.M. (1976) GCA 40, 149. (2) Bar-Matthews, M. *et al.* (1979) Meteoritics 14, 342. (3) Grossman, L. *et al.* (1979) GCA 43, 817. (4) MacPherson, G.J. *et al.* (1983) GCA 47, 823. (5) MacPherson, G.J. *et al.* (1981) PLPSC XII, 1079.

THE CHEMISTRY AND ORIGIN OF REFRACTORY METAL PARTICLES FROM Ca, Al-RICH INCLUSIONS IN CARBONACEOUS CHONDRITES; B. Fegley* and H. Palme, Max-Planck-Institut für Chemie, Saarstrasse 23, D-6500 Mainz, F.R. Germany (*Permanent Address: Dept. of Earth, Atmospheric, and Planetary Sciences, MIT, Cambridge, MA 02139, U.S.A.).

Refractory metal particles from Ca, Al-rich inclusions in Allende were independently discovered by Wark and Lovering (1) and Palme and Wlotzka (2). The metal particles, which are found separately and in more complex assemblages called Fremdlinge (3), are composed of different combinations of the Pt-metals Pt, Ru, Os, Rh, Ir and W, Mo, Re, Fe, Ni. Palme and Wlotzka (2) have proposed that the metal particles are direct condensates from a gas of solar composition and presented condensation calculations for these elements. Fegley and Kornacki (4-6) have suggested that the metal particles are formed from smaller grains of metal alloys and compounds during the evaporation and melting of primitive dust aggregates.

We have started a comprehensive set of condensation calculations to assess the effect of several factors such as activity coefficients, fractional condensation, and redox state on the composition of refractory metal particles. These calculations combined with partitioning experiments (7) and observations of metal particles in refractory inclusions provide important constraints on the origin of metal particles in refractory inclusions.

Preliminary calculations indicate that at a total pressure of 10^{-3} bars, the initial alloy forms at 1921 K and is 87 % Os, 11 % Re, and 2 % W. The low W content is due to the W activity coefficient of $\simeq 7$ in the W-Os system (8) and to the high W oxide/W metal ratio ($\simeq 200$) in the gas phase. This indicates the possibility of formation of almost pure Os grains by condensation. Under more reducing conditions the initial alloy would gradually become more W-rich and form at higher temperatures.

The REE pattern of Group II inclusions can be explained by condensation from a fractionated gas, produced by condensation and removal of an ultrarefractory component. Fractional condensation calculations were done to see what metal composition would result from removal of a high temperature metal alloy at the perovskite condensation temperature (1677 K). A Mo-Ru-Ir ternary alloy is initially formed but the composition at lower temperatures is dominated by Fe and Ni. So far no such alloys have been found in Group II inclusions.

Ref.: (1) D.A. Wark and J.F. Lovering (1976) LPS VII, 912. (2) H. Palme and F. Wlotzka (1976) EPSL 33, 45. (3) A. El Goresy et al. (1978) Proc. 9th LPSC, 1279. (4) A.G.W. Cameron and B. Fegley (1982) Icarus 52, 1. (5) A.S. Kornacki and R.E. Cohen (1982) CFA preprint no. 1617. (6) B. Fegley and A.S. Kornacki (1983) LPS XIV, 187; EPSL, in press. (7) H. Palme and W. Schmitt (1984) LPS XV, 623. (8) J.K.M. Gibson (1983) LBL report, 16233.

A SCANDALOUSLY REFRACTORY INCLUSION IN ORNANS: A. M. Davis, James Franck Institute, Univ. of Chicago, 5640 S. Ellis Ave., Chicago, IL 60637.

During a search for refractory inclusions in a polished thin section of the Ornans C3 chondrite, a remarkable inclusion was found. Named "**OSCAR**", it consists of pyroxene with 15% Sc_2O_3 and 4% ZrO_2 poikilitically enclosing perovskite with 6% Y_2O_3 and 2% heavy REE, spinel and hibonite. This compact 60 μm diameter inclusion has a lobate outline and is relatively unaltered in comparison to other refractory inclusions in carbonaceous chondrites. **OSCAR** is surrounded by normal Ornans matrix and is not in contact with any other object in the plane of the thin section. A band of 1 - 7 μm perovskites follows the outline of the inclusion through two lobes, about 10 μm inside the edge. Growing within and between these perovskites are minor spinel, unknown Sc-, Zr- rich minerals and Mo-, Os-, Ir-rich metal nuggets. In the center of the third lobe is a 15x20 μm intergrowth of spinel, perovskite and hibonite. A discontinuous 2 μm band of an unknown Ca-, Al-rich silicate (possibly glass), voids and alteration products (nepheline, sodalite and fayalitic olivine) occurs 2 μm inside the edge nearly all the way around **OSCAR**. Point counting (34933 points) of a backscattered electron mosaic established that **OSCAR** has an area of 2308 μm^2 and contains, by area, 69.56% Sc-pyroxene, 15.76% perovskite, 5.54% spinel, 4.74% voids and alteration products, 1.89% hibonite, 1.61% glass, 0.83% Sc-, Zr-rich phases and 0.06% refractory metal nuggets.

The pyroxene is a fassaite, as it contains 0.97-1.01 Ca atoms per 6 O atoms. The compositional ranges found in 9 analyses are 0.3-2.8% MgO, 23.1-27.9% Al_2O_3, 18.2-24.8% SiO_2, 22.7-24.2% CaO, 14.2-16.7% Sc_2O_3, 7.1-9.8% TiO_2, 0.57-0.68% Cr_2O_3, 0.35-0.69% FeO and 2.0-5.3% ZrO_2. Sc-pyroxenes with up to 6% Sc_2O_3 occur as a rare phase in two refractory inclusions in Efremovka [1] and Essebi [2]. Minor elements found in perovskite are 2.1% Al_2O_3, 0.9% Sc_2O_3, 1.6% FeO, 5.9% Y_2O_3, 1.5% ZrO_2, 1.2% Gd_2O_3, 1.0% Dy_2O_3 and 0.5% Er_2O_3. 2σ upper limits for Ce_2O_3 and Nd_2O_3 are 0.07 and 0.12%, respectively. Hibonite contains 2.8% MgO, 0.7% Sc_2O_3, 5.6% TiO_2, 0.3% FeO and 0.3% ZrO_2. REE were not detected in pyroxene and hibonite (<0.1% Nd_2O_3 and Gd_2O_3).

Relative to C1 chondrites, bulk **OSCAR** has the following enrichment factors: Sc - $13.4x10^3$, Y - $5.1x10^3$, Zr - $5.9x10^3$, Gd - $9.0x10^3$, Dy - $5.7x10^3$, Er - $4.7x10^3$, Ce - $<1.5x10^2$ and Nd - $<3.7x10^2$. Based on Ce and measured heavy REE, **OSCAR** is enriched in heavy relative to light REE by >30 to >60 times. By this criterion, **OSCAR** is more refractory than the ultrarefractory inclusions MH-115 [3] and SH-2 [4] and may be more refractory than RNZ [5]. Condensation calculations [6, 7] have assumed that refractory lithophile trace elements condense in solid solution in major element-bearing phases such as hibonite and perovskite. If Gd and Y entered perovskite during condensation, they must have done so after only 1-2% of the perovskite has condensed. Sc and Zr should have condensed into hibonite or perovskite, but perhaps Sc-pyroxene is as stable a condensate as hibonite and perovskite. The only calcic pyroxene included in condensation calculations, diopside, condenses well over 200° C lower than perovskite and hibonite [7, 8]. Further microbeam analyses of the chemical and isotopic composition of **OSCAR** are planned.

REFERENCES: [1] A. A. Ulyanov *et al.* (1982) *LPS XIII*, 813. [2] A. El Goresy *et al.* (1983) oral presentation at 14th LPSC. [3] W. V. Boynton *et al.* (1980) *LPS XI*, 103. [4] V. Ekambaram *et al.* (1984) *GCA*, in press. [5] H. Palme *et al.* (1982) *EPSL* **61**, 1. [6] W. V. Boynton and C. C. Cunningham (1981) *LPS XII*, 106. [7] A. M. Davis *et al.* (1982) *GCA* **46**, 1627. [8] J. M. Lattimer and L. Grossman (1978) *Moon and Planets* **19**, 169.

REFRACTORY INCLUSIONS IN THE MIGHEI C2 METEORITE

Glenn J. MacPherson, National Museum of Natural History, Smithsonian Institution, Washington, D.C. 20560.

Refractory inclusions in Mighei are small (generally 100-500 μm) but abundant (>30 in 3 thin sections). Many are nodular-structured spinel-pyroxene aggregates like ones described in Murchison (1). Like the latter; those in Mighei occur mostly in two structural varieties. The most abundant kind have a banded or sinuous form, consisting of contorted and commonly discontinuous chains of spinel crystals and crystal clumps, each mantled by successive rims of phyllosilicate + calcite and aluminous diopside. Perovskite inclusions in spinel are common, but accessory hibonite is rare. The spinel is usually near-end-member $MgAl_2O_4$, but in one inclusion it has up to 4 wt % Cr_2O_3. The individual clumps in the spinel chains are not always connected and in some cases are separated by up to 100 μm of matrix; such inclusions could not have originated as melt droplets. Another feature of some of these irregularly-shaped objects is a thick, multi-layered outer mantle in which each layer consists of phyllosilicate that differs in composition from those of other layers. These layers are thickest in topographic pockets on the surfaces of the inclusions, and may be the altered equivalents of sedimentary-like rim structures on Allende inclusions (2). Members of the second type of spinel-pyroxene aggregate have a compact nodular structure, with cores consisting of dense mosaics of polygonal spinel crystals. The cores are commonly mantled by a discontinuous band of phyllosilicate + calcite and, always, an outermost rim of aluminous diopside. Rare examples have an additional mantle of forsterite + Fe metal outside of the diopside rim. In both kinds of spinel-pyroxene inclusions, the pyroxene rims commonly have a comb-like structure in which elongate pyroxene crystals are aligned perpendicular to the surface of the underlying spinel. The pyroxene does not extend into the spinel. The pyroxene probably nucleated on the surface of pre-existing solid spinel, rather than ever having been part of a spinel-pyroxene-rich melt. A new type of inclusion consists of highly porous aggregates of individual spinel crystals ($\lesssim$ 10μm) ± accessory perovskite. Pyroxene, calcite and phyllosilicate are present in some cases but, unlike the spinel-pyroxene aggregates described above, do not form well-defined rim structures. One of these inclusions contains spinel crystals with highly unusual blade-like shapes, similar to spinel in two hibonite-rich inclusions described in Murchison (3). Such shapes apparently result from the pseudomorphous replacement of hibonite by spinel. This inclusion is unusual also because it contains at one end a spinel-rich spherule. Refractory spherules like this, and of the kind described in Murchison (1,3,4), are rare in Mighei. This one consists of spinel with interstitial pyroxene, mantled by a porous rim of phyllosilicate + calcite. Although the spheroidal shape and compact texture of this object suggest that it may have solidified from a melt droplet, the irregularly-shaped and porous spinel-rich aggregate enclosing it could not have formed in this manner.

REFERENCES: (1) MacPherson G.J. *et al.* (1983), *G.C.A.* 47, p.823-839; (2) MacPherson G.J. and Grossman L. (1981) *L.P.S. XII*, p.646-647; (3) MacPherson G.J. *et al.* (1984), *L.P.S. XV*, p.503-504; (4) Macdougall J.D. (1981), *Geophys. Res. Lett.* 8, p.966-969.

TRACE ELEMENTS IN HIGH-TEMPERATURE INCLUSIONS FROM MURCHISON. V. Ekambaram, S.M. Sluk & L. Grossman, Dept. Geophysical Sci., Univ. of Chicago, IL 60637

Refractory inclusions in Murchison differ from those in Allende in being more hibonite-rich(1,2) and, in some cases, in containing corundum(3). This suggests that the former have higher nebular equilibration temperatures, also supported by these features of the former: absence of group I REE patterns, high frequency of patterns in which refractory REE are enriched relative to volatile REE and sub-chondritic Ir/Os and Ru/Re(4). We report trace element data for 7 more inclusions from Murchison, some of which are splits of those in (3).

BBT-10 is a turquoise inclusion, thus probably hibonite-bearing. Relative to C1 chondrites, the Lu/Sm, Ho/Sm, Dy/Sm and Tb/Sm ratios are 10.4, <3.0, 3.0 and 2.6, resp. These fractionations among the most refractory REE, enrichments of these elements relative to Tm and light REE, and negative Eu and Yb anomalies are traits required of the condensate component postulated to have been lost prior to condensation of group II REE patterns(4-6). As this ultrarefractory REE pattern has a lower C1-normalized Lu/Tb ratio, 4.0, than SH-2 (4) and a higher one than that in(5), it is intermediate in refractoriness between them. This part of the REE pattern indicates the presence of a lithophile component with a much higher nebular equilibration temperature than that in Allende coarse-grained inclusions, most of which have group I patterns indicating low enough condensation temperatures that all REE condensed. As in SH-2, however, the relatively low Tb/Sm ratio indicates the presence of a second REE component in BBT-10, containing relatively volatile REE. Ir/Re and Ru/Re ratios are sub-chondritic, indicating that the siderophile component also has a higher equilibration temperature than in most Allende inclusions. SH-5 is a hibonite-spinel inclusion whose texture suggests vapor-solid condensation(3). Its C1-normalized Lu/Sm, Ho/Sm, Dy/Sm, Tb/Sm and Tm/Sm ratios of 14.1, <3.0, ?.4, 1.8 and <0.9, resp., indicate the presence of an ultrarefractory REE component more refractory than that of SH-2 and addition of a slightly larger amount of volatile REE. Like other ultrarefractory inclusions, SH-5 has a large negative Yb anomaly but, unlike the former, a large positive Eu anomaly which, because of the volatility of Eu, would not be expected here unless Eu were added with the other volatile REE. Ir/Re and Ru/Re ratios are sub-chondritic in SH-5, as in BBT-10.

BB-9 is a hibonite-spinel spherule with minor melilite and perovskite(3). Enrichments relative to C1's are ~50 for light REE, 14 and <1.8 for Eu and Yb, resp., 214, 33, <4.3 and <1.7 for Tb, Dy, Ho and Lu, resp., and 282 for Tm. Thus, it has a group II pattern but differs from all those reported so far in having much higher enrichments for Tb and Tm than for light REE. This could be the result of REE condensation into BB-9 at a higher temperature than for most group II inclusions. Refractory siderophiles are enriched by factors of 5 to 17 and Ir and Ru are again depleted relative to Re compared to C1's. GR-1, a corundum-hibonite inclusion(3), appears to have a group II REE pattern but the sample taken for INAA was so small that this is uncertain.

BLUB-1, an altered hibonite-spinel inclusion(3), and MUM-4, a melilite-rich inclusion(3), have group III patterns. The former has near-chondritic Ir/Os and Ru/Re; the latter is depleted in Ir and Ru relative to Os and Re compared to C1's. OC-12, a forsterite-rich inclusion(3), is uniformly enriched in most REE by a factor of 4 to 5 relative to C1's except for positive Eu and Yb anomalies. Relatively low enrichment factors may be due to dilution of refractories by forsterite.

Refs: (1) Macdougall, J.D. (1981) GRL 8, 966. (2) MacPherson, G.J. *et al.* (1983) GCA 47, 823 (3) MacPherson, G.J. *et al.* (1984) Subm. Proc. 15 LPSC (4) Ekambaram, V. *et al.* (1984) Subm. GCA. (5) Boynton, W.V. *et al.* (1980) LPS XI, 103. (6) Palme, H. *et al.* (1982) EPSL 61, 1.

THE IDENTIFICATION OF GROUP II INCLUSIONS BY ELECTRON MICROPROBE ANALYSIS OF PEROVSKITE.

A.S. Kornacki (Shell Oil Co., Box 527, Houston, TX 77001) and J.A. Wood (Smithsonian Astrophysical Obsv., Cambridge, MA 02138)

Ca,Al-rich inclusions (CAI's) with Group II REE patterns are relatively depleted in the super-refractory lithophile trace elements (SRE), including Zr and Y (1). The recent demonstration that Mg isotopic FUN anomalies are ubiquitous in Group II CAI's (2) supports our suggestion (3,4) that SRE depletions in these inclusions manifest the "chemical memory" (5) of presolar dust populations. Additional studies of Group II CAI's seem warranted, but are hindered by the difficulty of recognizing them (since Group II REE patterns occur in all mineralogical/textural varieties of inclusions). We demonstrate that Group II CAI's can be rapidly identified by electron microprobe analysis of perovskite (*pv*), a host for the SRE Zr and Y (6). On similar grounds, proton microprobe analysis of *pv* previously has been utilized to identify Group II CAI's (7).

Six *pv* analyses in each of four CAI's whose REE patterns have been determined (1,8) show that *pv* in a Group II CAI average <0.10 wt% ZrO_2, while *pv* in each Group III and VI CAI average >0.30 wt% ZrO_2 (Table 1). Two similar populations of *pv* occur in 12 other spinel-rich Allende inclusions, on which basis we characterize CAI's with Zr-poor *pv* as Group II inclusions. Y is somewhat less useful than Zr for this identification. All *pv* within an individual inclusion tend to be either Zr-rich or Zr-poor (Fig. 1), and only two or three *pv* analyses are sufficient to accurately characterize a CAI by this technique.

We identify ~67% of Type 2 inclusions (=spinel-rich, fine-grained CAI's; 9) as Group II CAI's, in close agreement with their abundance as determined by bulk trace-element analyses (1,8,10,11). A spinel-rich nodule in a rimmed olivine aggregate (#0505) also contains SRE-poor *pv*, supporting our proposal (9,12) that the spinel-rich nodules which occur in ~25% of olivine-rich Allende inclusions are the Group II REE carrier in "fractionated AOA's" (~30% of Allende AOA's) (10,13).

Table 1. Average perovskite compositions (wt%) (number of analyses shown in parentheses)

Inclusions with SRE-rich *pv*				Inclusions with SRE-poor *pv*			
Incl	Type	ZrO_2	Y_2O_3	Incl	Type	ZrO_2	Y_2O_3
3529-46*	3A	0.60	0.11 (6)	4692§	2	0.09	0.05 (6)
3593*	3B	0.34	0.05 (6)	0505	1B	<0.05	<0.05 (3)
3529-47*	3A	0.34	0.11 (6)	0702	2	0.06	<0.05 (9)
0506	2	0.48	0.28 (7)	0804	2	0.06	<0.05 (5)
0910	3B	1.00	0.39 (5)	1303	3B	0.06	0.06 (3)
1407	2	0.59	0.12 (4)	1409	2	0.06	<0.05 (2)
1412	3B	0.53	0.12 (4)	1501	3B	0.05	<0.05 (2)
1917**	2	0.18	0.06 (6)	1508	2	<0.05	<0.05 (3)
				1922	2	0.09	<0.05 (6)

*Group III CAI †Group VI CAI
§Group II CAI **CAI with intermediate level of SRE in *pv*

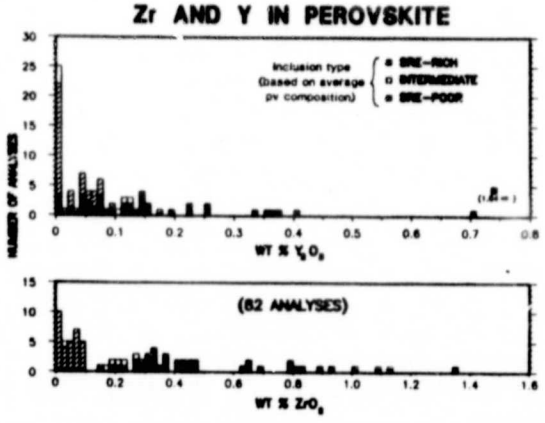

Fig. 1. SRE concentrations in *pv*.

Acknowledgements: This research was supported by NASA Grants NAG 9-28 to J.A.W. and NGL 22-009-527 to J.S. Lewis. We thank B. Mason and R.S. Clarke Jr. for the loan of USNM inclusions. A.S.K. also acknowledges technical support from Shell Oil Co.

References: (1) Mason B. and Martin P.M. (1977) *Smithson. Contrib. Earth Sci. 19*, 84-95. (2) Esat T.M. and Taylor S.R. (1984) *LPS XV*, 254-255. (3) Wood J.A. (1981) *EPSL 56*, 32-44. (4) Fegley B. Jr. and Kornacki A.S. (1984) *EPSL*, in press. (5) Clayton D.D. (1978) *Moon and Planets 19*, 109-137. (6) Kornacki A.S. (1984) *LPS XV*, 449-450. (7) Wark D.A. *et al.* (1980) *LPS XI*, 1205-1207. (8) Mason B. and Taylor S.R. (1982) *Smithsn. Contrib. Earth Sci. 25*. (9) Kornacki A.S. and Wood J.A. (1984) *Proc. 14th LPSC*, in *JGR 89*, B573-B587. (10) Grossman L. and Ganapathy R. (1976) *GCA 40*, 967-977. (11) Nagasawa H. *et al.* (1977) *GCA 41*, 1587-1600. (12) Kornacki A.S. (1983) *Meteoritics 18*, 328-329. (13) Grossman L. *et al.* (1979) *GCA 43*, 817-829.

ON THE RECORD OF GALACTIC COSMIC RAY FLUX AND TRAFFIC BREAK-UPS IN IRON METEORITES

S. Regnier, B. Lavielle,* K. Marti, G.N. SIMONOFF, Centre d'Etudes Nucléaires de Bordeaux-Gradignan, ERA 144, 33170 Gradignan-France.
* Also UCSD, Department of Chemistry, 92093 La Jolla - USA

Iron meteorites contain the record of the galactic cosmic ray intensity over a 10^2 - 10^3 Myr time scale. As early as 1962, Voshage[1] pointed out the systematic discrepancy between ^{40}K - ^{41}K cosmic ray exposure ages and other methods using radioisotopes with short half-life such as ^{39}Ar, ^{36}Cl and ^{26}Al. This discrepancy was later discussed in terms of space erosion[2] and nuclear reaction rates[3]. The most likely explanation is thought to be a "recent", 50 % increase of the galactic cosmic ray flux. Three of us[4] developed a method for calculating exposure ages of iron meteorites, which implies no assumptions about the constancy of cosmic ray flux, of exposure geometries, and of the production ratio $P(^{40}K)/P$ (isobar 40). The shielding (and time) dependent production rate of ^{38}Ar was fitted versus the $S = {}^4He/{}^{21}Ne$ parameter. Also the production ratio $M_0 = P(^{41}K)/P(^{40}K) - 0.07424\ P(^{39}K)/P(^{40}K)$ was recalculated independently and a nearly linear dependence with S was found. M_0 values differ slightly from the so-called N-parameter of Voshage[1], but the discrepancy between exposure ages clearly remains. From $P(^{38}Ar)$, exposure ages T_{38} as short as 10 Myr may be calculated. Two more indicators of complex exposure history become apparent, when the exposure age ratio T_{38}/T_K is significantly lower than 1, or when several samples of the same iron meteorite yield different T_{38} ages. About 25 % of studied irons experienced several collisions, from these indicators. Meteorites with $S > 330$ are more likely to belong to the complex population.

The T_{38} histogram is better documented than the T_K histogram and a structure appears which is group-dependent. Group I irons are distributed between 50 and 950 Myr. Almost half of group II irons have $T_{38} < 50$ Myr. Most group III meteorites belong to several peaks at 450 (mainly III E), 650 (III A) and may be 550 and 750 Myr. Group IV meteorites present a strong peak at 400 Myr (IV A). Anomalous (IRAN) meteorites look distributed. The peaks evidently imply several catastrophic traffic break-ups.

Most meteorites with $T_{38} < 150$ Myr have a T_{38}/T_K ratio clearly greater than 1. One more time, a recent increase of GCR flux should fill the gap. In this case, we could have an indication to constrain the timing of the flux change.

Alternative possible explanations to the general discrepancy are varying space erosion rates, a change in the energy spectrum of GCR, orbits out of ecliptic, or spacial (periodic) changes implying for example the galactic arms. Several models are under investigation to test some of these hypothesis and others.

References

1) H. Voshage, Z. für Naturf. 17a (1962) 422
2) O.A. Schaeffer, K. Nagel, H. Fechtig, G. Neukum, Planet. Space Sci. 29 (1981) 1109
3) S. Regnier, F. Baros, B. Lavielle, G.N. Simonoff, Meteoritics 18 (1983) 384
4) K. Marti, B. Lavielle, S. Regnier, LPSC 15th (1984) Houston

N85 15635

THE LOW-ENERGY SECONDARY COSMIC RAY FLUX: DETECTORS IN IRON METEORITES. S.V.S. Murty and K. Marti, Chemistry Dept., B-017, University of California, La Jolla, California 92093.

The cosmic ray produced nuclides in the interiors of very large bodies are mainly due to secondary particle reactions. The records of low-energy products, specifically the neutron capture products in meteorites, may provide new information regarding multi-stage irradiation and parent body breakups. Such multi-stage histories have recently been inferred for some irons (1). The nuclide pair ^{129}I - ^{129}Xe, produced chiefly through neutron capture $^{128}Te(n,\gamma,\beta)^{129}I \rightarrow {}^{129}Xe$, serves as a new chronometer, which for single exposures is independent of shielding and production rates. The study of a suitable set of nuclides should make it possible to obtain the energy spectrum of cosmic rays. Also, the ratio of protons to neutrons in the secondaries can be inferred, if high and low energy spallation products, as well as the (n,γ) products, can be unambiguously identified from similar target elements. Noble gas nuclides, in general, are the best candidates for these investigations. The troilite nodules of iron meteorites contain very low amounts of trapped gas and, because of their elemental abundance systematics of suitable target elements for low energy production of noble gas nuclides, they are ideal candidates for this purpose (2,3). We present results of a study of noble gases and nitrogen in a troilite nodule of the Cape York iron.

The small amount of cosmogenic ^{38}Ar ($\lesssim 10^{-9}$ cc STP/g) indicates very heavy shielding of this troilite nodule and the surrounding metal. Kr and Xe show excesses at masses 80, 82, 83 and 128, 129, 131 respectively. The largest ratios observed so far are $^{83}Kr/^{84}Kr = 2.59$ and $^{131}Xe/^{132}Xe = 1.34$. The most prominent target nuclides for the production of ^{83}Kr and ^{131}Xe are ^{82}Se and ^{130}Te respectively. Contributions from other target elements are small, due to lower abundances (4). Excess ^{83}Kr and ^{131}Xe, due to Se and Te, are observed in Mundrabilla troilite (2) and are used to study the neutron capture profile in Mundrabilla (3). The ratio of ^{83}Kr excess/^{82}Se to ^{38}Ar/Fe in Cape York troilite is 440, compared to a ratio of 80 in Mundrabilla troilite (2). This reflects a distinct energy spectrum and a relative increase (by a factor of 5) of the low-energy neutron component in the Cape York, as compared to Mundrabilla, pointing to heavier shielding for the Cape York sample.

References:

1. Marti, K., Lavielle, B. and Regnier, S. (1984), Lunar and Planet. Sci. Conf. XV, 511.
2. Kirsten, T. (1973), Meteoritics 8, 400.
3. Hagg, H. and Kirsten, T. (1975), Meteoritics 10, 408.
4. Jochum, K. P., Hintenberger, H. and Buchwald, V. F. (1975), Meteoritics 10, 419.

COSMOGENIC NUCLIDES IN PECULIAR METEORITES; K. Nishiizumi[1], D. Elmore[2], and J. R. Arnold[1], [1]Dept. of Chemistry, Univ. of Calif., San Diego, La Jolla CA 92093, [2]Nuclear Structure Research Lab., Univ. of Rochester, Rochester NY 14627.

At present we have much data on production of cosmogenic radionuclides in meteorites of moderate pre-atmospheric size, perhaps in the range of 1-1000 kg. Two or more cosmogenic nuclides in the same meteorite give us the size, exposure age and the terrestrial ages of the objects. The combination of accelerator mass spectrometry (^{10}Be and ^{36}Cl) and neutron activation (^{53}Mn) allow us to measure very low activities in meteorites which could not be measured previously. We are beginning a systematic search for peculiar meteorites which contain a very small amount of cosmogenic radionuclides due to several reasons.

New ^{53}Mn, ^{10}Be, and ^{36}Cl data for several meteorites are given in Table 1. The activity levels of the fresh fall Bogou are also listed as references because it contains typical concentrations of cosmogenic nuclides. (1) Long terrestrial age: A very low concentration of ^{36}Cl along with a relatively high concentration of ^{53}Mn indicates that the meteorite spent a long period on the earth. This feature is very common among Antarctic meteorites. Some of the iron meteorites have been known to have long terrestrial ages [1]. We found three iron meteorites with terrestrial ages over one million years: Tamarugal (3.6 My), Ider (2.5 My), and Negrillos (1.7 My). These meteorites have cosmic ray intensity records only before 1.7 My. (2) Large preatmospheric size: Very low cosmogenic nuclides, both ^{53}Mn and ^{36}Cl, indicate that the meteorite was heavily shielded from cosmic ray bombardment in space. Antarctic meteorite Derrick Peak is known to be a shower, with fragments labelled DRP78001-78009. Based on the low ^{53}Mn result, the preatmospheric diameter of this group of Derrick Peak iron meteorites was more than 3 m. The lowest amounts of cosmogenic nuclides were found in the Brenham pallasite. The preatmospheric diameter of Brenham was more than 6.5 m. This is consistent with ancient results from our laboratory [2]. Fuse and Anders explained that low ^{26}Al activity (5.7% of saturation value) in Serra de Mage (USNM839) was due to multi-stage irradiation [3]. However, our ^{53}Mn and ^{10}Be results in two different specimens of Serra de Mage indicate that this meteorite also had large preatmospheric size (4 m in diameter).

Further preliminary results will be presented at the meeting.

[1] Chang C. and Wänke H. (1969) in Meteorite Research (ed. Millman P. M.), pp. 397-406. Reidel Publishing Company Holland.
[2] Honda M., Umemoto S. and Arnold J. R. (1961) J. Geophys. Res. 66, 3541-3546.
[3] Fuse K. and Anders E. (1969) Geochim. Cosmochim. Acta 33, 653-670.

Table - 1.

Meteorite	Class	Recov. Mass (kg)	^{53}Mn dpm / kg (Fe+1/3Ni)	^{10}Be dpm / kg sample	^{36}Cl dpm / kg metal
Bogou	IA	8.8	471 ± 20	5.11 ± 0.41	22.2 ± 0.7
Ider	IIIA	140	280 ± 11	1.43 ± 0.07	0.071 ± 0.003
Negrillos	IIA	28.5	187 ± 8	0.37 ± 0.03	0.469 ± 0.018
Tamarugal	IIIA	320	170 ± 7	0.24 ± 0.02	0.0057± 0.0009
DRPA78008	IIB	59.4	2.7± 0.2		0.033 ± 0.004
DRPA78009	IIB	138.1	65 ± 3		0.198 ± 0.013
Brenham	Pal	>2000	0.81± 0.05		0.0173± 0.0013
Serra de Mage (USNM839)	Euc	2	42 ± 7	1.17 ± 0.06	
Serra de Mage (Paris 1606)	Euc	2	158 ± 9	6.24 ± 0.31	

^{22}NA, ^{60}CO AND LONG-LIVED COSMOGENIC RADIONUCLIDES IN METEORITE FALLS

U.Herpers and P.Englert
Institut für Kernchemie der Universität zu Köln, D-5000 Köln 1

Cosmogenic radionuclides were measured in seven fragments of the four meteorites Acapulco, Jilin, Nuevo Mercurio and Tuxtuac, which all fell within three years between 1975 and 1978. ^{22}Na (T=2.602a), ^{60}Co (T=5.272a), ^{26}Al (T=7.2x 10^5a) and ^{53}Mn (T=3.8x10^6a) were determined by nondestructive gamma-coincidence-counting techniques and radiochemical neutron activation analysis. Some results are given in table 1. Rare gas concentrations in aliquots of our

Meteorite	Date of Fall	Class	Sample	Recovered Mass [kg]	^{22}Na t=0 [dpm/kg]	^{26}Al [dpm/kg]	^{60}Co t=0 [dpm/kg]
Acapulco	8-22-1976	H	F6C	1,9	62±9	49±7 [5]	-
Jilin (Kirin)	3- 8-1976	H5	A	>4000	106±16	25±4	50±6
			B		98±15	35±5	209±21
			F		117±21	21±5	153±19
			Puchelt		133±15	38±4	149±18
Nuevo Mercurio	12-15-1978	H5	WIII,GI	>5	110±26	73±11	29±6
Tuxtuac	10-16-1975	LL	C204.1g	4,2	150±36	46±6	6±0,6

Table 1: ^{22}Na-, ^{26}Al- and ^{60}Co-concentrations of the meteorites included in this study

Acapulco and Jilin samples are described elsewhere [1,2]. Most of the meteorites analysed show very high activities of the short-lived ^{22}Na, which corresponds to their fall close to the minimum of the 11 years solar cycle in 1976-77 [3]. The apparently low ^{22}Na and ^{26}Al activities of Acapulco are caused by the location of our sample close to the surface of the preatmospherically small object [1,5]. The ^{60}Co-activity of Acapulco was below the detection limit. Shielding effects within the large body of Jilin, as documented by the high ^{60}Co-concentration between 50 to 209 dpm/kg, and a two stage exposure history [4] are responsable for their low ^{26}Al activities. The ^{60}Co-activity of (29±6) dpm/kg indicates that the preatmospheric size of the body, which caused the Nuevo Mercurio shower, must have been considerable, though the recovered mass is only about 5 kg. Tuxtuac (6±0.6 dpm ^{60}Co/kg) may have been a meteorite only slightly larger than Acapulco, however, its ^{22}Na activity is higher than expected for a small meteorite.

Acknowledgements
The authors wish to thank J.C.Lorin, Z.Ouyang, F.Begemann, H.Puchelt, E.Scott and K.Keil for providing the meteorite samples. This work was supported by the Bundesministerium für Forschung und Technologie.

References
[1] H.Palme, L.Schultz, B.Spettel, H.W.Weber, H.Wänke, M.Christophe Michel-Levy and J.C.Lorin, Geochim.Cosmochim.Acta 45, 727 (1981). [2] H.Weber, O.Braun and F.Begemann, Meteoritics 14, 588 (1979). [3] J.C.Evans, J.H.Reeves, L.A.Rancitelli and D.D.Bogard, J.Geophys.Res. 87, 5577 (1982). [4] G.Osadnik, P.Englert, U.Herpers and W.Herr, Meteoritics 16, 371 (1981). [5] P.Englert, U.Herpers and W.Herr, Proc.Lunar Planet.Sci. 12B, 1209 (1981)

^{26}Al, ^{60}Co, ^{53}Mn AND ^{22}Na PROFILES IN THE JILIN DRILL CORES.

G. Heusser, Z. Ouyang, E. Pernicka, W. Yi, W. Hampel and T. Kirsten,
Max-Planck-Institut f. Kernphysik, P.O.B. 103980, 6900 Heidelberg, F.R.G.

The size of the Jilin meteorite and, in particular, of its intact main mass (about 1.2 t) are exceptional for stones. Its two stage exposure history with a 2π geometry near the surface of its parent body and a 4π geometry after being expelled is well established (1,2). This exceptionality makes Jilin an interesting object for studying the systematics of cosmic ray-produced nuclides in stony meteorites.

Samples of two drill cores (3) have been analyzed for ^{26}Al, ^{60}Co, ^{53}Mn, and ^{22}Na activities. Drill core A has the direction perpendicular to the first stage surface. The other core, B, was oriented in parallel with that surface. Both cores meet the center of the second stage irradiation. ^{26}Al, ^{22}Na, and ^{60}Co were measured by three- and two-dimensional gamma-ray spectroscopy. ^{53}Mn was determined in the metallic phase by neutron activation.

In Fig. 1 the measured activities of ^{26}Al, ^{60}Co, and ^{22}Na (preliminary results) in core A are plotted against the distance from the entrance point of the core in the direction to the center of the last stage and towards the first stage surface. ^{60}Co increases with increasing shielding depth as expected from the model of Eberhardt et al. (4). ^{22}Na is constant within its error bars, whereas ^{26}Al increases due to the contribution from the first stage irradiation. The activity profiles of Jilin reconstructed from the drill cores and from other samples differently shielded during both stages are compared to calculated production rates.

(1) Honda M., Nishiizumi K., Imamura M., Takaoka N., Nitoh O., Horie K. and Komura K. (1982) Earth Planet.Sci.Lett., 57, p. 101-109.
(2) Heusser G. and Ouyang Z. (1981) Meteoritics, 16, p. 326-327.
(3) Heusser G., Kirsten T. and Ouyang Z. (1983) Meteoritics, 18, p. 312.
(4) Eberhardt P., Geiss J. and Lutz H. (1963) in Earth Science and Meteoritics (eds. J. Geiss and E.P. Goldberg), p. 143-168.

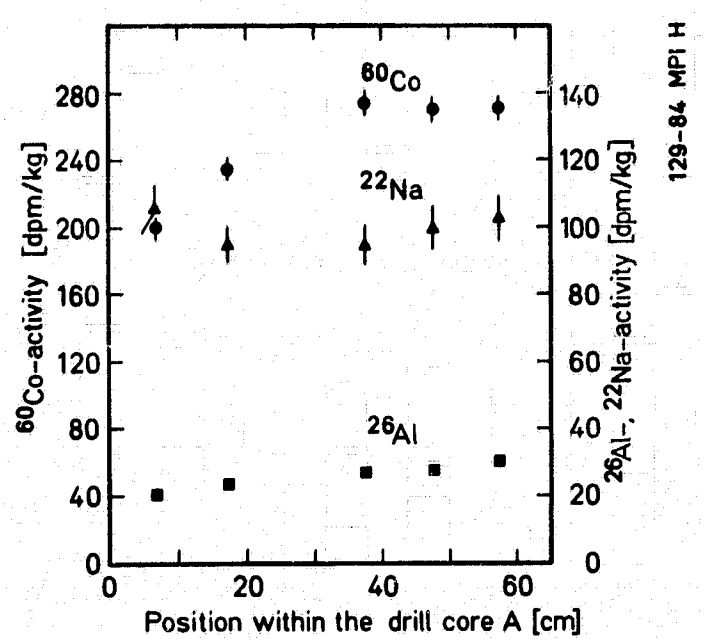

Fig.1: ^{26}Al, ^{60}Co and ^{22}Na in drill core A

COSMOGENIC RECORDS IN ANTARCTIC METEORITES-II; J. N. Goswami[1], K. Nishiizumi[2], and J. R. Arnold[2], [1]Physical Research Laboratory, Ahmedabad 380 009, India, [2]Dept. of Chemistry, Univ. of California, San Diego, La Jolla, CA 92093.

Studies of nuclear track records and ^{53}Mn activities in chondritic meteorites from the Antarctic meteorite collection are continued. Results obtained from the initial study of a set of about thirty meteorites were presented earlier(1). We have now extended this study to include about two dozen additional chondrites. Aliquot samples were used for nuclear track and ^{53}Mn studies. The data have been analyzed to obtain information on the cosmic ray exposure history of Antarctic meteorites, magnitude of their atmospheric mass-ablation and to check on the proposed pairing of some of these meteorites. An intercomparison of data from Antarctic and non-Antarctic meteorites will be presented.

Identification of Antarctic meteorites with small preatmospheric size (<10 cm) have also been attempted. This information will be extremely useful in consolidating our knowledge of the primary mass-spectrum of meteoroid in the cm to decimeter region, and to refine our understanding of production of cosmogenic nuclides in small objects exposed in space. The starting material for this study was a set of Antarctic meteorites with recovered mass less than 15 gm, that have already been studied for their petrographic records (2) and the possible survivors from individual falls. Nuclear track studies of spot samples taken from near center and the perimeter of about two dozen selected H and L chondrites, however, indicate that most of them were not fragments from small (<10 cm) meteoroids. Four specific samples having higher track densities were considered as suitable candidates for further investigation to check if they were indeed fragments of small meteoroids. Experimental approach used in this study and the preliminary results will be presented at the meeting.

(1). Goswami J. N. and Nishiizumi K., EPSL 64, 1-8, 1983.

(2) Keil K. (Personal communication), 1982.

^{53}MN IN MAIN FRAGMENTS OF THE NORTON COUNTY METEORITE

P.Englert and R.Sarafin
Institut für Kernchemie der Universität zu Köln, D-5000 Köln 1

The Norton County aubrite, which fell in 1948, was the largest stony meteorite known (preatm. mass ~3600 kg [1]) until the fall of the Jilin chondrite (preatm. mass ≥4000 kg [2]) in 1976. For the study of cosmic ray interaction effects it is valuable because, in contrast to Jilin, it was subjected to a very long and presumable one stage irradiation history [3]. As coring of the friable main fragment of the achondrite (mass ~1070 kg) might result in severely damaging the specimen, only surface samples were taken. Of the McKinley fragment also interior samples were available.

We have measured cosmogenic ^{53}Mn ($T_{1/2}$ = 3.8 x 10^6 a) in 10 Norton County samples. Five of them were taken from main fragment locations where cosmic ray tracks have been determined previously [1]. The abundance of iron, the main target element for ^{53}Mn production, is very low in aubrites. Therefore, enriched samples were prepared by handpicking and magnetic separation of dispersed metal. Starting with samples of 150 - 550 mg separates of 10 - 80 mg (45 - 68 % Fe) were obtained. A 44 mg chip from a large metallic inclusion was also investigated.

The figure shows the results of our ^{53}Mn-measurements as a function of the observed track density in pyroxenes. With decreasing track density the ^{53}Mn concentrations increase from 413 to a maximum of 559 dpm/kg Fe, which exceeds the ^{53}Mn center activities observed in the cores of the St.Severin and Keyes chondrites [4,5]. This behaviour is not compatible with theoretical predictions for spherical meteorites with preatmospheric masses of more than 3000 kg [e.g. 6].

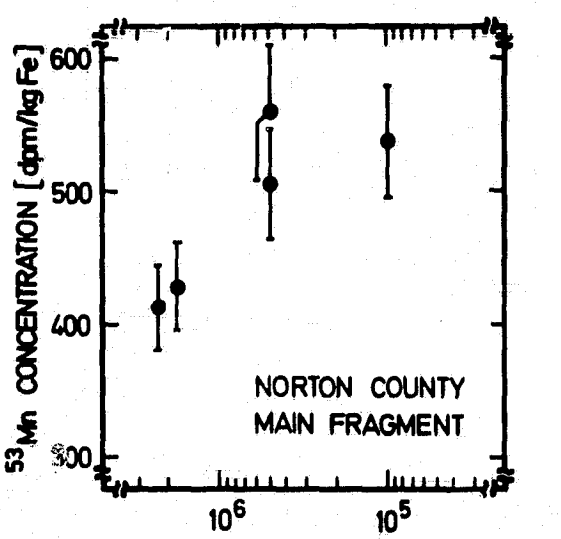

Acknowledgements
The authors wish to thank E.Scott, L.LaPaz and K.Keil for their assistance and for providing the samples. This work was supported by the Bundesministerium für Forschung und Technologie.

References
[1] N.Bhandari et al., Nucl.Tracks 4, 213-262 (1980). [2] M.Honda et al., Geochem.J. 14, 83-89 (1980). [3] G.F.Herzog et al., J.Geophys.Res. 82, 3430-3436 (1977). [4] P.Englert and W.Herr, Earth Planet.Sci.Lett. 47, 361-369 (1980). [5] P.Englert, Lunar Planet.Sci.Conf.XV, Abstr. 248-249 (1984). [6] T.P.Kohmann and M.L.Bender, in: High Energy Nuclear Reactions in Astrophysics, B.S.P.Shen (ed.), 169-245 (1967).

COSMOGENIC NUCLIDES IN A CROSS SECTION OF THE 300 KG KNYAHINYA CHONDRITE. R. Wieler, P. Signer, ETH Zürich, 8092 Zürich, Switzerland; U. Herpers, R. Sarafin, Univ. Cologne, 5000 Cologne, FRG; G. Bonani, H. J. Hofmann, E. Morenzoni, M. Nessi, M. Suter, W. Wölfli, ETH Zürich, 8093 Zürich, Switzerland.

We determined the production rates of 10-Be and 26-Al relative to those of He, Ne and Ar as a function of shielding in a cross section of the main fragment of the L5 chondrite Knyahinya. Weighing 293 kg, this stone, nearly totally covered by fusion crust, is one of the largest single chondrite pieces. It amounts to about 60 % of the total recovered mass of this meteorite. Upon impact, the fragment broke into two almost symmetrical parts. The diameters of the thereby exposed cross section range between 40 and 55 cm. Dr. G. Kurat kindly allowed us to take about 20 samples spread over the cross section. They were splitted into aliquots for the mass spectrometric analysis of He, Ne, and Ar, and the determination of 10-Be and 26-Al by accelerator mass spectrometry. The noble gas data are summarized here, the AMS determinations are in progress.

The correlation between the ratios 3-He/21-Ne and 22-Ne/21-Ne, known to be irradiation hardness indicators, are shown in Fig. 1. The open symbols represent the data from five 100 mg sized aliquot samples taken from a small Knyahinya fragment. The reproducibility of the noble gas concentrations in these aliquots are ±0.4%, ±2%, and ±2.5% for 3-He, 21-Ne, and 38-Ar, respectively. Weights for the other samples ranged between 150 and 200 mg.

21-Ne concentrations increase from the lowest towards the highest shielding by about 20%. The slope of the best fit straight line through the Knyahinya data (heavy line) is 20.8±1.6 and agrees with that of 23.4 ±2.4 for the "Bern-Line" (1) obtained from various chondrites. The Knyahinya line is, however, distinctly steeper than the correlation lines obtained on the L chondrite Keyes (3) and the LL chondrite St. Severin (4) (slopes of 13.6 ± 2.0 and 9.8 ± 1.9, respectively). To what extent these differences signal intrinsic properties of spallation systematics, secondary break-up, or interlaboratory biases is unclear and deserves further attention. Note that the extreme values of the 22-Ne/21-Ne ratio are lower for Knyahinya than for either Keyes or St. Severin, indicating a larger mean shielding of the Knyahinya samples. The distance between the samples with the lowest shielding (##8, 10, and 16) and the most heavily shielded one (#17) is 30 - 50 cm. All these samples are from about 1 cm below the fusion crust, showing that one side of the main fragment was close to the center of the meteoroid.

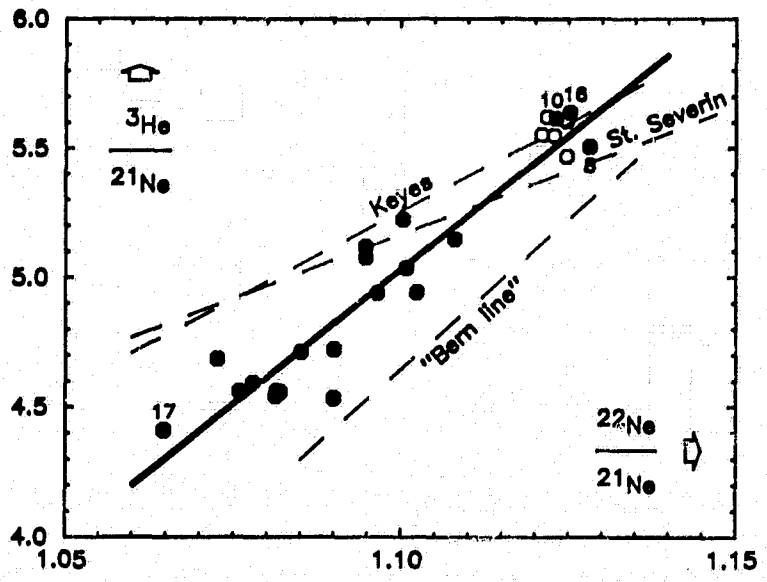

Refs: 1) Eberhardt et al, (1966) Z. Naturf. 21a, 414. 2) Wright et al., 1973 JGR 78, 1308. 3) Schultz and Signer, (1976) EPSL 30, 191.

Work supported by the Swiss National Science Foundation and The Bundesministerium für Forschung und Technologie.

THE IRRADIATION HISTORY OF DHURMSALA METEORITE, J.T. Padia, M.N. Rao, J.N. Goswami, Physical Research Laboratory, Ahmedabad 380 009, India and P. Englert, U. Herpers, Institute fur Kernchemie, University of Köln, Köln, FRG.

In Dhurmsala (LL6) Chondrite, Al-26 and Mn-53, particle tracks, He, Ne and Xe isotopes were measured in documented samples (over a distance of ~13 cm) from a single Dhurmsala fragment. Here we report data on He, Ne and Xe in three samples analysed at 600°C and 1600°C. Sample 1 is located near the fusion crust and samples 6 and 5 are located about 6.4 cm and 12.4 cm away from crust position respectively.

The He-3 found in samples 1, 6 and 5 are 14.09, 14.57 and 13.14 (all gas concentrations are given in units of 10^{-8} cc STP/g) respectively. Earlier Eberhardt et al. (1966) measured He-3 in some samples of Dhurmsala and found a value of 14 ± 0.7. The He-3/Ne-21 ratios in these three samples are 3.06, 3.07 and 2.77 respectively, which indicate loss of cosmogenic He-3. If we use the He-3 production rate of 2.46 x 10^{-8} cc STP/g m.y. for LL chondrites (Cressy and Bogard, 1976), we get a He-3 exposure age of 5.7 m.y. for Dhurmsala, on the average. The Ne-21 found in samples 1, 6 and 5 are 4.6, 4.7 and 4.8 respectively. Also the Ne-22/Ne-21 ratios in these samples are 1.075, 1.079 and 1.079 respectively. Earlier Eberhardt et al.(1966) measured a value of 1.075 in another Dhurmsala sample but the Ne-21 found by them was 4.65± 0.12. If we take the preatmospheric depth of sample 5 to be 20 cm based on neon ratio and use a depth dependent production rate of 0.37 x 10^{-8} cc STP/g. m.y. (Bhandari and Potdar, 1982), the Ne-21 based exposure age turns out to be 12.8 m.y. In sample 5, Xe isotopic composition was measured. The 131/132 ratio is found to be 0.8056 which does not show any neutron produced Xe-131 excess. The 129/132 ratio is 1.315 which indicates the presence of radiogenic Xe-129 excess. The 126/132 ratio of 0.0057 for this sample shows spallogenic Xe contribution.

The Mn-53 values measured in samples 1, 6 and 5 of Dhurmsala are 366 ± 21; 377 ± 16 and 410 ± 20 dpm/kg Fe respectively. The Al-26 values found in above samples are 64 ± 1.9; 61.1 ± 1.8 and 69.3 ± 4.8 dpm/kg respectively (Englert et al. 1982). The trend followed by these three samples is in general, consistent with that observed in the case of Ne-21.

In these three samples, the Ne-22/Ne-21 ratio does not vary much and this ratio indicates very deep shielding which is consistent with the track data for these samples. Based on all these results, we infer that the preatmospheric radius for Dhurmsala is about 50 cm and the samples under study seem to originate at a depth of ~ 20 to 30 cm location in that body.

References: Bhandari N. and M.B. Potdar (1982) E.P.S.L., 57, 143
Cressy P.J., Jn. and D.D. Bogard (1976) G.C.A., 40, 749
Englert P. et al. (1982) 5th Int'l Conf. Nikko Japan, 89
Eberhardt P. et al. (1966) Z. Naturf, 21A, 414.

SOLAR COSMIC RAY PRODUCED NEON IN LUNAR SOILS AND THEIR IMPLICATION FOR GAS-RICH METEORITE STUDIES, C.M. Nautiyal and M.N. Rao, Physical Research Laboratory, Ahmedabad 380 009, India.

Characteristic neon isotopic ratios, produced due to solar cosmic ray spallation (SCR) in lunar soils, are useful in deciphering and estimating the relative contributions of SCR and GCR spallation. To delineate these features, we have mass spectrometrically analysed etched mineral grains from mature and immature lunar soils, 14148 and 61221 respectively. Three size fractions of feldspars from soil 61221 and one size fraction of feldspars from soil 14148 were etched chemically (to a depth of several microns) to remove the surficial solar wind and stepwise heated using standard mass spectrometric procedures. The percentage of irradiated grains in 14148 is $\sim$90% and that in 61221 is $\sim$ 12%. All the points of 61221 feldspars, define a single line which passes through the GCR-end point on one side and the SF-Ne end point ($^{20}Ne/^{22}Ne$ = 11.6 + 0.2) on the other. The SF-Ne composition deduced in this work agrees with that obtained from our etched lunar pyroxene studies earlier (soils 24087 and 14148, two size fractions) (Nautiyal et al.,1983). The data points for mature soil 14148 define a line which significantly deviates from the 61221 tie line. This deviation is attributed to the presence of SCR spallation component.

In this context, we have studied neon isotopic compositions (step-wise heating) in Pantar and Leighton dark portions and compared these data with those of Fayetteville (Black, 1972). We find that the meteorite data points (Fig.1) deviate significantly from the tie line joining SF-Ne and GCR (pyroxene) end points. Based on our reasoning above, we attribute this deviation to SCR-spallation in gas-rich chondrites. However, in this case, this deviation could also be explained by a ^{22}Ne-enriched phase or by the addition of a carbonaceous chondrite component. The difficulties involved in various hypotheses are presented.

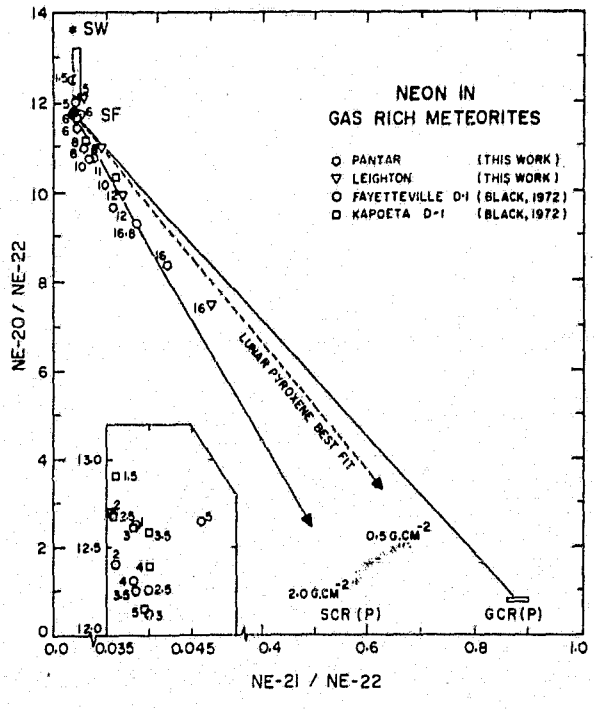

FIG.1.

References:

Black (1972) G.C.A. 36, 347.

Nautiyal et al. (1983) LPSC XV, 544.

SOLAR WIND AND COSMIC RAY IRRADIATION OF GRAINS AND ICES - APPLICATION TO EROSION AND SYNTHESIS OF ORGANIC COMPOUNDS IN THE SOLAR SYSTEM. Rocard F., Bénit J., Bibring J-P., Meunier R., and Vassent B., Laboratoire René Bernas, 91406 Orsay Campus, France

We have shown that the SW and CR irradiation of grains induces physical and chemical effects including their erosion and the synthesis of molecular compounds within the implanted layers (1). In this paper, we present the experiments performed with H_2O ice implanted by keV ions, intended to simulate the irradiation of comets, ring grains and satellites of outer planets, either by the primitive solar particles or by contemporary solar wind (SW) or solar cosmic rays (SCR) fluxes. The detection of molecules is obtained through in-situ infrared spectroscopy.

Thin films of H_2O ice, with thicknesses of a few thousands of Å, are made onto a KBr substrate maintained at liquid nitrogen temperature within a vacuum chamber, and implanted with D, He, ^{12}C, ^{13}C, ^{15}N, with fluences up to 10^{17} cm^{-2} and keV/uma energies. The spectra are obtained with a Nicolet MXS Fourier Transform Spectrometer, coupled with a LeCroy 3500 computer. This system is on line with an ion implanter. Moreover, the possibility of storing repetitive spectra allows the detection of synthesized molecules, down to levels smaller than 10^{14} molecules cm^{-2}.

In the 4300-400 cm^{-1} range, the H_2O ice presents a number of spectral features, around 3250 cm^{-1}, 830 cm^{-1}, 1620 cm^{-1} and 2250 cm^{-1}, in decreasing order of intensity. The erosion rates are measured by in situ observation of the decrease of the H_2O absorption bands.

After ^{12}C and ^{13}C implantations, the most intense lines that appear are those of $^{12}CO_2$ and $^{13}CO_2$, at 2340 and 2275 cm^{-1} respectively. As in the case of C implantation into silicates (2), the bands corresponding to implanted species are different from those of gaseous ones: instead of the usual P-R double structure due to vibration-rotation transitions, we observe single bands for implanted species; moreover, these bands are slightly shifted towards smaller wavenumbers in comparison with the center of the gaseous double structure. In contrast with the implantation within SiO_2, CO_2 remains the dominant C compounds at high fluences, instead of being partly transformed into CO.

It is interesting to note that hydrocarbides are not the dominant species upon the implantation of C into H_2O. Thus, the observations of CO and CO_2 in cometary tails, in large excesses as compared with molecules or radicals containing C-H boundings, would be consistent with an irradiation origin for the carbon chemistry in comets. Our experiments would also indicate that the primary molecules are CO_2, CO resulting from their partial photodissociation within the coma.

We propose a model for the formation of organic matter within icy solar system bodies, in agreement with our experimental results of erosion rates. The organic molecules, frozen-in within the icy mantles of the grains present in the protosolar nebula, would originate from their primitive irradiation. Such an irradiation would have taken place during an early stage of the proto-sun, when both the SW and SCR particles were by orders of magnitude more intense.

(1) Bibring J-P. and Rocard F. (1982), Ion implantation phenomena in space, Rad. Effects, 65, 159-165

(2) Rocard F. and Bibring J-P. (1982), Molecule formation by implantation in insulators, Phys. Rev. Lett., 48, 25, 1763-1766

COMPOSITIONS OF 7 ALLAN HILLS POLYMICT EUCRITES AND ONE DIOGENITE. Arch M. Reid and A.P. le Roex, Department of Geology, University of Cape Town Rondebosch, South Africa.

Bulk compositions were determined by X-ray fluorescence analysis of 7 Allan Hills polymict eucrites (ALHA 76005, 77302, 78040, 78132, 78158, 78165, 79017), one diogenite (ALHA 77256) and the eucrite Jonzac.

Despite small sample sizes (1-2g) and the polymict character of the eucrites, the bulk compositions show a restricted range in composition (Figure 1). The analyses of 76005 and 78132 are virtually identical and these appear to be fragments of the same meteorite. The two small eucrite samples 78158 and 78165 are also identical in bulk composition.

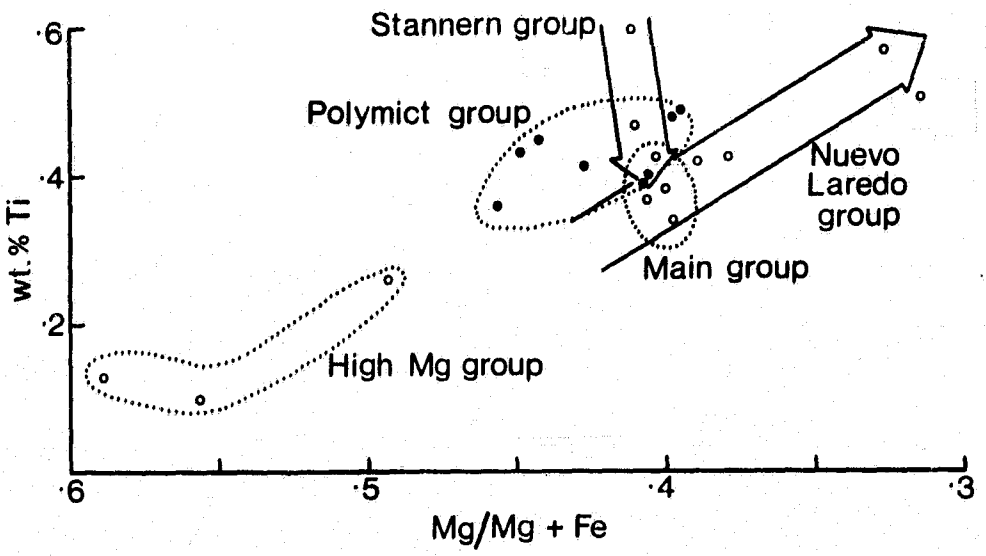

Figure 1. Plot of Ti (wt%) versus Mg/Mg+Fe (atomic). Closed circles are Allan Hills polymict eucrites plus Macibini. Open circles are monomict eucrites.

Petrographically the seven Allan Hills polymict eucrites are mixtures of fragments of cumulate materials and basaltic liquids. Chemically they may be derivatives from a single parent melt or from a small number of closely similar melts. The average Allan Hills polymict eucrite is closely comparable in composition to the main group eucrites (e.g. Sioux County) but somewhat enriched in incompatible elements. The average composition plots on the 'Stannern trend' (Figure 1) and the source liquids for the Allan Hills eucrites could derive from the same source region as the main group eucrites, but represent smaller degrees of partial melting. Alternatively these polymict eucrites could be mixtures of a wider range of eucritic materials, but including a 'Stannern-type' component.

COMPARISON OF CHEMICAL COMPOSITIONS OF YAMATO POLYMICT EUCRITES. T. Fukuoka, Department of Chemistry, Faculty of Science, Gakushuin University, Mejiro, Toshima-ku, Tokyo 171, Japan.

More than 5,000 specimens of meteorites were collected on the Antarctic ice field by both Japan and U.S. teams since 1969 (1). These collections include a large number of polymict eucrites which are typical achondrites in the Antarctic meteorite collection. Most of the specimens of the polymict eucrites are probably pieces of some falls. In order to know the number of meteorite falls for the Yamato polymict eucrites, the comparison of the chemical compositions of matrices of polymict eucrites is one of the useful tools because it is considered that the chemical compositions of matrix represent the average chemical compositions of polymict eucrite.

In this study, the abundances of 23 major, minor, and trace elements (Ti, Al, Fe, Mg, Ca, Na, Mn, Cr, V, Co, Sr, Ba, Sc, La, Nd, Sm, Eu, Tb, Yb, Lu, Hf, Th, and Ta) in 22 samples of matrices from 12 Yamato polymict eucrites (Table 1) have been determined by instrumental neutron activation analysis (INAA) for the above purpose. The matrix samples were provided from National Institute of Polar Research of Japan. The small chips of clasts were excluded from the sample specimens under a binocular type microscope to eliminate chemical effect from the clasts prior to INAA.

On Y74159, Y790020, and Y790122, the trace element compositions, especially rare earth elements (REE), of three samples from the same meteorite showed the different values one another over the analytical errors, although the major chemical compositions were not so different. In this case, we used the highest values for composition of the results for REE considering the weathering effect as pointed out by Shimizu et al. (2). We preliminarily distinguished twelve Yamato polymict eucrites into five groups (A, B, C, D and E, shown in Table 1) by the chemical compositions. Takeda et al.(3) distinguished those into three groups based on the mineralogical investigations. Our preliminary conclusion is generally consistent with them.

Table 1.

Name	No.of Anal.	Chem.group (Prelim.)
Y74159	3	A
Y74450	1	D
Y75011	1	A
Y75015	1	A
Y790006	1	A
Y790007	3	B
Y790020	3	B
Y790113	1	B
Y790122	3	A
Y790260	3	C
Y790266	1	C
Y791186	1	E

References:
(1) Yanai, K. compiler (1981) Photographic Catalog of Selected Antarctic Meteorites, p. 4.
(2) Shimizu, H. et al. (1983) Mem. Natl. Inst. Polar Res., Spec. Issue 30, 341-348.
(3) Takeda, H. et al. (1984) Ninth Symposium on Antarctic Meteorites, p.20-21.

POLYMICT EUCRITE ALHA81011: EQUILIBRATED CLASTS IN A GLASSY MATRIX. Allan H. Treiman, Lunar and Planetary Laboratory, University of Arizona, Tucson, AZ 85721, USA.

The polymict eucrite ALHA81011 is a suevite breccia of equilibrated basaltic and metamorphic fragments in a matrix of dark, vesicular glass (1). Although the meteorite resembles some lunar breccias, the FeO/MnO ratios of pyroxenes and glass ($\sim$35) are characteristic of the eucrites. The matrix of ALHA81011 resembles glasses in the Kapoeta and Malvern howardites (2).

Clasts in ALHA81011 are mostly of gabbroic and hornfelsic lithologies with subordinate basalts (variolitic and ophitic). All clasts show some textural re-equilibration (polygonized grains, 120° grain junctions) and the hornfelses retain little igneous texture. Some hornfels fragments may be metamorphosed breccias. Mineral compositions are uniform throughout the meteorite: plagioclase is An88; and pyroxenes are Wo43En35 and Wo02En37. The equilibration temperature for the pyroxenes is 775-800°C (3).

Clasts are set in a dark, glassy matrix (partly devitrified) which comprises $\sim$50% of the meteorite. The glass surrounds all clasts and has invaded some along fractures. Vesicles are scattered through the glass. Small vesicles ($\sim$0.3 mm) surround some smaller clasts and elsewhere are distributed randomly. Large vesicles (up to 7.5 mm) are confined to large clast-free areas of glass. The surfaces of the larger vesicles are frothy. The glass contains many small mineral fragments, mostly plagioclase (formerly maskelynite) and pyroxene, that are indistinguishable from those in the clasts. Plagioclase fragments and plagioclase from small clasts is commonly "swirled" into the dark matrix glass and folded against larger clasts, pyroxene fragments, and vesicles. Temperatures must have been high enough to have melted the plagioclase. The matrix glass has devitrified to varying degrees. Adjacent to large clasts, the matrix is dark and essentially undevitrified; far from the large clasts, pyroxene laths appear and coarsen. As in the Bununu howardite (4), this texture suggests that matrix melt quench-cooled against the clasts.

Compositionally, the glass is slightly inhomogeneous, reflecting variable normative plagioclase, pyroxene and alkali feldspar. The glass has Mg/(Mg+Fe)=0.38, essentially identical to that of the pyroxenes. Thus the matrix composition reflects minimal admixture of diogenite, chondrite, or iron-meteorite components.

ALHA81011 records a major impact on the eucrite parent body. The target material was an equilibrated fragmental breccia, now representated by the clasts in the stone. Parts of the target were shock-melted on impact to temperatures exceeding 1500°C (the melting temperature of plagioclase). Melt and cold clasts mixed during crater formation and emplacement of the breccia (5), chilling the melt adjacent to the clasts. Remaining melt cooled more slowly, but still in excess of 50°C/min (6) to yield the coarser-textured matrix.

(1) SCORE R. AND MASON B. (1983) Antarc. Meteorite Newsl. 6:1,6. (2) DYMEK R. ET AL. (1976) Geochim. Cosmochim. Acta 40, 1115-1130. DESNOYER C. AND JEROME D. (1977) Geochim. Cosmochim. Acta 41, 81-86. (3) ROSS M. AND HUEBNER S. (1975) Internat. Conf. Geothem Geobarom. LINDSLEY D. AND ANDERSON D. (1983) Proc. 13 Lunar Planet. Sci. Conf., A887-A906. (4) KLEIN L. AND HEWINS R. (1979) Proc. 10 Lunar Planet. Sci. Conf., 1127-1140. (5) GRIEVE ET AL. (1977) in Impact and Explosion Cratering, Pergamon, N.Y. (6) WALKER D. ET AL. (1978) Proc. 9 Lunar Planet. Sci. Conf., 1369-1391.

PETROLOGY OF THE PALO BLANCO CREEK EUCRITE; T. Dickinson, K. Keil, L. LaPaz, Dept. of Geology, Institute of Meteoritics, Univ. of New Mexico, Albuquerque, New Mexico 87131; R. A. Schmitt, M. R. Smith, Dept. of Chemistry and Radiation Center, Oregon State Univ., Corvallis, Oregon 97331; M. Rhodes, Dept. of Geology, Univ. of Massachusetts, Amherst, Massachusetts 01003.

The Palo Blanco Creek meteorite, a single stone weighing 1,482g, was found in 1954 by Mrs. Lincoln LaPaz in Colfax County, New Mexico (36°32'N, 104°4'W) and was donated by her to the Institute of Meteoritics in 1982. It was classified as a monomict pyroxene-plagioclase achondrite (eucrite) by (1) but was not previously studied in detail.

The meteorite is very fresh and has well-preserved fusion crust over much of its surface. The rock consists of light-colored, angular to rounded clasts, submillimeter to 4.5 cm in size, that are surrounded and occasionally cut by black shock veins. The clasts are subophitic in texture and consist of about 60% pyroxene (ferrohypersthene, avg. En35.7Fo61.0Wo3.4, with exsolution lamellae of augite, avg. En30.4Fs29.9Wo39.7, 4-24 μm in width), 30% plagioclase (An83-92), and 10% accessory phases including ilmenite, chromite, troilite, and very minor-shock produced glass veinlets. Plagioclase occurs as subhedral laths; adjacent to the shock veins, it often forms spherulites. Both plagioclase types have identical compositional ranges. The black shock veins consist of shock-produced mafic glass, ilmenite, chromite and metallic Ni-Fe and, in places, contain relict mafics.

Whole rock oxygen isotope ratios of δO^{18} = 3.74 and δO^{17} = 1.73 (R.N. Clayton, pers. comm.), mineral compositions and abundances, and bulk composition (Table 1) confirm that Palo Blanco Creek is a typical non-cumulate eucrite. Textural observations and similar bulk compositions of clasts and shock veins suggest that the rock is a basaltic eucrite whose monomict-brecciated appearance is the result of in situ shock blackening.

Table 1. Bulk compositions of shock veins and clasts in Palo Blanco Creek

	Shock veins*	Clast**	Clast***
SiO2 (wt.%)	n.d.	n.d.	48.74
TiO2	0.7	0.8	0.56
Al2O3	13.3	14.6	13.16
Cr2O3	0.28	0.27	n.d.
FeO	18.0	17.4	18.42
MnO	0.51	0.53	0.58
MgO	6.1	6.2	6.56
CaO	10.5	10.7	10.43
Na2O	0.43	0.42	0.25
K2O	0.06	0.06	0.064
P2O5	n.d.	n.d.	0.090
Sc (ppm)	30	28	
V	66	70	
Co	4.1	2.9	
La	2.9	2.8	
Sm	1.76	1.78	
Eu	0.64	0.55	
Tb	0.42	0.38	
Dy	2.9	3.4	
Yb	1.69	1.63	
Lu	0.29	0.24	
Hf	1.2	1.1	

*Avg. of four samples, total weight 505 mg; INAA. ** Weight 511 mg; INAA. *** Weight 3.93 g; XRF. n.d. = not determined.

(1) Mason, B., Smiths. Contr. Earth Sci. 14, 71-83, 1975.

ORDINARY EUCRITES WITH SLOWLY COOLED TEXTURES AND THEIR CRYSTALLIZATION HISTORY; Hiroshi Takeda[1], H. Mori[1], and Y. Ikeda[2], [1]Mineralogical Institute, Faculty of Science, University of Tokyo, Hongo, Tokyo 113, [2]Dept. of Earth Sci.,. Faculty of Science, Ibaraki Univ., Mito, Ibaraki, Japan.

The chemical compositions of known ordinary eucrites cluster around the peritectic point in the olivine-silica-plagioclase pseudo-ternary system. There is no individual noncumulate eucrite with slowly cooled textures or compositions between ordinary eucrites and the most Fe-rich cumulate eucrite, Moore County, except probably Pomozdino. Only small mineral and lithic fragments of this type have been found in polymict eucrites and howardites. We studied a new monomict eucrite and a lithic clast in a howardite of this type by X-ray diffraction and a microprobe.

Yamato 791186 shows a lightly brecciated coarse subophitic texture, and contains less plagioclase than ordinary eucrites. Pyroxene crystals up to 2.4 X 0.9 mm in size are penetrated by laths of plagioclase up to 1.5 X 0.6 mm in size, and often include ilmenite up to 0.3 mm in diameter. Large plagioclases include a thin hollow core of pigeonite. Pyroxenes often display well developed "herring-bone" texture of twinning. The bulk pigeonite compositions $Ca_{8.1}Mg_{37.4}Fe_{54.5}$ are among the most Mg-rich members in ordinary eucrites. Cores of the crystals show coarse exsolution lamellae of augite ($Ca_{43}Mg_{31}Fe_{26}$) up to 10 microns thick with (001) in common with the host ($Ca_{1.5}Mg_{38.4}Fe_{60.1}$). Unlike the ordinary eucrites, the host low-Ca pyroxene is partly inverted to orthopyroxene as confirmed by the X-ray diffraction. The rims are more Ca-rich (Ca_{24} Mg_{35} Fe_{41}) and display fine exsolution lamellae, indicating that they were originally zoned with subcalcic augite rims. The plagioclase crystals are strongly zoned from An_{90} to An_{76}. Mesostasis is not recognizable. The bulk chemical composition of Y791186 (Analysis by H. Haramura), which may contain a polymict area, is one of the noncumulate eucrites with the lowest FeO/(FeO+MgO)(=0.54 mole %).

A gabbroic clast in Y791208 2.6 X 2.3 mm in size consists of subround pigeonites (28 vol. %) and plagioclase (72 %). The pigeonite crystals show clouding and fine regular exsolution lamellae of augite on (001). This feature is very similar to that of ordinary eucrites, but the bulk chemical composition of pyroxene $Ca_{12}Mg_{40}Fe_{48}$ is more Mg-rich than Y791186. Plagioclase is uniform in composition with An_{90}. The presence of such eucrites between Moore County and the ordinary eucrites can be interpreted by the existing models as follows: (a) They are crystallization products from a more fractionated magma than Moore County for the fractional crystallization model; (b) they are quenched liquids (scum layer) of less fractionated residual magma than the ordinary eucrites of a model (1); or (c) they were crystallized from a melt produced by more advanced degree of partial melting than Sioux County for a partial melting model (2). If we introduce a model, in which crystal cumulation is involved, the above eucrites can be produced by slight cumulation of crystals and loss of small amounts of fractionated residual liquid from a primary eucritic magma.

Y791186 is the first ordinary eucrite with very slowly cooled textures. The degree of homogenization of pyroxene may be type 6 (3).

We thank Dr. K. Yanai, and National Inst. of Polar Res. for meteorites.
References: (1) Ikeda Y. and Takeda H. (1984) Lunar and Planetary Science XV, 391-392. (2) Stolper E. (1977) Geochim. Cosmochim. Acta, 41, 587-611. (3) Takeda H. et al. (1983) Mem. Natl. Inst. Polar Res. Spec. 30, 181-205.

The significance of two pyroxene mafic clasts in basaltic achondrites.
Jeremy S. Delaney, American Museum Natural Hist., New York, NY10024

Clasts in polymict achondrites vary from ultramafic, through mafic to silicic. Much of the variation observed within these clasts can be modelled by varying the amount of partial melting at low pressure of an olivine bearing source rock (1) and fractionating the melts so produced. Clasts with cocrystallizing pigeonite and augite are not, however, so readily explained. The bulk compositions of these pyroxene pairs (after correction for late stage exsolution) are compatible with crystallization temperatures greater than 1100°C (2). These pyroxenes, therefore, equilibrated with a magma that was significantly more calcic than typical eucrites. These clasts are present in polymict eucrites, howardites and especially in mesosiderites (3) but are not represented by any monomict meteorites. To produce these calcic magmas, it is suggested that the liquids formed in equilibrium with both olivine and orthopyroxene, thus maintaining a low SiO_2 relative to the eucrites. The formation of liquids in equilibrium with both opx and olivine requires that the orthopyroxene field expand at the expense of olivine relative to the iron free system (4) and may also require congruent melting of orthopyroxene. Two possibilities may produce this expansion of the orthopyroxene stability field: (a) Increasing pressure results in increased opx stability with congruent melting of pure enstatite occuring at > 1.4 kbars. (b) Increasing Fe/(Fe+Mg) increases the stability of orthopyroxene with congruent melting of orthopyroxene beginning at Fe/(Fe+Mg) ~0.15 (5). Increasing the pressure of melt generation tends to increase the cpx/opx of the liquid. Liquids produced at depth in the Basaltic Achondrite Parent body are, therefore, likely to be more calcic than those produced by low pressure melting of the same source rock. The effect of iron enrichment has not been systematically explored but the presence of liquidus olivine in eucrite melting experiments (1) suggests that Fe-enrichment alone cannot produce the required expansion of the orthopyroxene liquidus field needed to produce augite + pigeonite saturated melts. Increase of the iron content of the source region should, however, reduce the pressure necessary to stabilize two pyroxene melts. Since both pigeonite bearing mafics (eucrites) and pigeonite + augite bearing mafics are present in the polymict achondrites, these meteorites probably sample basaltic rocks derived from several source regions at different depths in their parent body. Those breccias that contain the most abundant "deep seated" clast types might be expected to contain more two-pyroxene mafics. The diogenite component is often equated with deeper levels in the crust of BAP and indeed those meteorites containing an abundant diogenite component appear to contain more two pyroxene mafic clasts (mesosiderites and howardite Y7308).

By terrestrial standards, the pressures necessary for two pyroxene basalt formation are modest (for an Fe-free system, 1.4 kbar: for Fe bearing system, lower pressures) but on an asteroid, these pressures may represent depths in excess of 100 km. The presence of two-pyroxene mafic clasts may, therefore, be direct evidence that the basaltic achondrite parent body was larger than 200 km in diameter and perhaps as large as 500 km if an unsampled mantle and core are present. Serial magmatism in a 100 km thick suite of mafic rocks may, therefore, explain much of the diversity of rock types (igneous and metamorphic) observed in basaltic achondrites breccias. The multiple parent body hypothesis (7) may, therefore, be unnecessary.

References: (1) Stolper (1977) G.C.A.40. (2) Lindsley, Anderson (1983) JGR 88, Supplement, A887. (3) Nehr et al. (1980) LPS XI, 803. (4) Anderson (1915). (5) Bower, Schairer (1935) Amer. J. Sci. (6) Walker et al. (1979) PLPSC 10th. (7) Delaney et al. (1981) LPS XII.

ORIGIN OF HOWARDITES, DIOGENITES AND EUCRITES: A MASS BALANCE CONSTRAINT

Paul H. Warren, Institute of Geophysics, Univ. Calif., Los Angeles, CA 90024

Howardites, which are regolith breccias, appear to be mixtures of two main components: eucrite-like basalts and diogenite-like pyroxenites. This association, as well as O-isotopic and FeO/MnO similarities, militates in favor of a genetic link between diogenites and eucrites. Non-cumulate (NC) eucrites are generally interpreted as 'primary' partial melts, but earlier models assumed that they formed as residual liquids from fractional crystallization (FC) of the magma(s) parental to the diogenites. Diogenites are px cumulates, sometimes with minor ol. Anatexis may have modified some diogenites, but their high px contents were not caused by melt removal, because during low-pressure melting residual solids always have higher ol/px ratios than initial solids. The diogenite parent magmas were probably saturated with px, and perhaps also with ol, but not with pl. During diogenite genesis, FC of px increased the Al content of the melt, and eventually pl saturation resulted, i.e., a basaltic residual liquid formed. Let f_x = the maximum fraction of melt during partial melting before pl is exhausted (a function of bulk mantle composition), A = the Al content of the melt. During genesis of a magma parental to diogenites (f reaches a maximum of f_d), $A_{min} = A_p \cdot (f_x/f_d)$, where A_p = the Al content of the melt at the ol-px-pl peritectic. Once the same melt begins to produce diogenites (by FC), $A = A_{min}/r$, where r = the fraction of the original melt that is still liquid. Substituting for A_{min} and rearranging, $r = (f_x/f_d) \cdot (A_p/A)$. To a good approximation, the residual liquid reaches pl saturation when A_p/A drops to unity. Thus r_b, the fraction of basaltic residuum, $= f_x/f_d$. Clearly (barring a mechanism which would add more material from the lower half of the diogenite pluton than from its upper half —— the reverse is probable), unless $f_d/f_x > 2$, the regolith (howardites) should receive more basaltic-residual-liquid material than diogenitic material, from any given diogenite-bearing pluton.

An average howardite contains about 55% basalt and 45% pyroxenite (Mittlefehldt et al., 1979). If, for every gram of pyroxenite there is also a gram of related basaltic-residual-liquid material, then <20% of the basaltic component is <u>not</u> of residual liquid origin. It might be argued that f_d/f_x was, on average, >2. But the NC eucrites cluster tightly around the ol-px-pl peritectic (Stolper, 1977), which (along with other evidence) implies that if NC eucrites formed by partial melting, f was seldom or never $> f_x$. Yet calculated <u>mg</u> ratios of the diogenitic parent melts are only marginally greater than <u>mg</u> ratios of some NC eucrites. The basaltic component in howardites is probably dominated by late differentiates of the magma(s) parental to the pyroxenitic component. If howardites are representative samples of the diogenite-eucrite parent body, then eucrites are probably dominated by late differentiates of the magma(s) parental to the diogenites.

Clustering of NC eucrites near the ol-px-pl peritectic is not a major objection to a FC origin for NC eucrites. The ol-px boundary is probably closer to px than shown on Stolper's Fig. 8. If so, his path P-Q-R-B exaggerates the distance (R-A) separating a FC residuum from the peritectic. Because the peritectic is close to the px-pl join, FC of px + pl by a melt near the peritectic scarcely changes the melt's Si/(Mg+Fe) ratio until the fraction of the original melt remaining (r) drops to <0.2. Meanwhile, primitive material of low Si/(Mg+Fe) might be added, either by further melting of the mantle (a common phenomenon in terrestrial layered intrusions) or by accretion. The low gravity field of an asteroid would not facilitate convection or crystal settling (the presumed mechanisms of FC) to particularly low values of r.

EVIDENCE FOR THE FORMATION AND THE SIZE OF A METAL CORE IN THE EUCRITE PARENT BODY; H.E. Newsom, Max-Planck Institut für Chemie, Abteilung Kosmochemie, Saarstrasse 23, D-6500 Mainz, F.R. Germany.

A new neutron activation method for determining molybdenum has been applied to the eucrites (1). The Mo data were obtained using metal extraction in a high temperature furnace before irradiation to avoid production of radioactive Mo by induced fission of ^{235}U (2). Molybdenum concentrations in eucrites are very low compared to chondrites, in agreement with the large depletions of other siderophile elements (3). Eucrites have a mean Mo/La ratio of 0.0066 (Fig. 1) which is a factor of 570 lower than the C1 chondritic ratio. The depletions of siderophile elements in eucrites were presumably caused by segregation of metal. The similar fractionation of siderophile and lithophile element pairs (e.g. Mo, La) imply that metal segregation in the Eucrite Parent Body occurred prior to formation of the eucrite magmas.

The observed depletions of siderophile elements in the eucrites can be used to place limits on the metal content of the Eucrite Parent Body (3,4). The amount of metal required to obtain the observed depletion of the Mo/La ratio depends on the degree of partial melting during metal silicate equilibrium. Because the concentration of the compatible element Co has a different dependence on the degree of partial melting than Mo and W, the Co data can be used together with Mo and W to estimate the metal content and degree of partial melting. A metal content of 30 % to 50 % and metal segregation at approximately 50 % partial melting of the silicates is consistent with the data. Because the metal segregation occurred at a large degree of partial melting, before the igneous fractionations which produced the eucrite magmas, the formation of the magmas requires either solidification of the eucrite source regions and then partial melting to generate the eucrite magmas (5), or production of the magmas by fractional crystallization (6). In addition, a metal core in the Eucrite Parent Body may be detectable from a spacecraft.

Refs. (1) Newsom, H.E. (1984) Proceedings Lunar Planet. Sci. Conf. 15, submitted. (2) Newsom, H.E. and Palme, H. (1984) Radioanal. and Nuc. Chem., Lett., in press. (3) Palme, H. and Rammensee, W. (1981) Proc. Lunar Planet Sci. 12, 949. (4) Newsom, H.E. and Drake, M.J. (1982) Geochim. Cosmochim. Acta 46, 2483. (5) Stolper, E. (1977) Geochim. Cosmochim. Acta 41, 587. (6) Mason, B. (1962) Meteorites, J. Wiley.

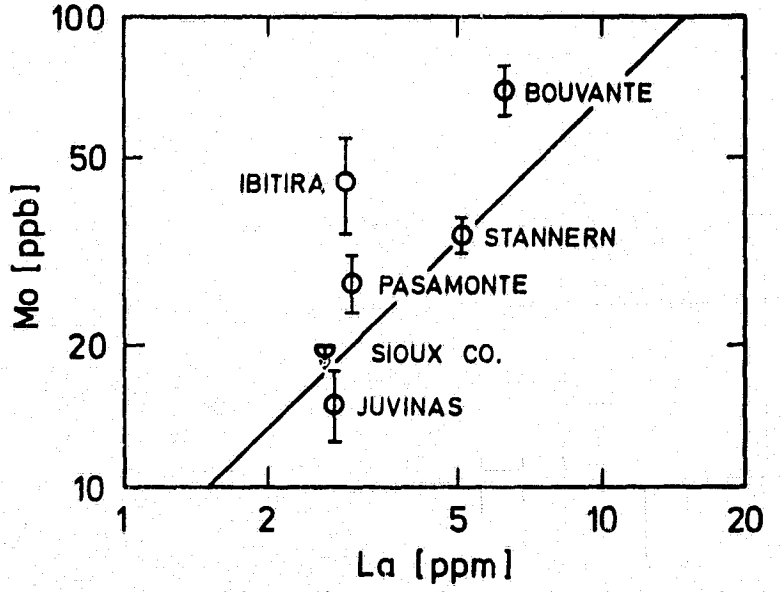

Fig. 1 Molybdenum and lanthanum concentrations in eucrites. The measured Mo concentrations (1) are: Bouvante 69.8 ppb, Stannern 34.2 ppb, Pasamonte 27.1 ppb, Juvinas 15.0 ppb, Sioux Co. <20 ppb, Ibitira 44.6 ppb. The errors are approximately 15%, but somewhat greater for Ibitira. Lanthanum data from (3).

The Fractionation of Siderophile and Volatile Elements on the Eucrite Parent Body (EPB)

W. Schmitt, G. Weckwerth and H. Wänke, Max-Planck-Institut für Chemie, 6500 Mainz, Federal Republic of Germany

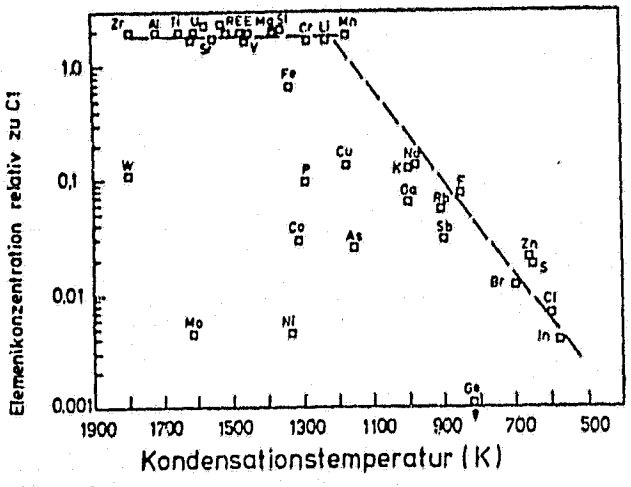

Fig. 1

The composition of the EPB, estimated by Dreibus and Wänke(1), shows a considerable depletion of volatile and siderophile elements relative to Cl-abundances. In fig.1 we plotted Cl-normalized concentrations from this estimation against the condensation temperatures published by Grossman (2), Wai and Wasson (3) and others, providing a scale of volatility of the respective elements. We see that the depletion of lithophile elements increases with volatility starting with condensation temperatures of about 1200 K (upper line).

Tab. 1 Element	$D_{M/S}$	Depletion calculated	observed
Ga	13	3	4
Cu	50	11	14
W	34	8	16
P	14	4	21
Co	157	32	73
Ge	1283	258	400
Ni	2389	479	500
Mo	1270	255	570

All siderophile elements have an additional depletion, which are compared in table 1 with experimentally determined metal/silicate-partition coefficients D, Schmitt (4), which are specified to assumed EPB-conditions (T=1300°C, p_{O_2}=6.9E-13). Assuming a metal content of the EPB of 20% we have calculated the expected element depletion using the measured metal/silicate-partition coefficients. As one can see there is a good agreement of the two sets of data leading us to the following conclusion:

In contrast to the earth on the EPB an almost complete equilibrium between core and mantle was achieved.

Ref.: (1) Dreibus and Wänke (1980), Z.Naturforsch. 35a, 204-216
(2) Grossman and Larimer (1974), Rev.Geophys.Space Phys. 12, 71-83
(3) Wai and Wasson (1977), Earth Planet Sci.Lett. 36, 1-13
(4) Schmitt and Wänke (1984), Lunar Planet.Sci.Conf. XV, 724-725

UREILITES: THE CASE OF MISSING DIAMONDS AND A NEW NEON COMPONENT;

U. Ott, H.P. Löhr and F. Begemann, Max-Planck-Inst. f. Chemie, Saarstraße 23, D-6500 Mainz, F.R.G.

For quite a while, a trademark of ureilites has been the occurrence in them of pronounced shock effects (1), of diamonds (2) and abundant trapped noble gases (e.g.3). However, in recent years, several relatively lightly shocked ureilites have been discovered (4,5,6,7), including two, Nilpena and ALHA 78019, that are reported to contain no diamonds (6,7). Such meteorites are of special interest. According to our earlier work (8) diamonds are the main carrier phase for trapped noble gases in ureilites. A second carrier had to be invoked, however, which could not be identified. Analysis of noble gas-bearing diamond-free ureilites might allow us to shed light on the nature of the putative second carrier phase.

Data obtained so far for Nilpena and ALHA 78019 have lived up to these expectations only in so far as both meteorites contain large amounts of trapped noble gases (Table 1). An acid-resistant residue (4.6 wt.%) from Nilpena, however, shows unambigously the x-ray diffraction pattern of diamonds, despite reports to the contrary (6). Except for the line systems of diamond and graphite, which are of about equal intensity, only very faint lines of unidentified origin are present. Nilpena, in this respect, is a perfectly normal ureilite. It remains to be seen, whether we will be similarly disappointed by ALHA 78019. Similar to North Haig (9), data for this weathered meteorite, taken at face value, indicate an extremely short cosmic ray exposure age of only $\sim 10^5$ years.

The new noble gas data confirm the presence of trapped He and Ne in ureilites. Previously (8) we had noted a similarity of the 20Ne/22Ne to that in Ne-C (10). Our new analyses show that the 21Ne/22Ne ratio is different, however. From analyses of acid-resistant residues of the Hajmah ureilite, which has high abundances of trapped gases and short c.r. exposure age, we obtain: 20Ne/22Ne=10.4±0.3, 21Ne/22Ne=0.027±0.003. Since this differs from all other known types (Fig.1), we propose the name Ne-U for this component.

	Nilpena	Nilp.res.	78019
3He	20.1	10.4	0.09
4He	456	2320	~17
20Ne	6.8	35	1.2
21Ne	4.3	0.30	0.03
36Ar	173	3618	118
84Kr	--	27	0.55
132Xe	--	18	0.32

Table1. Abundances in 10^{-8} cm³STP/g.

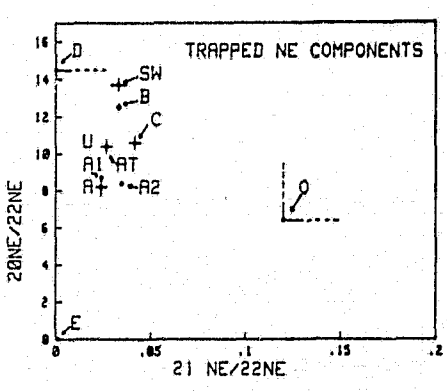

Fig. 1(right). Isotopic composition of trapped neon components. SW = solar wind, AT = terr. atmosphere.

References: (1) Vdovykin G.P., Space Sci. Rev. 10, 483. (2) Lipschutz M.E. (1964), Science 143, 1431. (3) Stauffer H. (1961), GCA 26, 70. (4) Takeda H. and Yanai K. (1982), Proc.7th Symp.Ant.Met., 97. (5) Mason B. and Clarke R.S. Jr. (1982), Proc. 7th Symp.Ant.Met., 17. (6) Jaques A.L. and Fitzgerald M.J. (1982), GCA 46, 893. (7) Berkley J.L. and Jones J.H. (1982) JGR 87 Suppl., A353. (8) Göbel R. et al. (1978), JGR 83, 855. (9) Bogard D.D. et al. (1973), GCA 37, 547. (10) Black D.C. (1972) GCA 36, 347.

NOBLE GASES IN THE UNSHOCKED UREILITE ALLAN HILLS 78019. John F. Wacker, Enrico Fermi Institute, University of Chicago, Chicago, IL 60637

One of the major questions about ureilites is how their two main constituents got together: olivine-rich rock and ~4% carbon, the latter containing very large amounts of planetary noble gases. About half of the C is diamond, apparently shock-produced and containing most of the noble gases *(1)*. The role of shock in ureilite genesis is not clear: did the shock bring the above two constituents together, or did they coexist before the shock? ALHA 78019 (hereafter 78019) is important as it contains only graphite (mainly as euhedral blades, ~0.5 mm long; *2*) but no diamonds and hence, was less shocked than other ureilites. I have measured noble gases in two bulk samples of 78019.

The ^{36}Ar, ^{84}Kr, and ^{132}Xe contents of 78019 are 160, 0.65, and 0.26×10^{-8} cc STP/g. They are comparable to other ureilites *(1,3)*, as are the elemental and isotopic ratios.

The He and cosmogenic Ne concentrations of 78019 are extremely low for ureilities. Ne is dominated by planetary gas (20/22 ~8-9) and the concentration of ^{21}Ne gives a cosmic-ray exposure age of only about 0.15 Myr, using the production rate of *(4)*. This exposure age is very similar to that of North Haig *(5)*, and since such low exposure ages are uncommon, their coincidence suggests that North Haig and 78019 came from the same parent body. As meteorite-forming impacts typically involve km-sized craters *(6)*, the similar ages imply that diamond-bearing and diamond-free ureilite material coexisted within a few km. However, the ^{21}Ne production rate depends on shielding, and to prove that the ages are identical, it will be necessary to measure ^{26}Al, cosmic-ray tracks, and the terrestrial ages of both meteorites.

The gases in one sample were extracted from 400 to 1800°C, in 200°C temperature steps. Except for the release of adsorbed atmospheric gases at 400°C, most of the trapped Ne to Xe was released between 1200 and 1800°C (≥50% betwwen 1400 and 1600°C). Despite the apparent lack of diamonds in 78019, the release temperatures were, at most, 100 to 200°C less than those for diamond-bearing ureilites *(1,3)*. Obviously, the carrier of trapped gases in 78019 is a refractory phase, the nature of which would have to be established by further experiments. But by analogy to other ureilites and to chondrites, it is probably carbonaceous. Crystalline graphite releases gases at relatively low T *(1,7)* and does not appear to be an important carrier in other ureilites *(1)*. I therefore suggest that the gas carrier in 78019 is some other kind of carbon, perhaps amorphous C. However, since all graphites aren't necessarily alike, even the large graphite blades cannot be ruled out yet. Nevertheless, there are indications that such a phase -- as yet unidentified -- may exist in other ureilites, judging by the similar concentrations of noble gases in samples of diamonds and diamonds + carbonaceous material in Haverö *(1)*.

Apparently, the noble gases were located in some part of the carbon prior to the shock that made the diamonds. Further work is needed to find out what this C is and whether the graphite blades in 78019 contain any noble gases.

(1) R. Göbel, U. Ott, and F. Begemann. *JGR 83*, 855 (1978).
(2) J.L. Berkley and J.H. Jones. *JGR 87*, A353 (1982).
(3) L.L. Wilkening and K. Marti. *GCA 40*, 1465 (1976).
(4) K. Nishiizumi, S. Regnier, and K. Marti. *EPSL 50*, 156 (1980).
(5) D.D. Bogard *et al. GCA 37*, 547 (1973).
(6) E. Anders. In *Asteroids: An Exploration Assessment*, NASA CP-2053, 57 (1978).
(7) T. Nakai *et al. Bull. Chem. Soc. Japan 33*, 497 (1960).

H-12

UREILITE PETROGENESIS: CLUES FROM A GRAPHITE AND METAL-BEARING INTRUSIVE COMPLEX, DISKO ISLAND, GREENLAND; C.A. Goodrich, Institute of Meteoritics, Department of Geology, University of New Mexico, Albuquerque, NM 87131

Models for ureilite petrogenesis state that they are partial melt residues into which carbonaceous material was introduced late, possibly in a shock event (e.g. 1), or igneous cumulates from a magma in which carbon was an abundant primary component (2,3). Olivine cumulates from the Hammer Dal Complex (HDC)--a complex of basaltic, subvolcanic intrusive bodies containing abundant graphite and iron-carbon alloy (4)--offer insight into processes important in the cumulate model for ureilite petrogenesis. Graphite in the HDC was derived from assimilated shale and is heterogeneously distributed in aluminous xenoliths derived from shale and as discrete crystals remaining after disaggregation of xenoliths; it was the reducing agent that led to formation of metal. Olivine cumulate zones 10-20 cm thick are overlain by 0.5-1.5 m thick iron cumulate zones with 15-25 vol. % metal (4). The metal accumulated as spongy bodies rather than a dense layer because the host magma was intruded near its solidus and cooled quickly.

The olivine cumulates consist of coarse (up to 2-3 cm), often skeletal, unzoned olivine crystals (Fo 80-86). Skeletal cavities and intergranular areas contain coarse pigeonite (Wo 2-4, mg 79-86) lining or rimming olivine, coarse plagioclase with calcic cores (An 92-94) and normally zoned overgrowths (An 81-54), and finer-grained diabasic material compositionally and texturally similar to the host rock surrounding cumulus olivine. The coarse grain size and homogeneity of the olivine, pigeonite, and calcic plagioclase are consistent with slow crystallization at depth before intrusion of the HDC. The diabasic material represents trapped liquid. The fine grain size of the diabase, lack of reaction between cumulus olivine and trapped liquid, and high CaO content of the olivine (avg. 0.23 wt.%, similar to ureilites) indicate rapid cooling of the HDC. NiO (70 ppm) and P_2O_5 (avg. 180 ppm) contents of the olivine are similar to ureilites and significantly lower than in typical terrestrial basalts and reflect fractionation of Ni and P into metal. Inclusions of low-Ni troilite in olivine represent trapped immiscible sulphide liquid that was in equilibrium with the metal phase. Nevertheless, chemical fractionation trends within the olivine cumulates and diabase are normal, which indicates that the bulk of the metal and sulphide were formed before crystallization of the silicates. This is in contrast to native iron-bearing extrusive rocks from Disko, which show strongly reverse-zoned orthopyroxene and progressive reduction recorded in Fe-Ti oxides (5), reflecting equilibration to lower pressures than the HDC. Chemical fractionation trends within ureilites are not well documented.

Mineral compositions suggest fO_2 conditions generally consistent with those expected from C-CO+CO_2 equilibria at pressures slightly greater than 150 bars (430 m depth, minimum estimate for HDC). However, fO_2 was not uniform in the magma and was probably controlled by proximity to heterogeneously distributed graphite. The low carbon content of the metal [0.7-1.4 wt.% (4)] indicates that it did not remain in equilibrium with graphite, and variations in C and P contents between metal in the cumulate zone and in the rest of the HDC (4) suggest lower fO_2 for the former. In contrast, the Disko extrusive rocks show more homogeneous fO_2 because shale inclusions were more completely assimilated and graphite more homogeneously distributed. Olivine compositions for the HDC and ureilites suggest similar fO_2; however other ureilite mineral compositions suggest greater reduction. This suggests that ureilites equilibrated at lower pressures than the HDC rocks. Carbon is more homogeneously distributed, and consequently fO_2 was probably more uniform in ureilites than in the HDC. This implies for the model of (2) that graphite occurred as discrete crystals in the ureilite magma (similar to the Disko extrusive magmas), in contrast to the HDC in which it was largely contained in xenoliths. Despite differences, the similarities between ureilites and HDC olivine cumulates, for which carbon was an abundant magmatic constituent, lend credence to the cumulate-primary carbon model for ureilite petrogenesis.

References: (1) Boynton, W.V. et al (1976) GCA 40, 1439-1448. (2) Berkeley, J.L. et al. (1980) GCA 44, 1579-1597. (3) Berkeley, J.L. and Jones, J. (1982) JGR 87, A353-A364. (4) Ulff-Moller, F. (1977) Rapp. GGU 81, 15-33. (5) Pedersen, A.K. (1981) Contr. Min. Pet. 77, 307-324.

TRACE ELEMENTS IN NATIVE IRON FROM DISKO ISLAND, WEST GREENLAND

W.Klöck[1], H.Palme[1] and H.J.Tobschall[2]. ([1]Max-Planck-Institut für Chemie, Mainz, FRG; [2]Mineralogisches Institut, Univ. Mainz, FRG.)

The most famous occurrences of metallic iron in terrestrial basalts are those of Disko Island, Westgreenland and Bühl near Kassel, FRG. Suggested origins include: a) meteoritic iron, [1] b) mantle xenoliths, [2] c.) origin by in situ reduction of iron oxide from the basaltic melt by graphite bearing sediments [3]. Trace element analyses of samples from Disko and Bühl were performed to clarify the origin of the metals and to throw some light on the behaviour of siderophile elements in naturally reduced systems.

Metal-bearing andesites from Disko Island are not different in major and trace element chemistry from normal metal-free andesites. This indicates in situ reduction of the silicate melt.

Table 1:

	A	B	C	D
Ni/Co	3 -3.8	20	6 - 85	21.5
Co/W	190-890	8750	600-1.2x10^5	5570
Ni/Ga	31-290	702	510-5x10^6	1180
Ge/W	8.7-50	100	0.001-7430	348
Ga/Au	350-3000	6000	0.01-500	64
Au/Ir	1.4-4.5	0.16	0.003-400	0.3

A = Disko metals C = Iron meteorites
B = Earth mantle D = Chondrite(Orgueil)

The relative abundances of siderophile trace elements (Ir, Ni, Au, As, Ga, etc) in the Disko iron are identical to that of the average earth crust. This pattern is distinct from the earth's mantle pattern and from the pattern of various types of meteorites in having higher abundances of the less siderophile elements. Some element ratios are given in table 1. These data exclude a meteoritic origin as well as a mantle origin for the Disko metals. In situ reduction of the iron oxide in the silicate melt is the only reasonable way to produce these metals.

Table 2:

	1	2	3
Ni	3120	5220	20450
Co	1044	1240	5366
Cu	778	1900	1665
Cr	30	14	80
Ga	99	76	70
Ge	48	70	300
As	47.4	133	168.6
Sb	1.5	5.7	3.3
Mo	14.9	20.8	57.8
W	5.5	11.3	6.0
Au	33 ppb	32.7 ppb	201 ppb
Re	64 ppb	63 ppb	316 ppb
Ir	7.4 ppb	6.7 ppb	146 ppb
P	6600	5800	1700

1 = small iron spherules (<1 mg); 2 = intermediate iron spherules (1-4 mg); 3 = massive iron.

From structural features we can distinguish three types of metallic iron from Disko : 1.) very small iron grains (<0.3 mm); 2.) larger iron spherules, consisting of a few sintered small grains (0.3 - 4 mm) and 3.) massive iron (up to a few tons), which obviously originated through accumulation of small iron spherules.

Trace element contents are different for the three structural types. The concentrations of most elements increase with increasing size and degree of accumulation of the spherules. The increase is more pronounced for the highly siderophile elements. The Ir content of the massive metal is more than a factor of 20 higher than that of the small spherules (Tab. 2). This behaviour can be explained by sinking of the small iron spherules through the magma accompanied by the accumulation of tiny iron particles into larger aggregates and simultaneously extraction of highly siderophile elements from a larger volume of magma.

Similar processes may have occurred on meteorite parent bodies. Different conditions of metal-silicate equilibration in those parent bodies may result in metals with variable concentrations of siderophile elements.

Ref: [1] Nordenskiöld, A.E. (1870) Öfvers. Kgl. Vetensk. Akad. Förh. 10, 973. [2] Fundal, E. (1975) Meddelelser om Grønland, Bd 195, Nr. 7, 1-28. [3] Pedersen, A.K. (1981) Contrib. Miner. Petrol. 77, 307.

GRAINSIZE EVOLUTION AND DIFFERENTIAL COMMINUTION IN AN EXPERIMENTAL REGOLITH; F. Hörz, M. Cintala, NASA/Johnson Space Center, Houston, TX 77058, and T. See, Lockheed EMSCO, Houston, TX 77058.

The comminution of planetary surfaces by exposure to continuous meteorite bombardment was simulated in the laboratory by impacting the same fragmental gabbro target 200 times. The target weighed 4000 gr and consisted of gabbro-fragments 2-32 mm in size. Stainless steel projectiles (D=6.3 mm; 1.02 g; Vi=1.35±.05 km/s) delivered 9.7×10^9 ergs per shot, or a specific energy of 2.5×10^6 ergs/g target mass. Peak pressures were <15 GPa and thus insufficient to cause significant melting. As a consequence, these experimental conditions were well suited to address the role of comminution and *in situ* gardening of planetary regoliths.

Mean grainsize continuously decreases with increasing shot number. Initially it decreases linearly with accumulated energy, but at some stage comminution efficiency starts to decrease gradually. Two factors contribute to this decrease: 1) a change in dominating fracture mechanism from intergranular to intragranular as grainsize decreases, and 2) a change in the partitioning of kinetic energy from one initially characterized by collisional fragmentation of coarse boulders and blocks to one dominated by genuine cratering in a fine-grained, homogeneous medium.

The gabbro was coarse-grained (1-5 mm) and had an initial mode of 54% plagioclase, 22% opx, 13% cpx, 5% orthoclase, 5% quartz, and the remainder (1%) being made up of biotite, ilmenite and magnetite. Point counting techniques, aided by the electron microprobe for mineral identification, were performed on a number of comminution products. The modal composition of the 125-250 μm fraction is enriched in plagioclase (65-70%) and depleted in opx + cpx (20-25%). These depletions/enrichments are present in the very first sample removed (after shot 5) and their magnitude is not time-dependent, i.e., degree of fractionation is about the same after shot 200. Identical conclusions are derived from bulk chemical analyses of specific grainsize fractions: Al_2O_3 enrichment and FeO+MgO depletion characterizes all grainsizes analyzed. The finest sizes (<10 μm) display generally the strongest enrichment/depletion factors.

Similar, if not exactly identical, trends are reported from lunar soils. It is, therefore, not necessarily correct to explain the chemical characteristics of various grainsizes (1,2,3) via different admixtures of materials from distant source terranes.(2) Differential comminution of local source rocks may be the dominating factor.(3)

References:

(1) Heiken, G. (1975) Rev. Geophys. Space Phys., 13, p. 567-587.
(2) Korotev, R. L. (1976) Proc. Lunar Sci. Conf. 7th, p. 695-726.
(3) Papike, J. J., Simon, S. B. and Laul, J. C. (1982) Rev. Geophys. Space Phys. 20, p. 761-826.

SPECTRAL REFLECTANCE STUDIES OF THE ORIENTALE REGION OF THE MOON; B. R. Hawke, P. Lucey, and J.F. Bell, Planet. Geosci. Div., Hawaii Inst. of Geophys., Univ. of Hawaii, Honolulu, HI 96822; and P.D. Spudis, Dept. of Geology, Arizona State Univ., Tempe, AZ 85281.

The Orientale impact occurred in rugged highlands on the southwestern limb of the Moon and was the last of the major basin-forming events. Valuable insight concerning lateral and vertical changes in the composition of the lunar crust can be provided by studies of material exposed by lunar impact basins. These impacts have excavated material from a variety of depths and deposited this ejecta in a systematic manner. In order to investigate the composition of materials exposed on the interior of Orientale basin, we have collected near-infrared reflectance spectra for units within the Cordillera ring.

Twelve near-infrared spectra (0.6-2.5μm) were recently (October, 1983) obtained at the Mauna Kea Observatory 2.2-m telescope using the Planetary Geosciences Division indium antimonide spectrometer. These include spectra obtained for two fresh surfaces on the inner Rook ring, two fresh craters in or adjacent to the outer Rook Mts. (Eichstadt K, 13-km. in diameter and an unnamed 15-km. crater), and two fresh 11-km. craters (Eichstadt G and H) which are located between the outer Rook ring and the Cordillera ring and expose material from within the knobby facies of the Montes Rook Formation. In addition, spectra were collected for portions of the Maunder Formation.

Analyses of the spectra obtained for the mare units on the interior of Orientale (Lacus Veris and Lacus Autumni) indicate that these surfaces are contaminated by variable amounts of local highland debris. This is not surprising in light of the limited areal extent of the mare units and the proximity of highland terrain. However, the presence of a highlands component complicates comparisons with spectra of common nearside mare deposits. Spectra obtained for mature highlands units on the interior of Orientale basin (e.g., Maunder Formation) are very similar to those of mature units in the vicinity of the Apollo 16 landing site. A similar composition is implied.

Special attention was paid to the spectra collected for six fresh features on the Orientale interior. Eichstadt G and H should be dominated by the material which comprises the knobby facies of the Montes Rook Formation. Eichstadt K and an unnamed crater in the outer Rook Mts. may expose the major components of the third Orientale (outer Rook) ring. The spectra for knobby facies and the outer Rook Mts., while differing in detail, exhibit many common spectral characteristics. All represent highlands rocks with abundant Fe-bearing plagioclase feldspar and Ca-poor pyroxene. Compositions ranging between noritic anorthosite and anorthositic norite are indicated. There is no evidence for the presence of an ultra-mafic component.

The spectra obtained for the fresh surfaces (a steep massif slope and a small crater on a massif) in the inner Rook Mts. are very distinct from the other spectra of Orientale-related features. These spectra exhibit no absorption bands. We interpret these spectra to represent areas composed of plagioclase feldspars which have been subjected to shock pressures in excess of 200 Kb (i.e., shocked anorthosite).

ASTEROID-METEORITE CONNECTION: REGOLITH EFFECTS IMPLIED BY LUNAR REFLECTANCE SPECTRA; C.M. Pieters, Brown University, Providence, R.I. 02912

A major component of absorbing lunar-like agglutinates is not expected in asteroid soils (1), (2), which should instead contain mostly lithic fragments. To estimate the effects of soil formation on the spectral characteristics of asteroids we thus need to consider in situ properties of materials affected by the space environment other than those associated with agglutinates.

In his initial survey of the reflectance properties of lunar samples, J.B. Adams measured a few chips from the exterior and interior of Apollo rocks. For Apollo 12 basalts [12053-12063] (3), the exterior and interior spectra exhibited strong absorption bands which were very similar in nature; the exterior fragment was a bit brighter, which was attributed to microbrecciation. Chips from an Apollo 16 fragmental polymict breccia [67016] exhibited notably different properties. Both chips exhibited spectra with low-Ca pyroxene absorption bands, but the exposed exterior chip was darker, the spectrum was distinctly redder, and spectral contrast was strongly reduced in the visible (Adams, unpublished data).

Mature lunar soils measured in the laboratory have the same spectral properties as telescopically measured undisturbed surface areas at the landing sites (4). It was hypothesized that freshly exposed material at fresh impact craters should be comparable to powdered rock samples in the laboratory. This expected trend seemed to be true with the early reflectance data (5), but as the more complete near-infrared data has become available it is clear that there is no simple correspondence of rock type (laboratory powder or chip measurement) to freshly exposed surface material (telescopic measurements of fresh crater classes). Small fresh craters in the mare are the exception; their reflectance spectra are directly comparable to laboratory spectra of lunar rock powder in nature and strength of absorption bands and, in some cases, the nature of the continuum. Highland or terra fresh craters, on the other hand, exhibit spectral properties that can be interpreted in terms of mineral assemblages present in the surface material, but the absorption bands are generally weaker than those observed in the laboratory for rocks and breccias and the continuum is almost always steeper (6).

Neither of these examples depend on accumulation of agglutinates to alter the optical properties. The first case dealt with effects from exposure to the space environment on an airless surface (at 1 AU); the second case concerns alteration possibly associated with the impact process. In both cases optical alteration was strongest for the brecciated highland material and weakest or nonexistant for basaltic material.

For asteroids this information indicates that examples such as the close association of the spectral properties of asteroid 4 Vesta with laboratory measurements of basaltic achondrite powders should not be extrapolated to infer that asteroid regolith soil is unaltered crushed fragments of the asteroid's surface. For non-basaltic asteroids the optical properties of asteroid soils are likely to contain subtle alteration effects that would make them different from the properties of rock fragments of their surface. These differences are likely to include a weakening of absorption bands and perhaps a reddening of continuum slope for the regolith soils of asteroids.

1) Housen and Wilkening (1982) Ann.Rev.Earth Planet.Sci., 10, 355-376. 2) Matson et al. (1977) Proc. Lunar Sci.Conf. 8th, 1001-1011. 3) Adams and McCord (1971) Proc. Lunar Sci.Conf. 2nd, 2183-2195. 4) McCord et al. (1972) The Moon, 5, 52-89. 5) Pieters (1977) Proc. Lunar Sci.Conf. 8th, 1037-1048. 6) Pieters (1983) Lunar Planet. Sci., XIV, 608-609.

SPECTROSCOPIC EVIDENCE OF REGOLITH MATURATION- T.V.V. King[1], M.J. Gaffey[1], and L.A. McFadden[2]. (1) H.I.G.-P.G.D., University of Hawaii, Honolulu, HI, 96822 (2) University of Maryland, College Park, MD,20742

In recent years much effort has been directed toward describng the character of regoliths on small bodies in the solar system (1,2,3,4, and others). These works have paid particular attention to the development, depth and distribution of regolith on asteroids. Here we address the question of the physio-chemical nature of the regoliths as determined by remote spectral reflectance measurements.

We have selected a group of eleven asteroids described by King et al.(5) to show evidence of regolith maturation. This group of asteroids has spectra that increase in reflectance, nearly linearly, through 0.3um to 0.9um. The reddened spectra, if not the result regolith maturation, may be attributed to early solar system condensation on the asteroid surface, because reddened spectra is characteristic of both mature regoliths and solar condensates of meteoritic origin (6). In each case the spectral character is attributed to the presence of elemental iron in non-crystallographic sites, as discrete grains or as a component in glassy material, such as lunar agglutinates. Although the number of agglutinates in meteorites is small (7,8) this is not surprising when one considers the processes involved in delivering a meteorite to Earth. The lack of abundant agglutinates in meteorites, in comparison to the Moon, has been interpreted to be indicative of: a.)short surface exposure, (9); b.) the coarse grain size of the surface layer of the meteorite parent associated with a relatively "benign bombardment environment" (2); c.) weaker gravity and in some cases, compositional differences (10) d.) differences in impact velocity (2,10); e.) the absence of processes, such as solar-wind implantation, due to variations as a function of heliocentric distance (10). Our bias between lunar soils and meteorites in terms of sampling methods precludes a comparison of their agglutinate contents. Spectral characeristics, eg. spectral reddening, are consistent with regolith processes acting on the outer most layers of the Moon and Mercury. It is interesting to note that the only known lunar meteorite, Antarctic meteorite ALHA81005, shows no evidence of spectral reddening. Hence, we would conclude that the solar wind emplacement and micrometeorite bombardment are viable processes on the surfaces of some asteroids. The physico-chemical expressions of these processes would not necessarily be evident in meteorites contained in the terrestrial collections. If the surfaces of these reddened asteroids represent the product of early solar system condensation, it implies that they have remained unaffected by the normal collisional and fragmentation processes which would be expected to remove this material from the exterior surface or to alter its physical state. Their exemption from such events remains to be explained. Nonetheless, the recognition of either mature regoliths or early solar system condensates on the surface of some asteroids testifies to the complexities of evolutionary processes in the asteroid belt. Further spectral measurements, in different wavelength regions, should clarify the exact character of these surfaces.

(1) Housen, K.R. and L.L. Wilkening (1982), Ann. Rev. Earth Planet. Sci., 10, pp.355-376.(2) Hora, F. and R.B. Schaal (1981), Icarus, 46, pp.337-353.(3) Lazovin, Y. and M. Maurette (1980), Lunar. Planet. Sci. XI, pp.602-604.(4) Gintala, M.J., J.W. Head, and L. Wilson (1979), Asteroids, pp.579-600.(5) King, T.V.V., L.A. McFadden, and M.J. Gaffey (1983), Meteoritics, 18, 4.

(6) King, T.V.V., M.J. Gaffey, and E.A. King (1982), Lunar Planet. Sci. XIV, pp.371-372.(7) Rajan, R.S., D.E. Brownlee, G.H. Heiken, and D.S. McKay (1974), Meteoritics, 9, pp.194-197.(8) Wilkening, L.L. (1977), In Relationships Between Comets, Minor Planets and Asteroids, pp.389-396,(9) Housen, K.R., L.L. Wilkening, C.R. Chapman, and R. Greenberg (1979), Asteroids, pp.601-627.(10) Matson, D.L., T.V. Johnson, and G.H. Veeder (1979), Proc. Lunar Sci. Conf. 4th, pp.1001-1011.

SPECTROSCOPIC IDENTIFICATION OF PROBABLE PALLASITE PARENT BODIES. J. F. Bell, M. J. Gaffey, and B. R. Hawke, Planetary Geosciences Div., Hawaii Inst. of Geophysics, University of Hawaii, Honolulu HI 96822.

Telescopic observations have recently revealed the existence of a class of asteroids whose surfaces show the spectral signature of abundant olivine. These objects were formerly grouped in the "R" class but are now separated into a new "A" class characterized by unusual broadband infrared colors (1). High-resolution IR spectra in the 0.8-2.6 micron wavelength region have been published for 246 Asporina (2), 289 Nenetta (2), and 446 Aeternitas (3). All three objects show the distinctive deep multiple absorption band of olivine near 1.1 μm. The overall slope of the continuum suggests the presence of a metal component. This interpretation implies that the A-type asteroids are potential parent bodies of pallasites. We have conducted laboratory studies to investigate this hypothesis. Olivine grains of three sizes (fayalite content similar to main-group pallasites) were scattered on a roughened iron background to simulate the multiple scattering expected in a regolith derived from pallasite bedrock. IR spectra were obtained for a variety of iron/olivine ratios within each olivine particle size. No simulation using 1mm olivine grains can reproduce the fine structure seen in the asteroid spectra; evidently the large olivine crystals found in pallasites do not survive regolith gardening. Simulations with 90-μm olivine grains provide excellent matches to the asteroids in band depth and shape, though continuum slopes indicate that the asteroidal metal phase has a more curved spectrum that does our artificial iron alloy. Apparent olivine content increases in the sequence Asporina-Aeternitas-Nenetta, from ≈30% to ≈40% to ≈70%. A third series of simulations employing a broad range of particle sizes <250μm also provides acceptable matches with slightly higher olivine contents. (In the case of Nenetta a 100% olivine regolith may be consistent with the somewhat noisy data available.) These results fully confirm the previous interpretations (2,3) of A-type asteroids as having pallasite-like surface mineralogy. Because of the unusual spectral signature of olivine this identification is of high reliability and uniqueness, comparable to the generally accepted identification of Vesta as a basaltic achondrite parent (4). Since these objects are as large as 60km in diameter and are apparently pallasitic over most of their surfaces, models in which pallasite formation is confined to small objects or restricted surface areas cannot explain them. The A-type asteroids are probably remnants of larger differentiated bodies which have been eroded down to the core/mantle interface zone where cumulate olivine crystals and nickel-iron metal coexist. The S-type asteroid 8 Flora has been shown to be a similar stripped core with an additional pyroxene component (5). We speculate that S-type and A-type asteroids are both derived from highly differentiated parent bodies with their upper layers eroded away to different depths. Vesta and Dembowska may represent two such bodies which happened to escape this massive erosion.

REFERENCES: 1) G. J. Veeder et al., Icarus 55, 177. 2) D. P. Cruikshank and W. K. Hartmann, Science 223, 281. 3) J. F. Bell et al., Lunar and Planetary Science XV, 48. 4) M. J. Gaffey, Lunar and Planetary Science XIV, 231. 5) M. J. Gaffey, Icarus, in press.

RADAR INVESTIGATION OF ASTEROIDS; S. J. Ostro, Department of Astronomy, Cornell University, Ithaca, NY 14853

Radar observations can provide useful constraints on an asteroid's size, shape, spin vector, topography, decimeter-scale morphology, density, and composition. Since radar techniques achieve spatial resolution of a planetary target in a manner that is independent of the target's apparent angular size, they provide a powerful ground-based tool for investigating asteroids, which generally remain unresolved by optical telescopes. By virtue of the long wavelengths employed, radar measurements furnish unique information about (i) near-surface structure at scales several orders of magnitude larger than the scales probed optically, but much smaller than typical asteroid dimensions; and (ii) regolith bulk density and metal content (i.e., two parameters that are not well constrained optically.)

An intensive series of asteroid investigations was initiated in 1980, using the Arecibo Observatory's λ13-cm (2380-MHz) radar system. So far, echoes have been detected from a total of 25 asteroids (16 mainbelt objects plus 9 Earth-approachers).

As a class of objects, asteroid echoes lack the sharply peaked spectral signature that dominates echoes from the quasi-specularly scattering bodies (e.g., the Moon). This result indicates that asteroid surfaces are rougher than the Moon at some scale(s) at least as large as a few centimeters.

The particular roughness scale can be constrained by measurements of the circular polarization ratio, μ_C, of echo power received in the same sense of circular polarization as transmitted (i.e., the "SC" sense) to that in the opposite (OC) sense. (For the Moon at λ13 cm, $\mu_C \approx 0.1$) Values of μ_C for individual asteroids range from ~ 0.0 to ~ 0.5; the lowest values require that the echo be due to single reflections from surfaces that are smooth at cm-to-m scales, whereas the highest indicate substantial multiple scattering and/or near-surface roughness. Values of μ_C apparently depend on target size and/or VIS-IR taxon, perhaps reflecting gravitational and/or compositional control of regolith processes. For at least some asteroids, μ_C varies across the disc, indicating heterogeneous near-surface structure.

The radar reflectivities of mainbelt asteroids span nearly an order of magnitude and apparently depend on VIS-IR taxon. This result indicates variations in the bulk densities and/or metal concentrations within the top few meters of these objects' regoliths.

This research was supported by NASA Grant NAGW-116. The Arecibo Observatory is part of NAIC, which is operated by Cornell under contract with NSF and with support from NASA.

Ostro, S. J., D. B. Campbell, and I. I. Shapiro (1981). Radar Detection of Iris, Psyche, Klotho, Apollo, and Quetzalcoatl. Bull. Amer. Astron. Soc. 13, 716.

Ostro, S. J., D. B. Campbell, I. I. Shapiro, and M. R. Showalter (1982). Radar Detection of 2 Pallas, 8 Flora, and 2100 Ra-Shalom. Bull. Amer. Astron. Soc. 14, 725.

Ostro, S. J., D. B. Campbell, and I. I. Shapiro (1983). Radar Observations of Asteroid 1685 Toro. Astron. J. 88, 565.

Ostro, S. J., D. B. Campbell, and I. I. Shapiro (1983). Radar Detection of Astraea, Victoria, Fortuna, Hestia, Juewa, Geographos, and Oljato. Bull. Amer. Astron. Soc. 15, 823.

HIGH-ENERGY NEUTRON INDUCED PROMPT GAMMA-RAYS; CHEMICAL REMOTE SENSING OF PLANETARY SURFACES. J. Brückner[1], P. Englert[2], R. C. Reedy[3], and H. Wänke[1]. ([1]Max-Planck-Institut für Chemie, Mainz, FRG; [2]Institut für Kernchemie, Köln, FRG; [3]Los Alamos National Laboratory, Los Alamos, NM, USA)

The distribution of certain elements over a planet's surface specifies constraints on models of its origin and evolution. Such information can be obtained by means of remote sensing γ-ray spectroscopy (1). Such γ-ray experiments are planned for a number of future space missions, as for Mars, Moon, asteroids or comets.

The surface of a planetary body is bombarded by energetic particles of cosmic-rays, which produce a cascade of secondary particles, such as neutrons. Nonelastic scattering and capture reactions of these neutrons play an important role in the production of discrete-energy γ-ray lines which can be measured by a γ-ray detector on board of an orbiter. This allows to determine the abundances of many elements, as O, Al, Si, K, Ca, Fe, Th, and U, in the first 50 centimeters of a planet's surface.

To investigate the γ-rays made by interactions of neutrons with matter, thin targets of different composition were placed between neutron-source and a high-resolution germanium spectrometer. γ-rays in the range of 0.1 to 8 MeV were accumulated. The detector was surrounded with paraffin, boron, and lead to shield it from neutrons and background radiation.

These in-beam γ-ray spectra consist of a rather high continuum and of narrow peaks, which in most cases show no broadening. Only a few nonelastic scattering γ-rays have noticeable Doppler broadening. As a result of the experimental set-up, there is a considerable background of discrete lines from surrounding material. A similar situation exists under planetary exploration conditions: γ-rays are induced as well in the planetary surface as in the spacecraft.

Unfolding of the spectra, subtraction of the γ-ray background, correction of detector efficiency, and correction of γ-absorption in the shielding material and in the target itself are necessary for determination of the target γ-intensities. A comparison of measured intensities of iron capture-lines with literatur values shows the validity of all these corrections.

In one set of experiments a 14-MeV neutron-generator using the T(d,n) reaction as neutron-source was placed in a small room. Scattering in surrounding walls produced a spectrum of neutron energies from 14 MeV down to thermal. This source induced mainly neutron-capture lines and some scattering lines. The complexity of the accumulated γ-ray spectra is similar to what planetary spectroscopy may encounter in an orbit.

To investigate the contribution of neutrons with higher energies, the same targets were irradiated with neutrons having energies up to 39 MeV provided by the Be(d,n) reaction of a cyclotron (KFA, Jülich, FRG). Here, the scattering and (n,2n) reaction γ-rays dominate the spectra. Capture lines are very week. The measured scattering γ-intensities, e. g. in the iron-spectrum, exceed those of the 14 MeV irradiation by one or two orders of magnitude. The number of detectable scattering lines increased by a factor of about three.

Combining the results of the two sets of experiments we get a rather realistic simulation of the expected planetary γ-ray spectra.

Ref.: (1) R. C. Reedy (1978) Proc. Lunar Planet. Sci. Conf. 9th, p. 2961

CLASTIC TEXTURE OF METEORITES; L.L. Wilkening, S.E. Jensen, and K. Schaudt, University of Arizona.

We have measured the sizes of hundreds of clasts in each of 17 meteorites of different chemical types. The long term goal of our study is to determine if there are differences in brecciation texture and clast sizes which might be correlated with different types of meteorites and, by inference, different spatial regimes in the asteroid belt or different locations on the meteorite parent bodies.

The areas of the clasts were measured with a digital planimeter on tracings of photographs of the meteorites. Assuming circular cross-sections, the areas were converted to diameters. The diameters were then converted to the phi-scale. Graphs of the clasts within each size-bin, differential probability, and total number of clasts within each size-bin, relative size frequency, were examined for inter- and intra-group similarities.

The first order finding is that all meteorite breccias are not alike in terms of the clast size distribution. Similar clast size distributions were found for the eucrites, ALHA 77302, 79017, 78132, and 80102. It has been suggested on petrographic evidence (Antarctic Newsletter,4,9) that these meteorites may be from the same fall. Our observations are consistent with this. Similarities were also found between the LL6 chondrite BTNA 78004 and the unusual eucritic breccia AHLA 81011. We included two gas-rich meteorites, Weston and Djermaia, in our study. Unfortunately, the quality of the photographs which we had to measure was not as high as desirable. At this point these meteorites appear distinctly different from the eucrite group and are similar to other chondrites. The aubrite, ALHA 78114, shows yet another pattern characterized by a relatively higher abundance of larger clasts.

The observations on the clast sizes generally correspond to the general breccia textures. We expect that the correlations will correspond to microscopic textural features as well (amount of glass present, degree of shock, grain size, etc.) as appears to be the case in our work to this point.

THE KENDLETON L4 FRAGMENTAL BRECCIA: PARENT BODY SURFACE HISTORY. A.J. Ehlmann[1], K. Keil, E.R.D. Scott, Dept. of Geology, Institute of Meteoritics, Univ. of New Mexico, Albuquerque, N.M. 87131. [1] Permanently at Dept. of Geology, Texas Christian Univ., Fort Worth, Texas. 76129. H.W. Weber, L. Schultz, Max-Planck-Institute of Chemistry, Mainz, F.R. of Germany.

The Kendleton chondrite (fall, 1925 hrs., May 2, 1939) is a fragmental breccia consisting of a dark, chondritic matrix (mostly L4 material) with light-colored chondritic (L5/6); shock-blackened, partly glassy; unequilibrated (type 3) chondritic; light-colored microporphyritic melt rock; and chondrule-free tridymite-low-Ca pyroxene clasts. Although macroscopically similar to a regolith breccia (light-dark structure), Kendleton does not contain solar wind implanted gases (3He 3.25, 4He 840, 20Ne 0.84, 21Ne 0.77, 22Ne 0.87, 36Ar 6.8, 38Ar 1.34, 40Ar 5300, 84Kr 0.10, 132Ne 0.14, in 10-8cc STP/g; also Taylor and Heyman, 1969). The rock was not appreciably outgassed and reheated during or after lithification, as indicated by 36Ar contents and lack of reaction between clasts and dark, chondritic matrix. There are no extensive rock-wide shock effects (only minor shock veins), although individual constituents and clasts are highly shocked.

The dark chondritic matrix consists of relatively homogeneous olivine and somewhat heterogeneous low-Ca pyroxenes: means in 9 sections are Fa 21.9-23.3, Fs 15.1-18.6. PMD of FeO in olivine is 0.9 to 3.7 (excluding one Fa6 grain), indicating type 4. Kendleton is unique in that it is mostly (about 80%) made of dark, chondritic matrix whose olivine and pyroxene compositions indicate heterogeneities on a thin section scale. Round to angular, light-colored chondritic clasts (the light portions of typical light-dark structured chondrites) have olivine of Fa 23.5 (σ = 0.6) and low-Ca pyroxene of Fs 19.2 (σ = 2.5); chondrules are less well-defined than those in the dark, chondritic matrix. Thus, these clasts are type L5/6. Shock-blackened, partly glassy clasts are angular to irregularly-shaped, up to 15 mm in size, and are the dominant clast type; boundaries are sharp to diffuse. They consist of faint, isolated to grouped chondrules; shock-melted Fe,Ni and FeS; glassy material; and olivines and pyroxenes with means in 5 clasts of Fa 22.2 - 24.2 and Fs 15.8 - 20.1. One clast contains a relict type 3 clast. This unequilibrated (type 3) clast has slightly turbid, igneous glass and mean olivine of Fa 17.9 (N = 35, σ = 8.9) and low-Ca pyroxene of Fs 15.9 (N = 14, σ = 6.1). One barred olivine chondrule has Fa 1-19.9. A light-colored microporphyritic clast has subhedral to euhedral olivine (mean Fa 21.9, N = 45, σ = 0.27), in a matrix of devitrified glass. This melt rock clast is depleted in Fe,Ni and FeS and equilibrated prior to rock lithification. A tridymite-low-Ca pyroxene clast, 6 mm in size, has no chondrules and consists of a large area of tridymite, intergrown with small and adjacent large low-Ca pyroxene (mean Fs 20.0, N=29, σ =1.0). Tridymite exhibits sharp boundaries with the dark, chondritic matrix and outlines suggesting crystal faces. It is intensely fractured and shocked.

Conclusions. Kendleton is a fragmental breccia that may have resided in a regolith, as indicated by the light-dark structure and presence of shock-blackened and a melt rock clast. Residence time in a regolith was short, as indicated by the absence of detectable solar wind gases and matrix heterogeneity on a thin section scale, (suggesting poor mixing and low maturity). Although all materials except the tridymite-low-Ca pyroxene clast are of L-group composition, compositional variabilities between clasts and presence of type 3 inclusions indicate heterogeneities across the source regions on the parent body. Further work is required on the tridymite-low-Ca pyroxene clast before genetic inferences can be made.

PETROLOGY OF SOME ORDINARY CHONDRITE REGOLITH BRECCIAS: IMPLICATIONS FOR PARENT BODY HISTORY: C.V. Williams, A.E. Rubin[1], K. Keil, Dept. of Geology, Institute of Meteoritics, Univ. of New Mexico, Albuquerque, New Mexico 87131; A. San Miguel, Museo Municipal de Geologia, Parque de la Ciudadela, Barcelona-3, Spain. [1] Inst. of Geophysics and Planetary Physics, UCLA, Los Angeles, CA 90024.

Regolith breccias are clastic rocks containing angular, fragmented mineral and rock clasts in a fine-grained matrix which are formed by the consolidation of loose, impact-produced material on the surfaces of their parent bodies. Here we report on detailed microscopic and electron microprobe studies of the chondrite regolith breccias Cangas de Onis (H), Nulles (H), Ipiranga (H), Mafra (L), and Rio Negro (L).

Studies of clasts and matrices in these breccias indicate that they are of the same compositional group but are, in some cases, of different petrologic type. Metallographic cooling rates for the equilibrated clasts are coherent, but indicate different burial depths for different clasts. Incoherent metallographic cooling rates of the clastic matrices also suggest a range of burial depths. For example, the most rapidly cooled metal grains (1000°C/Myr) in Cangas de Onis could have been derived from maximum depths of only a few kilometers and the most slowly cooled grains (1°C/Myr) from depths as great as 100 km on a parent body 400 km in diameter.

A mechanism capable of bringing material to the surface and accounting for the coexistence in the regolith of material derived from a wide range of depths is needed to explain the incoherent metallographic cooling rates of the clastic matrices. Excavation by single or multiple impacts does not explain the coexistence of material from a wide range of depths: an impact sufficiently energetic to excavate material from such depths would totally disrupt the parent body. It is therefore likely that the ordinary chondrite parent bodies were fragmented and gravitationally reassembled. This process would lead to a chaotic pile of debris with a surface regolith containing material derived from a variety of depths. Reworking and compaction of this regolith would produce rocks with characteristics of ordinary chondrite regolith breccias.

The diverse metallographic cooling rates of different H6 clasts in Cangas de Onis indicate that highly metamorphosed material was buried at different depths before incorporation into the regolith. This is inconsistent with the onion shell model of chondrite parent bodies, wherein the most metamorphosed material should be concentrated at the core. However, these data are consistent with the Scott-Rajan metamorphosed-plantesimal model which predicts no correlation between cooling rate and metamorphic grade. Collisional disruption and reassembly of the parent body dispersed fragments of the individual planetesimals; some were incorporated into the regolith.

CONFIRMATION OF COSMOGENIC NEON FROM PRECOMPACTION IRRADIATION OF KAPOETA AND MURCHISON; M.W. Caffee, C.M. Hohenberg, T.D. Swindle, McDonnell Center for the Space Sciences, Washington Univ., St. Louis, MO 63130; and J.N. Goswami, Physical Research Laboratory, India.

In a recent study [1] the neon isotopic records from individual meteorite grains having significant exposure to energetic particles, as evidenced by particle tracks, were compared with grains which did not show such pre-compaction exposure effects. The results can be summarized as follows: 1) Quantities of spallation-produced ^{21}Ne in irradiated grains from Kapoeta and Murchison exceed that plausibly attributable to either galactic or present-day solar cosmic ray irradiations. 2) Associated solar wind neon seems to be underabundant. Such observations seem to require substantial fluxes of energetic particles as might be expected from an early active sun. Information on the energy spectrum of the incident particles can be obtained from the isotopic composition of the cosmogenic neon [2]. The effect is most pronounced for plagioclase feldspars where the $^{21}Ne/^{22}Ne$ ratio is distinctly lower (around .5) for low energy particles, compared with $>$ .8 for more energetic particles. The previous studies involved olivines and pyroxenes, which exhibit less energy-dependent isotopic structure. In this study we have analyzed solar flare irradiated and unirradiated feldspar grains from Kapoeta. Additionally, we have repeated the experiment on olivine grains from Murchison.

The solar flare irradiated Kapoeta feldspar sample consisted of 9 grains weighing 70μg. The unirradiated sample consisted of 8 grains weighing 113μg. The irradiated feldspar grains would require a pre-compaction irradiation time of 40 m.y., were the effect due to galactic cosmic ray exposure (production rates from [3]), while the unirradiated grains provide a cosmic ray exposure age of 4 m.y., consistent with the accepted age. The $^{21}Ne/^{22}Ne$ ratio of the most spallation rich extraction approximates that of galactic cosmic rays, rather than lower energy particles, such as current solar flares.

The irradiated Murchison sample consisted of 8 grains weighing 55μg and the unirradiated sample had 9 grains weighing 74μg. Galactic cosmic ray exposure inferred from the unirradiated grains is 0.9 m.y., as expected from the accepted exposure age. If the pre-compaction exposure of the irradiated grains were due to galactic cosmic rays, a pre-compaction period of 10 m.y. would be required.

In all cases the unirradiated grains show fairly reproducible exposure ages that agree well with nominal values determined by other methods. However, the irradiated grains show large and variable pre-compaction exposure effects, suggesting wide differences in energetic particle doses to individual grains and energy spectra substantially harder than current solar flares. Some of the required pre-compaction exposure times exceed 200 million years [1] if due to either GCR or current SCR sources.

REFERENCES: 1) Caffee, M. W., et al.(1983), J. Geophys. Res., 88, B267-B273. 2) Walton, J. R., et al.(1974), Proc. Lunar Sci. Conf. 5th, 2045-2060. 3) Reedy, R. C., et al.(1979), Earth Planet. Sci. Lett., 44, 341-348.

COSMOGENIC RADIONUCLIDES AND EXPOSURE HISTORIES OF SNC METEORITES; Robert C. Reedy, Nuclear Chemistry Group, Mail Stop J514, Los Alamos National Laboratory, Los Alamos, NM 87545.

Chemical, petrological, and chronological measurements for Shergotty, Nakhla, Chassigny, and the 5 other SNC meteorites imply that these meteorites came from a large parent body (1). Trapped gases suggest that the SNC meteorites came from Mars; however, there are dynamical problems in ejecting them from Mars (2). The spallogenic noble gases for these SNC meteorites group into 3 sets of cosmic-ray exposure ages that require complex scenarios to explain them (2). Measurements of cosmogenic radionuclides and detailed calculated production rates are needed to help decipher the SNCs' cosmic-ray exposure histories. Calculated production rates of several cosmogenic noble-gas isotopes were recently reported (3). Presented here are production rates for the important long-lived cosmogenic radionuclides Be-10, Al-26, Cl-36, and Kr-81. The production of 3.7-Ma Mn-53 is mainly from Fe; existing measurements for Mn-53 per kg of iron can be used for the SNCs.

As in (3), the model of (4) for GCR-particle fluxes and evaluated cross sections for the main reactions producing these radionuclides were used. The SNC chemistries (3) vary considerably, especially for the important target elements for Al-26 (Mg, Al, and Si) and Cl-36 (Ca and Fe). Production rates for 6 SNC chemistries relative to those in L-chondrites are given in Table 1. As for Ne-21 and Ar-38 (3), some of these production ratios vary considerably among these SNCs and these ratios are shielding dependent. Preliminary measurements of 1.6-Ma Be-10 (G. Herzog, priv. comm.) in the SNCs are consistent with the 3 groups of noble-gas exposure ages (2). Activities of 0.7-Ma Al-26 in EETA79001 (J. Evans and U. Herpers, priv. comm.) imply its terrestrial age was not very long, which with its low exposure age means that it was ejected more recently from the shergottite parent body than the other 3 shergottites. While 0.3-Ma Cl-36 often is good for getting terrestrial ages, the unusual chemistries make it hard to accurately interpret Cl-36 activities in SNCs. Thus 0.2-Ma Kr-81 relative to Kr-78, which are made relatively well, would be better in getting terrestrial ages of the Antarctic shergottites. To help determine shielding conditions and find complex exposure histories, cosmic-ray-nuclei tracks and neutron-capture-produced nuclides are needed in additional to a variety of spallogenic nuclides.

(1) McSween, H. Y. (1984), Geology 12, 3-6. (2) Bogard D. D., Nyquist L. E., and Johnson P. (1984), Geochim. Cosmochim. Acta, in press. (3) Reedy R. C. (1984) Lunar Planet. Sci. XV, pp. 677-678. (4) Reedy R. C. (1984) Lunar Planet. Sci. XV, pp. 675-676; Proc. Lunar Planet. Sci. Conf. 15th, submitted.

Table 1. Ratios of calculated production rates in SNC meteorites relative to those in L-chondrites. The first ratio is for near the surface or in a very small meteoroid; the second is for fairly deep inside a large object.

	Shergotty	Nakhla	Chassigny	EETA79001B	EETA79001A	ALHA77005
Be-10	1.05-1.08	1.02-1.05	1.07-1.08	1.04-1.07	1.07-1.09	1.09-1.11
Al-26	1.48-1.54	1.21-1.20	0.91-0.89	1.57-1.67	1.36-1.40	1.10-1.11
Cl-36	2.6-3.6	3.5-4.9	0.7-0.5	2.7-3.8	1.9-2.5	1.1-1.3
Kr-81	7.4-6.6	3.65-3.65		6.7-5.8	3.3-2.8	2.0-1.8
Kr-78	9.8-9.2	3.4-3.5		9.9-9.3	4.8-4.5	2.8-2.6

COSMOGENIC NUCLIDES IN ANTARCTIC ACHONDRITES AND CHONDRITES

R.Sarafin[1], U.Herpers[1], R.Wieler[2] and P.Signer[2]

1 Institut für Kernchemie der Universität zu Köln, D-5000 Köln 1
2 Inst. f. Kristallographie u. Petrographie, ETH Zürich, CH-8092 Zürich

Among the numerous meteorites yet recovered from Antarctica there is a certain fraction of 'rare' types, which now become more easily available for investigation of cosmic ray induced effects. In documented samples of eight antarctic achondrites and three ordinary chondrites cosmogenic ^{53}Mn ($T_{1/2}$ = 3.8 x 10^6a) as well as the concentration and isotopic composition of light noble gases were determined by radiochemical neutron activation analysis and static mass spectrometry, respectively. Furthermore, in the case of the achondrites ^{26}Al ($T_{1/2}$ = 7.2 x 10^5a) was measured in adjacent samples by non-destructive γ-γ-coincidence spectrometry. First results of these measurements are given in table 1.

Meteorite	Type	^{26}Al [dpm/kg]
EETA 79001(A)	Shergottite	32.9 ± 1.6
EETA 79004,58	Eucrite	89.1 ± 4.3
EETA 79006, 2	Howardite	81.2 ± 4.9
ALHA 77257,14	Ureilite	33.2 ± 1.4
ALHA 78113,32	Aubrite	94.7 ± 6.8

Table 1: ^{26}Al concentrations of some selected antarctic achondrites

The concentrations of cosmogenic isotopes will be discussed with respect to exposure ages and terrestrial residence times. Special attention will be paid to the shergottite EETA 79001, for which a Martian origin has been proposed [1,2].

Acknowledgements
The authors wish to thank NASA for supplying the meteorite material. This work was supported by the Bundesministerium für Forschung und Technologie and the Swiss National Science Foundation grant No. 2.443-0.82.

References

[1] D.D.Bogard and P.Johnson, Science 221, 651 - 654 (1983).
[2] M.R.Smith et al., Proc.Lunar Planet.Sci.Conf.14th, in:J.Geophys.Res. 89, B612 - B630 (1984).

Evidence for ages older than 1.3 Gyr in the Elephant Morraine Shergottite.
R.S. Rajan[1], A.S. Tamhane[2], G. Poupeau[3], T.D. Swindle[4], M. Caffee[4], and C.M. Hohenberg[4]; 1. Jet Propulsion Laboratory, Caltech, Pasadena, CA 91109; 2. Tata Institute, Bombay, India; 3. CBPF, Rio de Janeiro, Brazil; 4. Mc Donnell Center, Washington Univ., St. Louis, MO 63130.

Shergottites are an extremely important group of meteorites to study because of their possible origin from Mars, e.g. (1). We have carried out nuclear track studies and uranium concentration measurements on samples from the Elephant Morraine shergottite. The study was initiated as part of the consortium effort over 2 years ago (H. McSween, Leader).

The pyroxene track densities range from 5×10^5 to $8 \times 10^5/cm^2$. Based on the short exposure age determined for this meteorite of 0.6 Myr (2), we infer that the samples had undergone little ablation and were very close to the pre-atmospheric surface. In fact, the preatmospheric depths of samples are tightly constrained to be between 1.5 and 2.5 cms, independent of the pre-atmospheric size.

Most of the phosphates in our sample were heavily shocked, as was expected. However, there is a small fraction of phosphates (1-2%), where the tracks can be observed clearly. The track densities seen in these crystals range from 3×10^6 to $9 \times 10^6/cm^2$. A study of the neighboring pyroxenes, discussed earlier, indicates that cosmic ray tracks can account for only 10 to 25% of the observed tracks. Accordingly, the majority of the tracks are indeed due to fission in the phosphates.

Uranium contents have been determined for over 50 phosphate grains and several of those have also been analyzed with the electron microprobe. All the phosphates analyzed were whitlockites and their uranium concentrations range from 0.3 to 1.5 ppm.

Using the highest uranium concentrations measured, we can calculate that the number of fission tracks expected over 1.3 Gyr is only $0.9 \times 10^6/cm^2$. It is thus clear that we are dealing with a population of phosphate grains which are substantially older, with nominal fission track ages ranging from 2.5 to 4.0 Gyr.

These observations are in apparent contradiction with the established radiometric chronologies of the shergottites. Efforts are presently underway to elucidate and understand these discrepancies, in light of models for the formation of shergottites. We hope that fission xenon measurements on these samples, which are currently in progress, will significantly help in constraining these models.

References: (1) C.Y. Shih et al., Geochim. Cosmochim. Acta, 46, 2323 (1982). (2) R.O. Pepin and R.H. Becker, LPSC XV, 637 (1984).

NOBLE GASES IN SNC METEORITES; T.D. Swindle, M.W. Caffee, C.M. Hohenberg, McDonnell Center for the Space Sciences, Washington Univ., St. Louis, MO 63130; and G.B. Hudson, Lawrence Livermore National Laboratory, Livermore, CA.

Shergotty and potentially related SNC meteorites are widely discussed as possible Martian samples. Many recent arguments in favor of a Martian origin for these meteorites have focused on noble gases in the glassy lithology C of EETA 79001 [1, 2]. We report on analyses of neon, argon, krypton and xenon from stepwise heating of EETA 79001,C, and xenon from ALHA 77005.

Results for EETA 79001,C confirm and extend many earlier findings [1, 2]. Enhanced $^{129}Xe/^{132}Xe$ ratios are seen in most temperature steps, up to 2.43, the highest value yet observed for an SNC sample, but still consistent with the measured Martian atmospheric ratio of 2.5 (+2,-1) [3]. $^{40}Ar/^{36}Ar$ ratios of 1000-2000 are observed at several consecutive temperature steps, consistent with a single component widely attributed to trapped argon. The measured ^{21}Ne is consistent with the reported exposure age of about .5 m.y. [4, 5].

A major motivation for this study of EETA 79001 is to delineate the isotopic structure of xenon at the heavier isotopes (131-136), since enhancements of the $^{136}Xe/^{132}Xe$ ratio have been noted [1]. Elevated $^{136}Xe/^{132}Xe$ ratios are, in fact, observed in some temperature steps, but they are rather modest, peaking at .353 (compared to .330 for air and .321 for AVCC). Release patterns are consistent with a mixture of two components, one of them enhanced in both ^{129}Xe and ^{136}Xe. However, attempts to derive a fission-yield spectrum, assuming addition of fissiogenic xenon to a known trapped component such as AVCC, U-Xe or air, are inconclusive, primarily because the calculations are extremely sensitive to corrections for the small spallation contribution to the fission-shielded isotopes (such as ^{130}Xe). Thus details of the isotopic structure of the heavy xenon isotopes in EETA 79001 remain undelineated.

Xenon from ALHA 77005 shows a slight enhancement in the $^{129}Xe/^{132}Xe$ ratio, with the highest of three temperature steps yielding a ratio of 1.13, approximately a 15 percent enhancement over terrestrial atmosphere. The $^{136}Xe/^{132}Xe$ ratio is also slightly enhanced in the same temperature step.

While the elevated $^{129}Xe/^{132}Xe$ ratio in these samples has usually been attributed to trapped xenon from the Martian atmosphere, many meteorites which are definitely not Martian contain enhancements much larger than those seen in EETA 79001. However, in those cases the excess ^{129}Xe is due to the *in situ* decay of the extinct radionuclide ^{129}I and therefore correlates with iodine. Since the iodine is normally present in variable proportion with the trapped xenon, the observed $^{129}Xe/^{132}Xe$ ratio varies substantially. This behavior, in fact, forms the basis for I-Xe dating. For EETA 79001,C we observe a relatively constant $^{129}Xe/^{132}Xe$ ratio in the higher temperature steps, suggesting either that the two isotopes come from a common source (not *in situ* decay) or that the xenon isotopic system has been homogenized (not implausible given the glassy lithology). An attempt was made to search for correlations between ^{129}Xe and iodine in ALHA 77005 by irradiating a sample with neutrons and looking for correlations between the release of ^{129}Xe and iodine-derived ^{128}Xe, in the usual fashion of I-Xe dating. However, the attempt was unsuccessful because ALHA 77005, like many Antarctic meteorites, contains an abnormally high amount of iodine, presumably contamination from terrestrial sources [6].

REFERENCES: 1) Pepin R.O., and R.H. Becker (1983) Met. 18, 375-376. 2) Bogard D.D., and P. Johnson (1983) Science, 221, 651-654. 3) Owen T., et al. (1977) J. Geophys. Res., 82, 4635-4639. 4) Pepin R.O., and R.H. Becker (1984) Lunar Planet. Sci. XV, 637-638. 5) Bogard D.D., et al. (1984) Lunar Planet. Sci. XV, 68-69. 6) Dreibus G., and H. Wanke (1983) Met. 18, 291-292.

ON THE ORIGIN OF EXCESS ^{40}Ar IN THE FOUR SHERGOTTITE-ACHONDRITES;
Donald Bogard, NASA, Johnson Space Center, Houston, TX 77058

The four shergottite-achondrites had their Rb-Sr isochron ages totally reset 180 My ago, probably by a common impact event which also produced the observed shock features. The apparent ^{39}Ar-^{40}Ar ages measured on whole rock and phase separates of the four shergottites, however, are poorly defined and range from 250 My to ~6000 My. The highest ages occur for shock-altered phases (e.g. glass) of EETA79001. The excess ^{40}Ar (relative to 180 My) in these phases is part of a trapped gas component whose diagnostic elemental and isotopic ratios suggest that the gas represents Martian atmosphere shock-implanted into the meteorite (Bogard & Johnson, Science 221, p651, 1983). Excess ^{40}Ar concentrations in Shergotty, Zagami, and ALHA77005 (~1-5 $x10^{-6} cm^3/g$) are about x10 smaller than in shocked phases of EETA79001. A significant question is whether this excess Ar might also represent shock-implanted Martian atmosphere, or can it be explained as radiogenic Ar not completely driven out of the sample by the shock event?

Excess ^{40}Ar is experimentally the most sensitive indicator of a Martian atmosphere component. IN EETA79001 the ratio of excess Ar to trapped Xe is $\sim 10^6$, essentially that measured in the martian atmosphere. The concentrations of Mars atmosphere CO_2 and N_2 to be expected in the EETA79001 glass sample with the largest excess ^{40}Ar are ~3ppm and ~0.1ppm, respectively. From the excess ^{40}Ar in the other three shergottites the largest CO_2 and N_2 concentrations consistent with Martian atmospheric composition are ~0.3ppm and ~0.01ppm, respectively. Such concentrations are quite small relative to those normally measured in meteorites and such components would be experimentally difficult to identify. ALHA77005 appears to have a small excess of ^{129}Xe, however, which is in approximately the same proportion to excess ^{40}Ar as gases in EETA79001. Terrestrial Ar is ruled out because of the strong retentivity of the gas and the observation of $^{40}Ar/^{36}Ar$ ratios greater than the value of terrestrial air.

If excess ^{40}Ar in Shergotty, Zagami, and ALHA77005 is *in situ* radiogenic gas not completely driven out by the shock event (or even inherited at the time of crystallization ~1.3 Gy ago) then Ar diffusion and loss would have to be slower than the extensive Sr diffusion that occurred 180 My ago. A comparison of literature data (e.g. D/a^2 values) for Sr diffusion in silicate minerals with data we measured for Ar diffusion in feldspar and pyroxene phases of the shergottites suggests that across a wide temperature range Ar diffusion should occur more readily than Sr diffusion. For our pyroxene separates Ar is strongly concentrated in tiny (~10 micron diameter), alkali-rich inclusions scattered throughout the pyroxene. Crushing which preceeded mineral separation probably exposed many of these inclusions and thereby artifically increased the ease of Ar diffusion from pyroxene during laboratory heating. Ar diffusion from uncrushed olivines in ALHA77005 (which also contain alkali-rich inclusions), for example, is up to several orders of magnitude slower (depending on the temperature) than Ar diffusion from feldspar, but comparable to Sr diffusion in some minerals. Concentrations of excess ^{40}Ar in different phases of Shergotty, Zagami, and ALHA77005 do not vary by large factors, however, in spite of large apparent differences in the ease of Ar diffusion. Available diffusion data, therefore, suggest that it would require special circumstances to explain the excess Ar in shergottites as due to incomplete loss of radiogenic Ar during the shock event, but we cannot rule out this explanation.

REMEASUREMENT OF NITROGEN IN EETA 79001 GLASS. R. C. Wiens, R. H. Becker, and R. O. Pepin, School of Physics and Astronomy, University of Minnesota, Minneapolis, Minnesota 55455.

Following the report (1) of trapped noble gases in the EETA 79001 shergottite closely resembling those measured in the atmosphere of Mars (2), we undertook an analysis of this meteorite to look for the presence of the isotopically heavy nitrogen which is also a characteristic of the martian atmosphere (3). Results of that analysis, reported previously(4), included a bulk $\delta^{15}N$ value of +180 permil for one sample of 79001 glass, with a maximum $\delta^{15}N$ of $\sim$200 permil in the gas released at the highest temperature. Although the value did not closely approach the $\sim$600 permil measured for Mars(3), it was demonstrated that the lower values could be explained by mixing of martian atmospheric gases with a second component, either indigenous to the silicates or adsorbed from the terrestrial atmosphere on the crushed samples. To distinguish between the two possibilities, we have reanalyzed EETA 79001 using an uncrushed glass sample with a much smaller surface-to-volume ratio.

We obtained a 110 mg sample of EETA 79001 glass in the form of a single, roughly spherical piece. The sample was inspected microscopically to verify that it was not microcracked or visibly vesicular. Analysis was carried out by stepwise heating, with He, Ne and Ar measured along with the nitrogen, in the same way as for the previous samples (4).

Preliminary nitrogen results are presented in the Table for the steps of interest. The data have not yet been corrected for blanks, and therefore represent minimum $\delta^{15}N$ values. Two points should be noted. One is that the maximum $\delta^{15}N$ obtained, which presumably represents a minimum value for the trapped component, is +290 permil (reduced to +265 permil if this step contains *all* the expected spallation N). This value, while not as high as one might hope given the presumed $\sim$600 permil composition of the pure end-member component, can be taken as strengthening the argument that the trapped component is Mars-like in its $\delta^{15}N$. The second point is that, even though the present sample had only $\sim$2.5% of the surface-to-volume ratio of the previous samples(4), the $\delta^{15}N$ of the sample as a whole is only marginally closer to the presumed value of the pure trapped component(blank corrections are expected to increase the numbers in the Table by $\lesssim$ 5-10%). We conclude from this, and the fact that the isotopic ratio does not reach a constant value at temperatures where surface-adsorbed N_2 should be gone, that the isotopically light component is inherent in the sample, though variable in amount, rather than adsorbed from the terrestrial atmosphere. The possibility that the pure trapped nitrogen is not characterized by $\delta^{15}N \simeq 600$ permil, but has some lower value, should not be overlooked as an explanation for the maximum of only $\sim$290 permil in this experiment, but the lack of a plateau in $\delta^{15}N$ argues for variable mixing of a two-component system in all but perhaps the highest temperature gas fraction.

Preliminary processing of argon data indicates that results from this sample are consistent with the N_2-^{40}Ar mixing line defined by the two glass samples previously analyzed (4).

T(^{0}C)	=	900	1030	1100	1180	$\sim$1500	Σ
$\delta^{15}N$(‰)	=	102	156	228	290	280	231

REFERENCES. (1)Bogard D.D.(1982)*Meteoritics 17*,185; (2)Owen T. *et al.*(1977) *J. Geophys. Res. 82*,4635; (3)Nier A.O. and McElroy M.B.(1977)*J. Geophys. Res. 82*,4341; (4)Becker R.H. and Pepin R.O.(1984)The case for a martian origin of the shergottites, *Earth Planet. Sci. Lett.* (in press).

MARTIAN ATMOSPHERIC CO_2 IN AN ANTARCTIC METEORITE ? R.H. Carr, I.P. Wright and C.T. Pillinger, Planetary Sciences Unit, Department of Earth Sciences, The Open University, Walton Hall, Milton Keynes MK7 6AA, U.K.

There is mounting evidence for a Martian origin for the SNC meteorites, although dynamical problems of ejecting suitably sized objects from planetary bodies still exist. Glassy-melt inclusions of the EETA 79001 shergottite release noble gases (1) and nitrogen (2) at high temperatures, during stepped heating experiments, with elemental and isotopic compositions which indicate the presence of trapped Martian atmospheric components. If this interpretation is correct, these gases should have been accompanied by ca. 5 ppm of the most abundant atmospheric component -- CO_2 (1). We have now measured, with high sensitivity mass spectrometric techniques, the isotopic composition of carbon released by stepped combustion from EETA 79001,149, a 14.8 mg fragment of a lithology C inclusion.

The fragment yielded a total of 48 ppm C, 80% of this comprising organic contamination and another low temperature component, as yet unidentified. Above 900°C (Fig. 1), 9.4 ppm C was evolved, with $\delta^{13}C$ (>900°C) = +6‰, equivalent to $^{13}C/^{12}C$ = 0.0114. These data are in agreement with the expected CO_2 content of the glass (1) and with the $^{13}C/^{12}C$ value of 0.0115 ± 0.0003 measured by the Viking spacecraft in the Martian atmosphere and are, therefore, consistent with previous interpretations of there being Martian atmospheric gases trapped in these inclusions.

It is interesting to note, however, that Nakhla (Fig. 2) and other SNC meteorites, including lithology A of EETA 79001 (4), release some carbon at similar temperatures. In each case, the $\delta^{13}C$ value shows a marked increase relative to that measured at lower temperatures, consistent with the presence of a proportion of the component seen in EETA 79001 lithology C.

In addition, Nakhla contains an isotopically heavy carbon component, $\delta^{13}C$ = +13‰, released ca. 400-600°C, confirming previous findings (5). Carbon dioxide probably plays an important role in chemical weathering on Mars; thus, considering the $\delta^{13}C$ values for CO_2 from EETA 79001 released above 900°C, the presence of a Martian carbonate in Nakhla is an intriguing possibility.

References: (1) Bogard & Johnson (1983) Science, 221, 651. (2) Becker & Pepin (1983) Meteoritics, 18, 264. (3) Nier et al. (1976) Science, 194, 68. (4) Carr, R.H. & Pillinger (1984) Lunar Planet. Sci. XV, 135. (5) Fallick et al. (1983) Lunar Planet. Sci. XIV, 183.

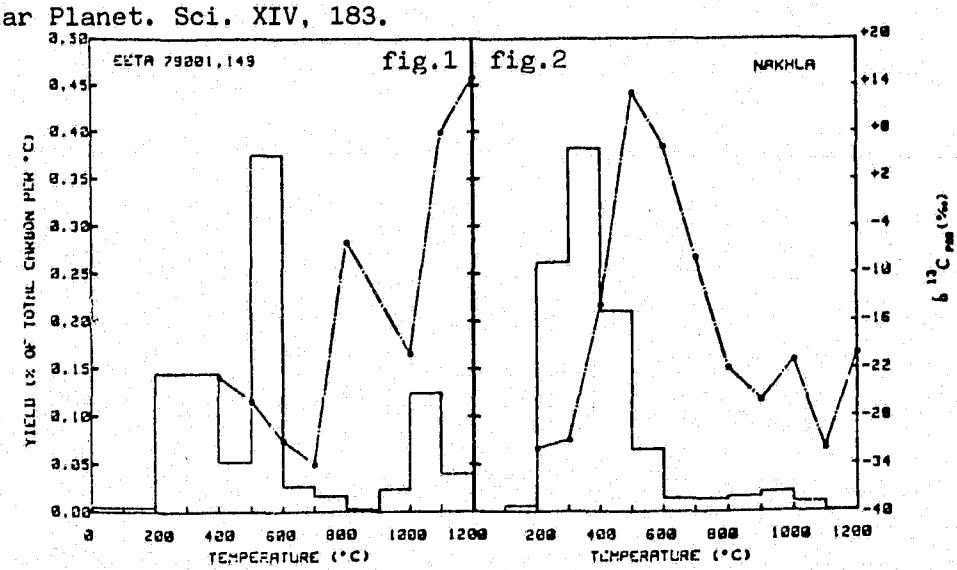

SHOCK DEFORMATION TEXTURE OF OLIVINE CRYSTALS OF THE EETA79001 SHERGOTTITE; Hiroshi Mori and H. Takeda, Mineralogical Institute, Faculty of Science, Univ. of Tokyo, Hongo, Tokyo 113, Japan.

All the shergottite meteorites display intense shock metamorphisms. Especially, plagioclase shows a characteristic shock feature: formation of diaplectic glass (maskelynite) or melting (1, 2, 3). By studying the shergottite meteorites, we can get a better understanding the nature of shock metamorphism of olivine, in comparison with that of coexisting plagioclase which is the most sensitive and well-characterized pressure indicator, in natural impact events. Olivine occurs in two shergottites, ALHA77005 and EETA79001. Previously we reported shock deformation microstructures of olivine crystals in the ALHA77005 shergottite (4).

Transmission electron microscopic (TEM) study was conducted to elucidate the shock deformation microstructure of olivine in the EETA79001 shergottite. One olivine megacryst was separated from the chip of EETA79001. The olivine crystal was examined on an X-ray precession camera to determine the crystallographic orientation and the diffraction asterism. Sample preparation for TEM study was performed using a conventional ion-thinning technique after X-ray study. Optically, the olivine shows irregular fractures and undulatory extinction. TEM observation reveals deformation microstructures characteristic of shock (i.e. dislocation, crack) are very common in the olivine. Long straight [001] screw dislocations are predominant. Some dislocations form dipole configurations. Ashworth and Barber (5) observed similar dislocation substructures of olivine in the Olivenza and Hedjaz chondrites. Dislocation densities are ca. 10^8 - 10^{10} cm^{-2} in EETA79001. Zones of very high dislocation density occur in association with microcracks. In some cases, small amounts of amorphous zone are observed along the microcracks. Such an amorphous zone may represent a diaplectic glass produced by shock compression (6) . Shock-induced thermal effect is apparently negligible in EETA79001, judging from the small degree of dislocation recovery and the preservation of the diaplectic glass.

McSween and Jarosewich (3) estimated peak shock pressures of 35-45 GPa experienced by EETA79001. Their estimate is based on the following diagnostic observations: mosaicism and granulation in olivine, formation of maskelynite, and production of melt pockets and veins. As far as our observation on the deformation microstructures of olivine is concerned, lower shock pressurs (ca. 20 -30 GPa) are inferred than those of McSween and Jarosewich (3). This may reflect a heterogeneous distribution of shock deformation or a refractory nature of olivine for shock deformation.

References:

(1) Duke M.B. (1968) In Shock Metamorphism of Natural Materials, p. 613-621.
(2) McSween H.Y. and Stöffler D. (1980) Lunar Planet. Sci. XI, p. 717-719.
(3) McSween H.Y. and Jarosewich E. (1983) Geochim. Cosmochim. Acta 47, 1501-1513.
(4) Mori H. and Takeda H. (1983) Proc. 16th ISAS Lunar and Planet. Symp., p. 105-108.
(5) Ashworth J.R. and Barber D.J. (1975) Earth Planet. Sci. Lett.,27, 43-50.
(6) Jeanloz et al. (1979) Science, 197, 457-459.

Sr and Nd ISOTOPIC SYSTEMATICS OF EETA 79001; L. Nyquist[1], J. Wooden[2], B. Bansal, H. Wiesmann, and C.-Y. Shih[3] ([1]SN4, NASA Johnson Space Center, Houston TX 77058; [2]MS 937, USGS, Menlo Park CA 94065; [3]Lockheed, 1830 NASA Rd. 1, Houston, TX 77058)

Additional Sm-Nd data for bulk rock and pyroxene separates of EETA 79001 refine and extend the results previously reported (1). The whole rock Sm-Nd age for all four shergottites is 1.27+/-0.04 Gyr and epsilon (Nd,1.27 Gyr) = -11. The whole rock age for only EETA 79001 and ALHA 77005 is 1.12+/-0.12 Gyr and epsilon (Nd,1.12 Gyr) = -10. The time significance of these ages depends on the extent to which the mantle sources of the shergottites had similar Sm-Nd histories. The model age, T_{CHUR}, of EETA 79001 is 0.78 Gyr, slightly older than the 0.72 Gyr model age of ALHA 77005. The pyroxene-whole rock age of EETA 79001 is 240+/-150 Myr and is within error limits of the 180 Myr Rb-Sr shock-metamorphic age of shergottites. Three of the four shergottites have pyroxene-whole rock ages which are consistent with the shock metamorphic age. Even for post-shock temperatures in the range of 800-1100°C, moderately large post-shock objects , ca. 3-30 m in radius, are implied in order for cooling times to be long enough for diffusive equilibration of the Nd isotopic composition in pyroxenes to occur.

As previously reported (1) internal Rb-Sr isochrons for lithologies A and B, respectively, are 173+/-10 Myr and 185+/-25 Myr. The corresponding initial ratios are I(0.18 Gyr) = 0.71217+/-3 and 0.71243+/-7, respectively. Rb-Sr data for handpicked xenocrysts lie below the lithology A isochron and correspond to I(0.18 Gyr) = 0.71187+/-7. This result is understandable if the xenocrysts represent a separate lithology as suggested by (2). These authors attribute the xenocrysts to the disaggregation and partial resorption of an olivine - pyroxene - chromite cumulate by the lithology A magma. The xenocrysts resemble olivine and pyroxene in ALHA 77005 in mineral chemistry (2). The Rb/Sr ratio of the xenocrysts is also similar to that of olivine separates from ALHA 77005 (3). These observations suggest a model of assimilation of ALHA 77005-like material by the lithology B magma to produce lithology A. A mass-balance calculation suggests that a mixed magma containing 44% ALHA 77005 and 56% EETA 79001 B would have the observed Sr-isotopic composition of EETA 79001 A. These mixing proportions are similar to those obtained by (4) from a mixing model including major, minor, and siderophile elements. However, Nd isotopic compositions of EETA 79001 A and B show no evidence of admixture of a component like ALHA 77005 to EETA 79001 B. The expected effect on EETA 79001 A of an admixture of 44% ALHA 77005 to EETA 79001 B is only slightly greater than typical analytical uncertainties, however. The absence of an observable Nd-isotopic effect may imply that $^{143}Nd/^{144}Nd$ of the assimilated material was more similar to that of the EETA 79001 B magma than to that of ALHA 77005 or that REE abundances in the assimilated material were lower than in ALHA 77005. In this connection it is noteworthy that the mixing models overestimate REE abundances in lithology A by ca. 25-50%.

(1) Wooden J., Shih C.-Y., Nyquist L., Bansal B., Wiesmann H., and McKay G. (1982) Lunar and Planet. Sci. XIII, p. 879-880. (2) Steele I.M. and Smith J.V. (1982) Proc. Lunar Planet. Sci. Conf. 13th, in Journal of Geophysical Research, 87, p. A375-A384. (3) Shih C.-Y., Nyquist L., Bogard D., McKay G., Wooden J., Bansal B., and Wiesmann H. (1982) Geochim. et Cosmochim. Acta 46, p. 2323-2344. (4) Smith M., Laul J., Ma M., Huston T., Verkouteren R., Lipschutz M., and Schmitt R. (1984) Proc. Lunar Planet. Sci. Conf. 14th, in Journal of Geophysical Research 89, p. B612-B630.

CORE FORMATION IN THE SHERGOTTITE PARENT BODY (SPB) Allan H. Treiman and Michael J. Drake, Lunar and Planetary Laboratory, University of Arizona, Tucson, AZ 85721.

The signature of metal/silicate fractionation during core formation in the SPB can be seen in the abundances of the siderophile elements in the SNC meteorites, after corrections for effects of volatility-controlled fractionation and silicate mineral/melt fractionation. Contrary to our previous report [1], which was based on a less sophisticated analysis of published data which did not explicitly consider post-accretional silicate fractionation during magmatic events, there is no evidence that the shergottites, nakhlites, and Chassigny were derived from a mantle with variable siderophile element concentrations. The signature of core-formation in the SPB is similar to that of the Earth and different from those of the Moon and Eucrite Parent Body.

Our method is like that of [2]; we compare abundances of an incompatible siderophile element to abundances of a lithophile element of similar volatility and compatibility. We recognize two groups of elements whose abundances in the SNC meteorites are strongly correlated on log. element vs. log element diagrams with slopes approximating unity: highly incompatible elements (Ag, As, Au, Ba, Cs, and moderately incompatible elements (Al, Eu, Ga, Hf, HREE, Na, P, Ti). Within each group, a ratio of element abundances (e.g., P/Ti) may vary by a factor of 3, mostly because of sample heterogeneity. However, abundance ratios for an element in one group versus an element in the other group (e.g., P/La) may vary by a factor of 25 as a result of silicate mineral/melt fractionation. By separating elements into these two groups we attempt to see through the effects of silicate fractionation in the SPB. Among the highly incompatible elements, the lithophile refractory elements (Ba, La, Ta, Th, U) are present in chondritic relative proportions. Volatile lithophile elements (Li, K, Rb, Cs) are depleted by a factor of 3 relative to the refractories (3), probably as a result of volatility-controlled processes during planetary accretion. We expect that any element more volatile than Li will be similarly depleted in the SPB.

Highly incompatible elements with siderophile character (Ag, As, Au, Sb, W) are depleted in the SNC meteorites more than would be expected from volatility alone. Abundances relative to La and CI are: Ag, 0.025; As, 0.002; Au, 0.005; Sb, 0.08; and W, 0.3. Abundances of the first four elements are affected by volatility, but the depletion of W must be ascribed to metal/silicate fractionation alone, presumably core formation.

Among the moderately incompatible elements, Ga, P and Na may be affected by volatility, but other elemental abundances are not explained by volatility alone (e.g., Al/Hf < Eu/Hf). After correction for volatility, elemental abundances in the mantle of the SPB relative to Hf and estimated bulk SPB are: P, 0.35; Eu, 1.0; Ti, 0.7; Tb, 0.7; Lu, 0.5; Na, 0.45; Al, 0.35; and Ga, 0.35. Except for P, abundances are inversely correlated with compatibility in a silicate mantle [4] which lacks residual feldspar. Excess depletion of P may be ascribed to metal/silicate fractionation. Depletion of Ga relative to Al in the SNC's is completely explained by volatility; there is no need to separate Ga into a metal phase.

After correction for effects of pre-accretional volatility and post-accretional silicate fractionation events, abundances of siderophile elements in the mantle of the SPB (relative to bulk SPB and an appropriate lithophile element) are: 1=Ga>Sb>W>P>Ag>Au ≈ As. This order of relative depletion is identical to that of the Earth and different from that of the Moon or Eucrite Parent Body [2]. W, Ga and P are less depleted in the SPB than the Earth; thus core formation in the SPB may have involved higher $f(O_2)$, lower temperature, and/or less efficient separation of metal than in the Earth.

[1] TREIMAN A. ET AL. (1984) Lunar Planet. Sci. XV, 864. [2] DRAKE M.J. (1983) Geochim. Cosmochim. Acta 47, 1759. [3] LAUL J. ET AL. (1972) Geochim. Cosmochim. Acta 36, 329. [4] SUN S. ET AL. (1979) Earth Planet. Sci. Lett 44, 119.

CHEMICAL RELATIONSHIPS AMONG SHERGOTTITES, NAKHLITES, AND CHASSIGNY

G. Weckwerth and H. Wänke, Max-Planck-Institut für Chemie, 65 Mainz, F.R.G.

In respect to their chemical and mineral composition both, the shergottites and the nakhlites, form distinct groups. The different mineral composition of shergottites (orthopyroxene and plagioclase), nakhlites (clinopyroxene-rich) and Chassigny (olivine-rich) makes it more difficult to judge, whether all these groups have a related origin. One possibility to perform this, is to compare the ratios of incompatible elements, which are known to stay relatively constant during partial melting or fractional cristallization processes. Using mainly data of Burghele et al. (1) and Dreibus et al. (2) we studied the ratios of all incompatible elements relative to REE.

The incompatible elements can be devided into two groups. The first one includes all highly incompatible elements (K, Rb, Cs, Ba, La, and Ce). These elements are correlated with each other in all SNC-meteorites. The second group is composed of Ca, Al, Ti, P, Sc, Na. They have constant ratios in shergottites and Chassigny with heavy REE. Only Nakhla deviates in some cases more than 50% from the mean ratios in both element groups. These differences are strongest for the elements Ca and Sc, which have high partition-coefficients between clinopyroxene and basaltic melts. Therefore it is not unreasonable to find them enriched in Nakhla, which consists to 80% out of augite. The P/HREE-ratios of Nakhla, which are between two and three times lower than those of the other SNC-meteorites, can be explained in a similar way. Measurements of clinopyroxene from terrestrial peridotites show also depletions of the P/REE-ratios relative to the other mineral phases (3). Treiman et al. (4) took the high variation of P/La-ratios as an indicator for a distinct origin of SNC-meteorites. In contrast to this, we think that the correlation of P with more heavy REEs indicates a more compatible behaviour of P, possibly caused by residual phosphate or a higher olivine/plagioclase-ratio in the source-region of SPB.

W and Ta have constant ratios with the other highly incompatible elements in shergottites, but in Nakhla and Chassigny the W/La and the Ta/La ratios are about a factor of three lower (4). In light of the correlations of all SNC-meteorites for the other highly incompatible elements and the common age, we do not believe that the postulation of an inhomogeneous SPB-mantle or different parent bodies is justified.

References: (1) A. Burghele et al. (1983) Lunar Planet.Sci.XIV, 80
(2) G. Dreibus et al. (1982) Lunar Planet.Sci.XIII, 186
(3) G. Weckwerth (1983) Thesis, University of Mainz
(4) A. Treiman et al. (1984) Lunar Planet.Sci.XV, 864

THERMOLUMINESCENCE AS A PALEOTHERMOMETER?;

R.K. Guimon, K.S. Weeks, B.D. Keck and D.W.G. Sears. Dept. of Chemistry, Univ. of Arkansas, Fayetteville, AR 72701.

An important phase in the history of chondritic meteorites is a period of metamorphism. Thermoluminescence has been shown to be a powerful technique for investigating metamorphic effects, particularly for the least metamorphosed meteorites (1). The ordinary chondrites as a whole exhibit a 10^5-fold range in their TL sensitivities, while the least metamorphosed type 3 ordinary chondrites show a 10^3-fold range. Associated with this range in TL sensitivity are variations in the temperature at which maximum TL emission occurs and also in the range of temperature over which emission occurs (2).

In the present paper, we present the results of annealing experiments on a little-metamorphosed ordinary chondrite (A77011, type 3.5). Samples were annealed for 100 hours at temperatures ranging from 500 to 1000 C in a nitrogen atmosphere. The TL emission characteristics of the annealed samples show trends which are very similar to those observed in meteorites which have been naturally metamorphosed to different extents. The temperature at which maximum emission occurs in both our annealed samples and in naturally metamorphosed type 3 chondrites shows an increase of 80 - 100 C relative to the unannealed or least metamorphosed samples. The temperature range in which TL emission is observed shows corresponding increases of about 50%. This broadening and movement to higher temperatures of the peak is also similar to the effects produced by experiments on terrestrial albite (3,4) where the changes observed were associated with a low to high temperature transformation. These data suggest that the TL phosphor is feldspar and also that TL may be used to estimate paleotemperatures for little-metamorphosed, unequilibrated meteorites.

References. 1. Sears, D.W., Grossman, J.N. and Melcher, C.L. (1980) Nature 287, 791-796. 2. Sears, D.W., Grossman, J.N. and Melcher, C.L. (1982) Geochim. Cosmochim. Acta 46, 2471-2481. 3. Pasternak, E.S., (1978) Ph.D. Thesis, Univ. of Pennsylvania. 4. Pasternak, E.S., Gains A.M. and Levy, P.W. (1976) Geol. Soc. Amer. Abstracts with Program 8, 1044.

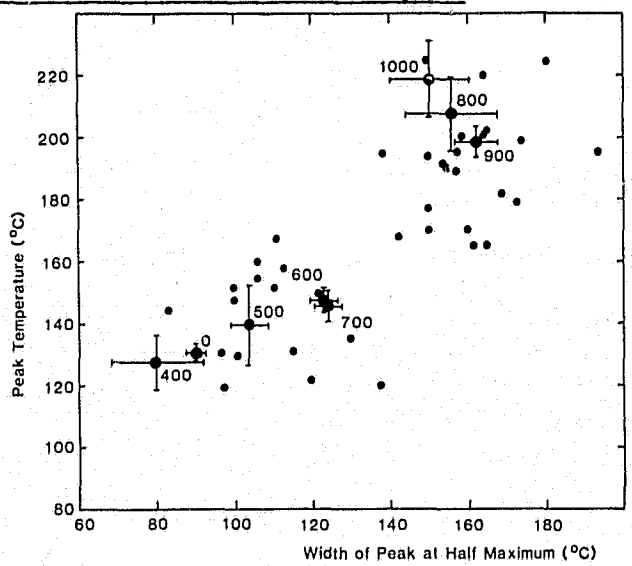

Fig 1. TL peak temperature vs. peak width for samples of Allan Hills A77011 annealed to various temperatures (large points, temperatures in C) and type 3 ordinary chondrites (small points).

A QUANTITATIVE LOOK AT CHONDRITE METAMORPHISM. G. Jeffrey Taylor and Edward R. D. Scott, Institute of Meteoritics and Department of Geology, University of New Mexico, Albuquerque, NM 87131.

The most prominent metamorphic effects in chondrites include homogenization of olivine and pyroxene, devitrification of glass, and obscuration of originally distinct chondritic texture, accompanied by minor increase in grain size. To clarify chondrite metamorphic histories, we modeled changes in grain size that would take place during protracted heating and cooling of chondritic rock. We also investigated constraints on thermal history of type 3-6 chondrites imposed by the homogeneity or lack of it in olivine and low-Ca pyroxene. We modeled grain coarsening of polycrystalline olivine assuming a rate law of the form $R^3 = R_o^3 + Kt$, where R and R_o are the final and initial particle radii, respectively, and t is time. K is a function of the diffusion coefficient, temperature, surface energy, etc. We used a surface energy of 10^3 ergs/cm^2 and modeled the growth in small isothermal steps. To estimate the amount of diffusion in olivine, we used the relation $X^2 = 2Dt$, in which X is the average diffusion distance, D is the olivine diffusion coefficient, and t is time.

Our calculations indicate that Fe-Mg equilibration in olivine is much faster than grain growth at all subsolidus temperatures. For example, the average diffusion distance in olivine heated to 900°C for 10 years is 70 μm, but grains larger than 10 μm would not grow at all during this time (although one micron grains would grow to 4 μm). It seems possible to homogenize mineral compositions without significant grain growth, contrary to some opinions [1].

If type 6 chondrites cooled from 900°C at <10°C/Myr [2,3], their average grain sizes would be >600 μm, which is not the case. Even if the peak temperature was 800°C, their average grain sizes would be larger (>375 μm) than observed. This suggests that type 6 chondrites (and type 5 as well) cooled rapidly (>1000°C/Myr) from peak metamorphic temperatures down to 500°C, at which point they cooled as slowly as cooling-rate measurements indicate. There is sufficient time for minerals to equilibrate during rapid cooling from peak temperatures: the average diffusion distance in olivine in a rock cooling at 10^4 °C/Myr from 900°C is 2 cm, enough to homogenize even mm-sized olivine grains. Assuming diffusion in pyroxene is 10^3 times slower, the average diffusion distance would be 700 μm, enough to homogenize it also. If the average grain size were 10 μm to begin with, cooling at this rate from 900°C would cause growth to 30 μm; no significant additional coarsening would occur during cooling from 500°C at 1 °C/Myr. Type 4 chondrites were probably heated to <800°C, but our analysis indicates that they also cooled faster above 500°C than below. The calculations point toward a two-stage cooling history for chondrites, consistent with the idea that chondrites were metamorphosed in km-sized bodies that subsequently accreted to form parent bodies. Our results are also consistent with models [4] calling for accretion at >800°C, during which minerals homogenize, followed by rapid cooling to lower temperatures, but we believe that such models require implausible physical settings.

The few type 3 chondrites with well-defined cooling rates, such as Tieschitz, Chainpur, and Mezo-Madaras, pose some problems. The lowest Ni contents in taenite centers in these chondrites indicate they were heated to >450°C. Cooling from this temperature at a rate of only a few °C/Myr, however, would cause fine-grained matrix and chondrule rim materials to coarsen from <1 μm to >10 μm, and would cause olivine to become completely homogenized, contrary to observations. This indicates that either a) the cooling rates are incorrect, b) growth and olivine diffusion are much slower than calculated, or c) both. Although cooling rates are subject to question when peak temperatures are < 600°C, it seems likely that there are kinetic barriers (e.g., glass in chondrules) to grain growth and diffusion [5]. At higher temperatures, these barriers may be quickly overcome so that our conclusions about type 4-6 chondrites are probably not affected.

References: 1) Fredriksson, K. (1983) Chondrules and Their Origins, 44-52. 2) Wood, J.A. (1967) Icarus **6**, 1-49. 3) Pellas, P. and Storzer, D. (1981) Proc. Royal Soc. London **Ser. A**, 253-270. 4) Ashworth, J. R. et al. (1984) Nature **308**, 259-261. 5) Sears, D. et al. (1984) GCA, in press.

METAMORPHISM OF TYPE 3 CARBONACEOUS AND ORDINARY CHONDRITES; Edward R.D. Scott and G. Jeffrey Taylor, Institute of Meteoritics, Dept. of Geology, University of New Mexico, Albuquerque, NM 87131.

We have analyzed silicates in ~15 porphyritic olivine (PO) chondrules in each of six CO3 chondrites to understand how and where metamorphism occurred, and to help distinguish primary and metamorphic features. We found previously (1) that 17 out of 20 type 3.4-3.9 ordinary chondrites appear to be mixtures of equilibrated and unequilibrated chondrules suggesting that these chondrites are breccias of materials with different metamorphic histories. We wish to know whether metamorphic effects in CO3's resemble those in H-L-LL3 chondrites, and whether they were produced by similar processes.

Mean compositions of olivine and low-Ca pyroxene are shown below for type I and type II PO chondrules; meteorites are arranged in order of increasing metamorphism (2). In A77307 and Kainsaz, as in other primitive chondrites, most Type I PO chondrules have olivine with 0-4 mole% Fa and 0.2-0.4 wt.% CaO. With increasing metamorphism and consequent chondrule-matrix equilibration, Fa increases and CaO decreases. Thus in Warrenton, the most metamorphosed CO3, olivines in all Type I chondrules are zoned, typically with Fa 5-35 and 0.1-0.3% CaO. As in H-L-LL3 chondrites, low-Ca pyroxene lags behind olivine during equilibration because of 10^3-fold slower diffusion; average compositions in Warrenton are Fs 2-6. Type II chondrules in the six CO3 chondrites show smaller metamorphic changes, but olivines in Warrenton are appreciably more homogeneous and lower in CaO than those in Kainsaz and 77307. Recrystallization in types I and II is limited to the mesostases of type I.

Despite similarities between metamorphic trends in O and C type 3 chondrites, metamorphosed CO3's tend to show a much narrower range of Fe/(Fe+Mg) concentrations, e.g. Fa 1-30 in Ngawi type I chondrules, but Fa 15-20 in Warrenton. This is more consistent with *in situ* metamorphism, but metamorphically zoned, broken olivines (3), and significant variations in type I chondrule Fe/(Fe+Mg) ratios in a single chondrite suggest that CO3 chondrites, like H-L-LL3's, are breccias of material with diverse metamorphic histories. In Lancé, 77029, 77003, and Warrenton, we did not find a single chondrule with type 4 levels of homogeneity and CaO in olivine, or one with Fa 0.7-3 like those in 77307; such chondrules are relatively common in type 3.5-4 O chondrites. CO3's may come from a body with no type 4 material, in which mixing was less severe than in ordinary chondrite parent bodies.

Our studies of CO3 and C4 chondrites indicate that metamorphic effects in carbonaceous chondrites resulted from processes similar to those that affected ordinary chondrites. Heating probably occurred in km-sized planetesimals. Requirements that silicate homogenization occurred at ~1000°C before quenching and proto→clinoenstatite conversion (4) imply that planetesimals were broken up and reassembled before O chondrite parent bodies formed.

References: (1) Scott E.R.D. et al. (1983) Meteoritics 18, 392. (2) McSween H.Y. Jr. (1977) Geochim. Cosmochim. Acta 41, 477-491. (3) Van Schmus W.R. (1969) In "Meteorite Research" edited by P.M. Millman, pp. 480-491. (4) Ashworth J.R. et al. (1984) Nature 308, 259-261.

	Type I			Type II	
	Fa	CaO in ol.	Fs	Fa	CaO in ol.
ALHA77307	0.7-2.5	0.20-0.35	0.9-1.1	27-35	0.15-0.35
Kainsaz	1.2-6.8	0.20-0.40	1.0-2.5	26-31	0.07-0.24
Lancé	1.0-7.9	0.10-0.6	1.0-1.5	31-43	0.15-0.20
ALHA77029	4.3-10	0.15-0.35	0.9-2.0	32-41	0.15-0.20
ALHA77003	12-29	0.10-0.20	1.0-2.8	36-42	0.07-0.15
Warrenton	15-20	0.10-0.25	2-6	24-36	0.10-0.15

CHEMICAL ZONING AND HOMOGENIZATION OF OLIVINES IN ORDINARY CHONDRITES

M. Miyamoto, D. S. McKay, G. A. McKay, and M. B. Duke, SN4/NASA-JSC, Houston, TX 77058.

Petrologic types (from 3 to 6) of ordinary chondrites are generally thought to be produced by thermal metamorphism in their parent bodies [e.g. 1]. For example, Mg-Fe variations and CaO contents of olivines decrease with increasing petrologic type, that is, CaO content of type 3 is >0.1 wt%; that of type 4 is ca. 0.06 %; that of types 5 and 6 is 0.02-0.05 % [e.g. 1]. We have accurately measured CaO contents of olivines in ALHA77278(LL3),ALHA77299 (H3) [2], and Yamato-75028(H5) with a microprobe by the method described by [3] in order to better understand conditions of the thermal metamorphism.

Mg-Fe-Ca variations in olivines from the core to rim can be tentatively classified into several types. (a) Both Fa component and CaO content (~0.1-0.3 wt%) increase gradually (zoning). (b) Fa component increases but CaO content (~0.5-0.1 %) decreases gradually. (c) Fa component is almost constant and CaO decreases gradually (~0.4-0.05 %). (d) Both high Fa component (Fa=~20-30) and CaO content (~0.03-0.05 %) are almost constant. All zoning types are present in a type 3 chondrite.

By employing Mg-Fe-Ca zoning profiles as initial values, we have calculated the expected homogenization path of CaO content in olivine by numerically solving the diffusion equation. The assumed boundary condition is that CaO content at the rim is 0.02 wt%. This value is based on the CaO content in type 6 olivines and distribution coefficient of CaO between olivine and glass. Some calculated profiles match the observed profiles. Mg-Fe-Ca variations and negative correlation between CaO content and Fa component in olivines [4] may be explained by thermal metamorphism, because of differences of both diffusion coefficient [5] and boundary conditions between Ca and Fe [Fig. 1].

We have also calculated the burial depths to homogenize the type (a) CaO variation. The parent body (R=85km) is assumed to be heated internally by decay energy of Aluminum-26 [6]. If burial depth is less than ca. 3km, the CaO variation does not change, If burial depth is more than ca. 8km, the CaO is homogenized completely to 0.02 %.

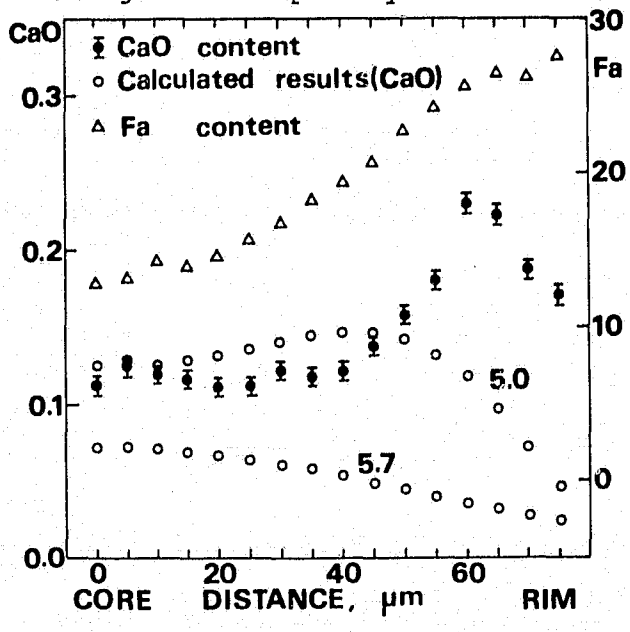

Fig. 1. CaO content (wt%) and Fa component of an olivine in ALHA77278 (LL3). Data are 5 micron interval from core to rim. Solid circles indicate CaO (wt%) (left-hand scale). Error bar shows ±2-sigma. Triangles indicate Fa component (right-hand scale). Open circles show calculted homogenization paths of CaO, internally heated by Aluminum-26. Numbers show burial depths in km.

References: [1] R. T. Dodd, Meteorites, Cambridge Univ. Press, 1981. [2] E. R. D. Scott, Meteoritics, 17, 393, 1984. [3] G. A. McKay, GCA 1984(submitted). [4] E. R. D. Scott and G. J. Taylor, Proc. 14th Lunar & Planet. Sci. Conf. B275, 1983. [5] M. Morioka, GCA, 45, 1573, 1981. [6] M. Miyamoto, N. Fujii, and H. Takeda, Proc. Lunar & Planet Sci. Conf. 12B, 1145, 1981.

NOBLE GAS CHRONOLOGY OF LL CHONDRITES; T. Bernatowicz, M. Honda and F. Podosek, McDonnell Center for the Space Sciences, Washington University, St. Louis, MO USA.

In the simplest model for the structure and evolution of a chondritic parent body there should be univariant correlations among various parameters reflecting parent body metamorphism, including radiometric chronometers. Such correlations, even among chronometers, have proved elusive. This abstract is a preliminary report of experiments exploring how well (or poorly) the noble gas methodologies, ^{129}Xe-^{128}Xe and ^{40}Ar-^{39}Ar, can be related to the chronology of metamorphism of the LL chondrites. We have analyzed samples of Soko-Banja (LL4) and Alta Ameen (LL5), and experiments on additional samples, selected for low degree of shock, are underway.

Neither Alta Ameen nor Soko-Banja give easily interpretable ^{40}Ar-^{39}Ar apparent age release patterns with well-defined plateaux. Both, however, give well-defined linear correlations between $^{129}Xe/^{130}Xe$ and $^{128}Xe/^{130}Xe$ (cf. Fig. 1), indicating the existence of correspondingly well-defined trapped and radiogenic components (Table 1).

Even with the present results, I-Xe data for LL chondrites are sparse (Fig. 2). One generalization does suggest itself, however. Data for the highest petrographic grade, all various samples of the LL6 condrite St. Severin, indicate relatively late formation (isotopic closure for Xe) and relatively high trapped $^{129}Xe/^{130}Xe$, consistent with accumulation of radiogenic ^{129}Xe prior to closure (in both cases the comparison is with lower metamorphic grade). Qualitatively, this distinction is in the same sense as that noted by Pellas and Storzer (1981), who found that, in comparison with lower grade samples including Soko-Banja and Alta Ameen, differential phosphate/pyroxene track retention intervals indicate a substantially lower cooling rate for St. Severin. Further data will determine whether this tentative conclusion can be generalized.

References: (1) Hohenberg, C.M., et al. (1981), Geochimica 45, 535. (2) Pellas, P. and Storzer (1981) Proc.Roy.Soc.Lond.A 374,253. (3) Pellas, P. et al. (1983) Meteoritics 18, 374. (4) Podosek, F.A. (1970) Geochimica 34, 341.

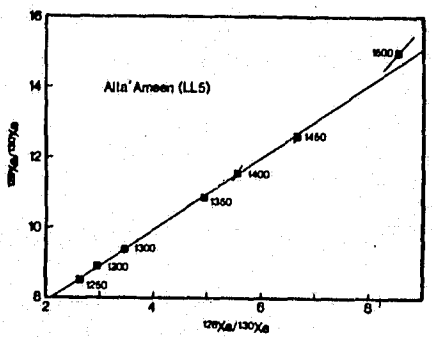

Fig.1: I-Xe Correlation diagram for Alta Ameen

Fig.2: I-Xe age (relative to Bjurbole) and trapped $^{129}Xe/^{130}Xe$ for LL chondrites (additional data from Podosek, 1970, and Hohenberg et al., 1981).

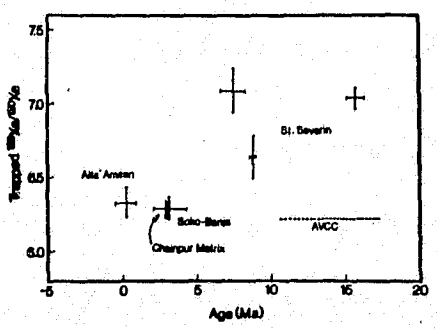

Table 1. Noble Gas Results for LL Chondrites

Sample	K-Ar age (Ga)	I-Xe age[a] (Ma)	$^{129}Xe/^{130}Xe$ (trapped)
Soko-Banja (LL4)	3.91	+3.2 ±1.1	6.29 ±.08
Alta Ameen (LL5)	4.20	+0.3 ±0.8	6.33 ±.10

[a] Ages relative to Bjurbole; positive ages indicate later formation.

THERMAL HISTORY OF THE PEACE RIVER L6 CHONDRITE BASED ON 40AR-39AR MEASUREMENTS; P.McConville and G.Turner, Physics Department, Sheffield University, Sheffield S3 7RH, England.

Peace River is an L6 chondrite with abundant glassy veins and other features characteristic of a moderate to high degree of shock, presumed to be the result of a major collision involving a former parent body. A previous 40Ar-39Ar analysis of this meteorite gave a remarkably flat 'low temperature age plateau' which indicated that around 99% of the radiogenic argon had been driven off in an intense heating event 420 Ma ago. In contrast to this extensive argon loss, the published Rb-Sr systematics show little or no evidence for this late heating. In an attempt to understand the detailed implications of these observations we have carried out further 40Ar-39Ar studies involving both stepped heating and the use of a laser probe. The work was carried out on a sample selected on account of the presence of a large glassy vein. Stepped heating measurements were carried out on three samples of matrix and a small, 2.5mg, sample of glass from the vein. In addition laser probe measurements were carried out on a section of meteorite containing both matrix and glass. The stepped heating data for all three matrix samples were very similar to each other and, more significantly, to the results obtained ten years previously on an unrelated sample. Two sets of results are shown in figure 1. The central plateau regions are indistinguishable for all four samples and indicate an outgassing age of 430+-30 Ma. In contrast to the matrix, the glass gave high and variable ages for all but a small part of the release. The most likely explanation of this observation seems to us to be the incorporation of 'excess' 40Ar into the glass when it was injected in a molten state through the matrix at the time of the impact. An earlier laboratory experiment on the Barwell meteorite also indicated a tendency for takeup of degassed radiogenic argon by molten silicate. The laser probe was used to selectively degas localised regions of the meteorite of the order of 10 - 100ug in weight. The results are summarised in figure 2 and confirm that the matrix was rather uniformly outgassed, presumably by the annealing following the impact, while the glass acquired excess argon which it retained at least in part through the annealing period. The diffusion properties as a function of temperature have been inferred from the release patterns and appear to indicate rapid annealing at a high temperature.

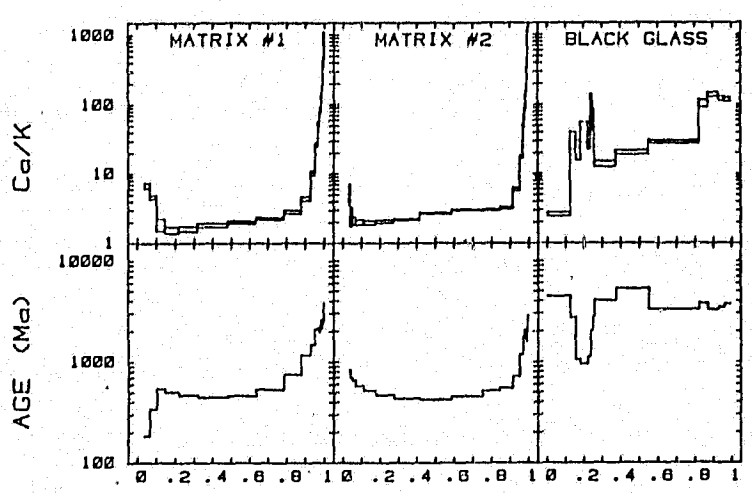

Fig 1 FRACTION OF 39Ar RELEASED

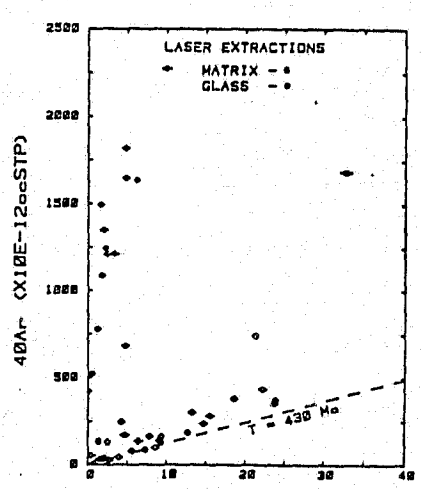

Fig 2 39Ar (X10E-12ccSTP)

CUMBERLAND FALLS (CHONDRITE), SUWAHIB (BUWAH) AND OTHER ORDINARY CHONDRITES SHOWING EVIDENCE OF POSTACCRETIONAL REDUCTION. John T. Wasson and Gregory W. Kallemeyn, University of California, Los Angeles, CA 90024, USA.

Instrumental neutron-activation analysis (INAA) of the Cumberland Falls chondrite (CFC) yielded refractory lithophile abundances in the ordinary chondrite range and siderophile and Se abundances in the LL range, consistent with earlier data of Jarosewich and Easton indicating an LL composition. In contrast, FeO/(FeO + MgO) ratios in the low-Ca pyroxene are generally near 10 mol %, far below the LL range, and ratios in the olivine are still lower, $\leq$4 mol %, too low to be in equilibrium with the pyroxene. Because diffusion is more rapid in olivine than in pyroxene, the lower ratio in the olivine is an indication of incomplete reduction of the chondritic silicates resulting from metamorphic interaction with the highly reduced aubritic host. Rubin finds petrographic evidence supporting such a reduction. Clayton and Mayeda's O-isotope data are near but outside the fields of equilibrated ordinary chondrites; $\Delta^{17}O$ ($=\delta^{17}O - 0.52\delta^{18}O$) is $\sim$0.8 ‰, between the H and L ranges, but $\delta^{18}O$ is $\sim$5.7 ‰, 1 ‰ above the field of equilibrated L chondrites. The O-isotope composition is roughly similar to that of the unique ordinary chondrites Suwahib (Buwah), Semarkona and Cynthiana. These results indicate that CFC is not as exotic as suggested by Lipschutz and coworkers, but is closely related to the LL chondrites.

Mason reported that the Suwahib (Buwah) find has slightly unequilibrated olivine with a mean composition near Fa15. Our analysis of the first of two samples indicates an L-group composition; we speculate that this small (240 g) meteorite also experienced postaccretional reduction, and predict that petrographic studies will show that FeO/(FeO + MgO) in its olivine will be lower than that in the orthopyroxene. Several years ago we showed that a chondritic clast in the Bencubbin meteoritic melange had an LL composition despite an olivine composition of Fa14-19; we also predict that its olivine is more reduced than its pyroxene. The O-isotope composition of the Bencubbin LL clast shows $\Delta^{17}O$=0.8 ‰, but $\delta^{18}O$ of 6.4 ‰, still higher than the values cited above. Cynthiana, which also has a $\delta^{18}O$ value above the normal L range, has an olivine composition in the L range but siderophile abundances in the LL range. All these meteorites have L or LL compositions, reduced silicates, and ^{18}O-rich oxygen; they may all be unequilibrated in the primitive, nebular sense but this requires a careful petrologic investigation. The unusual O-isotope compositions may reflect a primitive unequilibrated nature or they may reflect formation at nebular locations and/or times slightly different from those that left their signature in the L and LL chondrites.

METEORITE Hg DIFFUSION STUDIES; S. Jovanovic and G. W. Reed, Jr., Chemistry Division, Argonne National Laboratory, Argonne, IL 60439

The behavior of volatiles is most important for understanding the thermal and non-thermal processes to which meteorites have been subjected. Our interest is primarily in Hg; however, some of the fundamental information regarding the history of meteorites and solar system matter is obtained from rare gas studies. Primordial ^{129}Xe and its I parent are notable cases as are ^{244}Pu spontaneous fission Xe and ^{40}Ar. Disturbances of initial distributions of Xe-I (1) and the ^{40}Ar system (2) have recently been treated in detail. Previously (3,4), we attempted to rationalize the behavior of Hg in meteorites on the basis of the amounts in labile and retentive sites. Hg data will be examined here with the objective of contributing to the rare gas discussions. Linear and isothermal heating procedures are used to obtain data on the energetics of Hg mobilization via the Arrhenius equation. Treatment of the data will be discussed. Typical results are plotted in Fig. 1; the bottom part gives the isothermal data. Activation energies cluster between 8 and 12 kcal/mole suggesting grain boundary type sites. There appears to be no correlation with the degree of thermal or shock alteration, e.g. (5). We have presented evidence that the relative amount of Hg in high temperature sites is correlated with equilibration temperatures (4). Emplacement of Hg into minerals by shock may accomplish the same effect, i.e. transfer from labile to retentive sites. Possible evidence for an effect of shock may be seen when the total Hg is compared with the total diffusion-related Hg, Fig. 2. The data suggest two parallel trends. The significant observation may be that dark and light Pantar and Breitsheid samples are separated with the dark falling close to the curve through Farmington and Barrata, both of which exhibit high shock facies. References: (1) Caffee M. W., et al. (1982) J. Geophys. Res. 87, A318-A320. (2) Bogard D. D. and Hirsch W. C. (1980) Geochim. Cosmochim. Acta 44, 1667-1682. (3) Reed G. W. and Jovanovic S. (1967) J. Geophys. Res. 72, 2219-2228 and (4) (1968) in Origin and Distribution of the Elements (L. H. Ahrens, ed.) 321-328. (5) Dodd R. T. and Jarosewich E. (1979) EPSL 44, 335-340.

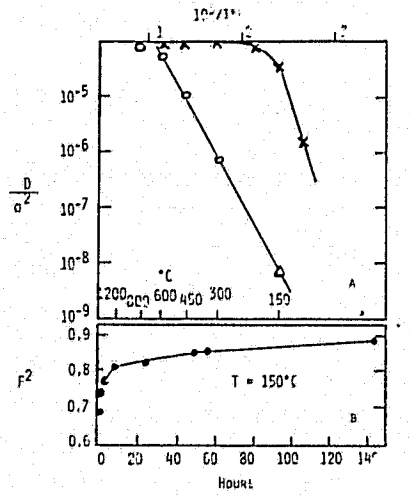

Fig. 1. Linear (A), Isothermal (B) Diffusion Plots. Δ-isothermal point

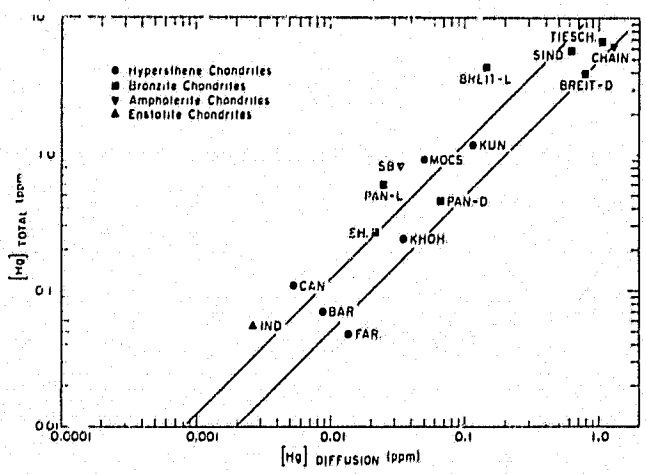

Fig. 2. Total vs. diffusion-related Hg.

MOBILE TRACE ELEMENTS AND THERMAL HISTORIES OF H4-6 CHONDRITES COMPARISON WITH L4-6 CHONDRITES. D. W. Lingner, T. J. Huston and M. E. Lipschutz, Dept. of Chemistry, Purdue University, W. Lafayette, Indiana 47907 USA

Extended laboratory heating of primitive chondrites under ambient atmospheric conditions and over a temperature range appropriate for meteoritic parent body fractionation processes and for shock-heated collisional debris results in significant mobilization (i.e. vaporization and loss) of a number of trace elements. In L4-6 chondrites, shock-heating predominates in determining contents of and trends among siderophilic trace elements and those mobilized in laboratory heating experiments [1-3]. For example, strongly shocked L4-6 chondrites, i.e. those of shock facies d-f (exhibiting mineralogic evidence for shock-loading to pressures >22 GPa) and/or loss of radiogenic gas (e.g. $\geq$25% loss of ^{40}Ar), contain significantly less ($\geq$90% confidence level) siderophilic Co, Au and Ga and mobile Cs, Te, Bi, Ag, In, Tl, Zn and perhaps Cd than do mildly shocked samples. On average, L4-6 chondrites exhibiting radiogenic gas loss seem to have been more heavily shocked during parent body breakup ~0.5 Gy ago than were those of shock facies d-f [3].

We measured 16 trace elements - Co, Au, As, Sb, K, Se, Ga, Rb, Cs, Te, Bi, Ag, In, Tl, Zn, and Cd (arranged in order of increasing mobility) - by RNAA in 43 H4-6 chondrites exhibiting a variety of K/Ar and U,Th/He ages. As in L4-6 chondrites, we compared trends in the mildly-shocked sample population (K/Ar age >3.75 Gy, or >75% retention of ^{40}Ar) to those in the sample population with disturbed K/Ar age ($\leq$3.75 Gy or $\geq$25% loss of ^{40}Ar).

Only In is significantly less abundant in the H4-6 population with disturbed K/Ar age than in the mildly shocked one: Se and Ag are more abundant in the former population.

When mildly shocked populations are compared, H4-6 chondrites reveal significant depletion of Sb and mobile Bi, Ag, In, Tl, Zn and possibly Te and Cd and the expected enrichment of siderophilic Co, Au, As and Ga relative to L4-6 chondrites. Siderophile enrichments need no further comment. Significant mobile element depletions in H4-6 chondrites indicate early high temperatures that the L4-6 chondrites do not record. This could involve higher nebular condensation/accretion temperatures [4] or an early shock erased by subsequent extended cooling [5] of H chondrite parent material.

REFERENCES: [1] C. W. Neal, R. T. Dodd, E. Jarosewich and M. E. Lipschutz, Geochim. Cosmochim. Acta **45**, 891-898 (1981). [2] T. M. Walsh and M. E. Lipschutz, ibid **46**, 2491-2500 (1982). [3] T. J. Huston and M. E. Lipschutz, ibid **48**, in press (1984). [4] R. Hutchison, A. W. R. Bevan, A. J. Easton and S. O. Agrell, Proc. Roy. Soc. London A **374**, 159-178 (1981). [5] P. Pellas and D. Störzer, ibid **374**, 253-270 (1981).

HEAVY NOBLE GASES ASSOCIATED WITH NEON-E; O. K. Manuel, Chemistry Department, University of Missouri, Rolla, MO 65401; Rama and S. Ramaduri, Tata Institute of Fundamental Research, Bombay 400 005

Data on the isotopic and elemental abundances of He, Ne and Ar in the G5 mineral separates of the Orgueil CI carbonaceous chondrite have been presented by Eberhardt et al. (1981) with a description of experimental techniques, extraction blanks, etc. We use the results of Eberhardt et al. (1981) to seek answers to some of the questions raised by Sabu and Manuel (1980) but not addressed by the Bern group.

Blanks: For those temperature fractions in which Eberhardt et al. (1981) report Ne-20/Ne-22 < 1, the blank signal at m/q = 20 amounts to 52-83% of the signal assigned to singly ionized Ne-20. Density fractions of the Orgueil G5 minerals were separated in thallium malonate, $TlHCO_2CH_2CO_2$, and thallium formate, $TlHCO_2$. The CO_2^{+2} ions from adsorbed trace organics might appear to be monoisotopic Ne-22, but Eberhardt et al. (1981) report that interference at m/q = 22 from doubly ionized CO_2 is negligible.

Heavy Noble Gases with Neon-E: Eberhardt et al. (1981) report that their results support the conclusion of earlier studies at Bern and Chicago in showing "that Ne-E is not associated with any sizable amounts of other trapped noble gases." However, a plot of Ne-22/Ne-20 vs Ar-36/Ne-20 for the noble gases in the G5 mineral separates demonstrates a correlation of excess Ne-22 with Ar-36, as shown in Fig. 1. If there are no systematic errors in these results, then the Orgueil separates with $\rho \geq 3.15$ appear to contain (a) one noble gas component in the lower left corner of Fig. 1 containing only He-3, He-4, Ne-20 & Ne-21, and (b) a mirror image component containing Ar-36, Ar-38 & Ne-22. The latter contains Ne-E (h) and atomic abundances with Ne-22 = Ar-38. The Orgueil separates with $\rho \leq 3.15$ may contain another noble gas component, (c) with Ar-36, Ar-38 & Ne-22. This component contains Ne-E(ℓ) and atomic abundances with Ne-22 = Ar-36 = 5.4 x Ar-38. Prominent excesses of spallogenic He-3 and Ne-21 are observed in separate G5f, and spallogenic Ne-22 is probably responsible for the position of the one data point (G5f) above the correlation line in Fig. 1.

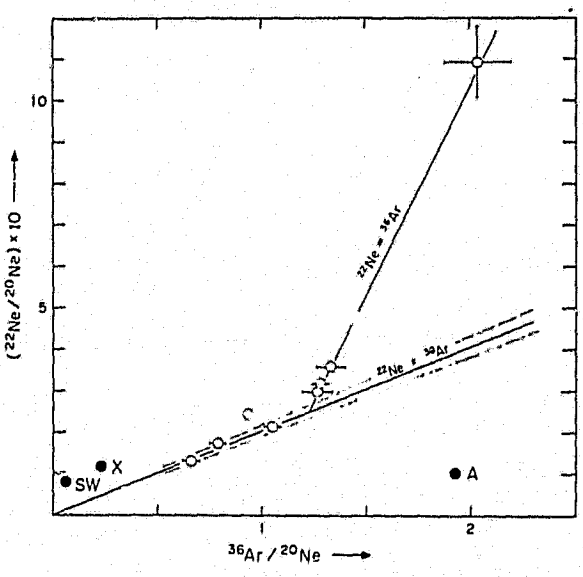

Fig. 1 Correlations of the $^{22}Ne/^{20}Ne$ isotopic ratio with the $^{36}Ar/^{20}Ne$ elemental ratio in G5 separates of Orgueil (Eberhardt et al., 1981) compared with noble gases in air, A, in the solar wind, SW, and in planetary type X noble gases (Sabu and Manuel, 1980b).

Eberhardt, P., M. H. A. Jungck, F. O. Meier and F. R. Niederer, 1981. Geochim. Cosmochim. Acta **45**, 1515-1528.

Sabu, D. D. and O. K. Manuel, 1980. Proc. Lunar Planet. Sci. Conf. 11th, 879-899.

NOBLE GASES IN THE BELLS (C2) AND SHARPS (H3) METEORITES. M.G. Zadnik
Enrico Fermi Institute, University of Chicago, Chicago, IL 60637

Bells. This meteorite was initially classified as a C2 chondrite *(1)*, but recent work *(2)* suggests that it is intermediate between C2's and C1's. To see whether noble gases could contribute anything to this problem, I analyzed two samples obtained from O.E. Monnig.

The primordial gases shed little light on the classification. The neon is mainly planetary (Ne-A) with some spallogenic but no solar Ne. Some Ne-E shows up at 1000°C, as in other C1 and C2 chondrites *(3)*. The elemental abundances of the heavier gases (Ar^{36} = 88 and $Xe^{132} = 1.10 \times 10^{-8}$ cc STP/g) are at the high end of the C1 and C2 ranges, being slightly exceeded only by a single Murray sample *(4)*. Planetary Ne^{20}, however, is distinctly lower than in C1's, but fits well in the C2 range (Bells 10, C1's 13 to 37, C2's 5.2 to 42, all 10^{-8} cc/g).

The radiogenic and especially cosmogenic gases point more clearly, even decisively, to a link with C2's. Ar^{40}, at 970×10^{-8} cc/g, is higher than in any C1 chondrite. Moreover, the Ne^{21}-exposure ages, 0.31±0.15 or 0.43±0.07 Myr, are extraordinarily short, and nearly coincide with the distinctive cluster of five C2's (0.15-0.65 Myr). Very likely Bells belongs to the same cluster, in which case it comes from the C2 parent body. Thus the C2 parent body must have contained transitional C1-C2 material like Bells within ≈1 km of the region of C2 chondrites proper.

Thus, though some of the data are consistent with either a C2 or a C1 affinity, the low Ne^{20}, high Ar^{40}, and especially the short exposure age link Bells to C2's.

Sharps. This meteorite has been classified as H3.4 *(5)*, but its high Bi,In, and Tl content *(6)* suggests that it may be more primitive. Two chips from USNM sample No. 640 were analyzed; both were free of carbonaceous or other obvious xenoliths.

The elemental concentrations of primordial Ar,Kr,Xe indeed are ≥3x higher than for other H3 chondrites, except ALHA 77003 *(7)*: Ar^{36} = 127, Kr^{84} = 0.76, and $Xe^{132} = 0.52 \times 10^{-8}$ cc STP/g. The Ar^{36}/Xe^{132} ratio of 240 is near the top of the UOC range, close to the values for the unique chondrite Kakangari and C3O's *(8)*, but well above the C1-C2-C3V range. One other property suggests a very primitive character: the isotopically anomalous CCFXe component ($Xe^{136}/Xe^{132} \approx 0.66$) resolves quite well from primordial Xe ($Xe^{136}/Xe^{132} \approx 0.31$) in stepped heating. The maximum 136/132 ratio for Sharps bulk, 0.54±0.03, was markedly higher than that for carbonaceous separates of lower petrologic type, e.g. Krymka (3.0) 0.46 or Bishunpur (3.1) 0.35 *(9)*. Apparently the CCF and planetary Xe components in Sharps have not been fully homogenized by metamorphism. Coupled with the high concentration of Ar^{36} and volatile trace elements, this suggests a more primitive classification than 3.4 for this meteorite. The high Ar/Xe ratio and the high release temperature for the maximum 136/132 ratio (1600°C, vs 800°C and 600°C for Allende and Chainpur) suggests that the noble gas carriers in Sharps have some unusual features that merit closer study.

A small amount of trapped Ne is present ($Ne^{20} \approx 2.5 \times 10^{-10}$ cc/g). Its isotopic ratio cannot be characterized owing to the large spallogenic component, but the low Ne^{20}/Ar^{36} ratio of ≈0.02 suggests that it is planetary; solar gas seems to be absent. Only a few UOC's contain planetary Ne. The cosmic ray exposure age based on Ne^{21} is 26±3 Myr, placing Sharps in the second-largest peak of the H-chondrite distribution *(10)*. The nominal K-Ar and U,Th-He ages [based on average H-chondrite values of K = 800 ppm, U = 13 ppb; *(11)*] are 4.6±0.1 and 4.3±0.7 Gyr, suggesting that Sharps has remained at low temperatures since its early days.

(1) Mason B. *Space Sci. Rev. 1*, 621 (1963). *(2)* Lewis A.M. and Olsen E. *LPS 15*, 190 (1984).
(3) Black D.C. and Pepin R.O. *EPSL 6*, 395 (1969). *(4)* Pepin R.O., unpublished data (1969).
(5) Sears D.W., Grossman J.N. Melcher C.L., Ross L.M., and Mills A.A. *Nature 287*, 791 (1980).
(6) Laul J.C., Ganapathy R., Anders E., and Morgan J.W. *GCA 36*, 329 (1973).
(7) Takaoka N., Saito K., Ohba Y., and Nagao K. *Proc. Symp. on Antarctic Meteorites 6*, 264 (1981).
(8) Srinivasan B. and Anders E. *Meteoritics 12*,417 (1977). *(9)* Alaerts L., Lewis R.S., and Anders E. *GCA 43*, 1399 (1979).
(10) Crabb J. and Schultz L. *GCA 45*, 2151 (1981). *(11)* Mason B. *Geological Survey Professional Paper 440-D-1*, Dept. of the Interior (1979).

s-PROCESS Nd IN ALLENDE RESIDUES; Donald D. Clayton, Rice University, Houston, TX 77251.

My purpose here is to reexamine my interpretation (1) of Nd isotopic anomalies in acid-resistant Allende residues as being an excess of s-process Nd in view of a subsequent publication (2) by its discoverers and in light of new measurements of the Nd cross sections (3), which I had been forced to predict in a way to preserve both the essential correctness of s-process theory and the essential smoothness of the r-process yield curve. The issue is whether ^{146}Sm was alive in the Allende residues at a concentration level that would require a large $^{146}Sm/^{144}Sm$ production ratio (2, 1) or whether the ^{142}Nd excess is primarily part of a general s-process excess, augmented if required by ^{146}Sm decay in interstellar grains.

Lugmair et al.'s (2) published data confirms an odd-even pattern of anomalies. They did not address that pattern, nor my interpretation of it. But it must be counted a plus for the s-process interpretation that it accounts for the whole pattern, rather than merely for the excess ^{142}Nd. Moreover, the subsequent measurements by Mathews and Käppeler (3) of the Nd capture cross sections confirms the reasoning I had used (1) in assigning their values in a way to conform to general nucleosynthesis theory. This measurement is also a plus for the s-process interpretation.

In their footnote 10, Lugmair et al. (2) discount my procedure for renormalization of their data, in which I postulated a mass fractionation m = 2/3 ppm/amu during nature's preparation of the carbonaceous sample. Above and beyond the riskiness of ruling out isotopic fractionation on grounds so shaky as the relative abundances of elements in the sample, their footnote overlooks the natural expectation that interstellar-dust components may be strongly fractionated by interstellar sputtering (4), which affects different elements in very complex ways — in some cases not at all.

Shimamura and Lugmair (5) have measured ^{234}U excesses in the same samples, and advance that discovery as evidence that ^{143}Nd and ^{142}Nd excesses are also the result of decay-recoil enhancement. Their argument is convincing for ^{143}Nd, because the ratio of its excess in CF-1 to that in CG-1 is 1.8, exactly as it is for ^{234}U. But for ^{142}Nd the excesses stand in the significantly smaller ratio 1.3. Their data itself therefore suggest a different process. The one I proposed is that carbonaceous dust from red giants traps s-process Nd in the interstellar medium, that this dust is mixed with carbonaceous mantles in cold clouds of the ISM, and that these mantles reorganized into the present carriers during Allende's thermal fixation.

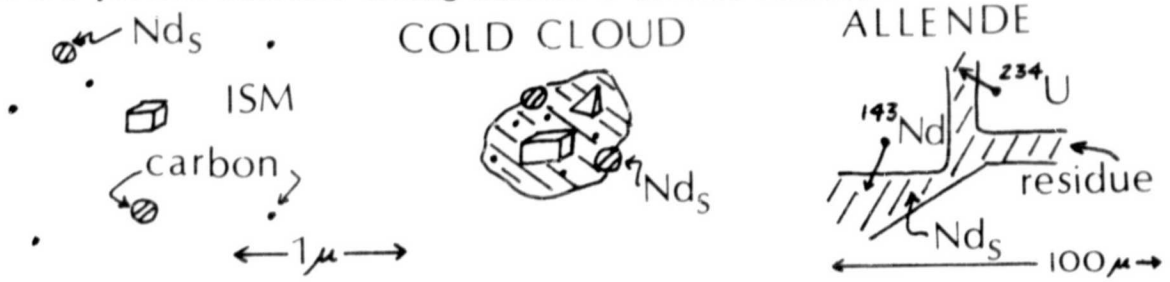

(1) Clayton, D. D. (1983) Astrophys. J., 271, L107
(2) Lugmair, G. W., Shimamura, T., Lewis, R. S., and Anders, E. (1983) Science, 222, 1015
(3) Mathews, G. J., and Käppeler, F. (1984) Astrophys. J. (in press)
(4) Clayton, D. D. (1981) Astrophys. J., 251, 374
(5) Shimamura, T., and Lugmair, G. W. (1984) Lunar Planet. Sci. XV, 776.

ANOMALOUS ISOTOPIC COMPOSITION OF CHROMIUM IN ALLENDE INCLUSIONS ;
J.L. BIRCK and C.J. ALLEGRE, Laboratoire de Géochimie et Cosmochimie, I.P.G., 4, place Jussieu, 75230 PARIS Cedex 05.

The discovery of isotopic anomalies in Allende inclusions have shown that the different nucleosynthetic components of the solar system have not been isotopically homogeneized. Anomalies were first discovered for light elements and for heavy elements from the rare earth group.
The focal point of current research in this field is the iron group nucléi. This group of elements from Ti to Cu is astrophysically important since they are believed to be products of silicon burning at high temperature which can take place close to the core of massive stars. Cr is of particular interrest since it is close to Ca and Ti where widespread anomalies have already been detected in the Allende inclusions. On the other band, for nickel which is in the high mass range of this group no anomaly has been found.
Former studies (1,2,3) on chromium isotopes in Allende inclusions have failed to produce any detectable anomaly. We have readressed this problem with an improved experimental technique which allows us to resolve differences as small as 2.10^{-4} for any ratio ; especially $^{54}Cr/^{52}$ Cr the value of which is close to 0.0282.

Among other samples, four total rock samples of Allende inclusions have been investigated : 2 coarse grained inclusion and 2 fine grained inclusion. For three of them, non linear effects are clearly evidenced. According to the very small size of the effects, there exist several prossibilities for instrumental mass fractionation correction (normalization). According to titanium and calcium isotopic date the most likely possibility is that the samples have a terrestrial $^{52}Cr/^{50}Cr$ ratio. The $^{54}Cr/^{52}Cr$ ratio displays excesses ranging from 0 to 8 ε units ($1\varepsilon = 10^{-4}$ relative deviation) relatively to the others samples including the bulk of Allende. There is also a hint for a deficit of around 1ε for the $^{53}Cr/^{52}Cr$ ratio but more work is needed to ascertain it. The Cr 54 excess are correlated with Ti 50 excesses. These samples don't display nuclear effects in nickel . There are numerous proccesses to produce the neutron rich isotopes of the iron group nuclei but considering all the date available on these samples, the most likely way to account for the effects observed in both Ti and Cr is that the inclusions have received an extra addition of matter processed in neutron rich equilibrium (4), when compared to usual solar system material.

1)Nitoh, O., Kamata M., and Honda M. (1978) USGS Open File Rep. 78-701, p. 308-310
2)Birck J.L., Ricard L.P. and Allègre C.J. (1980) Meteoritics 15, p.266.
3)Lee T. and Tera F. (1983) Meteoritics 18, p.337-338
4)Cameron A.G.W. (1979) Ap.J 230, p.L53-L57

CORRELATED ISOTOPIC ANOMALIES IN THE ELEMENTS SILICON AND MAGNESIUM FROM ALLENDE INCLUSIONS C. Molini-Velsko*, T. K. Mayeda and R. N. Clayton, The University of Chicago, Chicago, IL 60637 *currently at Lawrence Livermore Laboratory, P.O. Box 808 L-396, Livermore, CA 94550

Five coarse-grained Allende inclusions show effects in silicon and magnesium isotopic abundance ratio measurements that cannot be attributed to mass dependent isotopic fractionation. For each element, the pattern of the effect on a three isotope diagram is identical, but the magnitude for silicon is about half that of magnesium. The results in Table 1 reflect a choice of normalization ratio which yields apparent excesses in $^{25}Mg/^{24}Mg$ and $^{29}Si/^{28}Si$ ratios. The other normalization would lead to apparent deficits in $\delta^{26}Mg$ and $\delta^{30}Si$. With either choice, a linear relationship between the magnitudes of the effects is evident. A linear regression of the data yields a slope of 0.648 and an intercept of -0.14, with δMg displayed along the x axis. The correlation coefficient, r^2=0.945 is quite good for measurements that were carried out on different pieces of the inclusions, especially since the effects are somewhat heterogeneously distributed within the inclusions (1). The inclusions with excess $\delta^{29}Si$ are coarse-grained, but of variable chemical compositions and mineralogies that fall into Type A, Type B (2) and forsterite-rich (3) groups. The silicon anomalies are more common than the light and heavy element anomalies that characterize FUN samples C1 and EK 1-4-1. The excess $\delta^{29}Si$ has no simple relationship to the range of mass-fractionation in these coarse-grained inclusions so we assume that mass-fractionation and the nuclear anomalies were generated by separate events. An excess in ^{25}Mg,^{29}Si, a deficit in ^{24}Mg or ^{26}Mg,^{28}Si or ^{30}Si could produce the effects shown in Table 1. If the effects are nucleosynthetic, some anomalous material may have mixed with material in the nebula to produce the anomalies. Explosive nucleosynthesis, ie. carbon-burning, produces excesses in the neutron-rich isotopes of silicon but not magnesium, whose isotopes are produced in nearly solar abundance. In that process, the isotopic effects for silicon are calculated to be about 75 times those of magnesium and of opposite sign (4). The data in Table 1 suggest that the correlated anomalies should differ by no more than a factor of 2 and be in the same direction. Nucleosynthetic processes other than explosive burning may be more appropriate for producing correlated effects. Measurements of isotopic abundances in the interstellar medium (5) and galactic cosmic rays (6) indicate possible enhancements of the neutron-rich Mg and Si isotopes relative to the most abundant isotope of each element. Another possible source of the effects could be nuclear reactions. Excitation functions for various reactions are being investigated to consider this hypothesis.

Table 1

Inclusion	Excess $\delta^{29}Si$	Excess $\delta^{25}Mg$
TE	0.00[a]	0.4+0.1[b]
Egg 3	0.30	0.4+0.1[c]
CG 14	0.35	0.9+0.7[d]
C1	0.45	0.9+0.2[e]
EK 1-4-1	1.00[f]	1.7+0.2[e]

[a] 2σ precision +.06‰ except EK 1-4-1 [b] Papanastassiou and Wasserburg 1983, Meteoritics 18, 370-1. [c] Esat et al. 1980, LPS XI,262-64. [d] Ref. (3). [e] Ref. (1). [f] Yeh and Epstein 1977, LPS VIII, 287-89.

REFERENCES (1)Wasserburg et al. 1977, Geophys. Res. Lett. 4, 299-302. (2)Grossman, L. 1975, GCA 39, 433-54. (3)Clayton, R.N. et al. 1984, GCA 48, 535-48. (4)Lee, T. et al. 1979, Ap. J. 232 854-62. (5)Penzias, A.A. 1980, Science 208, 663-65. (6)Wiedenbeck, M.E. and Greiner, D., 1981, Ap. J. Lett. 247,L119.

MAGNESIUM AND SILICON ISOTOPIC COMPOSITION OF INTERPLANETARY DUST PARTICLES; E. Zinner, A. Fahey, and K. D. McKeegan, McDonnell Center for the Space Sciences, Washington University, St. Louis, MO 63130

We have used our modified Cameca IMS-3f ion probe to measure Mg and Si isotopes in 3 interplanetary dust particles (IDP's) of chondritic composition. In contrast to the hydrogen in these particles, all of which showed large D excesses [1,2,3], the isotopic compositions of Mg and Si were found to be terrestrial within errors. Measurements were performed by oxygen bombardment at a mass resolution of 3500 in an automatic peak switching mode (60 cycles of the mass sequence 24, 25, 26, 28, 29 and 30). Terrestrial pyroxene and olivine grains served as standards to monitor instrumental mass fractionation. Plotted in figure 1 are the isotope ratios (2σ errors) for Mosquito and Skywalker, along with the standard deviation envelopes for repeated measurements of the pyroxenes and olivines. The third IDP, Spray-2, (not plotted) has errors roughly twice those of Mosquito and Skywalker due to the small amount of material available for analysis. Skywalker had abundant silicates in every fragment, 7 of which were measured. In contrast, only one fragment of Mosquito consisted of predominantly silicates. Total amounts of particle mass consumed during the measurement of a fragment was $<5 \times 10^{-11}$ g. The measured isotopic ratios from the pyroxenes and olivines are shifted relative to one another demonstrating the matrix dependence of mass fractionation in SIMS analysis. In addition, the absolute value of the mass fractionation depends on instrumental conditions; Mosquito and Skywalker and their terrestrial standards were measured under different tuning conditions. Esat et. al. [4] have measured Mg in individual IDP's by solid source mass spectrometry and found significant mass fractionation in one sphere and a hint of non-linear effects in several chondritic aggregates. If only Mg were measured for a whole IDP, the precision of the ion probe to measure non-linear effects approaches that reported by Esat et. al. [4,5]. However, because of the matrix dependence, the ability of the ion probe to measure indigenous mass fractionation effects in Mg and Si would be much less. Nevertheless, the ion probe has already been used to measure linear mass fractionation of Mg and Si in FUN inclusions [6,7] and a mass fractionation of >1%/amu as reported in [4] would have been seen by us even under present conditions.

References: [1] E. Zinner et al (1983), Nature 305,119. [2] E. Zinner and K.D. McKeegan (1984) LPSC XV,961. [3] K.D. McKeegan et al, this conference. [4] T.M. Esat et al (1979) Science 206,190. [5] I.D. Hutcheon (1982) ACS Symp. Ser. No 176,95. [6] J.C. Huneke et al (1983) GCA 47,1635. [7] R.N. Clayton et al (1984) GCA 48,535. [8] E.J. Catanzaro et al (1966) J.Res.Nat. Bur.Stand. 70A,453 [9] I.L. Barnes et al (1975) J.Res.Nat.Bur.Stand. 79A,727.

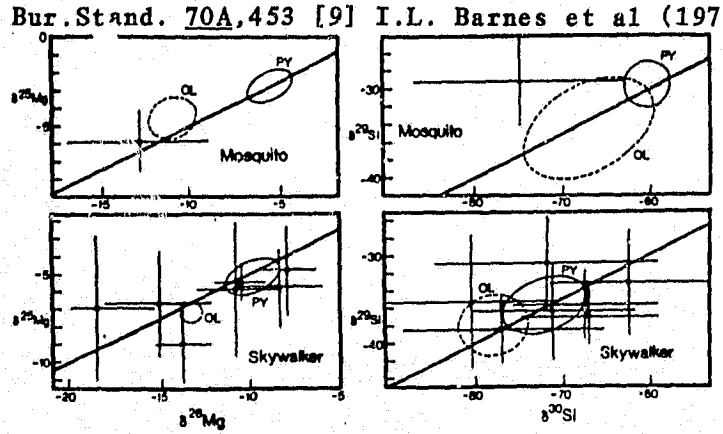

Fig. 1a: Isotope correlation plots of $^{25}Mg/^{24}Mg$ vs. $^{26}Mg/^{24}Mg$ in 2 IDP's and terrestrial olivines (OL) and pyroxenes (PY). Plotted are $\delta^{25}Mg$ values in ‰ relative to $^{25}Mg/^{24}Mg = 0.12663$ [8] and $\delta^{26}Mg$ relative to $^{26}Mg/^{24}Mg = 0.13928$ obtained from a fit to our terrestrial measurements. Fig. 1b: Isotope correlation of $^{29}Si/^{28}Si$ vs. $^{30}Si/^{28}Si$ in the same IDP's and terrestrial standards. $\delta^{29}Si$ is relative to $^{29}Si/^{28}Si = 0.050633$ [9] and $\delta^{30}Si$ relative to the best fit value $^{30}Si/^{28}Si = 0.03357$ of our terrestrial measurements.

SEARCH FOR ISOTOPIC ANOMALIES IN ODESSA(IA), OCHANSK(H4), PLAINVIEW (H5), AND GLADSTONE(H6); J. Yang and S. Epstein, Division of Geological and Planetary Sciences, California Institute of Technology, Pasadena, CA 91125.

Both unusually D-rich hydrogen and ^{13}C-rich carbon have been found in Murchison acid residues [1,2,3]. The ^{13}C-rich carbon ($\delta^{13}C \approx 1500‰$) was attributed to a stellar condensate and the D-rich hydrogen to ion-molecule enrichment in interstellar clouds. The simultaneous $\delta^{13}C$ and δD analyses of various extracts from the Murchison HCl-HF residues showed no correlation between these values, indicating a lack of a common origin [2,3].

The ^{13}C-rich carbon resides in a form which is resistant to strong oxidizing chemicals and to pyrolysis in presence of O_2 up to 800°C. This suggests that this form of carbon might survive a high temperature history in metamorphosed and iron meteorites. Thus, the following analyses were made.

Odessa IA, Ochansk H4, Planview H5, and Gladstone H6 were demineralized by acids, HCl, HF, $HClO_4$, HNO_3, H_2O_2, NaOH-NaOCl, and washed in acetone. The residues (CFO) ranged between 0.37 and 1.03% in weight (Table 1). The CFO residue of the Odessa iron meteorite was further treated by boiling $HClO_4$ and the residue, CFOP, weighed 0.32%.

Table 1 shows the data of H, C, N, and S. All samples contained small amounts of hydrogen, 0.8-4.2 μmoles/g (C/H ratio ranges 1.2 to 70). Unlike Murchison residues, these meteorite residues gave negative δD values, down to -280‰. $\delta^{13}C$ values of carbon are also negative, below -4.7‰, except the highest temperature steps of three residue samples of Plainview and Odessa.

Amounts of the positive $\delta^{13}C$ carbon, 12 to 50‰, are very small, less than 0.05 μmoles/g. If we assume that positive $\delta^{13}C$ values are due to the presence of 1500‰ $\delta^{13}C$ carbon originated from stellar condensates, then the concentrations of such heavy carbon are only $(1\text{-}6)\times10^{-4}$ μmoles/g which are about three orders of magnitude less than those found in Murchison meteorite residues.

Table 1. The concentrations and isotopic data of H and C released by stepwise oxidation-pyrolysis of acid residues of meteorites.

Sample*	T† °C	H_2 μmoles/g‡	δD	CO_2 μmoles/g‡	$\delta^{13}C$	C/H
Ochansk CFO	(350)	2.91	-10	0.59	-25.7	0.10
1.03%	700	0.85	-76	32.7	-25.6	19
167 mg	800	0.29	-148	3.1	-25.3	5.3
	900	~0.04	~-190	0.12	-34.7	~2
	1100	~0.08	~-217	0.21	-22.2	~1
	Total	4.17	-39	36.7	-25.6	4.4
Plainview CFO	(350)	0.62	-50	0.18	-22.5	0.15
0.84%	800	0.18	-56	11.5	-17.3	32
191 mg	900	~0.02	~-196	0.044	~-55	~1
	1100	~0.02	~-177	~0.003	~50	~0.1
	Total	0.84	-58	11.7	-17.5	7.0
Gladstone CFO	(350)	4.56	-9	0.35	-28.8	0.038
1.02%	800	1.32	-68	13.1	-22.9	5.0
132 mg	900	~0.09	-206	0.17	-8.8	~0.9
	1100	~0.05	~-280	0.31	-25.1	~3
	Total	6.02	-27	13.9	-22.9	1.2
Odessa CFO	(350)	1.09	-59	1.1	-24.4	0.50
0.37%	700	0.63	-106	45	-6.2	36
22.4 mg	800	0.28	-68	20	-4.7	360
	900	~0.02	~-62	~0.026	~-31	~0.7
	1100	~0.07	~-39	~0.012	~31	~0.1
	Total	2.09	-74	247	-5.1	59
Odessa CFOP	(350)	0.58	~-17	0.48	-19.5	0.41
0.32%	700	0.61	~-5	55	-5.4	45
173 mg	800	0.20	-216	42	-5.0	105
	900	0.18	-160	18	-5.3	51
	900	0.12	-209	120	-4.8	480
	900	<0.02	--	2.6	-4.7	>65
	1000	<0.01	--	0.015	~19	>0.7
	1100	<0.01	--	0.031	~12	>1.5
	Total	1.69	-65	238	-5.0	70

Above 5 samples contain total nitrogen of 0.1-0.2 μmoles/g and total sulfur of 0.01-2 μmoles/g.
*C≡HCl, F≡HF, O≡H_2O_2, HNO_3, NaOH-NaOCl, $HClO_4$, P≡boiling $HClO_4$.
†T in parentheses represnts the heating step without oxygen.
‡Yields are given in μmoles/gram of bulk meteorites.

REFERENCES [1] Swart P.K. et al.(1983) Science 220, 406. [2] Yang J. and Epstein S. (1983) Meteoritics 18, 429. [3] Yang J. and Epstein S. (1984) LPS XV, 949.

INTERSTELLAR CARBON GRAINS FROM THE MURCHISON METEORITE: ELECTRON MICROSCOPY. Roy S. Lewis and Mitsuo Ohtsuki, Enrico Fermi Institute, University of Chicago, Chicago, IL 60637

The Murchison C2 chondrite contains several kinds of anomalous carbon, whose interstellar origin is suggested by gross isotopic anomalies in C,N, or associated noble gases *(1,2,3)*. Three types have been characterized thus far:

Type	δC^{13} ‰	δN^{15} ‰	Enriched in	Abundance ppm	Grain Size μm	Release T °C
Cα	+340		Ne^{22}	<5	3 - 10	600
Cβ	+1100		Xe^{130}	<5	1 - 3	1400
Cδ	-38	-330	Xe^{136}	200	0.002	1000

Having previously imaged the relatively abundant Cδ *(3)*, we have now tried to obtain electron micrographs of the much rarer Cα and Cβ. As they constitute less than 5 ppm of the meteorite and only ~0.2% of our most enriched sample, we tried to concentrate them further. The starting material, Murchison DG, was an acid-resistant carbon-spinel fraction of 1-3 μm grain size (formerly known as Murchison 2C10m; *4*). It was treated with H_3PO_4 at 240°C for 16 hrs to dissolve spinel. Most of the remaining inorganic phases were removed by density separation at $\rho = 2.6$ g/cm^3, and the light fraction was examined on the electron microscope.

The electron energy used for the imaging was 75 kV, and magnification was set at 42,000x. For the electron diffraction study, a single crystal of gold, which was prepared epitaxially on the surface of a NaCl crystal, and a natural graphite crystal were used to obtain the precise camera length of the microscope.

The sample still contained some Cr-rich grains and other inorganic phases that had survived the treatment, along with carbon particles of the right size, about 1 μm. These carbon particles are coherent aggregates of smaller, generally elongated grains, ranging from 100-200 Å in the short dimension up to 1000 Å in the long dimension. They somewhat resemble amorphous carbon that has been graphitized at >2000°C, but the grain size is considerably smaller.

The electron diffraction patterns of these aggregates are quite sharp, and give 4 rings corresponding exactly to the strongest reflections of graphite (002, 100, 101, and 110). The sharpness of the pattern shows that the basal plane spacings are constant, as for crystalline graphite but not for amorphous carbon.

We have indirect evidence that these carbon aggregates are Cβ rather than Cα, as a parallel experiment on another sample showed that Cα does not survive the H_3PO_4 treatment. Murchison DF (formerly 2C10c), the 3-10 μm sister sample of DG, contains only Cα, judging from the absence of s-Xe *(4)* and the isotopic composition and combustion temperature of the carbon ($\delta C^{13} = +340$‰; $T_c = 650$°C; *5*). When DF was processed exactly like DG, no carbon particles were detectable by SEM in the low-density fraction. This is not surprising, as Cα is quite labile and reactive, judging from its low gas release and combustion temperatures.

The morphology and cohesiveness of these carbon aggregates is rather surprising. The presence of s-Xe implies that the carbon was ejected from a star in or past the red giant stage, and on the simplest model, one might have expected single graphite crystals condensed from the vapor phase. The aggregate morphology suggests a more complex history, which remains to be deciphered.

Acknowledgments. We are indebted to Leo Alaerts and Tang Ming for preparation of the samples. This work was supported in part by NASA Grant NAG 9-52 (E. Anders) and DOE Grant DE-AC02-76-EV02398 (A.V. Crewe).

(1) Swart P.K., Grady M.M., Pillinger C.T., Lewis R.S., and Anders E. *Science 220*, 406 (1983). *(2)* Lewis R.S., Anders E., Wright I.P., Norris S.J., and Pillinger C.T. *Nature 305*, 767 (1983). *(3)* Lewis R.S. and Anders E. *Sci. Am. 249* [2], 66 (1983). *(4)* Alaerts L., Lewis R.S., Matsuda J., and Anders E. *GCA 44*, 189 (1980). *(5)* Carr R.H., Wright I.P., Pillinger C.T., Lewis R.S., and Anders E. *Meteoritics 18*, 277 (1983).

WHERE IS THE EARTH'S MISSING XENON?

John F. Wacker and Edward Anders, Enrico Fermi Institute, University of Chicago, Chicago, IL 60637

Highly volatile elements (e.g. Tl,Pb,B,Cl,Br,etc.) in the Earth's crust occur in C-chondrite proportions, and so do the atmospheric noble gases Ne,Ar, and Kr. This has led to the suggestion that the Earth acquired its volatiles from a late "veneer" of C-chondrite-like material *(1,2)*. A glaring exception is Xe, which is depleted ~20× relative to Ne,Ar,Kr. Three explanations have been proposed for the depletion: (1) Xe is preferentially trapped in the crust, either in sediments *(3)* or in Antarctic ice *(4)*; (2) the Earth's noble gas inventory is non-chondritic *(5)*; or (3) Xe is incompletely outgassed from the mantle *(6)*.

(1) Sediments at best account for a minor part of the missing Xe *(4,5)*. If the missing Xe were located in the Antarctic ice cap, then K_{Xe} for ice would have to be ~3000 cc STP/g atm. Complementing direct measurements of Antarctic ice at Washington University *(7)*, we have measured K_{Xe} for ice at -20 to -60°C, using Xe^{127} tracer. K for trapping is only 0.098±0.004 cc/g atm, close to the value for liquid water at 0°C. K for adsorption plus trapping is larger but poorly determined (1.9±1.7 cc/g atm). Both values fall $\geq 10^3$× short of the required value of 3000, so unless some unknown factor greatly raises K under natural conditions, the Antarctic ice cap does not account for the missing Xe.

(2) A totally "non-chondritic" source seems implausible. All other volatiles require a chondritic source, and as noble gases in chondrites strongly correlate with other volatiles *(2)*, the chondritic material that supplied the Earth's volatiles must have supplied noble gases as well. A more reasonable possibility is that the material was chondritic, but with an unusual, Xe-poor noble gas pattern -- like the "subsolar" component in E-chondrites *(8,9)*.

(3) Retention of Xe in the mantle also seems plausible, even though no mantle rock analyzed to date has been sufficiently rich in Xe. The high abundance and chondritic pattern of Pt-metals in the mantle *(10)* -- including xenoliths from depths of >150 km *(11)* -- suggest that ~1% of a Cl-like component was present during accretion of at least the outermost 150 km of the Earth. The noble gases contained in this component thus would have to outgas from a great range of depths. If Xe lagged behind for some reason, then the atmosphere would be depleted in Xe.

Experiments on the trapping of Xe by amorphous carbon *(12)* suggest a reason why Xe might lag behind during such outgassing. The basal plane spacings in amorphous carbon are of the same order (3.5 to 5.0 Å) as the atomic diameters of the heavy noble gas atoms, 3.8 to 4.4 Å. Thus amorphous carbon can act as a "molecular sieve," preferentially trapping the heavier noble gases *(12)*. In terms of this model, the "missing Xe" would be located in a few specific minerals in the crust and mantle: amorphous carbon and any other minerals capable of acting as "molecular sieves" for Xe. Although no mantle rock analyzed to date has shown the required high Xe contents, none of these rocks contained significant amounts of amorphous carbon, and even if they had, the carbon could have been outgassed during ascent.

The same "molecular sieve" effect may have caused Xe depletions in nebular dust, e.g. in E-chondrites or in the source material of the volatiles on Venus, Mars, and Earth. We cannot tell from present evidence how much of the Xe depletion occurred before and how much after accretion. The essential point is, however, that the fortuitous match of the atomic size of Xe and the pore size of amorphous C may have caused preferential fractionation of Xe before or after accretion.

(1) Anders, E., 1968. *Acc. Chem. Res. 1*, 289; Turekian, K.K. and S.P. Clark, Jr., 1969. *EPSL 6*, 346.
(2) Anders, E. and T. Owen, 1977. *Science 198*, 453. *(3)* Canalas, R.A., E.C. Alexander, Jr., and O.K. Manuel, 1968. *J. Geophys. Res. 73*, 3331. *(4)* Podosek, F.A., M. Honda, and M. Ozima, 1980. *GCA 44*, 1875.
(5) Bernatowicz, T.J., F.A. Podosek, M. Honda, and F.E. Kramer, 1983. *LPS 14*, 31.
(6) Bernatowicz, T.J. and F.A. Podosek, 1978. In *Terrestrial Gases*, E.C. Alexander, Jr. and M. Ozima, (eds), 99.
(7) Podosek, F.A., 1983, private communication. *(8)* Crabb, J. and E. Anders, 1981. *GCA 45*, 2443; _____, 1982. *GCA 46*, 2351.
(9) Wacker, J.F. and K. Marti, 1983. *EPSL 62*, 147. *(10)* Chou, C.-L., 1978. *PLSC 9*, 219; Chou, C.-L. *et al.*, 1983. *JGR 88*, A507.
(11) Morgan, J.W. *et al.*, 1981. *Tectonophysics 75*, 47. *(12)* Wacker, J.F. and M. Zadnik, 1983. *Meteoritics 18*, 415; Zadnik, M. and J.F. Wacker, 1983. *Meteoritics 18*, 431; Wacker, J.F. *et al.*, 1984, paper in preparation.

M-2 N85 15642

BORON COSMOCHEMISTRY. David B. Curtis and Ernest S. Gladney, Los Alamos National Laboratory, Los Alamos, NM 87545.

Curtis et al. (1) demonstrated that interior pieces of chondrites contain significantly less boron than had been thought to be indigenous to this type of meteorite. The mean and range of boron abundances in 16 internal pieces of 10 chondrites were significantly smaller than in 126 pieces of 40 chondrites with unknown terrestrial histories. For lack of a more substantive criteria, it was assumed that samples not known to have been recently extracted from the interior were contaminated with boron, and only the analyses of interior pieces yielded results that were representative of indigenous meteoritic boron. The few analyses of interior pieces presented in that work showed no systematic relationship between boron abundance and meteorite type. Consequently, a new value of the "cosmic" abundance of boron was determined using the geometric average of the results from interior pieces of 10 chondrites. The result was about 7 times less than had been previously estimated from the analyses of meteorites.

Based upon the thermodynamic assessment of the cosmochemical properties of boron by Cameron et al. (2), Anders and Ebihara (3) assumed that boron was a "moderately volatile" element. They renormalized the data of Curtis et al. (1) to a chondrule free basis and thus inferred that the "cosmic" abundance of boron was about 3 times greater than that proposed by Curtis et al. (1). The difference between the two estimates stems basically from different assumptions about the cosmochemistry of the element rather than any fundamental disagreement about the data. To resolve these differences we have measured the relative abundances of several elements including boron in 38 carefully prepared interior pieces of 26 different chondrites. The elements are those that can be measured by the spectrometry of prompt gamma rays--the technique used to measure the boron abundances. This work was initiated in the hope that interelement relationships in individual pieces of chondritic material would elucidate the cosmochemistry of boron.

Silicon normalized abundances of sulfur (Fig. 1) show the distinct clustering as a function of meteorite type that is characteristic of "moderately volatile" elements. However, there is no correlation between boron and sulfur abundances, which indicates that, contrary to the conclusions of Cameron et al. (2), boron is not a "moderately volatile" element.

Abundances of other elements will be measured on samples selected from this set to try to distinguish a correlation with boron concentrations.

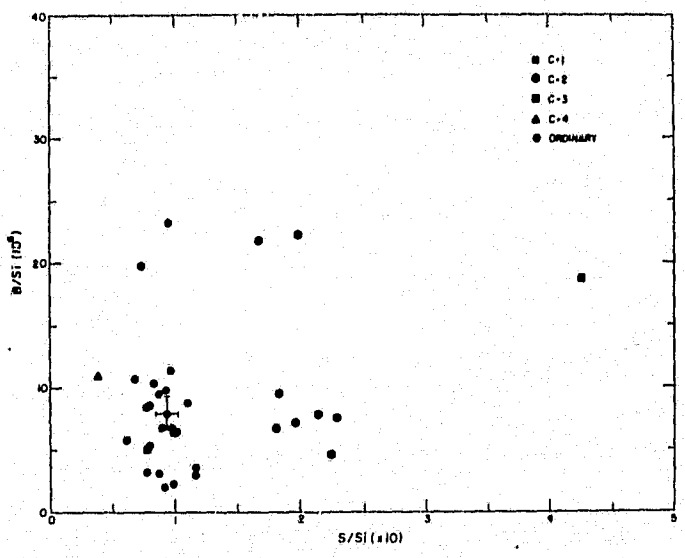

References: (1) Curtis D. B., Gladney E. S., and Jurney E. T. (1980) A Revision of the Meteorite Based Cosmic Abundance of Boron, Geochim. Cosmochim. Acta, 44, 1945-1953. (2) Cameron A. G. W., Colgate S. A., and Grossman L. (1973) Cosmic Abundance of Boron, Nature 243, 204-207. (3) Anders E. and Ebihara M. (1982) Solar System Abundance of the Elements, Geochim. Cosmochim. Acta 31, 1025-1034.

ACTINIDE CHEMISTRY OF ALLENDE COMPONENTS; M. T. Murrell and D. S. Burnett, Div. of Geol. & Planet. Sci., Caltech, Pasadena, CA 91125

U and Th in inclusions. Previous reports of high Th/U in Allende Ca,Al-rich inclusions (1, 2, 3) may indicate that U was not acting as a refractory element. The apparent ease of Th/U fractionation in the earliest material makes the ubiquity of Th/U = 3.8 in the solar system hard to understand. U-Th fission track radiography offers the possibility of a better understanding of actinide chemistry in Allende Ca,Al-rich inclusions. Volatility and valence differences between Th and U make these elements potentially useful in distinguishing between primary (condensation?) characteristics and those produced later by alteration. A preliminary examination of TS-23 (a type B inclusion provided by L. Grossman (4)) shows U to be highly enriched in the inclusion rim. This result is qualitatively similar to that found for U and Th in type A inclusions by Stapanian (3). The rim sequence in TS-23 consists of layers of (moving inwards): olivine, aluminous diopside + Ti,Al-rich clinopyroxene, nepheline, and Fe-rich spinel + perovskite. U is enriched in two of these layers. The band containing the Ti,Al-rich clinopyroxene is about 5- 10 μm thick and contains U at the 1 ppm level. The distribution of U in this band is fairly uniform but submicron U-rich phases (perovskite?) cannot be ruled out as the source of tracks at this time. The Fe-rich spinel layer is also high in U due to perovskite grains which contain $\geq$ 3 ppm U. Away from the rim, the major phases are fassaite, melilite, and anorthite which contain 40, 60, and $\leq$ 20 ppb U, respectively. For U to be enriched by 17x Cl values (5), the majority of the U must lie in the rim. However, U enrichments are also observed along some grain boundaries, within fractures, and as $\lesssim$ 10 μm hot spots within fine grained interstitial phases (Cl-rich in many cases). The extent to which these enrichments as well as those in the rims represent alteration may become apparent in our upcoming Th measurements in this and other inclusions.

Pu in chondrules. Mesostasis in chondrules from ordinary unequilibrated chondrites show enrichments in U and REE but no evidence for ^{244}Pu which instead appears to be concentrated in Ca-phosphates (6). This indicates either an initial Pu-REE, U fractionation or early migration of Pu from chondrules into phosphates. Neither of these alternatives are easy to explain. ^{244}Pu-Xe excesses have been measured in some Allende chondrules (7) and U enrichments are observed by us in mesostasis from some Allende chondrules. We have etched Allende chondrules to reveal fission tracks in olivine from ^{244}Pu in adjacent mesostasis, see (6). Reconnaissance examination of twenty chondrules showed a definite excess of tracks in olivine-mesostasis contacts in one chondrule (^{244}Pu content of ~0.4 ppb at the time of track retention); three other chondrules gave only a marginal indication of tracks originating from mesostasis, and the rest gave no indication. Therefore, we tentatively conclude that, in at least one chondrule, ^{244}Pu was present initially in mesostasis. The compatibility of our results with the fission Xe data (7) is unclear at present.

References: (1) Boynton, W. V. (1978) EPSL 40, 63-70. (2) Chen J.H. and Wasserburg G.J. (1981) Lunar Planet. Sci. XII, 132-133. (3) Stapanian M.I. (1981) Ph.D. thesis, Caltech. (4) Grossman L. (1975) GCA 39, 433-454. (5) Grossman L. et al. (1977) GCA 41, 1647-1664. (6) Murrell M.T. and Burnett D.S. (1983) GCA 47 1999-2014. (7) Swindle T.D. et al. (1983) GCA 47, 2157-2177.

PLUTONIUM AND URANIUM IN INDIVIDUAL CRYSTALS OF MERRILLITE AND APATITE OF ST. SEVERIN; S. de Chazal[1], G. Crozaz[1], M. Bourot-Denise[2] and P. Pellas[2], [1]Earth and Planetary Sciences Department and McDonnell Center for the Space Sciences, Washington University, St. Louis, MO 63130, USA; [2]Laboratoire de Minéralogie du Muséum et C.N.R.S., 61 Rue Buffon, 75005, Paris, France.

The hope of using ^{244}Pu as a chronometer to measure differences in meteorite formation times has been largely frustrated since it was realized that Pu and U (the normalizing element generally used because of the lack of a stable or long-lived plutonium isotope) chemically fractionate (see for ex., 1, 2, and 3). Lugmair and Marti (4) and Marti et al (5) observed that the Pu/Nd ratio in different meteoritic phases is constant and suggested that the Pu/Nd rather than the Pu/U ratio might be used for chronology. However, Ebihara and Honda (6) have recently challenged this hypothesis. They studied, by INAA in 3 ordinary chondrites, the REE concentrations of various phosphate size separates containing different proportions of merrillite and apatite and concluded that while the Pu abundances of these two phases differ by approximately a factor of 5, their light REE abundances are comparable. In turn, this study has been challenged by Woolum et al (7) and Reed et al (8) who have made in-situ measurements of light REE in a few chondritic phosphates. The results indicate that the light REE (like Pu) are enriched in the merrillite as opposed to apatite. The goal of the present research is to study the partitioning of Pu, U and the REE in individual crystals of merrillite and apatite from different chondrites. In a companion paper (9), we demonstrate our ability to measure rare earths in individual meteoritic phosphate grains using a Cameca IMS-3F Ion Probe.

In this work the $^{244}Pu/^{238}U$ ratios were determined in 48 phosphate grains from the dark portion of the St. Severin amphoterite. Twenty-nine of the grains consist of merrillite and nineteen of apatite (an unusually high concentration for this meteorite). The grains were mounted in epoxy, polished, and etched in HNO_3. The fossil fission track density of each grain was determined. The U concentrations of individual grains were measured using induced fission track densities in an external mica detector after neutron irradiation. The uranium concentrations, the Pu concentrations and the Pu/U ratios are listed in the table below. On a grain to grain basis there is no strong correlation between U, Pu, and the Pu/U ratio in either the apatites or the merrillites.

Table 1

	Uranium		Plutonium		Pu/U	
	Average	Range	Average	Range	Average	Range
Apatite	3.3±0.3ppm	2.3-4.2ppm	4.0±0.4ppb	2.4-5.3ppb	$1.3\times10^{-3}\pm0.3\times10^{-3}$	0.9×10^{-3} - 2.1×10^{-3}
Merrillite	0.32±.03ppm	0.13-0.46ppm	14 ± 1 ppb	8.6 - 18ppb	$50\times10^{-3}\pm12\times10^{-3}$	24×10^{-3} - 100×10^{-3}

(1) Crozaz, G. (1974) EPSL 23, p. 164-169. (2) Pellas, P. and Storzer, D. (1975) Meteoritics 10, p. 471-473. (3) Murrell, M. T. and Burnett, D. S. (1983) GCA 47, p. 1999-2014. (4) Lugmair, G. W. and Marti, K. (1977) EPSL 35, p. 273-284. (5) Marti, K. et al. (1977) Lunar Science VIII, p. 619-621. (6) Ebihara, M. and Honda, M. (1983) EPSL 63, p. 433-445. (7) Woolum, D. S. et al. (1983) Lunar Planet. Sci. XIV, p. 859-860. (8) Reed, S. J. B., et al. (1983) Nature 306, p. 172-173. (9) Crozaz, G. and Zinner E. (this conference).

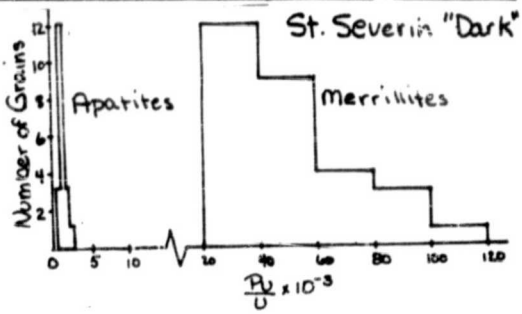

ION PROBE DETERMINATIONS OF THE REE CONTENTS OF INDIVIDUAL METEORITIC PHOSPHATE GRAINS; Ghislaine Crozaz and Ernst Zinner, McDonnell Center for the Space Sciences, Washington University, St. Louis, MO 63130.

We have measured the abundances of all the REE in individual phosphate crystals using a Cameca IMS-3F ion probe with an oxygen beam 5μm to 20μm in diameter. In order to determine elemental abundances, one has to eliminate molecular interferences or estimate their contribution to the ion signals, and determine the ionization yields of all the elements of interest relative to a reference element, for the matrix analyzed. Energy filtering of ~80V was sufficient to remove the less energetic molecular interferences (mainly complex compounds of the major elements). Oxides of light REE elements at the masses of heavier ones could not be eliminated completely but were the only remaining interferences. Atomic ion counts of the REE were obtained by taking into account the known relative abundances of the isotopes of all rare earth elements as well as their oxides at each measured mass (133 to 191). A second correction was made to an oxide/element ratio pattern for La to Sm as well as for Gd and Tb - obtained from high precision measurements of an apatite standard which also served for the determination of REE elemental sensitivities relative to Ca. The relative ion counts for all REE were found not to depend on the level of energy filtering (Fig.1). Agreement between our data on Angra dos Reis and those of Ma et al. [1] is very good (Fig. 2).

One of the main motivations of this work is to test whether or not the Pu/Nd ratio in meteorites can be used to determine relative formation times for these objects (see companion paper at this meeting by deChazal et al.). In this context, we analyzed both merrillite and apatite from the LL6 chondrite St. Severin. The merrillite has a flat REE profile at ~250 x chondritic with a pronounced Eu anomaly. REE concentrations in apatite range from 38 to 28 x chondritic with a distinct but small Eu anomaly. The ratios of the various REE concentrations in merrillite to that of apatite are between 2.7 and 16; the ratio for Nd is 9.2.

In addition, we analyzed 3 merrillite grains from the mesosiderite Emery. The grains have the same REE concentrations and the REE profile is flat from Sm to Dy (at ~90 x chondritic). The REE lighter than Sm are depleted whereas the ones heavier than Dy are enriched.

References: [1] M.-S. Ma et al. (1977) Earth Planet.Sci.Lett. 35, 331.

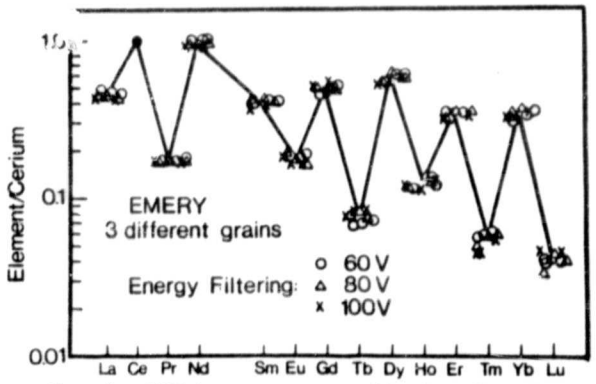

Fig. 1: REE ion counts normalized to Ce = 1 for the Emery mesosiderite merrillite.

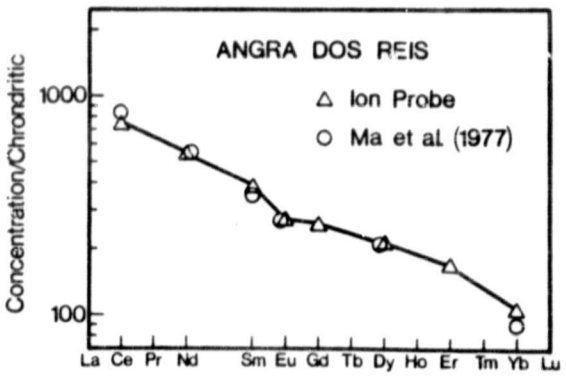

Fig. 2: REE abundances (normalized to chondrites) in the Angra dos Reis merrillite.

THE CHEMISTRY OF RARE EARTH ELEMENTS IN THE SOLAR NEBULA;

J. W. Larimer, H. A. Bartholomay, and B. Fegley[1]
Department of Geology and Center for Meteorite Studies, ASU, Tempe, AZ 85287
[1]Ceramic Processing Lab, MIT, Cambridge, MA 02138

The high concentration of REE in primitive CaS suggests that the REE along with other normally lithophile elements form stable sulfides under the unusual conditions which existed during the formation of enstatite chrondites.(1) In order to acquire a more quantitative framework in which to interpret these data, we are studying the behavior of the REE in systems with solar, or slightly fractionated solar, compositions. As a first step, we accumulated and put into a usable form, all the most recent (some unpublished) thermodynamic data on a large number of potentially significant species: gas and solid elemental, mono- and sesqui- oxides and sulfides.

These new data introduce modest changes in the behavior of some of the REE when compared to previous studies. For example, the largest differences are in the stabilities of the gaseous monoxides of Ce, Eu, Tb, Ho, and Tm, all of which now appear to be less stable than previously thought, and YbO(g) which is somewhat more stable. However, while these differences introduce some changes in the distribution of the REE in the gas they do not change the general pattern, only the details, of the predicted condensation sequence in comparison to that determined previously.(2)

Much more significant are the changes in REE distribution in the gas phase in fractionated systems, especially those made more reducing by changing the C/O ratio from the solar value of 0.6 to about 1.0. In almost all cases, the exceptions being Eu, Tm and Yb whose elemental gaseous species dominate, the monosulfides become more abundant. Moreover, the solid oxides of Eu, Tm and Yb become less stable under more reducing conditions which, in effect, should reduce the condensation temperature of all REE in more reduced systems. The stabilities of solid monosulfides increase also, achieving maximum values between about 1500 and 1000°K (at $P_T = 10^{-4}$ atm). In most cases the monosulfides of the light REE are more stable than the monosulfides of the heavier REE. This mimics the fractionation pattern observed in more primitive CaS grains.

Since CaS achieves its greatest stability under the same conditions, T = 1500 to 1000°K and C/O > 0.8, the incorporation of the REE into CaS is to be expected. The observed enrichment of all REE, slightly greater for LREE relative to HREE, in CaS can plausibly be explained on the basis of these predictions.

(1) Larimer, J. W., and Ganapathy, R., 1983, Meteoritics 18, 334

(2) Boynton, W. V., 1985, Geochimica et Cosmochimica Acta 39, 569-584

CHEMICAL VARIATIONS AMONG CHONDRULES FROM QINGZHEN (EH3).

J.N. Grossman[1], A.E. Rubin[2], E.R. Rambaldi[1], R.S. Rajan[1] and J.T. Wasson[2]. [1]Jet Propulsion Laboratory, California Institute of Technology, Pasadena, CA, 91109. [2]Institute of Geophysics and Planetary Physics, Univ. Calif., Los Angeles, CA, 90024, USA.

Recent studies have shown that chondrules in H-L-LL3 chondrites formed by melting heterogeneous nebular components similar to those involved in the fractionations among the chondrite groups. We report here the first detailed study of chondrules from a type-3 enstatite chondrite, Qingzhen (EH3). While many of the compositional properties are similar to those in ordinary chondrite (OC) chondrules, these enstatite chondrite (EC) chondrules do not preserve evidence of the same precursor materials.

Sixty-three chondrules were removed from Qingzhen by firmly crushing ~2 g of rock. The 15 largest ones (1-45 mg; 0.86-3.4 mm diam.) were chosen for this study. Preliminary examination shows that 8 of the 15 are radial pyroxene (RP) chondrules. In contrast, study of a thin section of Qingzhen reveals smaller chondrules (0.04-1.35 mm diam.) and fewer (21%) with RP textures. We do not yet know what effect these biases may have on our conclusions. The 15 chondrules were analyzed by INAA for ~30 elements.

Qingzhen chondrules are similar to OC chondrules in several important ways. Many elements show wide variations in abundance. The average chondrule is similar to the host rock in the Si-normalized abundances of nonvolatile lithophiles, and greatly depleted in siderophiles. Volatiles (Na, K, Cs, Se, Zn, Br, Cl, Ga) are not highly depleted in the chondrules. Porphyritic chondrules show subtle differences in composition from nonporphyritic chondrules along continuous chemical trends: the porphyritic chondrules are richer in siderophiles, Mg and Mn, and poorer in Cr and K. As in OC chondrules, the largest chondrules approach the composition of the whole rock minus metal and sulfide.

In contrast to OC chondrules, Qingzhen chondrules show relatively little variation in their abundances of refractory lithophiles, and thus there is little difference between porphyritic and nonporphyritic chondrules for these elements. Olivine has previously been linked to refractories in ordinary chondrites; the rarity of olivine in Qingzhen may be related to the lack of variation in refractory lithophiles.

Interelement correlations are very different between OC and EC chondrules. In Qingzhen, the elements that intercorrelate strongly are: 1) Fe-Co-Ni-Ir-Au; 2) Na-Al-REE-Hf; 3) Ca-Se-Eu; 4) Cl-Br. Only group 1, the siderophiles, is known to intercorrelate in OC chondrules. Groups 2 and 3 are similar to those found previously in Indarch (EH4) chondrules, although interelement ratios are quite different. Unlike the OC chondrules, many elements in Qingzhen chondrules seem to vary independently: Mg, Si, K, V, Cr, Mn, Zn, Cs.

Thus, the precursor components in Qingzhen chondrules differ from those in OC chondrules. The components of Qingzhen are not obviously related to the fractionations of enstatite chondrites from other chondrite groups. There is no evidence for a refractory lithophile component. Possibly, Qingzhen has experienced *in situ* alteration, changing the chondrule compositions enough to erase evidence for primitive components. A second alternative is that the precursor components were not produced early in the history of the nebula, but resulted from later alteration processes due, e.g., to temperature cycling. Sulfides bearing Ca, REE, etc., may have formed in this way before chondrule formation. A third alternative is that components which are abundant in the OC chondrules are greatly depleted in EC chondrules. In this case, the compositions of less-depleted components control chondrule variability.

A NEW CLASS OF ENSTATITE CHONDRITE?; K.S. Weeks and D.W.G. Sears, Department of Chemistry, University of Arkansas, Fayetteville, AR 72701, USA.

Several enstatite chondrites (Qingzhen, Parsa, Kota Kota, Allan Hills A77156, Yamato 69001, Galim and Yamato 74370) have a variety of petrographic and mineralogic properties which set them apart from the other enstatite chondrites (1-4). Most of these properties can be considered an extrapolation of the type 6 to type 4 trends, suggesting that these meteorites have suffered less metamorphic alteration, and equilibrated at lower temperatures, than the others. A few properties are not consistent with this trend, such as the Si content of the metal which is intermediate between EH and EL chondrites. On an Mg/Si vs. Fe/Si plot these meteorites fall with the EH chondrites, and well resolved from the EL chondrites. It has been suggested that this group of enstatite chondrites represent a new class of meteorites, perhaps sampling a new parent body (1,2).

We have performed an INAA on two of these chondrites, Qingzhen (3 irradiations) and Allan Hills A77156 (A77295, 2 irradiations) and present the results in Fig. 1, with literature data for Parsa (5) and Yamato 69001 (6). Ni, Co, Fe, Au and As (to a lesser extent Ir) are probably the elements which best resolve the EH and EL classes and Qingzhen, Parsa, Yamato 69001 and Allan Hills A77295 plot clearly among EH chondrites and well away from the EL chondrites. Al, Sc, Ca, REE and V do not readily resolve the EH and EL classes, although they do distinguish the enstatite chondrites from the other chondrites. Sb, Se and Zn are highly scattered, but are essentially consistent with a low petrologic type. Mn, Na and K are the only elements with abundances intermediate between the EH and EL chondrites (our 77295 K value excepted).

We suggest that this group of meteorites are EH chondrites whose mineralogical and petrologic properties reflect a lower petrologic type than the other EH chondrites (complicated in some cases, e.g. Si in the metal, by a differing bulk composition compared with the type 6 chondrites which to date are all EL chondrites). The low Mn, Na and K values may be associated with the unusual mineral distribution of these elements and which ElGoresy et al. interpreted as reflecting a parent-body process (1).

1. ElGoresy A. et al. Meteoritics 18,293 (1983). 2. Prinz M. et al. LPS XV 653 (1984). 3. McKinley S.G. et al. Meteoritics 17,251 (1984). 4. Nagahara H. LPS XV 583 (1984). 5. Sears D.W. et al. GCA 46,597 (1982). 6. Shima M. and Shima M. Mem. NIPR Spec. Iss. No. 5, 9 (1975).

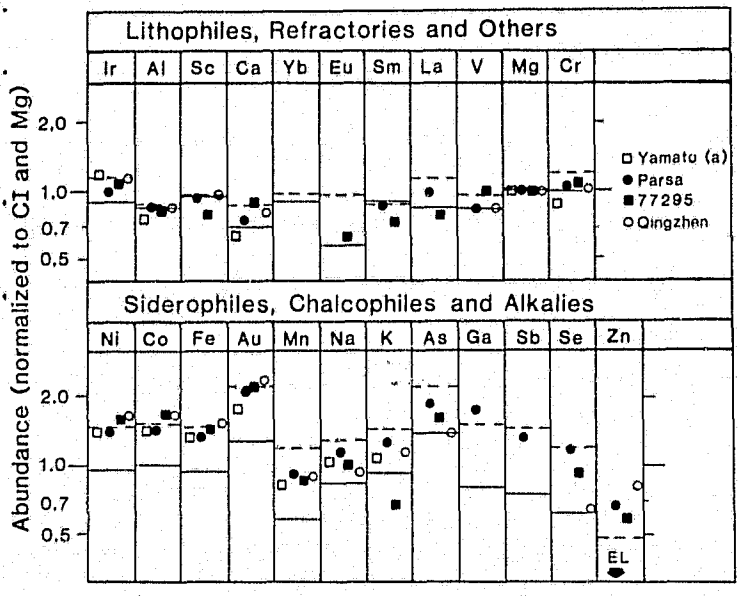

Fig. 1. CI and Mg-normalized element abundances in Yamato 69001 (a), Parsa, Allan Hills A77295 and Qingzhen compared with EH (broken bars) and EL (solid bars).

C-3

THE COMPOSITION OF ENSTATITE CHONDRITES. G.W. Kallemeyn and J.T. Wasson, Institute of Geophysics and Planetary Physics, University of California, Los Angeles, CA 90024, USA.

With the recent availability of new Antarctic and Chinese enstatite chondrites and the recognition of the first EH3 chondrites there is renewed interest in the study of these meteorites. We report new INAA analysis on 7 enstatite chondrites, including 5 grouped as EH3 or EH3,4 (ALHA77295, Kota-Kota, Parsa, Qingzhen, YAM74370) by several researchers and one proposed by Sears and coworkers to be the first EL5. Combining these with our previous data on 7 other enstatite chondrites, several distinct compositional differences between the EH and EL groups are apparent, and insights can be made regarding the compositional effects of weathering.

The EH and EL chondrites form narrow peaks on Mg (101-107, 135-140 mg/g) and Al (7.7-8.1, 9.3-10.1 mg/g) histograms, with broad hiatus between the two groups. Other normally lithophile elements such as Ca and Na show more scatter probably reflecting their greater tendency to form highly soluble reduced sulfides. Ranges of Fe and Ni are broad (215-315 abd 14.7-20.2 mg/g) with EH > EL, with some overlapping of values in the midrange. These wide-ranging values are probably mainly a sampling effect resulting from differing proportions of metal and sulfides, as opposed to weathering effects because of the small scatter in major lithophile concentrations. Nonrefractory siderophile abundances (Mg-normalized) show broad hiatus between H and L. Both Na and K, which commonly show weathering effects in other chondrite groups, appear to be depleted among EH finds relative to falls; they also show much more scatter among finds, probably the result of weathering.

The EH and EL chondrites have similar Mg-normalized lithophile and refractory siderophile abundances. Common siderophiles are distinctly higher in EH (1.45X CI) than in EL (1.05X CI). Volatile element abundances also show the same trend although to a highly variable degree with much more scatter among the two groups. There appears to be no correlation between petrologic type and abundances of the most volatile elements determined (Te, Br, Se, Zn). The EH3 (including EH3,4) chondrites show no tendency toward higher volatile abundances than the EH5 chondrites. In fact, the EH3 chondrites do not appear to define any bulk compositional property distinct from the other EH chondrites.

The alleged EL5 chondrite RKPA80259 shows a remarkable similarity to EH3,4 YAM74370. Abundances of 16 elements in the two meteorites agree to within 5 % of each other, and only the abundances of Na, K, Br and Zn among 29 elements determined disagree by more than 10 %. Our abundance data on RKPA80259 place it on the low end of the EH group, with only an unusally low Zn abundance being seriously out of line. The high abundance data for the common siderophiles Ni, Co, Fe (1.37X CI) and the concentration data for Mg (103 mg/g) and Al (8.06 mg/g) in our sample clearly favors an EH rather than an EL classification.

SILICA-NININGERITE-ENSTATITE CLASTS IN THE PRIMITIVE ENSTATITE CHONDRITES

Hiroko Nagahara, Geol. Inst., Univ. Tokyo, Hongo, Tokyo 113, Japan

Silica-niningerite-ensatatite clasts with igneous texture were found in Y-74370 EH chondrite (1). Their chemical compositions are shown on MgO-SiO2-MgS diagram (Fig. 1). Crystallization sequence of most clasts (■) is enstatite→niningerite→albite→SiO2, and rarely SiO2→devitrified glass of enstatite composition (□) which are considered to be formed as droplets. The latter is more enriched in MgO than the former, which is inconsistent with the crystallization sequence. Further, the similar texture as the former is observed in the interstitial part of large porphyritic pyroxene chondrules. Consequently, the clasts are not peculiar chondrules but are parts of chondrules. Clasts with silica mineral and pyroxene glass were probably formed by rapid cooling. A few spherical chondrules composed of tridymite, niningerite and troilite are free from MgO (●). Porphyritic pyroxene chondrules often contain silica and niningerite in the interstices (○).

Silica-niningerite-enstatite clasts are often observed in Qingzhen and Indarch (about 10% of fairly large objects other than mineral fragmentsin Qingzhen), and their textures are similar to those in Y-74370. However, they have neither chondrules with silica-niningerite assemblage nor clasts with silica and enstatite glass. Kota Kota has few clasts and Y-691 does not have any clasts.

Abundance of olivine-bearing chondrules and free olivine in the matrix is consistent with that of the clasts: Y-74370 and Indarch have very small amounts of olivine-bearing chondrules and olivine is always included in pyroxene, but Qingzhen, Kota Kota and Y-691 have more olivine-bearing chondrules which contain even porphyritic olivine and barred olivine chondrules.

Coexistence of silica mineral and niningerite shows that reducing and figh fS_2 conditions were important for the crystallization of silica minerals. Difference of silica-niningerite-bearing clasts and olivine-bearing chondrules among those primitive enstatite chondrites show that chondrules and clasts were formed under slightly deviated oxidizing-reducing conditions and that they accreted heterogeneously.

(1) Nagahara, H. and El Goresy, A. (1984) Lunar Planet. Sci., XV, 583-584.

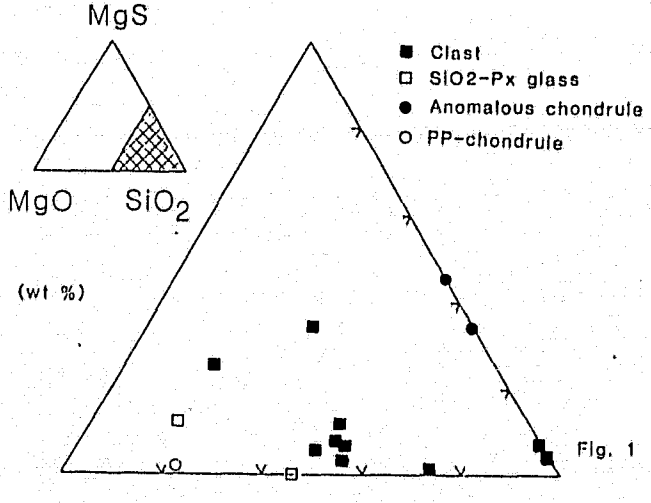

Fig. 1

COEXISTING CHALCOPHILE AND LITHOPHILE URANIUM IN QINGZHEN (EH3) CHONDRITE; E.R. Rambaldi[1], M.T. Murrell[2], R.S. Rajan[1] and D.S. Burnett[2], [1]Jet Propulsion Lab, Caltech, Pasadena, CA 91109; [2]Division of Geological Sciences, Caltech, Pasadena, CA 91125.

Mineralogical and textural studies of Qingzhen have shown that it is highly unequilibrated and that it contains a population of chondrules and isolated enstatite grains which preserve the record of more oxidizing nebular conditions(1,2). Even though in the majority of cases these objects have been affected by various degrees of reduction, some still contain silicates with high (up to 10%) FeO contents. The discovery of oxidized materials within an otherwise reduced meteorite, makes it an interesting candidate for U-distribution studies. Previous work by Murrell and Burnett(3) has shown that in the EL6 chondrites oldhamite (CaS) accounts for more than 80% of the total U content, while in the EH4 chondrite, Abee both oldhamite and niningerite (MgS) are important U-bearing phases.

Five polished sections of Qingzhen were irradiated and the U-bearing phases identified using the fission track technique. Mean U concentrations of 300 ± 20 ppb were found in oldhamite, which compare well with the value of 260 ± 20 ppb found in Abee oldhamite. Niningerite in Qingzhen contains only ≈ 2 ppb U in contrast to Abee niningerite (45 ppb). This is probably the result of considerable chemical differences in the composition of this mineral in the two meteorites. For example, in the case of Ca, its abundance in the Qingzhen niningerite (0.5%) is a factor of six lower than that from Abee[4]. No U (< 1 ppb) was found in the K-bearing sulfide, djerfisherite.

We have identified several chondrules in Qingzhen which contain large 50-100 μm areas of mesostasis which have high U contents. Similar U enrichments in chondrule mesostasis have been found in ordinary chondrites[5].

Chondrule A is a porphyritic chondrule consisting mainly of enstatite and interstitial albitic glass plus minor amounts of troilite, oldhamite, niningerite and metal. The glass in the chondrule core contains crystallites of a Ca,Al and Ti-rich pyroxene, which appear to be the site of high U concentrations (140 ppb). On the other hand in the outer portion of the chondrule, the glass is devoid of pyroxene crystallites and Ca is predominantly present as large isolated oldhamite grains with ≈ 300 ppb U. The presence of U-bearing Ca-pyroxene suggests that the precursor material of chondrule A must have originated under more oxidizing and less sulfurizing conditions than the bulk Qingzhen. Subsequently, the material was probably transported into a reducing environment where it was mixed with CaS and other sulfides prior to the melting involved in the chondrule formation event.

References: [1]Rambaldi, E.R., Rajan, R.S., Wang, D. and Housley, R.M. (1983) Earth Planet. Sci. Letters, 66, p.11-24. [2]Rambaldi, E.R., Housley, R.M. and Rajan, R.S. (1984) Nature, in press. [3]Murrell, M.T. and Burnett, D.S. (1982) Geochim. Cosmochim. Acta, 46, p.2453-2460. [4]Rubin, A.E. and Keil, K. (1983) Earth Planet. Sci. Letters, 62, p. 118-131. [5]Murrell, M.T. and Burnett, D.S. (1983) Geochim. Cosmochim. Acta, 47, p. 1999-2014.

HIGH TEMPERATURE PHASE EQUILIBRIA IN THE ENSTATITE CHONDRITE SYSTEM: W. A. Cassidy, University of Pittsburgh

Chondrules and lithic fragments that could not be derived through normal igneous processes seem to occur commonly in enstatite chondrites and unequilibrated H-chondrites (1,2). For enstatite chondrites, phase relations in the system Fe-Mg_2SiO_4-SiO_2 suggest that these particles probably condensed directly from vapor and passed through conditions in which two or three immiscible liquids were produced (for convenience, the additional sulfide liquid is ignored). The system contains three intersecting 2-liquid domes which envelop an underlying 3-liquid volume. As total pressure in this system decreases, the vaporus surface intersects the 2-liquid domes at lower and lower temperatures, eventually intersecting the 3-liquid volume also. At even lower total pressures for these compositions, crystalline cristobalite would condense directly from the vapor, accompanied by two immiscible liquids. Textural relations in some of the enstatite chondrite particles suggest that temperatures and pressures were high enough so that at least two of the liquids considered here were present. Composition of the high-silica phase often suggests that it was present as a third liquid. This would require rather high temperatures and pressures in that part of the primitive solar nebula where these particles were produced.

(1) Brigham, C., Murrell, M. T., and Burnett, D. S. (1982) (abstract) In Papers Presented to the Conference on Chondrules and their Origins, p. 4, Lunar and Planetary Institute, Houston.

(2) Nagahara, H. and El-Goresy, A. (1984) (abstract) In Lunar and Planetary Science XV, pp. 118-19. Lunar and Planetary Institute, Houston.

$Na_{0.3}(H_2O)_1[CrS_2]$, A NEW MINERAL IN THE NORTON COUNTY ENSTATITE ACHONDRITE

A. Okada (1), K. Keil, Dept. of Geology, Institute of Meteoritics, Univ. of New Mexico, Albuquerque, N.M. 87131; B.F. Leonard, U.S. Geological Survey, Box 25046, Federal Center, Denver, Colorado 80225; I.D. Hutcheon (2), Enrico Fermi Institute, Univ. of Chicago, Chicago, Illinois 60637. (1) The Institute of Physical and Chemical Research, Wako, Saitama, Japan. (2) Div. of Geological and Planetary Sciences, California Institute of Technology, Pasadena, California 91125.

A new mineral, ideally $Na_{0.3}(H_2O)_1[CrS_2]$, occurs in the Norton County enstatite achondrite as thin bands a few μm wide in caswellsilverite, $NaCrS_2$, and as individual grains up to 250 μm in size, adjacent to caswellsilverite. Other associated phases are daubreelite, titanoan troilite, ferromagnesian alabandite, oldhamite, kamacite and perryite. In reflected light, the mineral is gray in air and bluish gray in oil. It has distinct reflection pleochroism: in air, brownish gray (brighter) and bluish gray (darker); in oil, gray with an extremely faint yellowish tint (brighter) and bluish gray (darker). Anisotropism is strong and the phase is uniaxial (-). Electron microprobe and ion microprobe analyses show the mineral to be (ideally) $Na_{0.3}(H_2O)_1[CrS_2]$, with only minor Ti and Mn (avg. 0.17 wt.% each). The natural and synthetic phases have identical X-ray powder diffraction patterns with the following lines (in Å): 8.85 (vs) (003); 4.43 (w) (006); 2.80 (m) (102); 2.53 (m) (105); 2.21 (vvw) (00,12); 1.67 (m) (110). Because of the small amount of the natural phase available for X-ray studies, the weak (006) and very, very weak (00,12) lines could not be reliably measured. Lattice constants are a = 3.32Å and c = 26.6Å, based on a hexagonal setting. Possible space groups are R3m, $R\bar{3}m$ and R32. The measured density of the synthetic phase is 2.70 g/cm^3 and the calculated density is 2.74 g/cm^3. Experimental work by us and others shows that sodium chromium sulfide hydrate (bilayered molecular water form) is readily produced by the partial hydration of caswellsilverite ($NaCrS_2$) in aqueous solution at room temperature. The monolayered molecular water form, the new mineral, forms by subsequent partial dehydration of the bilayered phase. Based on its intergrowth with caswellsilverite, its composition, water content and structure and the lack of indigeneous water in the highly reduced Norton County enstatite achondrite, we propose that the new mineral is the terrestrial weathering product of caswellsilverite. We conclude that caswellsilverite was altered to the bilayered sodium chromium sulfide hydrate through reaction with moisture while the meteorite specimens rested in the soil of Nebraska. During subsequent storage and drying in the arid atmosphere of New Mexico, the bilayered phase converted into the monolayered sodium chromium sulfide hydrate.

BISHOPVILLE: THE IMPORTANCE OF A FIELD SEARCH; H. H. Nininger, 7891 Osceola St., Westminster, Colorado 80030

The Bishopville, Sumter County, South Carolina, meteorite fell during the daylight hours of March 25, 1843. Its meteor and the explosion which accompanied the fall were witnessed over an area 30 to 40 miles in diameter. The six-kilogram stone was seen to strike the earth and recovered from a depth of about three feet in the soft soil. The meteorite was brought to the attention of science in 1846 when J. C. Haynsworth purchased the stone from its owner and presented it to Professor C. U. Shepard.

So far as can be determined, no ground search was ever made for other pieces of the stone which were freed from the descending mass by the terminal explosion. It is now 141 years since the fall of this unique meteorite. A field search of the area could well bring to light other specimens of the Bishopville meteorite and give science a much needed insight into the terrestrialization or preservation of a meteorite of this variety.

NORTH AMERICAN TEKTITES AND MICROTEKTITES FROM BARBADOS, WEST INDIES: B.P. Glass[1], Annika Sanfilippo[2], C.A. Burns[1], D.H. Lerner[1]; [1]Geology Dept., Univ. of Delaware, Newark, DE 19716; [2]Scripps Institution of Oceanography, Univ. of California at San Diego, La Jolla, CA 92093.

In the summer of 1982, one of us (A.S.) discovered a layer of microtektites in late Eocene deep-sea deposits at Bath Cliff, Barbados. Late Eocene microtektites have now been found in two sites on Barbados: 1) Bath Cliff and 2) Gay's Cove. The Barbados microtektites are similar in appearance and major oxide composition (Table 1) to late Eocene microtektites found in the Caribbean Sea and Gulf of Mexico. In general, however, they are paler in color and more silica-rich. The microtektite layer found on Barbados differs from the late Eocene microtektite layer in the Caribbean Sea and Gulf of Mexico in at least three other respects: 1) the microtektites are not as abundant; 2) no clinopyroxene-bearing glass spherules are found associated with the microtektites; and 3) tektite fragments, up to ~2 mm in length, are common. The lower abundance of microtektites at the Barbados site may indicate that this site is closer to the edge of the strewn field. The tektite fragments are for the most part all similar in appearance suggesting rather uniform composition. The major oxide compositions of several fragments, determined by energy dispersive x-ray analysis, are similar to the major oxide compositions of North American tektites (Table 1). Furthermore, the ^{40}Ar - ^{39}Ar ages of several tektite fragments are indistinguishable from previously reported ^{40}Ar - ^{39}Ar and K-Ar ages of North American tektites (D. York and C.M. Hall, personal communication, 1984). We therefore conclude that the Barbados tektite fragments and microtektites belong to the North American tektite strewn field.

Table 1

Major Oxide Compositions of Barbados Microtektites, and Tektites, and Selected North American Tektites (Determined by EDS Analysis)

SiO_2	Al_2O_3	FeO	MgO	CaO	Na_2O	K_2O	TiO_2
			Barbados Microtektites				
84.2	10.4	1.48	0.45	0.20	0.60	1.77	0.49
79.5	12.5	2.35	0.74	0.19	1.17	2.49	0.62
79.1	12.1	2.42	0.92	0.74	1.24	2.71	0.43
77.4	12.9	3.02	0.80	0.75	1.23	2.73	0.69
73.2	12.6	4.65	1.32	4.46	0.92	1.84	0.56
			Barbados Tektites				
83.5	9.18	2.06	0.39	0.42	1.24	2.56	0.21
81.3	9.91	2.12	0.55	0.80	1.93	2.54	0.38
78.8	13.0	2.76	0.66	0.24	1.40	2.14	0.62
78.3	12.4	3.07	0.61	0.21	1.57	2.17	0.68
78.2	12.6	3.21	0.75	0.26	1.75	2.21	0.66
			North American Tektites				
81.3	11.0	2.43	0.53	0.50	1.50	2.17	0.53
81.0	11.0	2.58	0.60	0.36	0.84	2.61	0.52
78.4	12.9	3.40	0.54	0.26	1.41	2.01	0.67

RELICT MINERALS IN A MUONG NONG TEKTITE; R. F. Fudali, Daphne Ross, Daniel E. Appleman, Dept. of Mineral Sciences, Smithsonian Institution, Washington, D. C. 20560.

Zircon, corundum (probably a decomposition product of an Al_2SiO_5 mineral), rutile, chromite and monazite have previously been reported as inclusions in Muong Nong tektites (1). This assemblage, and the mean diameters of the recovered crystals (~20 to 160 microns), have been cited as evidence of a very fine-grained sedimentary precursor for the Australasian tektites.

We have subjected a much coarser fraction (370 to 710 microns) of a crushed Muong Nong specimen, weighing 649 grams, to a heavy liquid separation and have identified the following minerals in the heavy fraction: quartz, orthopyroxene, clinopyroxene, albite, microcline, biotite, muscovite, diaspore and corundum. The corundum is associated with and is a decomposition product of the diaspore ($2AlOOH \rightarrow Al_2O_3 + H_2O$). All the minerals examined, with the exception of diaspore, show only modest asterism. Diaspore exhibits extreme asterism.

The "average" refractive index of our Muong Nong glass (~1.512) puts it in the group where Glass and Barlow (1), working with much smaller amounts of material, were unable to find any relict minerals whatsoever.

The predominant mineral in the crystal fraction is a biotite with a rather distinctive combination of features; it has a high titanium content, contains tiny zircons surrounded by pleochroic halos and appears to have an unusual stacking arrangement.

The preservation of relict, hydrous minerals in this tektite is remarkable. Diaspore readily decomposes above 300°C and the micas readily decompose above 700°C in the absence of extreme water vapor pressures--temperatures far lower than this tektite has obviously experienced. Whatever, their presence is simple and irrefutable proof of a terrestrial origin for the Australasian tektites as such hydrous minerals are not present on the Moon.

The relict mineral association reported herein, and the relative coarseness of the individual grains, strongly suggests the parent rock for this particular tektite was an arkose. This mineral assemblage, plus the composition and structural state of the biotite, may be diagnostic enough to allow a positive identification of the parent terrain when and if likely candidates can be located. Whether the finer fraction of our crushed specimen contains a mineral assemblage similar to that reported by Glass and Barlow remains to be determined.

1. Glass, B. P. and Rodney A. Barlow, Meteoritics V. 14, no. 1, 55-67, 1979.

GEOCHEMISTRY OF MUONG-NONG TYPE TEKTITES V: UNUSUAL FERRIC/FERROUS RATIOS. C.Koeberl, F.Kluger, and W.Kiesl, Institute for Analytical Chemistry,University of Vienna,P.O.Box 73, A-1094 Vienna, Austria.

The geochemistry of Muong-Nong type tektites displays some anomalies when compared with the chemistry of normal splash-form tektites. One of the most important anomalies is the fact that volatile elements like the halogens or copper, boron, zinc, arsenic and others are significantly enriched, when compared with the abundances usually present in splash-form tektites. Another difference between these two groups of tektites of probable genetic significance is the high ferric/ferrous ratio. For splash-form tektites this ratio is generally less than 0.15 (O'Keefe, 1976). However, the assumption of Chapman and Scheiber (1969) that this is true also for Muong-Nong type tektites (their high Cu,B group), which led them to report all Fe as FeO, is not correct. Although there is some scatter in the Fe(III)/Fe(II) ratios of splash-form tektites, only very rarely the Fe(II) share of the the total iron amounts less than 80% (Schnetzler and Pinson, 1963). Our analyses of Muong-Nong samples from Ubon Ratchathani (Thailand) for ferric/ferrous ratios showed that significantly more iron is in the oxidized state than in the splash-form tektites. In table 1 we give our results for 18 Muong-Nong samples. Total iron has been determined with instrumental neutron activation analysis, and Fe(II) has been determined using a wet-chemical technique involving dissolution in HF and addition of NH_4VO_3 and a titration step. From the difference between the total iron and the Fe(II) as determined with this method the content of Fe(III) was calculated and reported as Fe_2O_3. In the case of the Muong-Nong type tektites, in contrary to splash-form tektites, Fe(II) only rarely amounts more than 80% of the total iron. The average for Fe(II) in our 18 samples is 75.3±9.4% of the total iron. Although it has been suggested that this ratio may be due to secondary alteration (O'Keefe, 1984), we feel that this has some genetic significance (i.e. a low-temperature origin of these tektites). This will be discussed in a later paper.

References: Chapman and Scheiber (1969) JGR 74,6737; O'Keefe,J.A., (1976) Tektites and their origin,Elsevier; O'Keefe,J.A. (1984) personal communication; Schnetzler and Pinson (1963), in:Tektites, ed. J.A.O'Keefe, p.95.

Table 1

Sample No.	FeO (%)	Fe_2O_3 (%)	Sample No.	FeO (%)	Fe_2O_3 (%)
MN8301	3.31	1.12	MN8310	3.45	0.57
MN8302	2.25	0.88	MN8311	3.35	1.22
MN8303	3.31	2.24	MN8312	3.20	0.39
MN8304	2.61	1.93	MN8313	3.55	1.48
MN8305	2.88	2.00	MN8314	3.42	1.36
MN8306	3.45	1.28	MN8316	3.67	0.85
MN8307	3.37	1.43	MN8317	3.23	1.86
MN8308	3.18	1.25	MN8318	3.07	0.26
MN8309	3.68	1.56	MN8319	3.91	1.08

GEOCHEMISTRY OF MUONG-NONG TYPE TEKTITES VI: MAJOR ELEMENT DETERMINATIONS AND INHOMOGENITIES. H.H.Weinke and C.Koeberl, Institute for Analytical Chemistry, University of Vienna, P.O.Box 73, A-1094 Vienna, Austria.

The shape and the over-all appearance of Muong-Nong type tektites as well as the appearance in the optical microscope leds to the idea, that these tektites may be significantly inhomogenous. We report here data on the homogenity of 19 Muong-Nong tektite samples. The analyses have been performed with a computer-controlled ARL SEMQ microprobe on random selected spots. Typically about 20-30 random spots have been used to evaluate the mean data reported in table 1. No attempts have been made for the case of these analyses to distinguish between light and dark layers present in the material. In table 1 only means of the major elements are given, and (for space reasons) no standard deviations. However, there is a large difference in the scatter (=inhomogenity) for different elements. The elements distributed most homogenous are Na and K with a variation of only less than 5% relative. The most inhomogenous elements are Al,Si, and Fe with variations of about 10% relative. The agreement between NAA and AAS data and the microprobe data reported here is generally very good for homogenous elements, but affected with larger differences for inhomogenous elements (especially Fe). Investigations concerning the small chemical variations between the dark and the light layers are in progress.

Table 1

Sample No.	K_2O	Na_2O	SiO_2	FeO	MgO	Al_2O_3	CaO	TiO_2
MN8301	2.50	1.01	76.73	3.95	1.57	11.41	1.25	0.67
MN8302	2.36	1.04	79.65	3.27	1.32	9.64	1.14	0.59
MN8303	2.25	1.01	80.54	3.18	1.20	8.53	1.17	0.53
MN8304	2.47	0.97	77.78	3.80	1.40	10.34	1.10	0.62
MN8305	2.26	0.87	79.50	3.24	1.33	8.89	1.39	0.59
MN8306	2.49	0.82	76.86	4.15	1.51	10.69	1.20	0.67
MN8307	2.46	0.77	77.28	3.92	1.47	10.65	1.09	0.63
MN8308	2.33	0.96	77.35	3.75	1.65	10.18	1.63	0.72
MN8309	2.55	0.77	77.80	4.05	1.49	11.06	1.04	0.65
MN8310	2.52	0.82	77.11	4.04	1.51	10.97	1.11	0.66
MN8311	2.37	0.87	78.86	3.97	1.38	9.53	1.21	0.60
MN8312	2.28	0.86	81.35	3.18	1.19	8.60	1.19	0.56
MN8313	2.50	0.95	76.62	4.10	1.53	11.19	1.16	0.67
MN8314	2.38	1.07	78.20	3.77	1.50	10.21	1.44	0.66
MN8315	2.51	0.92	77.08	4.06	1.52	11.26	1.16	0.68
MN8316	2.37	1.03	79.72	3.48	1.33	9.39	1.36	0.58
MN8317	2.52	0.95	77.28	4.00	1.48	11.13	1.15	0.65
MN8318	2.24	0.92	81.24	3.23	1.26	8.58	1.03	0.59
MN8319	2.52	0.95	76.67	4.02	1.58	11.22	1.26	0.66

All data in wt.%, all Fe as FeO.

A NEW H-3 CHONDRITE FROM STUDY BUTTE, TEXAS; K. Fredriksson*, R. S. Clarke, Jr.* and R. Pugh**, *Department of Mineral Sciences, National Museum of Natural History, Smithsonian Institution, Washington, D.C. 20560, and **4617 N.E. 26th Ave., Portland, OR 97211

The single weathered individual, weighing 417 grams, was found on Sept. 30, 1983, by Mr. Tim Turrentine approximately 2.2km SSE of Study Butte, Texas (29° 18' 6" N, 104° 30' 0" W). It was recognized as a meteorite by one of us (RP) and subsequently obtained by the Smithsonian Institution. The name Study Butte has been submitted to the "Meteoritical Bulletin". Macroscopically the specimen was almost completely enveloped in dark brown fusion crust; only a small part had been broken off. The first cut showed numerous chondrules and a few irregular, both light and dark, fragments, in a mottled matrix. A preliminary chemical analysis gave ~31% total Fe (Table 1) indicating that the meteorite belongs to the H (high iron) group chondrites. Microscopic and electronprobe studies on polished thin sections revealed a highly chondritic structure and a great variation in olivine (Fa 0.1 to 26 with a PMD of ~50%) and orthopyroxene (Fs 1 to 16%) compositions. According to current criteria this meteorite is therefore of petrographic grade 3. The modal composition is 77% silicates, 5.5% FeS, 8.4% metal, and 9.3% "oxide", apparently mostly oxidized metal; thus the original metal content also indicates the H-group. The metal grains, often intergrown with sulphides, are complex; kamacite (~6% Ni, 0.4% Co), taenite (15-32% Ni) and tetrataenite (up to 57% Ni) have been identified. Thin sections reveal numerous lithic fragments, both light and dark, mostly finegrained and with compositions near that of ordinary H-chondrites. However, a small achondritic fragment (0.2 x 0.3mm) is unique; it has andesitic bulk composition (Table 1) and texture and contains diopsidic pyroxene and twinned plagioclase (~An40) in a glassy matrix. This chondrite is clearly a complex breccia and probably gas rich; further studies seem warranted.

Table 1. Composition of Chondrite from Study Butte; wt %

	Bulk	"Andesitic" fragment
SiO_2	34.9	57.-
Al_2O_3	2.00	17.-
FeO	26.0-	2.5
MgO	22.7-	5.5
CaO	1.73	9.-
Na_2O	0.69	5.-
K_2O	0.12	0.4
FeS	4.5	-
Ni[1)]	1.2-	-
SUM[2)]	94.3-	-
Fe_{Tot}[3)]	~31.--	-

Bulk, Mode (1221 points)	
Silicates	77.-
Metal	8.4
Troilite	5.4
Chromite	0.1
"Oxides"	9.3

1. Ni mostly in oxides.
2. Low summation due to weathering (Fe^{3+}, H_2O). Includes Cr_2O_3 0.48%.
3. Assuming 10% Ni in metal and "oxides".

A NEW H-3 CHONDRITE FROM STUDY BUTTE, TEXAS; K. Fredriksson*, R. S. Clarke, Jr.* and R. Pugh**, *Department of Mineral Sciences, National Museum of Natural History, Smithsonian Institution, Washington, D.C. 20560, and **4617 N.E. 26th Ave., Portland, OR 97211

The single weathered individual, weighing 417 grams, was found on Sept. 30, 1983, by Mr. Tim Turrentine approximately 2.2km SSE of Study Butte, Texas (29° 18' 6" N, 104° 30' 0" W). It was recognized as a meteorite by one of us (RP) and subsequently obtained by the Smithsonian Institution. The name Study Butte has been submitted to the "Meteoritical Bulletin". Macroscopically the specimen was almost completely enveloped in dark brown fusion crust; only a small part had been broken off. The first cut showed numerous chondrules and a few irregular, both light and dark, fragments, in a mottled matrix. A preliminary chemical analysis gave ~31% total Fe (Table 1) indicating that the meteorite belongs to the H (high iron) group chondrites. Microscopic and electronprobe studies on polished thin sections revealed a highly chondritic structure and a great variation in olivine (Fa 0.1 to 26 with a PMD of ~50%) and orthopyroxene (Fs 1 to 16%) compositions. According to current criteria this meteorite is therefore of petrographic grade 3. The modal composition is 77% silicates, 5.5% FeS, 8.4% metal, and 9.3% "oxide", apparently mostly oxidized metal; thus the original metal content also indicates the H-group. The metal grains, often intergrown with sulphides, are complex; kamacite (~6% Ni, 0.4% Co), taenite (15-32% Ni) and tetrataenite (up to 57% Ni) have been identified. Thin sections reveal numerous lithic fragments, both light and dark, mostly finegrained and with compositions near that of ordinary H-chondrites. However, a small achondritic fragment (0.2 x 0.3mm) is unique; it has andesitic bulk composition (Table 1) and texture and contains diopsidic pyroxene and twinned plagioclase (~An40) in a glassy matrix. This chondrite is clearly a complex breccia and probably gas rich; further studies seem warranted.

Table 1. Composition of Chondrite from Study Butte; wt %

	Bulk	"Andesitic" fragment
SiO_2	34.9	57.-
Al_2O_3	2.00	17.-
FeO	26.0-	2.5
MgO	22.7-	5.5
CaO	1.73	9.-
Na_2O	0.69	5.-
K_2O	0.12	0.4
FeS	4.5	-
Ni[1)]	1.2-	-
SUM[2)]	94.3-	-
Fe_{Tot}[3)]	~31.--	-

Bulk, Mode (1221 points)	
Silicates	77.-
Metal	8.4
Troilite	5.4
Chromite	0.1
"Oxides"	9.3

1. Ni mostly in oxides.
2. Low summation due to weathering (Fe^{3+}, H_2O). Includes Cr_2O_3 0.48%.
3. Assuming 10% Ni in metal and "oxides".

THREE NEW CHONDRITE FINDS FROM ROOSEVELT COUNTY, NEW MEXICO;
Paul P. Sipiera, Department of Geology, University of Otago, New Zealand.

In recent years numerous chondrites have been recovered from the sandhills and blowout areas of eastern New Mexico. Considering the ever-increasing number of finds from in and around Roosevelt County, their study may provide additional information on meteorite type distribution and concentration mechanisms. In this study, three recent chondrite finds have been examined to determine their principal silicate mineralogy and petrographic type. All three were found in the vicinity of Milnesand, New Mexico at approximately 33°38' N, 103°20' W. Until more appropriate names can be assigned, the three chondrites will be referred to as Roosevelt County 1983a, 1983b, and 1983c respectively for the year and order in which they were reported. It is hoped that the data presented will contribute to the possible pairing of finds from within this relatively small geographical area.

Electron microprobe analyses of representative olivine and pyroxene grains are summarized in the Table below for each of the three chondrites. The first, Roosevelt County 1983a, is a weathered 96 gram chondrite fragment. In thin section its petrography is dominated by lithic fragments, relic chondrules and a few fresh metallic grains in a recrystallized matrix. Troilite and plagioclase were not observed in the section. Based on the data obtained, 1983a is described as an equilibrated H-5 chondrite. Roosevelt County 1983b is a weathered stone of 528 gram mass. Petrographically, lithic fragments, partial chondrules and a recrystallized matrix are evident. Kamacite, taenite and troilite are common, but plagioclase was not noted. This second stone is described as an equilibrated L-5 chondrite. The third stone, Roosevelt County 1983c is the largest and least weathered of the three, with a mass of 4.4kg . In thin section, a variety of whole chondrules are readily apparent. Metallic grains are few but fresh, with kamacite, taenite and troilite being noted. No plagioclase was observed. Based on its petrography and mineralogy, this third stone is described as an equilibrated H-4 chondrite.

TABLE 1.

Roosevelt county	Olivine	Pyroxene
1983a	Fa18.3 (PMD=2.18, N=11)	Fs16.2 (PMD=2.96, N=10)
1983b	Fa25 (PMD=1.60, N=13)	Fs21.1 (PMD=2.84, N=11)
1983c	Fa18.7 (PMD=2.35, N=12)	Fs16.9 (PMD=4.02, N=11)

SALEM METEORITE; Richard N. Pugh
Science Department, Cleveland High School, 3400 S.E. 26th, Portland, Ore. 97202

The Salem meteorite fell on a house in Salem, Oregon May 13, 1981. The time of the fall was 1:05 a.m., Pacific daylight time (07:05 G.M.T.). The location of the fall was lat. 44 degrees 58' 45" N., long. 123 degrees 58' 10" W., Marion County, Oregon.

Five fragments of the meteorite were recovered with a total mass of 61.28g. From studying the fragments it is believed about two-thirds of the total meteorite were recovered.

Dr. J.C. Evans, Senior Research Scientist, Bettelle Pacific Northwest Laboratories in Richland, Wasnington was sent the meteorite for analysis. The meteorite was found to be a LL5 amphoterite.

THE CHONDRITE HIGASHI-KOEN

A. Okada*, Masako Shima**, N. Takaoka*** and S. Murayama**
* The Institute of Physical & Chemical Research, Wako, Saitama
** National Science Museum, Ueno-Park, Taito-ku, Tokyo
*** Dept. Earth Sciences, Yamagata University, Yamagata

Higashi-koen meteorite fell in Fukuoka-ken, Japan (33°36'N, 136°26'E), on August 11, 1897. This stone was first described by Jimbo (1906), and later it was assigned to H5 chondrite (Van Schmus and Wood, 1967). After that no detailed work on the chemistry, mineralogy and petrography of the meteorite has been done. The fall of Higashi-koen was just three days after that of Nio (H3) in Yamaguchi-ken, Japan (34°12'N, 131°34'E) on August 8, 1897. Both sites are about 200 km distant one another. From this fact, we were interested in whether or not both meteorites had been derived from a single meteoritic body. Higashi-koen sample in Japan lost during the confusion after the World War II. The specimen used in this work was supplied from the British Museum by courtesy of Dr. R. Hutchison.

Chondrules and their fragments, 0.1-0.8 mm across, are buried in the fragile and granulated matrix which contains considerable amount of Ni-Fe and troilite. The outline of most chondrules is poorly defined from the surrounding matrix. The mesostasis between olivine and pyroxene crystals in chondrules is composed of clear plagioclase and fine-grained aggregate of plagioclase and clinopyroxene. The evidence of light to moderate shock effect is indicated by the presence of distinct undulatory extinction in every silicate grain and kink bands in a few olivine grains. Electron probe microanalysis shows that olivine is Fa:15-20 (Av. 18), ortho- and clinopyroxene are Fs: 14-19 (Av. 17), plagioclase is An:12, and kamacite contains 6.0 and 0.4 wt.% of Ni and Co, respectively. The thin section of Higashi-koen includes a basaltic fragment, 1.5 mm across, comprising 67 wt.% of plagioclase (An:24), 13 wt.% of olivine (Fa:17) and 16 wt.% of diopsidic pyroxene with very minor opaque grains. The lithic fragment could be a fractionation product from H-chondritic melt. Bulk chemical analysis and rare gas study of Higashi-koen are in progress.

References

Jimbo, K. (1906), T. Wada's Beiträge Min. Japan, No.2, p.50.
Van Schmus, W. R. and Wood, J. A. (1967), Geochim. Cosmochim. Acta, 31, 747.

Unique clasts with V-shaped REE pattern in L6 chondrites

N. Nakamura, Dept. Earth Sci., Kobe University, Nada, Kobe 657
K. Yanai, Natl. Inst. Polar Res., Kaga, Itabashi, Tokyo 173
Y. Matsumoto, Dept. Mineral. Sci. Geol., Yamaguchi University, Yoshida, Yamaguchi 753, Japan

We report here analyses of REE, Ba, Sr, Rb, K, Ca and Mg (by I.D.) and Rb-Sr isotopic measurements for two unique achondritic clasts in L6 chondrites, Yamato-75097 and -793241. The mineral composition of the clasts in Y-75097 is rather similar to but substantially different in details from Brachina (Yanai et al., 1983).

The Rb-Sr analyses for whole rock of Y-75097 clast (#64) yield $^{87}Rb/^{86}Sr=0.199$ and $^{87}Sr/^{86}Sr=0.71177\pm4$. The model age calculated from the Rb-Sr data and the Allende initial (Gray et al., 1973) is 4.5 ± 0.1 b.y. and thus compatible with an early igneous formation of the clast. The clast analysed in this work contains more CaO and K_2O and less MgO compared to that of Yanai et al., indicating heterogeneous distributions of minerals. From chemical data (Table 1) the mineral composition is estimated to be: olivine 75, plagioclase 25, merrillite $\leq$0.1%. Therefore, the sample analysed here may not sufficiently represent the whole clast but still show the unique chemical features as found by Yanai et al. Two clasts show the quite similar and remarkable REE fractionation with large positive Eu anomaly and V-shaped REE pattern (Fig. 1). This type of REE pattern would be the first ever reported for achondrites. It is worth noting that in spite of major-chemical similarity with Brachina (Nehru et al., 1983) these two clasts show marked difference in REE characteristics. The large positive Eu anomaly and the V-shaped REE pattern (Fig.1) suggest that plagioclase(+olivine) was the major phase which controlled the solid/liquid REE partitioning during the magmatic process resulting in formation of the clasts. It is thus considered that the clasts had been originally formed as solid (plagioclase + olivine) in fractional crystallisation or partial melting process followed by strong impact producing maskelynite.

Table 1. Chemical compositions

	Y-75097,64	Y-793241,81
MgO(%)	28.9(35.3*)	30.1
CaO(%)	0.58(0.30*)	0.65
K_2O(%)	0.11(0.08*)	0.06
Rb(ppm)	1.39	1.20
Sr(ppm)	20.2	17.7
Ba(ppm)	5.21	3.53

* Yanai et al. (1983)

Fig. 1. REE patterns

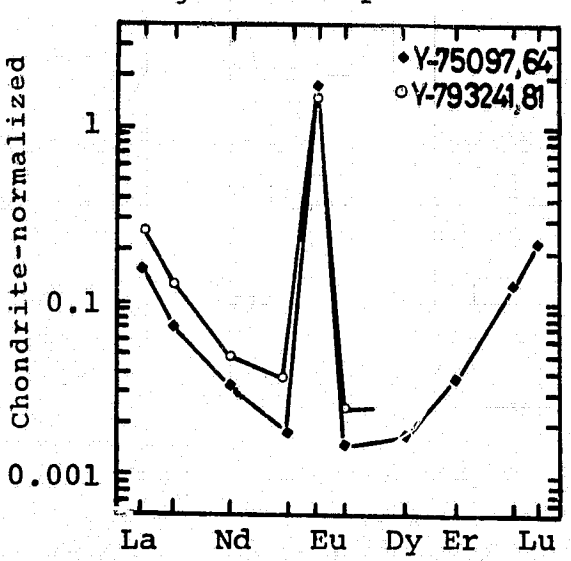

H CHONDRITIC CLASTS IN A YAMATO L6 CHONDRITE: IMPLICATIONS FOR METAMORPHISM; M. Prinz,[1] C.E Nehru,[1,2] M.K. Weisberg,[1,2] J.S. Delaney,[1] K. Yanai,[3] H. Kojima,[3] (1) AMNH, NY, NY 10024, (2) Brooklyn College, NY 11210, (3) NIPR, Tokyo 173, Japan.

Yanai et al. (1) gave preliminary results on a Brachina-like olivine-rich clast in the Yamato 75097 (Y75) L6 chondrite. The clast and host chondrite were analyzed for oxygen isotopes (2) and found to be H and L chondritic, respectively. Recently, a similar clast in the Yamato 793241 (Y79) L6 chondrite was found. The present study indicates that the two meteorites are paired and thus two clasts of this type are present in the meteorite. This is the first occurrence of H chondritic clasts in an L chondrite and the study was undertaken to determine the nature and significance of the clasts to chondrite genesis.

The Y75 clast is 2.5x2.5x0.8 cm, and the Y79 clast is of similar size. Both have sharp curved contact with the host. **Texture.** The clasts are fine to medium grained equigranular aggregates mainly of olivine and plagioclase; no pyroxene is found in either clast. A large (2 mm) relict barred olivine (BO) chondrule was found in the Y79 clast, which implies that this type of chondrule may be related to the clast origin. **Mode.** The two-clast average is 82% ol, 14% plag, 3% phosphate, 1% chromite. Phosphate is chloropatite and merrillite and is inhomogeneously distributed, with areas from 0-11% in the Y75 clast, and 0% in the Y79 clast; P_2O_5 in the wet chemical analysis of the Y79 clast indicates phos must be present. **Mineralogy.** The chondrite is typical of L group: ol, Fo_{76}; opx, En_{79}; cpx, Wo_8En_{48}; plag, An_{10}. The clasts are very similar to one another, and have the same ol and phos compositions as the host chondrite. The plag, however, is zonally distributed with distance from the clast-host boundary, and increases systematically from An_{10-22} in Y75, and An_{10-36} in Y79, over distances of about one cm; contour lines of the decrease in An content towards the host can be drawn. Portions of the Y79 clast have inhomogeneous plag compositions. Rare ilmenite is found in the Y79 clast. **Chemical Data.** Both clasts have been wet chemically analyzed (by H. Haramura) and are near-identical. Since the clast is olivine-rich the bulk composition differs significantly from average H chondrite; SiO_2, FeO and MgO are higher, and CaO and Al_2O_3 are lower. **Implications and Conclusions** of this study are: (1) The clasts in this L6 chondrite are superficially Brachina-like, but are related to H chondritic BO chondrules. (2) The host L6 chondrite is equilibrated, but the clasts are not. H chondritic olivine equilibrated with the host and developed the Fe/Mg ratio of L chondrites, but plag is not equilibrated. Since plag decreases in An content towards the host chondrite value, the original plag in the clast must have been considerably more calcic and was exchanging CaAl for NaSi with the host in an attempt to equilibrate with it. Since such diffusion is sluggish it has not reached the center of the clasts. (3) Oxygen isotopes have not equilibrated between clast and host, probably because there was no chemical potential or phase change to reorganize the oxygen. Olsen et al. (3) also showed that oxygen isotope exchange in an L6 chondrite involves transport of only a few millimeters. (4) Preliminary results on a study of BO chondrules in ordinary chondrites indicate that they are enriched in ol and plag, but often contain pyx in the higher grades. Pyx is not found in type 3 BO chondrules, but its components may be present in the glass. Thus, metamorphosed pyroxene-free BO chondrule material may represent a pyx-deficient end member of the BO chondrule compositional range. (5) The presence of H chondritic BO chondrule material in an equilibrated L chondrite implies incorporation and survival of fragments from another part of the solar nebula either early, during, or late in the L chondrite accretional history. (6) The lack of other recognizable H chondritic material in this meteorite implies that BO chondrule material can act as an independent entity at some stage in the chondrite formation process.

METEORITE CONCENTRATIONS IN ANTARCTICA -- HOW COMPLETE IS THE PICTURE?

J. O. Annexstad, NASA Johnson Space Center, Code SN2, Houston, TX 77058.

The importance of ice sheet flow as part of the process of concentrating meteorites in Antarctica is well known. Ford and Tabor (2) were the first to surmise that some type of ice sheet transport of Antarctic meteorites was likely considering that the Thiel Mountains pallasite was found on glacier ice without evidence of impact. Cassidy et al. (1) concluded that meteorites were carried by the ice to regions of high ablation where they were periodically uncovered. Three models of concentration have been proposed to explain the phenomena of meteorite accumulations on blue ice fields. Model I, suggested by Nagata (3) and illustrated pictorially by Yanai, is a general picture relating meteorite fall and accumulation to the entire Antarctic continent. Model II (4) is based upon the petrographic examination of an 8m ice core from the Allan Hills Icefield and suggests a local origin of ice from the catchment basin. The third picture is presented by Whillans and Cassidy (5) who infer, by using conventional ice flow concepts, a path length as long as 1,000km from the sites of fall to recovery for Allan Hills specimens. The Nagata-Yanai model assumes a steady state balance in the meteorite concentration zone between emergent ice gain and ablation losses. The model is useful in the macro sense but fails to account for the long terrestrial ages of the meteorites. Nishio et. al. suggest a fairly young age for the emergent ice at the Allan Hills using a short path length but fail to explain convincingly the large numbers of specimens found and the old terrestrial meteorite ages. The Whillans-Cassidy model assumes a steady state accumulation and ablation rate which needs to be tested with field data. Despite achievement of these working hypotheses, a number of questions must be resolved before a comprehensive model can be presented. Why are meteorites not found on every blue ice field? What is the flow path from the accumulation zone to the emergent zone? Are terrestrial ages of specimens related primarily to time spent encased within the ice? How rapidly does weathering deteriorate the meteorites? Does weathering occur while the meteorite is covered by ice? How old is the ice in the ablation area? Are the meteorite accumulation zones in steady state, are they growing or are they just local deficit areas? How important is the sub-glacial topography to meteorite concentration? Is there a relationship between the isotopic composition of the emerging ice and meteorite terrestrial ages? Some of these questions are under investigation and others will be examined in the future. As the search for meteorites continues it seems practical to continue the investigation of the role of blue ice in the concentration of specimens. The periodic remeasurement of established stake networks such as the Allan Hills triangulation net will help by providing long term base line data.

References:

(1) Cassidy, W.A., E. Olsen, and K. Yanai, (1977). Antarctica: A Deep-Freeze Storehouse for Meteorites. Science, 198, 727-731.

(2) Ford, A.B. and R.W. Tabor (1971). The Thiel Mountains Pallasite of Antarctica. U.S.G.S. Prof. Paper 750-D, D56-D60.

(3) Nagata T. (1978). A Possible Mechanism of Concentration of Meteorites Within the Meteorite Icefield in Antarctica. Mem. Natl. Inst. of Polar Res. (Japan), Spec. Issue 8, 70-92.

(4) Nishio F., N. Azuma, A. Higashi, and J.O. Annexstad (1982). Structural Studies of Bare Ice Near the Allan Hills, Victoria Land, Antarctica: A Mechanism of Meteorite Concentration. Ann. of Glac., 3, 222-226.

(5) Willians, I.A. and W.A. Cassidy (1983). Catch a Falling Star: Meteorites and Old Ice. Science, 222, 55-57.

PAIRING IN ANTARCTIC MESOSIDERITES; R.H. Hewins, Dept. of Geological Sciences, Rutgers University, New Brunswick, New Jersey 08903

Mesosiderites are classified according to their silicate matrix, which should also be used as the basis for pairing. ALHA 77219 and 81059 have very similar, fine-grained, little-recrystallized, plagioclase-poor matrix (subgroup 1B). Modal proportions of silicate minerals in matrix in ALHA 77219,8 are intermediate between those for ALHA 81059,13 and 81059,15. Matrix pyroxenes are very similar in Fe/Mg and Fe/Mn. ALHA 77219 and 81059 are probably a paired fall.

RKPA 80258 differs from the other Reckling Peak mesosiderites in containg some silicate matrix. This matrix consists of small plagioclase grains enclosing orthopyroxene grains poikilitically. This is thus a subgroup 2B mesosiderite and cannot be paired with the Allan Hills meteorites. Pyroxene in RKPA 80258,5 is dominantly En77-80, i.e. more magnesian than most pyroxene in all other Antarctic mesosiderites.

RKPA 79015, 80229, 80246 and 80263 must be classified as anomalous mesosiderites, since they lack silicate matrix. Orthopyroxenite clasts in ALHA 81059 are very similar in textures and modes to bulk RKPA 79015 but contain more Fe-rich pyroxene (En69 vs. En74). RKPA 79015 etc. can be paired with RKPA 80258 only on circumstantial evidence: it is necessary to find silicate matrix in the former or orthopyroxenite clasts in the latter to be certain of this pairing.

AN APPROACH TO THE METEORITE PAIRING PROBLEM AT THE ALLAN HILLS, ANTARCTICA. Ursula B. Marvin, Harvard-Smithsonian Center for Astrophysics, 60 Garden Street, Cambridge, Massachusetts, 02138

The distributions of all of the classified meteorite specimens collected during the 1976 through the 1982 field seasons on the Main and Near Western icefields of the Allan Hills region, Antarctica, have been plotted on a 1:8000-scale map. Separate overlays have been prepared to display the distribution pattern of each meteorite class. Several groups of specimens have been identified as possible candidates for pairing. For each of these groups, the thin sections are being reexamined and other types of available data (e. g. chemical analyses, age determinations, particle track histories) consulted in order to judge whether or not pairing is justified. Early results show fifteen L6 chondrite fragments in a tight cluster, which looks like a strewnfield, at the southern extremity of the Main Icefield. One group of L3 chondrites can probably be paired, as can a few other clusters. However, certain eucrites which were collected side by side, have markedly different textures and compositions, but other eucrites, lying farther apart and collected in different seasons, are virtually identical. The map patterns will be useful not only to indicate which specimens should be considered for pairing, but also which unpaired fragments may show comparable terrestrial ages or weathering histories. Detailed results of this analysis, which is still in progress, will be presented at the meeting.

TERRESTRIAL AGES OF ANTARCTIC METEORITES: L. Schultz and M. Freundel
Max-Planck-Institut für Chemie, D-65 Mainz, W-Germany

Terrestrial ages of Antarctic meteorites are important for an explanation of mechanisms of meteorite concentration on some blue ice fields in Antarctica. This timespan between the fall of a meteorite and the present can be obtained by the measurement of radioactive cosmic-ray-produced nuclides with suitable half-lives (e.g. 14-C, 81-Kr, 36-Cl, or 26-Al).

We have measured Ar, Kr (including 81-Kr) and Xe in three Antarctic meteorites: Allan Hills 77005 (shergottite), Pecora Escarpment 82502 (eucrite) and Elephant Moraine 82600 (eucrite). The terrestrial age of these meteorites is calculated from the "true" exposure age (derived from cosmogenic 38-Ar) and the "apparent" Kr-81-Kr-exposure age.Because of the decreasing activity of 81-Kr while meteorites are on earth the latter increases with terrestrial age of the meteorites.

At the moment preliminary results can be given only because the chemical composition of the measured samples is not yet available. For ALH77005 an exposure age of 3.6 mys and a terrestrial age of about 150 000 yrs are obtained. Due to the relatively large amounts of trapped Kr in this meteorite the terrestrial age is calculated using 78-Kr as stable monitor isotope and a production rate P(81)/P(78) of 2.5.

The exposure age of PCA82502 - found at a new meteorite concentration area about 2000 km from the Allan Hills region - is 21 mys and its terrestrial age is about 320 000 years. This terrestrial age is close to the mean terrestrial age of Antarctic meteorites. Exposure age and terrestrial age of EET82600 are 24 mys and 180 000 yrs, respectively. According to these preliminary data EET82600 may be paired with other Elephant Moraine eucrites like EET79005 or 79006.

The distribution of terrestrial ages of Allan Hills meteorites is compatible with a transport of meteorites in the ice without weathering and a destruction by weathering while lying on the surface of the ice. However, the rate of weathering in the Antarctic is smaller than that in moderate climats.

TRACE ELEMENTS IN ANTARCTIC H5 CHONDRITES: WEATHERING EFFECTS AND COMPARISON WITH NON-ANTARCTIC FALLS. J. E. Dennison, D. W. Lingner and M. E. Lipschutz, Dept. of Chemistry, Purdue Univ., W. Lafayette, IN 47907 USA

Of nearly 7000 Antarctic meteorites only relatively few are extensively studied as yet. However, these few show the Antarctic collection constitutes a trove for extraterrestrial genetic processes and terrestrial ice sheet dynamics [1]. Trace (ppm-ppt) elements provide important information since perturbing forces magnify small absolute concentration differences into large relative ones. The elements - Ag, Au, Bi, Cd, Co, Cs, In, Rb, Sb, Se, Te, Tl, Zn - provide significant genetic clues to because of geochemistry, volatility or mobility [e.g. 2-4].

For genetic inferences, we must know if Antarctic residence affects meteoritic compositions. We studied both this and the constancy over time of the near-earth meteoroid complex by using RNAA to determine these trace elements in numerous H5 chondrites. We chose unpaired samples of weathering types A-C (i.e. minor to extensive metal grains alteration) or that contain weathering rind: most have known cosmogenic radionuclide contents.

We have completed 2 type A, 6 type B (plus 3 weathering rinds) and 8 type C chondrites: others are in progress. We compare data for various populations using a single-sided upper-tail t test. Interior portions of weathering type C differ most clearly from those of type A and B: Bi, Cs and Sb differ significantly at >90% confidence level with Ag, In, Se and Tl being possibly significant (i.e. 85-89% confidence level). All indicate leaching from H5 chondrites of weathering type C. Data for weathering rinds define no coherent trend. Thus, meteorites of types A and B are compositionally unaffected by Antarctic residence and are as reliable as those for non-Antarctic falls [5]. Even the most heavily weathered H5 chondrites seem little affected.

For comparison with non-Antarctic H5 falls [4], we used chondrites of weathering types A and B, including type C only for Au, Cd, Co, Cs, Rb, Te, and Zn. Au, Bi, Sb, Se and Tl are significantly higher in Antarctic samples with Cd, In, Rb, Zn and possibly Ag being significantly lower. Hence, significant reason exists to doubt parent population identity in the meteoroid complex sampled 0.1-0.7 My ago by Antarctica and today by earth. This reflects differing debris proportions from major impacts on different H5 parent regions with time [cf. 6]. If a temporal change in the near-earth meteoroid complex is borne out by further experiment, the Antarctic collection provides a snapshot in time and is even more valuable than thought.

REFERENCES: [1] C. B. B. Bull and M. E. Lipschutz, Workshop on Antarctic Glaciology and Meteorites, LPI Tech. Report 82-03, 57 pp. (1982). [2] S. Biswas, T. Walsh, G. Bart and M. E. Lipschutz, Geochim. Cosmochim. Acta 44, 2097-2110 (1980). [3] T. J. Huston and M. E. Lipschutz, Geochim. Cosmochim. Acta 48, in press (1984). [4] D. W. Lingner, T. J. Huston and M. E. Lipschutz, 47th Annual Meeting, Meteoritical Soc. (1984). [5] S. Biswas, T. M. Walsh, H. T. Ngo and M. E. Lipschutz, Proc. Sixth Symp. Antarctic Meteorites, 221-228 (1981). [6] J. N. Goswami and K. Nishiizumi, Earth Planet. Sci. Lett. 64, 1-8 (1983).

LUNAR METEORITES IN JAPANESE COLLECTION OF THE YAMATO METEORITES

K. Yanai and H. Kojima; National Institute of Polar Research, Tokyo 173
T. Katsushima; Hokkaido University, Sapporo 060

Yamato-791197 meteorite collected in November 1979 had been reported as an anorthositic breccia which is very similar to the some of lunar rocks(Yanai and Kojima). One another specimen of the Yamato meteorites has been classified as more an anorthositic breccia. This specimen was collected on the bare ice surface near the Yamato Mountains by Japanese Antarctic Research Expedition Team in 1982-1983 field season. This specimen is nearly half stone, 36.67 grams and covered with less fusion crust, but it has some smooth surface which is corted with yellowish-tan colored. Fresh surface and interior show grey to light grey color. This specimen consists of aboundant clasts which range from millimeter to one centimeter, and they show dark to black and white in color in a light grey matrix.

The section of the specimen shows numerous clasts which made of melt fragments, crystalline fragments and brecciated lithic fragments in matrix. There are two type clasts of polymineral and monomineral in the section. The clasts are polymineralic which are composed of most plagioclase with minor pyroxene and olivine, and plagioclase-pyroxene. The smaller clasts are individual mineral fragments of most plagioclase and with some pyroxenes and minor of olivine. Most of melt fragments showing brown color are divitrified and contain fine plagioclases and minor pyroxenes. In the rare case the specimen contains small glass spherules. The clasts of the crystalline rock fragments show a variety of texture including diabasic, basltic and granulitic, and most of them have been shocked more or less. Matrices of the specimen consist of two part of brown color area and light area which shows a divitrified and recrystallized textures.

Microprobe analyses show that feldspar ranges from An88 to 97.6 with most analysis following between An93.5 and An96.5, and they are containing 1.3% (maximum) of Or component; pyroxene and olivine is variable in composition, pyroxene: Wo2.9-43.2, En13.8-79.1, Fs8.1-57.6 and olivine, Fo61.3-89.1 were analyzed. MnO content of the both pyroxene and olivine are lower than theirs of the all achondrites, but they are very similar to the some of lunar rocks, especially anorthositic breccia.

This specimen shows a brecciated texture of numerous lithic fragments, which is common occurrences in the most polymict eucrites and howardites, but it is different from eucrites and howardites in most respects of mineralogically, chemically and others.

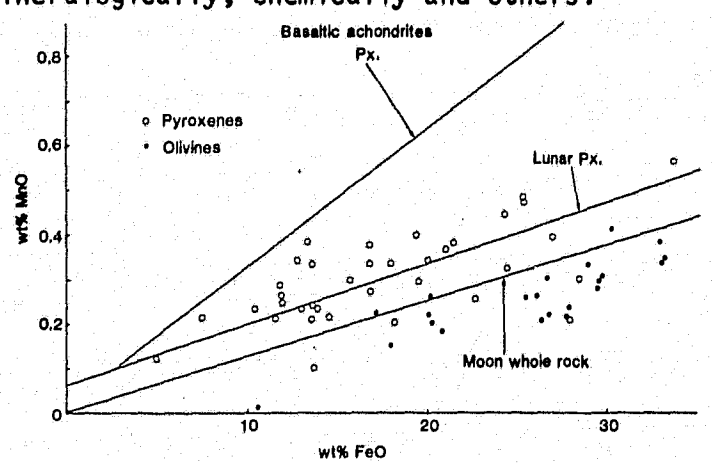

Figure 1. MnO-FeO value of pyroxens and olivines as compared with those of lunar and achondritic pyroxens and moon whole rock analyses. (After Stolper et al. 1979)

CRATER AGES, COMET SHOWERS, AND THE PUTATIVE "DEATH STAR";

E. M. Shoemaker and R. F. Wolfe, U.S. Geological Survey, Flagstaff, AZ 86001

Ages of relatively well dated impact structures larger than 3 km diameter formed in the last 150 Ma are distributed chiefly in clusters. Aside from a cluster near the present, which can be explained by a bias in the recognition of young craters, the three most prominent clusters are centered around ~38 Ma, ~67 Ma, and ~98 Ma. The 38 Ma cluster is broadly associated in time with two globally distributed microtektite horizons; the 67 Ma cluster is roughly centered around a globally distributed noble metal-bearing claystone at the Cretaceous-Tertiary boundary. All three clusters are broadly associated in time with major mass extinctions identified by Raup and Sepkoski (1). These associations suggest that the clusters of crater ages may reflect genuine surges or peaks in the rate of bombardment of the Earth.

As first noted by Hills (2), surges in the flux of Earth-crossing comets might be produced by occassional close encounters of stars with the sun. These near encounters would induce showers of Earth-crossing comets from a postulated massive reservoir of comets inside the Oort halo of the comet cloud. From our theoretical study of the structure of the inner comet reservior (3), we conclude that relatively strong comet showers have been produced at an average interval of a few tens of millions of years from the combined perturbations of the inner reservoir by passing stars and by giant molecular clouds. These showers should have been largely episodic, but they may have been weakly periodic as a result of periodic motion of the sun normal to the plane of the galaxy (cf. 4) and quasiperiodic passage of the sun through galactic spiral arms (cf. 5).

Alvarez and Muller (6) and Rampino and Stothers (4) suggested that the surges in cratering rate have been strongly periodic, and they linked this periodicity with an apparent strong periodicity in mass extinctions found by Raup and Sepkoski (1). The latter apparent periodicity has inspired the hypothesis of a distant solar companion star that produces a death-dealing comet shower at each perihelion passage (7,8). From 2,000 Monte Carlo simulations of the dynamical history of relatively distant hypothetical solar companions, we find that there is, at most, one chance in 1,000 that the sun had a companion star at the distance required to account for the apparent period of recurrence of mass extinctions and whose orbit was also sufficiently stable to cause a periodic sequence of extinctions over the last 245 Ma. If the apparent strong periodicity of mass extinctions and correlated crater ages is not a statistical fluke, we are unaware of a satisfactory explanation for it.

References: (1) Raup, D. M., and Sepkoski, J. J., 1984, Proc. Nat. Acad. Sci, v. 81, p. 801-805; (2) Hills, J. G., 1981, Astron. Jour., v. 86, p. 1730-1740; (3) Shoemaker, E. M., and Wolfe, R. F., 1984, Lunar and Planet. Sci. XV, pt. 2, p. 780-781; (4) Rampino, M. R., and Stothers, R. B., 1984, Nature, v. 308, p. 707-712; (5) Napier, W. M., and Clube, S. V. M., 1979, Nature, v. 282, p. 449-455; (6) Alvarez, Walter, and Muller, R.A., Nature, v. 308, p. 718-720; (7) Whitmore, D. P., and Jackson, A. A., 1984, Nature, v. 308, p. 713-715; (8) Davis, Marc, Hut, Piet, and Muller, R. A., 1984, Nature, v. 308, p. 715-717.

IRIDIUM SEDIMENTATION IN THE CENOZOIC; NO EVIDENCE FOR A DEATH STAR

Frank T. Kyte, Institute of Geophysics and Planetary Physics, University of California, Los Angeles, CA 90024, USA.

LL44 GPC-3 is an abyssal clay piston core from the central North Pacific which contains a nearly complete record of sedimentation for the last 70 Ma. To date, we have determined Ir in sections covering approximate time spans of 1.5-4 Ma, 32-43 Ma, and 63-66 Ma, including much of the Pliocene and the Eocene-Oligocene (EO) and Cretaceous-Tertiary (KT) boundaries. We have preliminary data on a new section which connects the EO and KT sections, giving continuous coverage from 32-66 Ma. These profiles will be useful in determining fluctuations in Ir sedimentation in the Cenozoic which may reflect major accretionary events, fluctuations in the interplanetary dust density, or terrestrial processes. They can also be used to constrain models such as the periodic comet showers recently proposed to explain a reported periodicity in terrestrial extinctions.

For comparison to recent abyssal clays we can use the inverse correlation between sedimentation rate and Ir concentration noted by Barker and Anders (1968) where $Ir(ng/g)=(0.14\pm0.07)/r(m\ Ma^{-1})$. This is equivalent to an Ir accumulation rate of 14 ng cm^{-2} Ma^{-1} for sediments with a bulk dry density of 1 g cm^{-3}. A lower limit on the extraterrestrial Ir fraction is ~10 %, or a flux of 1.4 ng cm^{-2} Ma^{-1}, similar to estimates from astronomical and microcrater studies of the micrometeoroid flux (Hughes, 1976). The actual extraterrestrial fraction is probably somewhat higher.

In the analyzed sections, the KT boundary remains unique in having a large excess of Ir relative to recent sediments. High Ir concentrations are mainly in a 30 cm section from 20.3 to 20.6 m. The total Ir across a 90 cm section bracketed by 0.4 ng/g Ir backgrounds is 190 ng cm^{-2} and the excess is estimated at 150 ng cm^{-2}. Our data also show small Ir peaks with approximate ages of 35, 40, and 46 Ma, but these contain <30 ng cm^{-2} excess Ir and may in part reflect variations in sedimentation rates. Possible and more interesting sources are the Late Eocene North American microtektite event or ejecta from the 100 km Popigai crater (39±9 Ma).

These results impose some rather severe constraints on recently proposed periodic comet showers. Events of this magnitude (incursion of a cloud of $>10^9$ comets into the inner solar system over ~1 Ma) should increase the interplanetary dust cloud sufficiently to cause large increases in Ir background sedimentation rates. Since most stratospheric dust appears to have a cometary origin, the conservative estimate of 1.4 ng cm^{-2} Ma^{-1} for the extraterrestrial contribution to Ir sedimentation can be used as an estimate of the modern cometary dust component. The influx during a cloud incursion of as much as 10 to 100 times more comets than during between-shower periods (~25 Ma) predicts an excess of 350 to 3500 ng Ir cm^{-2} during each shower. The KT Ir excess of 150 ng cm^{-2} is >2 to 20 times lower than expected. Comparison with other KT boundaries in locations with higher sedimentation rates indicate that the breadth (30 cm) of the peak resulted from bioturbation, not increased backgrounds. The EO portion of the section, another proposed comet shower period, provides a more severe test of the comet shower models. There is no evidence of worldwide siderophile deposition at this time. The Ir excess is at least a factor of 10 to 100 times less than expected. One could attempt to salvage the model by adjusting the orbital properties of the Death Star to scale down the size of the cometary cloud, but this reduces the impact rate proportionately and makes it less likely that this model can account for the major mass extinction events.

KILAUEA VOLCANO AEROSOLS: EVIDENCE IN SIDEROPHILE ELEMENT ABUNDANCES FOR IMPACT-INDUCED OCEANIC VOLCANISM AT THE K/T BOUNDARY.

A. R. Hildebrand,[1] W. V. Boynton,[1] and W. H. Zoller,[2] [1] University of Arizona, Tucson AZ 85721,[2] Los Alamos National Laboratory, Los Alamos NM 87545.

The Kilauea volcano on Hawaii represents hot spot volcanism in oceanic crust. Eruptive activity increased in 1983, resulting in the discovery of siderophile element enrichments in Kilauean aerosols, including an Ir:Al ratio 17,000 times its value in Hawaiian basalts.[1] The mechanism of siderophile element enrichment is poorly understood, particularly for normally refractory elements such as Ir, but it may be related to Kilauean volcanism having a mantle source. No other sampled volcano has shown such siderophile element enrichment, but no other volcano representing hot spot volcanism in oceanic crust has yet been sampled for siderophile elements.

Instrumental neutron activation analyses of Kilauean aerosols collected in 1984 show Ir:Au:Re ratios of 1:13:2000 normalized to CI chondrites. The large Re enrichment in these volcanic aerosols may explain the 3 to 15-fold Re excess, relative to chondritic, in the observed siderophile element signature of the Cretaceous-Tertiary boundary clay layer.[2,3] Strong evidence exists that an impact of an extraterrestrial body on the Earth caused mass extinctions at the end of the Cretaceous period.[4,5] If the projectile impacted ocean crust, fracturing of the lithosphere may have allowed volcanism to begin. A Kilauean aerosol contribution of only 0.01% of the chondritic component in the boundary clay layer would produce the observed Re enrichments. However, Kilauean-type aerosols cannot account for the other observed siderophile element abundances in the boundary clay layer. Alternate mechanisms for the observed Re enrichments include deposition of terrestrial rhenium from seawater because of a change in marine chemistry, or a Re-enriched projectile. The latter hypothesis seems unlikely since Re is not known to fractionate from Ir in any siderophile element-rich meteorites; the former hypothesis can be tested with analyses of non-marine boundary clays.

Impact-induced volcanism may have contributed to extinction mechanisms based on acidification or atmospheric dust. If the volcanism were of sufficient duration and magnitude, an atmospheric dust load could have been maintained for years instead of the months predicted from an impact.[6] Acids produced from the volcanogenic sulfur emissions could have augmented the nitrogen oxide acids produced by the shock wave of the projectile.[7]

Even if no bioturbation or secondary chemical dispersion occurred, Re should be distributed through the boundary clay layer for a thickness representing the duration of the volcanism. Because the volcanogenic Re is dispersed only by the atmosphere, a Re "halo," modified by prevailing winds, should surround the impact site, unlike the other siderophile elements, which were probably dispersed globally on ballistic trajectories.

A high velocity comet may produce approximately the same extinction effect as a low velocity nickel-iron asteroid, but will produce a siderophile element geochemical signature two orders of magnitude smaller. If the projectile impacts ocean crust, the volcanogenic Re signature will be the salient siderophile element signature of the extinction-causing impact.

1. Zoller, W. H., et al., Science, 222, 1118-1121, 1984. 2. Ganapathy, R., Science, 209, 921-923, 1980. 3. Kyte, F. T., et al., Nature, 288, 651-656, 1980. 4. Alvarez, W., et al., Science, 223, 1135-1141, 1984. 5. Bohor, B. F., et al., Science, 224, 867-869, 1984. 6. Pollack, et al., Science, 219, 287-289, 1983. 7. Lewis, J. S., et al., Special Paper 190, 215-221, 1982.

HYDROTHERMAL ALTERATION OF SUEVITE IMPACT EJECTA AT THE RIES METEORITE CRATER, F.R. GERMANY; H.E. Newsom[1] and G. Graup[2], [1]Max-Planck-Inst. f. Chemie, 6500 Mainz, F.R.G., [2]Inst. Geowissenschaften, Univ. Mainz, FRG.

We are studying alteration processes in suevite at the Ries crater to address two problems. First, was the observed alteration produced by hydrothermal fluids circulating through the hot ejecta after emplacement (1) or by alteration during ejection (2)? Second, were impact ejecta deposits on Mars similarly altered to have provided a significant source of clay minerals to the martian soil (1,3)?

Our field investigation of suevite at the Otting outcrop has revealed evidence for alteration by hot fluids. The most obvious evidence is the abundance of vertical channels (4) also seen in some other Ries outcrops. We have measured the number and width of channels in 36 sections 2 m wide. Most of the channels are 2 to 4 cm wide (Fig. 1) and the channels occupy 5 to 10% of the upper portions of the outcrop (Fig. 2). The size and number of channels seems to decrease toward the base of the suevite. Within the channels the fine grained matrix has been removed, possibly by rising steam, leaving only coarse fragments which appear to be coated with a light brown clay. Other evidence for hydrothermal fluids in the Otting suevite include the presence of quartz amygdules and previous observations of calcite cementation and deposition of calcite in the upper portion of the underlying bunte breccia (5). In thin section, we and others have observed clay coatings on vesicle walls and other alteration minerals such as calcite and zeolites (4, 6). Despite the evidence for hydrothermal alteration, significant amounts of glass in the suevite at Otting remains unaltered, even in the vicinity of the channels. The Otting site is outside of the morphologic crater rim and the suevite overlies 45 m of bunte breccia, suggesting a limited supply of groundwater. The crater suevite, in contrast, is much more extensively altered to clays and zeolites (7), because more groundwater was available.

We conclude that alteration of suevite impact deposits, both inside and outside of the crater, has occurred by hydrothermal circulation of groundwater, and has produced the observed clays and channel features. The magnitude of alteration in impact deposits can be easily underestimated from studying coherent and intact samples or cores (e.g. 6). Hydrothermal alteration of suevite was important at the Ries crater, and the alteration of impact ejecta may also provide a major source of clay minerals in the martian soil.

Refs. (1) Newsom (1980) Icarus 44, 207. (2) Kieffer and Simonds (1980) Rev. Geophys. and Space Phys. 18, 143. (3) Berkley and Drake (1981) Icarus 45, 231. (4) v. Engelhardt (1972) Contrib. Min. Pet. 36, 265. (5) Wagner (1965) Jh. Geol. Landesamt Baden-Württemburg, 199. (6) Allen et al. (1982) J.Geophys. Res. 87, 10083. (7) Stähle and Ottemann (1977) Geologica Bavarica 75, 191.

Fig. 1

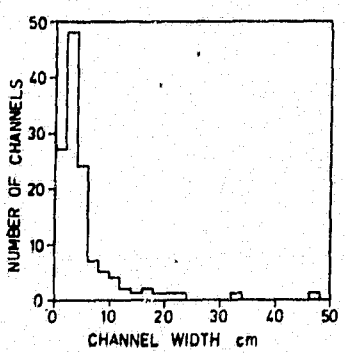

Fig. 2

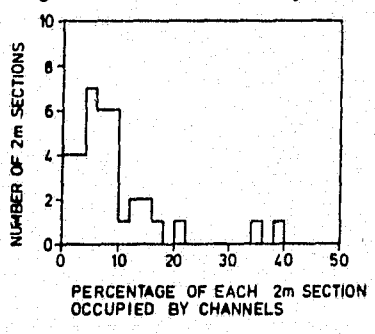

SEARCHING FOR IMPACT CRATERS USING SPACE SHUTTLE PHOTOGRAPHY;
C. A. Wood, NASA/Johnson Space Center, Houston, TX 77058; and C. Dailey, W. Daley, and G. Wells, LEMSCO, Houston, TX 77058.

Extrapolation of impact cratering rates derived from Canada and Europe[1] suggests that in the cratonic regions of Australia, India, Africa, and Brazil, 14-15 impact craters >20 km diameter should have formed during the last 120 my, and survived erosional erasure. In fact, in these areas, only 2 craters are known that approximately qualify: Gosses Bluff, 22 km, 130±6 my old, and Strangways, 24 km and 150±70 my old. It is therefore likely that about a dozen relatively large and preserved impact craters await discovery in these less explored cratons. A larger number of younger and smaller craters must also exist. We now report an informal search for impact craters using photographs obtained by Shuttle astronauts. Photographs taken with the 250 mm lens on Hassalblad cameras have a resolution of >25 m and cover a nominal area of 60x60 km^2. A larger format Linhof camera with similar resolution but 4 times larger area was flown March 1984, and will fly again in the future. Shuttle imagery has numerous advantages in looking for impact craters and for other types of earth observations. The cameras use color film, and pictures can be taken at any sun angle (thus emphasizing low relief structures or, alternatively, albedo contrasts), and at any look angle (oblique to vertical). Most importantly, the cameras are in the hands of intelligent and trained observers ("smart sensors") who can recognize and photograph unusual structures in real time. One final advantage of the astronaut photography -- it is essentially free, whereas it now costs $1000 to request that LANDSAT obtain an image of a particular scene!

During the first 11 missions of the Space Shuttle, 5 known impact craters have been photographed, as have at least 5 additional crater-like structures. The known impact craters are Manicouagan, Gosses Bluff, Bushveld, Vredefort, and Roter Kamm. During future flights, other known impact sites will be targeted for photography, allowing the gradual compilation of an atlas of terrestrial impact craters for comparative studies.

Of the 5 crater-like objects thus far seen, one, the Richat structure, is a well-known eroded anticline. A second structure is a 5 km wide, central-peak crater in Paraguay. Although located within 250 km from the Parana flood basalts, this unknown crater seems more likely to be associated with volcanism than impact. Another fresh-looking, 8 km wide crater was photographed in eastern Siberia. This structure occurs in a non-volcanic area and appeared very likely to be a previously unrecognized impact. A literature search revealed, however, that it is a 120 my-old pluton! A much larger (130 km) but more poorly defined semi-circular feature was noticed by the crew of the STS-11 mission while passing over NE Australia. The circularity is largely due to the arcuate trace of the northern end of the Diamantina River; the rocks in this area are Mesozoic and non-volcanic. Should this be an ancient impact crater, little surface expression remains. The Aorounga structure of northern Chad might be an impact. It is a 12 km wide, double ring crater with a central mound. Although it is only 80 km south of the Tibesti volcanic complex, the structure is formed in Devonian sandstones. No one has visited Aorounga; it might be a ring dike or it could be an impact crater.

The uncertainty in interpretation of the crateriform structures described here is a warning against too glib an acceptance of an impact origin for various unusual circular features on Venus and Mars.

Ref. (1): Grieve, R. A. F. (1984) Proc. Lunar Sci. Conf. 14th, p. 3403-8; JGR 89 supplement.

SHATTER CONES: DIFINITIVE CRITERIA FOR METEORITE IMPACT;

Robert S. Dietz and John F. McHone, Department of Geology, Arizona State Univ. Tempe, AZ 85287

Shatter coning, a distinct form of shock fracturing, creates cones of rock on which are superimposed packets of horsetail-like striations. Cone apexes commonly point toward ground zero and thus vector the explosion and show that a force came from above--as from an exogenic event. Shatter cones are currently identified in 51 astroblemes (ancient impact scars) and one modern meteorite crater (Bosumptwi, Ghana). Conical structures (e.g. cone-in-cone) are widespread in geology, but shatter cones are distinct and usually are positively identifiable. No example has yet been found in explosion structures which are clearly volcanic. In many cases, shatter coning was the initial field indication of a putative astrobleme. When shatter coning is unquestionably identified we regard this as a definitive criterion of impact.

There are rare occurrences of inverted cones with apexes pointing in the direction of shock wave propagation. These appear never to be isolated but are associated point-to-point or base-to-base with normal shatter cones. Although best developed in limestones and dolomites, and most rudely developed in granites, shatter coning is independent of rock type. Shatter cones were first reported by Branca and Frass from the Steinheim Basin in Germany in 1903, but it remained to Dietz in 1947 to associate them with meteorite impact. Two recent discoveries are at Logancha, Siberia and at Glover Bluff, Wisconsin where they were found in 1983 by William Reed.

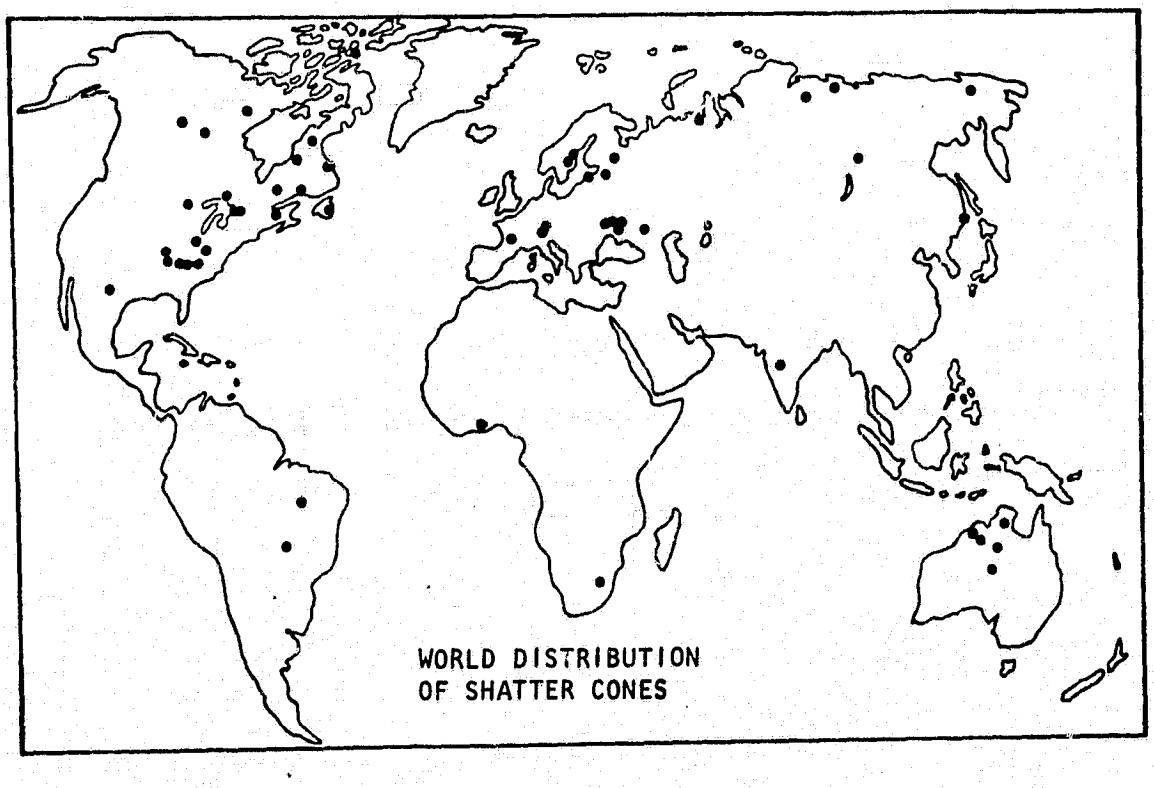

WORLD DISTRIBUTION
OF SHATTER CONES

COESITE AND STISHOVITE DETECTED IN NATURAL CONCENTRATIONS BY SOLID-STATE SILICON-29 NUCLEAR MAGNETIC RESONANCE; John F. McHone, Tryggvi I. Emilsson, Wang-Hong Yang, R. James Kirkpatrick, Norma Vergo, and Eric Oldfield
University of Illinois, Urbana, IL 61801

Coesite and stishovite, minerals important for verifying suspected impact structures, are silica polymorphs formed by strong pressure pulses from meteoroid impacts and large synthetic explosions. Conventionally, these phases are detected on X-ray diffractograms of insoluble residues from quartz-rich samples digested in aqueous HF. This method has several disadvantages: the procedure is destructive, glassy fractions and some coesite are destroyed by HF; pressure polymorphs typically form in microscopic granules which can be lost during concentration or may be too small for X-ray analysis; and X-ray peak positions may be superimposed and difficult to identify with certainty.

Smith and Blackwell, using magic angle sample spinning (MASS) solid-state silicon-29 nuclear magnetic resonance (NMR) techniques, examined silica polymorphs and characterized MASS NMR spectra for purified samples of natural coesite and stishovite (1). NMR theory and techniques are presented in the literature (2,3). We have examined with NMR a whole rock sample of shocked Coconino sandstone from Barringer (Meteor) Crater, Arizona. The resulting spectrum, referenced to a tetramethylsilane standard, (Fig. A) clearly shows twin peaks diagnostic of coesite (-108.652 and -114.434 ppm) and a smaller single peak indicative of stishovite (-191.693 ppm). Although more than 70% of this sample is quartz, the quartz NMR signal has been selectively eliminated by using a short 5 second recycle interval between radio bursts. Areas beneath the remaining polymorph peaks provide an estimate of the abundance of coesite relative to stishovite - in this case about 30 to one, respectively. A powder X-ray diffractogram of the same whole rock sample (Fig. B) clearly shows peaks attributable only to quartz and coesite; stishovite signals are too weak to be identified with confidence. X-ray data also indicate a lack of significant glassy components in the sample.

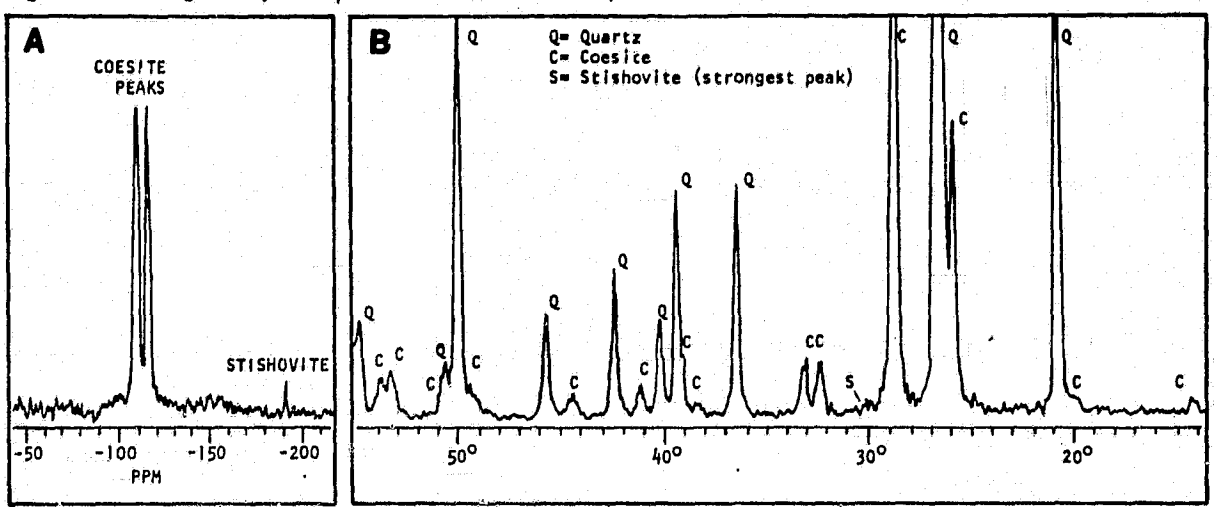

Nuclear magnetic resonance (A) and X-ray diffraction (B) spectra for shocked Coconino sandstone containing coesite and stishovite.

References: (1) Smith, J.V. & Blackwell, C.S. Nature 303, 223 (1983). (2) Lippmaa, E., Magi, M., Samoson, A., Engelhardt, G., & Grimmer, A.-R. J. Am. chem. Soc. 102, 4889 (1980). (3) Lippmaa, E., Magi, M., Samoson, A., Tarmak, M. & Engelhardt, G. J. Am. chem. Soc. 103, 4992 (1981).

THERMOLUMINESCENCE AGE OF METEOR CRATER, ARIZONA S. R. Sutton, Earth and Planetary Sciences Department and McDonnell Center for the Space Sciences, Washington University, St. Louis, MO 63130 USA.

Thermoluminescence (TL) dating has been applied to shocked sedimentary rocks from Meteor Crater, Arizona. Impact craters are, in principle, datable using TL because the high temperatures experienced by the target rocks resets their "pre-impact" TL and TL reaccumulation then occurs due to natural radioactivity exposure. The TL emitted by these rocks today is, therefore, a measure of the crater's age. Crucial to the success of this application was the identification of sufficiently shock-heated specimens. The shock threshold for resetting Coconino sandstone natural TL was evaluated using two approaches, one empirical and the other theoretical. The empirical determination was obtained from the observed dependence of natural TL (expressed as equivalent dose) on petrographic shock grade (1). The theoretical estimation was based on a kinetic model for thermal decay of TL and previous shock temperature calculations (2). The two results are consistent and indicate a shock threshold for TL resetting corresponding to petrographic shock class 2 as defined by Kieffer (1), a shock pressure of 100 kbars (10 GPa) and shock temperature of 680 °C.

Suitable Coconino specimens for TL dating are, therefore, those shocked to shock class 3 (i.e., exhibit plastically-deformed grains, cryptocrystalline coesite cores and abundant quartz cleavage) or greater. Such samples have TL sensitivities less than 0.45 that of unshocked Coconino and exhibit equivalent dose (E.D.) curves which are much lower than those of unshocked specimens and possess extended plateaus. Kaibab specimens possess E.D. curves analogous to those of Coconino sandstone and suitable Kaibab specimens for dating were, therefore, identified as those with extended plateaus. In this manner, 4 sandstones and 4 dolomites were selected for the dating measurements.

Accurate TL dating required the evaluation of two quantities for each of the eight shock-metamorphosed rocks, post-impact radiation dose and dose-rate. The former was evaluated using TL measurements on quartz mineral separates. Evaluation of the latter required detailed knowledge of the mineralogy, petrology and radioactivity of each specimen, properties which were studied using INAA, AAS, fission tracks, electron microprobe and cathodoluminescence. The mean ages for sandstones and dolomites were reasonably consistent, 51,300 and 46,000 years, respectively. Considering the fact that the doses and dose-rates varied by up to an order of magnitude, this age concordancy for the two different rock types is considered good evidence that pre-impact TL was indeed sufficiently reduced by shock heating. The overall mean age, 49,900 ± 2,900 years, is a factor of two older than the previous best estimate, 25,000 ± 5,000 years (3), which was based on the inferred correlation of pluvial episodes at the crater with $\delta^{18}O$ maxima observed in lake and ocean sediment sequences.

REFERENCES: (1) Kieffer, S. W. (1971) "Shock metamorphism of the Coconino sandstone at Meteor Crater, Arizona," JGR 76, 5449-5473. (2) Ahrens, T. J. and V. G. Gregson, Jr. (1964) "Shock compression of crustal rocks: data for quartz, calcite and plagioclase rocks, JGR 69, 4839-4874. (3) Shoemaker, E. M. (1983) "Asteroid and comet bombardment of the Earth", Ann. Rev. Earth Planet. Sci. 11, 461-494.

THE CIRCULAR STRUCTURE AT GLOVER BLUFF: WHAT AND WHERE IT IS

W. F. Read, Dept. of Geology, Lawrence University, Appleton, Wis.

Impact structures are generally circular in plan: a circle of excavated rock in the case of a crater, of deformed rock if the crater has been eroded away and only its underpinnings remain. Assuming, on the strength of its shatter cones, that Glover Bluff is indeed an impact structure, we infer that the circle in this case is concealed under glacial drift.

It is clear that the deformed Ordovician dolomite of the Bluff has been dropped down a couple of hundred feet. Two mechanisms for dropping down are commonly evident in impact structures: slumping on the sides of craters, peripheral downwarping or downfaulting in crater substructures. Fortunately, a fair number of water wells have been drilled down to bedrock around Glover Bluff. In all known cases the first, usually the only, bedrock encountered is sandstone. Evidently there is no circular belt of dolomite extending under cover beyond the Bluff. So slumping on the side of a crater appears in this case to be the better bet. A conglomerate between the dolomite and underlying Cambrian sandstone in the Bluff contains as much or more material derived from the dolomite as from the sandstone. It can reasonably be explained as the product of friction between a downsliding slab of fairly well indurated dolomite and less well indurated sandstone beneath it. Both dolomite and sandstone seem to have undergone a good deal of internal plastic deformation. Impact may have occurred while sedimentation was still in progress.

In both quarries where the dolomite is well exposed its overall dip is northward. This suggests that the crater into which it was sliding lies to the north--a conclusion apparently consistent with the orientation of shatter cones though it is difficult, where the shatter cones are developed, to restore the rock layers to their pre-impact position. The fact that water wells to the north, as elsewhere, have run into sandstone where they reached bedrock and have run into it at random depths suggests that the crater was filled with sand. It would be a simple matter to plot the crater's outlines from well records if there were some conspicuous difference between the sandstone inside the crater and the Cambrian sandstone around it. Unfortunately there are no known exposures of the fill. However, sandstone drill cuttings from a limited area north of the Bluff are known or said to be nearly pure white as compared with the shades of yellow and red characteristic of the Cambrian. Microfossils, especially conodonts, seem to offer the best hope of identifying the crater fill as definitely post-Cambrian. Where wells have gone on through the fill, cuttings from a layer of fallback material may be recognizable.

Exposures of what appears to be undeformed Cambrian sandstone, capped in some cases by dolomite, set limits to the extent of the crater. To the south, southwest, and southeast of the proposed crater site, the nearest of these exposures lie in an arcuate pattern. If the arc is extended it forms a circle something like seven miles in diameter with its center bearing about 15° west of north from Glover Bluff. A single small exposure to the north happens to lie just outside this circle. The boundaries of the crater, or what remains of it, must lie on or inside this circle.

LUNAR PALAEOMAGNETISM, POLAR WANDERING AND THE EXISTENCE OF PRIMEVAL LUNAR SATELLITES.

S.K.Runcorn, School of Physics, The University, Newcastle upon Tyne, NE1 7RU, England.

Magnetism was discovered in the returned Apollo samples from the Moon and parts of the lunar crust were found to be magnetized from satellites. The origin of this magnetism has been a mystery because it is known that the Moon today, unlike the Earth, has no magnetic field. The strength of the magnetic field responsible for the magnetization 4×10^9 years ago is twice the present Earth's field and decayed exponentially to about 1/5th of this value at 3.2×10^9 years. From palaeomagnetic directions conclusive evidence has been obtained that the Moon had a magnetic field at least between 4.2×10^9 and 3.2×10^9 years ago and it is concluded that this was generated in a small iron core. Determinations by Coleman, Russell and Hood of the directions of magnetization of the crust from the Apollo 15 and 16 subsatellite magnetometers has been an important step forward. I find that the pole positions calculated from this data fall into 3 or 4 bipolar groups along different axes inclined to the present axis of rotation. The antipodal groupings suggest reversals of the lunar dynamo. I identify the different axes with different times of magnetization, i.e. Pre-Nectarian 4.2×10^9 years, Lower Nectarian 4.0×10^9 years, Upper Nectarian 3.9×10^9 years and Imbrian 3.85×10^9 years. I explain successive re-orientations of the Moon with respect to its axis of rotation by the creation of the large basins which tend to move towards the pole. The striking association of the multi ring basins with the palaeoequators of corresponding age excludes the possibility that they are high velocity impacts of asteroids in a heliocentric orbit and gives the first observational evidence that there were satellites around the Moon. The directions of the incoming body obtained from studies of assymetry of the multi ring basins supports this view.

Bodies coming in at 1-2 km per second would be quite massive, 100 km and consequently the Lunar regolith will contain a large amount of primeval solar system material. The existence of the satellite system and/or an iron core are important constraints on the origin of the Earth-Moon system.

A HYDRATED INTERPLANETARY DUST PARTICLE CONTAINING CALCIUM- AND ALUMINUM-RICH REFRACTORY MINERAL: POSSIBLE RELATIONS TO CARBONACEOUS CHONDRITES. K. Tomeoka and P.R. Buseck, Departments of Geology and Chemistry, Arizona State University, Tempe, Arizona 85287

Transmission electron microscopy (TEM) of the "LOW-CA" hydrated interplanetary dust particle (IDP) showed it consists largely of poorly crystalline phyllosilicate containing Fe, Mg and Al (called "FMA-silicate") [1]. The FMA-silicate was identified as Fe- and Mg-rich smectite or mica. The LOW-CA particle also showed many unique mineralogical features that are not known from other IDPs.

We present here results of our TEM observations of another unusual IDP, called "SKYWALKER" (#r21-M3-5A), which had previously been studied by the Washington University group using infrared spectroscopy and ion microprobe. They showed that its infrared spectrum is characteristic of the hydrated chondritic class [2], and that this particle shows unusual deuterium enrichment similar to the primitive carbonaceous chondrites [3].

TEM study has revealed that SKYWALKER contains mainly two compositionally distinct types of poorly crystalline phyllosilicates: (1) FMA-silicate (smectite or mica) and (2) Fe-rich and Mg-poor phyllosilicate. The FMA-silicate typically occurs in close association with Fe-Ni sulfide grains as in the case of LOW-CA, while the Fe-rich phyllosilicate is rarely associated with sulfides.

One of the most interesting results is that we found a large cluster ($\sim$6 μm in diameter) of a Ca-, Al- and Mg-rich silicate that contains minor amounts of Ti and Cr. Based on electron diffraction patterns and quantitative microanalysis data, the silicate was identified as fassaite, Ca- and Al-rich clinopyroxene. Fassaite is a major constituent of Ca- and Al-rich refractory inclusions (CAI) in C2 and C3 carbonaceous chondrites [4,5]. Cation to silicon ratios of the IDP fassaite are 0.55 (Ca/Si), 0.36 (Al/Si) and 0.46 (Mg/Si), in good agreement with those in the type B CAIs in Allende [5].

Fe-Ni sulfides, mostly rounded grains (<1000 A) of pyrrhotite, is common. Euhedral, low-Ni pentlandite, characteristic of LOW-CA, is rare. Olivine grains and pyroxene platelets (<1 μm in diameter) with stacking disorder of clino- and orthoenstatite are abundant in SKYWALKER, which is in marked contrast to LOW-CA, where olivine is rare and no pyroxene was observed. The Fe-, Mg-, Si-, Ca- and Mn-containing mineral [1] is pervasive in SKYWALKER. So far, this mineral appears to be unique to hydrated IDP.

The detailed mineralogy of SKYWALKER shows considerable differences from LOW-CA, although both particles contain Fe- and Mg-rich smectite or mica as a major hydrated phase. The results indicate there are considerable mineralogical differences in the hydrated subsets of IDP. The presence of Ca- and Al-rich refractory mineral together with the hydrated silicates makes this IDP bear a close resemblance to the C2 carbonaceous chondrites and strongly suggests a link between hydrated IDPs and the carbonaceous chondrites in their formation histories.

REFERENCES: [1] K. Tomeoka and P.R. Buseck (1984) Earth Planet. Sci. Let. (in press) [2] S. A. Sandford, P. Fraundorf, R. Patel and R.M. Walker (1982) Meteoritics 17, 276. [3] E. Zinner and K.D. McKeegan (1984) Lunar Planet. Sci. 15, 961. [4] G.J. MacPherson, M. Bar-Matthews, T. Tanaka, E. Olsen and L. Grossman (1983) Geochim. Cosmochim. Acta 47, 823. [5] L. Grossman (1975) Geochim. Cosmochim. Acta 39, 433.

DIAGENESIS IN INTERPLANETARY DUST: CHONDRITIC POROUS AGGREGATE W7029*A.
Frans J. M. Rietmeijer and Ian D. R. Mackinnon, Code SN4, NASA/Johnson Space Center, Houston, Tx 77058, USA.

Samples from Chondritic Porous Aggregate (CPA) W7029*A [1] have been studied by Analytical Electron Microscopy. In previous studies we have reported on the presence of layer silicates [2,3] and metal oxide phases [2,4] in CPA W7029*A. We present here a continuation of this detailed mineralogical study and propose a diagenetic scenario which may account for the variety and types of phases observed in this aggregate. At least 50% of CPA W7029*A is carbonaceous material, primarily poorly graphitised carbon (PGC) with morphologies similar to PGC in acid residues of carbonaceous chondrites [5,6]. The basal spacing of graphite in CPA W7029*A ranges from 3.47 - 3.52 Å and compares with d_{002} of graphite in the Allende residues [5,6]. Low-temperature phases comprise 20% of CPA W7029*A and include layer silicates, BaS_2O_7, Bi_2O_3, goethite [2,3] and pentlandite-violarite. Clusters of Mg-rich olivine and pyroxene and clusters of thin Ti_4O_7 plates also occur and make up 16% of the aggregate.

Many of the mineral assemblages within CPA W7029*A can be explained by in situ diagenesis of individual solid grains within a carbonaceous matrix prior to entry into the Earth's atmosphere. For example, we have shown that layer silicates may have formed by decomposition ($T < 100\ ^{o}C$) of an amorphous phase of hydrous cordierite composition [7]. In addition, Ti_4O_7 and BaS_2O_7 can be formed in situ by diagenesis:

$$4\ BaTiO_3 + (Fe,Ni)_9S_8 + 23\ CO = 4\ BaS_2O_7 + Ti_4O_7 + 3\ (Fe,Ni)_3C + 20\ C$$

Ba-titanite is a rare condensate [8] but has been observed in Allende CAI [9]. Low-temperature epsilon Fe,Ni-carbide is present in some CPA's [10]. Carbon-rich CPA's form an uncommmon subset of interplanetary dust which do not appear greatly affected by pulse-heating during atmospheric entry [11]. Our observations and interpretations of CPA W7029*A mineralogy support this conclusion. Some phases within this CPA may have only been heated to 300 - 400 ^{o}C [2,4]. We believe that CPA W7029*A will show some minor effects of limited heating and that its present form will reflect some of the original particle texture. Thus, we can use Fraundorf's [11] model (solid grains embedded in a carbonaceous matrix) to propose a probable environment in which changes of individual components may occur. Using this model, we can infer from d_{002} values of graphite that graphitisation within the PGC-matrix of this CPA would occur between 275 - 300 ^{o}C. Reaction rates at these low temperatures are measured on a geological timescale [12]. We propose that diagenesis [cf. 13] at temperatures between ~80 ^{o}C and 300 ^{o}C may take place in the earliest stage of sub-planetary body formation [cf. 14] when the parent body is a loosely accumulated "cosmic sediment". Diagenesis precedes aqueous alteration in a parent body regolith [15] that may produce layer silicates, sulfates and carbonates in C1 and C2 carbonaceous chondrites.

REFERENCES. 1. Clanton US et al. (1982) CD Catalog JSC Publ, 62; 2. Rietmeijer FJM and Mackinnon IDR (1984) LPS, XV, 687-688; 3. Mackinnon IDR and Rietmeijer FJM (1983) Meteoritics, 18, 343-344; 4. Mackinnon IDR and Rietmeijer FJM (1984) Subm. Nature; 5. Smith PPK and Buseck PR (1981) Science, 212, 322-324; 6. Lumpkin GR (1983) LPS, XIV, 450-451; 7. Rietmeijer FJM and Mackinnon IDR (1984) subm. JGR, Supl.; 8. Fegley, MB (1980) LPS, XI, 279-281; 9. Masuda A and Tanaka T (1977) Nature, 267, 231-233; 10. Christofferson R and Buseck PR (1983) Science, 222, 1327-1329; 11. Fraundorf P. (1981) GCA, 45, 915-943; 12. Grew ES (1974) J. Geol., 82, 50-73; 13. Berner RA (1980) Early Diagenesis, 241 p. (Princeton Univ. Press NJ); 14. DuFresne ER and Anders E (1962) GCA, 26, 1085- 1114; 15. Bunch TE and Chang S (1980) GCA, 44, 1543-1577.

LINKS BETWEEN ASTRONOMICAL OBSERVATIONS OF PROTOSTELLAR CLOUDS AND LABORATORY MEASUREMENTS OF INTERPLANETARY DUST: THE 6.8 μm CARBONATE BAND;

S.A. Sandford and R.M. Walker, McDonnell Center for the Space Sciences, Washington University, St. Louis, MO

It has previously been shown that interplanetary dust grains (IDP's) collected in the Earth's stratosphere fall predominantly into 3 infrared spectral groups referred to as "olivines", "pyroxenes", and "hydrated layer-lattice silicates" (1). Particles in the last group are characterized by featureless, narrow 10 μm silicate absorption bands, and have broad absorption bands at 3.4 and 6.0 μm that are attributed to the presence of water. Bands associated with structural OH are rarely seen in the spectra. A broad band at 6.8 μm is also usually observed in the spectra of this class of particles and is attributed here to carbonates. The carbonate identification has been confirmed in one of these particles, which contains a particularly strong band at 6.8 μm, by the observation of a second weaker infrared band at 11.4 μm. No large carbonate grains have yet been seen in the TEM and indications are that this mineral phase resides in very small crystals. Preliminary quasi-powder electron diffraction data are consistent with the carbonate interpretation (2).

The infrared spectra of these particles match telescopic observations of protostars like W33A (3) in several important respects (see Fig. 1), including the presence of the 6.8 μm feature. This astronomical band was once thought to be caused by hydrocarbons (4) but this identification was since been shown to be inconsistent with other aspects of the spectra (3). Large enrichments in D/H are seen in radio telescopic observations of simple molecules in interstellar molecular-dust clouds and some IDP's have also been shown to have large D/H enrichments (5). We consider that these connections are highly suggestive, raising the possibility that the 6.8 μm protostellar feature is also due to the presence of carbonates. Further, it suggests that at least some IDP's may be residual, preserved solids from the molecular-dust cloud which preceded the formation of the solar system. Experiments are in progress to delineate the chemical and physical nature of the carbonates in IDP's to see, for example, if they are present primarily as coatings on grains. W33A shows an absorption band at 4.6 μm (not seen in the IDP's) which has been attributed to CO adsorbed onto dust grains (3). Conceivably there are reactions which could catalyze the formation of carbonates on such grain surfaces.

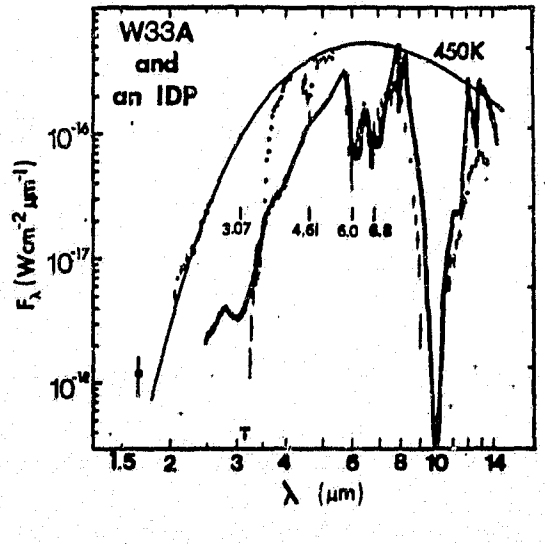

References:
(1) S.A. Sandford, et al, Meteoritics 17, 276, 1982.
(2) P. Fraundorf, private communication.
(3) B.T. Soifer, et al, Ap.J. 232, L53, 1979.
(4) R.C. Puetter, Ap.J. 228, 118, 1979.
(5) K.D. McKeegan, et al, this conference.

D/H RATIOS IN INTERPLANETARY DUST AND THEIR RELATIONSHIP TO IR, RAMAN, AND EDX OBSERVATIONS; K. D. McKeegan, S. A. Sandford, R. M. Walker, B. Wopenka, and E. Zinner, McDonnell Center for the Space Sciences, Washington University, St. Louis, Mo. 63130, USA.

We have continued our ion probe investigation of D/H anomalies in Interplanetary Dust Particles (IDP's) [1,2] extending the range of observed δD values from -280 to 2590 °/oo (relative to terrestrial actinolite) in 8 particles measured thus far. In an effort to understand the relationship between these D/H effects and other properties of the particles, we have performed complementary measurements on the same individual IDP's by other techniques including Fourier Transform Infared Spectroscopy (FTIR), Raman Microprobe Spectroscopy, and SEM/EDX. We have also measured C, Mg, and Si isotopes on selected particles [2,3]. The results are summarized in Table 1. TEM observations on fragments from some of the particles are being performed by the group at Arizona State University and are reported in a separate abstract [4]. We have previously shown that IDP's generally fall into one of 3 IR spectral classes which we labelled olivine (O), pyroxene (P), and hydrated silicate (HS) [5]. Two of the three HS particles show very large D excesses as does the one P type studied to date. The single O type particle with a chondritic EDX spectrum (Essex) which has been measured is slightly depleted in deuterium. Thus at least two of the IR classes are demonstrably extraterrestrial, although the D excess is not constant within a given class. All the Raman spectra exhibit graphite features of varying degrees of crystallinity but no correlation with isotopic structures is immediately apparent from this limited data base. The extraterrestrial nature of a HS particle with an extraordinarily strong carbonate feature in the IR is comfirmed by its large D excess. The astrophysical significance of a carbonate component in interplanetary dust is discussed in a companion abstract [6].

Table 1

Particle	EDX[a]	IR	Raman[b]	δD (°/oo)[c]	other isotopic measurements
Solo	c			556 > 894	
Mosquito	c		C type a little fluor.	191 > 2591	C, Mg, Si
Skywalker	c	HS	C type a moderate fluor.	117 > 767	C, Mg, Si
Essex	c	O	C type b	-193 > -120	
Lea	c	HS	C type a strong fluor.	-280 > +199	
Spray-2	c	P	C type a little fluor. Pyroxene	373 > 993	Mg, Si
Calrissian	c	HS[d]	C type?	373 > 1913	C
Attila[e]	Si,Fe,Ca,Mg,Al Cr,K,Cl,Mn,Ti	O	Same as Essex	-21 > +73	

(a) c = within factor of 3 of chondritic abundances. (b) C indicates graphite lines are seen at ~1330 and 1575-1600 cm^{-1}. The first is present only for disordered graphite, a shift of the second one toward higher wave numbers increases with the amount of disorder [7]. Type a: line 2 dominates line 1, Type b: both lines are of comparable strength. The fluorescence background is mainly seen between 2000 and 3000 cm^{-1}. Strong fluorescence like in Lea is observed in Orgueil and Murchison. (c) The range of observed δD values relative to D/H ratios measured in terrestrial actinolite. The standard deviation of these measurements during a run of an IDP is ~50 °/oo. (d) with very strong carbonate bands. (e) probably of terrestrial origin.

References: [1] E. Zinner et. al. (1983), Nature 305, 119. [2] E. Zinner and K. D. McKeegan (1984) LPSC XV, 961. [3] E. Zinner et. al., this conference. [4] K. Tomeoka and P. Buseck, this conference. [5] S. A. Sandford et. al. (1982), Meteoritics 17, 276. [6] S. A. Sandford and R. M. Walker, this conference. [7] B. Wopenka and S. A. Sandford, this conference.

LASER RAMAN MICROPROBE STUDY OF MINERAL PHASES IN METEORITES;

B. Wopenka[1,2] and S.A. Sandford[2], [1]Dept. of Earth and Planetary Sciences, [2]McDonnell Center for the Space Sci., Washington Univ., St.Louis, MO 63130

The Laser Raman Microprobe (LRM) gives characteristic spectra for most of the common rock-forming minerals, but its application on extraterrestrial materials has been limited to Tieschitz and Allende [1,2]. We have obtained Raman spectra of matrix samples from 13 additional meteorites using a RAMANOR U-1000 LRM in the spectral range of 100 - 2000 cm^{-1}.

Pyroxene spectra show large variations in the relative intensities and widths of their characteristic Raman peaks which, in some cases, may reflect the shock history of a meteorite. Fig. 1 displays the spectra of Nakhla and Shergotty, the latter of which is known to be heavily shocked. Nakhla shows both the Raman-active lattice modes between 300 and 400 cm^{-1} and the internal vibration peaks at ~660 and ~1000 cm^{-1}. In Shergotty the lattice modes are not seen and the internal peaks are smaller and wider than those observed in Nakhla. Measurements on a suite of meteorites with different shock histories and on laboratory-shocked specimens are in progress.

A series of carbonaceous and unequilibrated chondrites has been studied for comparison with similar measurements on interplanetary dust particles [3]. As is the case for reflection spectroscopy in the visible [4], the presence of highly opaque carbonaceous matrix suppresses most of the Raman peaks for other minerals. The spectra usually show only graphitic features, whose relative strengths, widths, and positions of the peaks at 1360 and 1585 cm^{-1} vary with the abundance of disordered and crystalline graphite [5,6]. Fig. 2 shows the Raman spectra of annealed pyrolitic carbon (crystalline graphite), Orgueil, Felix, and soot (disordered carbon). Leoville and Felix (Fig. 2), both C3's, show a higher abundance of disordered graphite than Orgueil, a C1. In addition to the Raman-active peaks, some of the spectra (e.g. Orgueil in fig.2) also show contributions from photo-luminescence. In principle, the shape of this smoothly varying background can give information about the chemical forms of carbon, although at present, no sources have been identified.

References: [1] M.C. Michel-Levy and A. Lautie (1981) Nature 292, 321. [2] P. Fraundorf et al. (1983) LPSC XIII, 231, [3] K. McKeegan et al. (1984) This conference, [4] S. Rajan and M.J. Gaffey (1984) LPSC XV, 659, [5] P. Tuinstra and J.L. Koenig (1970) J.Chem.Phys.53, 1126, [6] R. Vidano and D.B. Fischbach (1978) J.Am.Ceram.Soc.61, 13.

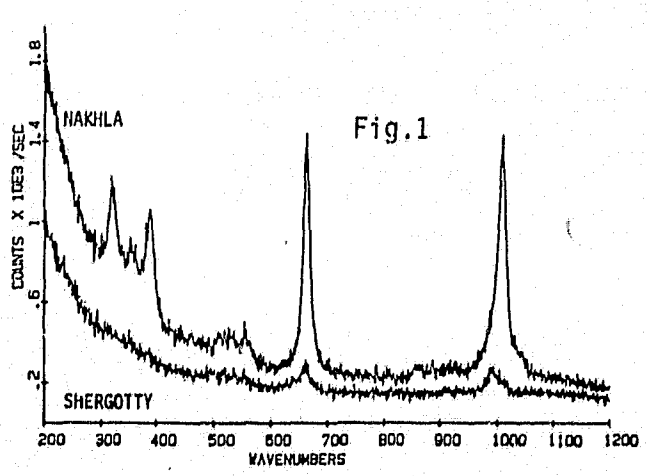

Fig.1

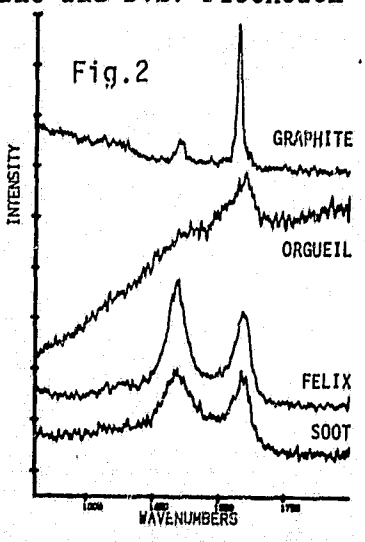

Fig.2

RAMAN MICROSCOPY OF THE LODRAN METEORITE*; R. W. Bild and D. R. Tallant, Sandia National Laboratories, Albuquerque, NM 87185

The Lodran meteorite fell in 1868 and was classified by Prior (1) as the only member of his "lodranite" group of stony-irons. The meteorite was described by Tschermak (2) and was the subject of an extensive electron microprobe study by Bild and Wasson (3). Bild and Wasson found that Lodran consists of roughly equal amounts of metal, olivine (Fa~15), and orthopyroxene (Fs~14). Grains are large (typically 0.5 to 2 mm), equant, and show a well recrystallized texture. Minor phases include troilite, chromite, schreibersite, chrome-diopside and an unnamed phase with a composition close to $(K,Na)AlSi_5O_{12}$. No feldspar was found. The unnamed phase occurs as small (<40 μm) oval inclusions in olivine. Since Bild and Wasson found the unknown phase only in a microprobe thick section (BM44003, P911), they were not able to determine optical properties. The rarity of Lodran material ruled out any sort of destructive analysis. It was not even possible to determine whether the phase is glass or crystalline, though the latter was considered more likely because of the stoichiometry of the material.

Raman microscopy is a relatively new tool for nondestructively obtaining structural information about materials of microscopic proportions. The technique involves focusing a laser beam through a microscope onto the phase of interest and analyzing the scattered light for Raman shifted components using an optical spectrometer. The horizontal spatial resolution is about 1 micron. We have applied this technique to troilite, metal, chromite, olivine, orthopyroxene and the unnamed $(K,Na)AlSi_5O_{12}$ phase in Lodran. Spectra of olivine and orthopyroxene are consistent with spectra for crystalline silicates in the literature (e.g. ref. 4) with olivine showing bands characteristic of silicate monomers and the orthopyroxene showing bands characteristic of chain silicates. The spectra from the unnamed phase has Raman bands from the surrounding olivine plus a relatively intense band at 963 cm^{-1} and a weaker band at 1036 cm^{-1} which are not due to the olivine. A Raman band at 589 cm^{-1} (only a shoulder in the olivine spectrum) also appears to be associated with the unknown phase. The Raman spectra indicate that the unnamed phase is crystalline rather than glass. Evidence for this is the narrow (~15 cm^{-1}) FWHM of the bands. Glasses have much broader (50 to 100+ cm^{-1}) FWHM values. We have not yet been able to make structural assignments for the bands in the unnamed phase, but we are in the process of obtaining spectra on other minerals with related compositions which may aid in making these assignments.

References: (1)Prior,G.T.(1916)Min.Mag. 18, 26-44; (2)Tschermak, G. (1870) Sitzber. Akad. Wiss. Wien, Math-naturwiss. Kl., Abt. 2, 61, 465-75; (3)Bild,R.W. & Wasson,J.T.)1976) Min. Mag. 40, 721-35; (4)Brawer,S.A. & White,W.B. (1975) J. Chem. Phys. 63,2421-32.

---

*This work performed at Sandia National Laboratories supported by the U.S. Dept. of Energy under Contract No. DE-AC04-76DP00789.

THE PERSEIDS AND COMET SWIFT-TUTTLE 1862 III

John A. Russell, University of Southern California, Los Angeles

Comet Swift-Tuttle, parent comet of the Perseid meteors, was first observed in 1862. Brian Marsden, using all available data, recently calculated a period of 120 ± 2 years. The comet should therefore appear between 1980-84. It has not been observed as of the date of this writing.

Have Perseids shown any significant differences in recent years attributable to the proximity of the comet? Mean hourly counts, heights of appearance and disappearance, and the % of spectra showing emission at 5577 Å have been compared for the years 1977,78,80 and 81 (Russell 1982). Figure 1 shows the annual mean hourly rate plot extended to include the 1983 counts. The downward trend since the 1980 high continues. The heights were unexpectedly great in 1983, probably attributable to high solar activity during the period of shower maximum.

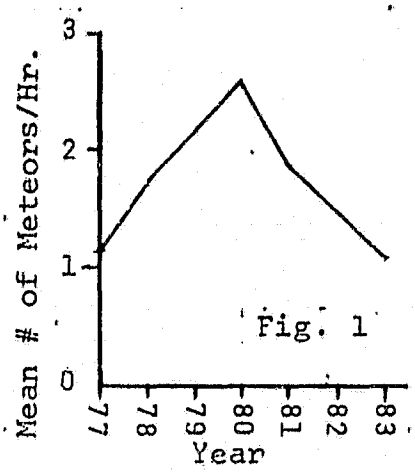

Fig. 1

To see if the average brightness varied significantly from year to year, absolute magnitudes were determined photographically for 82 meteors. Mean values for '80 and '83 (times of high solar activity) were 1.2 magnitudes fainter than the average for the other three years. The average number of breaks in the trails of meteors directly photographed through a rotating shutter were essentially the same for each of the 5 years. Where spectra are available, if the absolute magnitude is plotted against the number of shutter breaks, Figure 2 results. The dots indicate meteors in whose spectra the 5577 Å forbidden oxygen radiation is the strongest spectral feature. The x's indicate spectra in which the H and K lines of ionized calcium are visible. There is essentially no overlap in magnitudes between these two groups. For about the same number of shutter breaks, the meteors showing H and K lines average 33 times the maximum brightness of the meteors in which 5577 Å radiation is the strongest. It is known that the former appear lower in the atmosphere than the latter (Russell 1980). Some difference in meteoroidal structure is indicated, governing the height of maximum radiation and the rate of ablation.

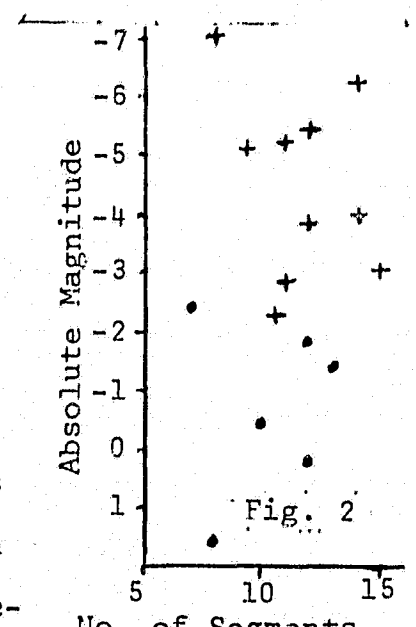

Fig. 2

REFERENCES

Russell, J. A. 1981, Ap. J. 243, 317-21
1982, Sky & Tel., 63, 10-11

THE GIOTTO MISSION TO HALLEY'S COMET; A. D. Johnstone, Mullard Space Science Lab., Univ. College London, Holmbury St. Mary, England; and R. Reinhard, Space Science Dept. of ESA, Estec, Noordwijk, The Netherlands

The European Space Agency (ESA) is carrying out a fast flyby mission to Halley's Comet with an encounter on 13 March 1986, about 4 weeks after the comet's perihelion passage. The mission is named "Giotto" after the Italian painter Giotto Di Bondone who, in 1304 AD, depicted Halley's Comet realistically in a chapel in Padua. At the time of the encounter, the comet's heliocentric distance is 0.9 AU and its geocentric distance is 1 AU. Because Halley's orbit is retrograde, the relative flyby velocity is rather high (69 km/s). The scientific payload comprises 10 experiments with a total mass of about 60 kg. The payload includes a narrow angle camera for imaging the comet nucleus (resolution 22 m from 1000 km); three mass spectrometers for analysis of the elemental and isotopic composition of the cometary neutrals, ions, and dust particles; various dust impact detectors; a photopolarimeter for measurements of the coma brightness; and a set of plasma sensors for studies of the solar wind/comet interaction. During the encounter scientific data are transmitted at a rate of 40 kbps. The Giotto spacecraft is cylindrical in shape (diameter: 1.84 m, height: 3 m, mass: 950 kg). During the encounter it will spin at 15 rpm. It carries a despun high gain parabolic dish antenna inclined at 44.3 degrees to point at the earth during the encounter while a specially designed dual-sheet bumper shield at the other end protects the spacecraft from being destroyed by hypervelocity dust impacts. A centrally mounted solid propellant boost motor is used for injection into the heliocentric transfer trajectory.

Presently under study is a cooperative NASA/ESA mission to another periodic comet with a launch between 1988 and 1990. ESA would procure a second Giotto spacecraft which would be modified by NASA to allow a coma sample (dust and gas) to be returned to Earth. The next two papers in this series will discuss this mission opportunity in greater detail and the scientific rationale for such a mission.

A PROPOSED GIOTTO/COMET COMA SAMPLE RETURN MISSION; B. L. Swenson, NASA Ames Research Center, Moffett Field, CA; Dr. P. Tsou, Jet Propulsion Laboratory, Pasadena, CA; A. Friedlander, Science Applications, Inc., Schaumburg, IL; and A. C. Mascy, NASA Ames Research Center, Moffett Field, CA

The Solar System Exploration Committee of the NASA Advisory Council has strongly recommended, as part of an overall core strategy for the future exploration of the solar system, that two programs be initiated for the exploration and characterization of comets. These missions are a rendezvous with a short period comet and the return to Earth of an atomized sample of the coma of a comet. The implementation of the rendezvous mission to comet Kopff is currently under intensive study and a launch in 1990 is contemplated.

Recently, a proposal has been made by NASA to ESA regarding the possible implementation of the coma sample return mission. The proposal is for a cooperative mission utilizing a second Giotto spacecraft provided by ESA to carry an appropriate collection device and an Earth atmospheric entry system for sample recovery provided by NASA. The spacecraft, collection device, and Earth entry system would be launched by Shuttle on a free-return trajectory to an appropriate cometary target. During the coma fly-thru dust would be collected and placed within the Earth entry vehicle. After return to Earth, the entry vehicle decelerates in the atmosphere and is air-snatched by an aircraft during the descent on a parachute.

The purpose of this paper is to provide a description of possible mission alternatives, an examination of alternate sample collection techniques and devices, a discussion of the engineering aspects of the design of the Earth entry system, and finally a discussion of the integration of the collection device and entry vehicle to the existing Giotto spacecraft.

S-10 N85 15646

SAMPLE RETURN FROM A COMET FLYBY

D.E. Brownlee, Dept. of Astronomy, Univ. of Washington

Sample collection and return to the Earth from a fast fly through of a cometary coma is the simplest sample return mission possible from any extraterrestrial body. The mission can provide valuable laboratory samples from a known cometary body and it can do it at low cost, within our lifetimes. In the flyby mission, dust particles and possibly some gas samples are collected at high velocity and then sealed into a capsule until return to the laboratory. The spacecraft itself is launched on a free return trajectory and the capsule is recoverable, either by direct entry into the atmosphere or by aerobraking and recovery from Earth orbit.

In comparison with a robotic surface collection approach, such as was used with the Soviet Luna missions, the coma collection is straightforward and simple, but the return is also limited and the science must be focused only on few aspects of sample analysis. On the coma mission only a small mass of sample is collected and it is not returned in pristine condition. The primary goal of the coma collection is to collect several hundred individual particles ranging in size up to 0.5mm. It may also be possible to collect some coma gas. The particles are collected either as debris in the bottoms of craters in selected substrates or as material trapped in individual sealed "capture cells" that particles enter by penetration of a thin metal diaphragm. Although the physical forms of particles are altered during collection, their bulk composition does not change. The fundamental scientific output from the mission will be the precise elemental and isotopic compositions for a large set of individual particles. This data set will provide a very powerful means for comparing a bona fide comet sample with known types of meteoritic materials.

Mg ISOTOPIC MEASUREMENTS IN FINE-GRAINED Ca-Al-RICH INCLUSIONS

C. A. Brigham, D. A. Papanastassiou, and G. J. Wasserburg, The Lunatic Asylum, Div. Geol. & Planet. Sci., California Inst. of Tech., Pasadena, CA 91125.

A study of the Mg isotopic composition and mineralogy of fine-grained, Ca-Al-rich inclusions has been initiated, to search for isotope fractionation and for excess $^{26}Mg^*$ due to the decay of ^{26}Al. It is important to establish whether there is evidence, in these inclusions, of isotopic heterogeneity, whether $^{26}Mg^*$ is correlated with Al/Mg, and whether there is a correlation of the isotopic effects with mineralogy. Fine-grained inclusions were identified in slabs of Allende; half of each inclusion was used for a thin-section and the other half was sampled and analyzed for Mg, either by the direct-loading technique or after dissolution and chemical separation. Analyses of both acid soluble phases and residues were obtained. The mineralogy of most of the inclusions, determined on the SEM, consists of sodalite, nepheline, and Mg-spinel, with minor plagioclase and Fe-Mg-pyroxene. One inclusion (BG82D-I) is distinctive, and consists primarily of hibonite, sodalite, and nepheline with trace anorthite and hercynite; no Mg-spinel was observed. We show (Table 1) Mg isotope fractionation factors (F_{Mg}) and $\delta^{26}Mg$ values. Most inclusions display small isotope fractionation favoring the lighter isotopes (negative F_{Mg}) and hints of excesses in ^{26}Mg. The small $\delta^{26}Mg$ in bulk aggregates are consistent with relatively high Mg concentrations and low Al/Mg (3.4% Mg for BG82C-M and 3.7% for A47-2). The hibonite-rich inclusion (BG82D-I) displays a significant isotope fractionation factor and a large $^{26}Mg^*$; the latter is correlated with high Al/Mg (0.2% Mg for the soluble portion and 0.1% Mg for the hibonite residue). There is a hint of intrinsic isotopic heterogeneity in this inclusion as seen by the small differences in F_{Mg} between the residue and soluble parts. The significant differences in $\delta^{26}Mg$ show that this inclusion was not homogenized after ^{26}Al decay. In summary, one halogen-rich inclusion with a high Al/Mg displays large excesses in ^{26}Mg and large isotope fractionation favoring the lighter isotopes, while most other fine-grained inclusions show small F_{Mg} in the same direction[1-3]. This is in contrast to the positive fractionation factors typical of coarse-grained CAI. It is difficult to reconcile the fractionation effects and low Mg content of BG82D-I with a replacement process, originating from a coarse-grained CAI. Fractionation factors favoring the lighter isotopes may be indicative of kinetic effects due to formation of the fine-grained inclusions by "early" condensation or by later condensation from a vapor phase enriched in lighter isotopes.[1]

[1]F.R. Niederer, D.A. Papanastassiou (1984) Geochim. Cosmochim. Acta 48 (in press). [2]D.A. Papanastassiou, C.A. Brigham, G.J. Wasserburg (1984) Lunar & Planet. Sci. XV, p. 629. [3]T.M. Esat and S.R. Taylor (1984) ibid., p. 254.

Table 1. Mg Analytical Results

Sample[a]	$F(Mg)^b$ °/oo amu^{-1}	$\delta(^{26}Mg)^c$ °/oo	DLT[d]
BG82D-I-s	-5.6±0.7	21.0±0.1	N
-r	-9.3±0.5	47.2±0.2	Y
-t[e]	-6.3±1.9	35.2±0.6	Y
A47-2 -s	-0.2±0.3	1.0±0.1	N
-r	-1.5±0.3	0.74±0.07	Y
BG82C-M-s	-1.8±0.3	1.1±0.2	N
-r	-3.6±0.3	1.3±0.2	Y
A47-1 -t	-1.6±0.6	0.6±0.1	Y
BG82I-C-t	-2.7±0.5	1.4±0.2	Y
BG82I-I-t	-3.0±0.2	0.98±0.07	Y

[a]s=Soluble; r=Residue; t=Total.
[b]Fractionation factor (2σ) is calculated from the measured values for $^{25}Mg/^{24}Mg$ relative to the raw measured value for normal, $(^{25}Mg/^{24}Mg)_N = 0.12475$. Reproducibility for F_{Mg} is ±1.5°/oo amu^{-1}.
[c]Deviations in $^{26}Mg/^{24}Mg$ (2σ mean) from normal after fractionation correction.
[d]Y: Samples analyzed by the direct loading technique (DLT). For these samples a bias of 1.5°/oo has been added to the reported $^{26}Mg/^{24}Mg$ due to high $^{27}Al^+/^{24}Mg^+$. N: Mg chemically separated; not subject to bias.
[e]From ref. 2.

EXCESS ^{41}K IN ALLENDE CAI: A HINT RE-EXAMINED; I.D. Hutcheon, J.T. Armstrong and G.J. Wasserburg, The Lunatic Asylum, Div. Geol. & Planet. Sci., California Institute of Technology, Pasadena, CA 91125.

The timescale for injection of fresh nucleosynthetic material and for the formation of the first solids in the early solar system is determined by the existence and abundance of short-lived nuclei. The presence of live ^{26}Al with $^{26}Al/^{27}Al \sim 5\times10^{-5}$ in numerous CAI from C2 and C3 meteorites places an upper limit to this timescale of $\sim 8\times10^{6}$y but the lower limit is poorly constrained. The short half-line of ^{41}Ca ($\bar{\tau} = 0.19\times10^{6}$y), which decays to ^{41}K, makes the abundance of ^{41}K a very sensitive indicator of the minimum time interval. Initial evidence for excess radiogenic $^{41}K(^{41}K^{*})$ was reported by HAW[1] and HAW[2], who found $^{41}K^{*}$ in fassaite from Allende CAI at a level $^{41}K^{*}/^{40}Ca \sim 0.5\text{-}1\times10^{-7}$. The search for $^{41}K^{*}$ is a difficult experiment because very high Ca/K ratios are required with K < 200 ppb. The resulting $^{41}K^{+}$ signal in fassaite is < 0.5 c/s with $^{41}K^{*+} \sim 0.1$ c/s. A major concern of [1] and [2] was the magnitude of molecular ion interferences in the region of ^{41}K, particularly $^{40}Ca^{42}Ca^{++}$, which is indistinguishable from $^{41}K^{+}$ at any available mass resolution. Both [1] and [2] evaluated the intensity of $^{40}Ca^{42}Ca^{++}$ by measuring the K isotopic composition of optical calcite containing < 50 ppb K. In the present study we have directly measured $^{40}Ca^{43}Ca^{++}$ in calcite and fassaite (typically ~ 0.06 c/s) and find that the yield of doubly-charged species is strongly matrix dependent; the intensity of $^{40}Ca^{42}Ca^{++}$ relative to $^{42}Ca^{+}$ in fassaite is ~ 10 times that in calcite. These new data indicate that in Allende fassaite $^{40}Ca^{42}Ca^{++}$ comprises up to 80% of the signal at mass 41 and that the ^{41}K excesses previously reported were overestimated by a factor of ~ 8 to 12. This report, therefore, supercedes our previous studies.

After correcting for $^{40}Ca^{42}Ca^{++}$ (using the measured $^{40}Ca^{43}Ca^{++}$ signal), fassaites from two Allende Type B1 CAI, Egg 3 and 3529Z, show excesses at mass 41 of up to 350%, which are linearly correlated with $^{40}Ca/^{39}K$ in each sample. The extent to which this correlation may be attributed to in situ decay of ^{41}Ca requires additional measurements and more careful characterization of contributions from possible interferences such as $^{26}Mg^{56}Fe^{++}$. Assuming the excesses are from $^{41}K^{*}$, the data define a line with slope $^{41}K^{*}/^{40}Ca = (8\pm3)\times10^{-9}$ (2σ) and intercept $^{41}K/^{39}K = 0.072$. The present data clearly show that ^{41}Ca was not abundant when two Allende CAI formed and place a firm upper limit on the abundance of $^{41}K^{*}$, <1 ppb. In contrast, $^{26}Mg^{*}$ is ~ 5 ppm in these CAI. The near absence of $^{41}K^{*}$ requires either that $^{41}K^{*}$ was lost during CAI metamorphism or that the time interval between ^{41}Ca production and CAI formation was $\sim 2\times10^{6}$y, an interval fully compatible with that inferred from ^{26}Al.

[1] LPS XII, 381 (1981);
[2] LPS XV, 387 (1984)

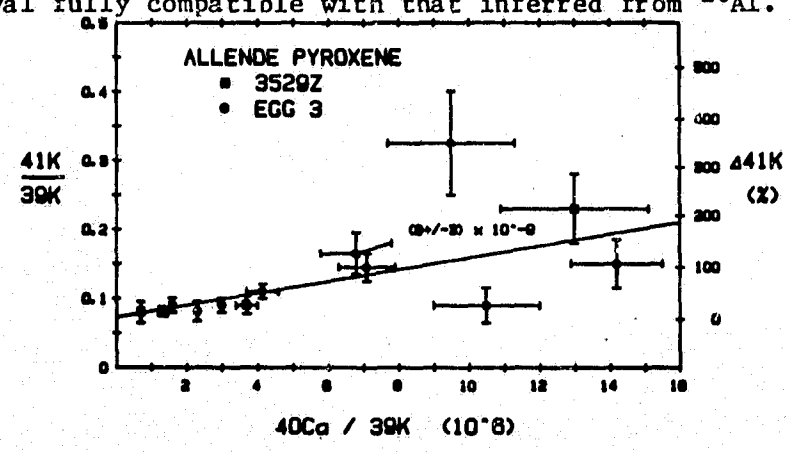

Ca-K evolution diagram for Allende fassaite.

MAGNESIUM ISOTOPIC ANALYSIS OF GR-1 - - A SECOND CORUNDUM-RICH MURCHISON INCLUSION. R.W. Hinton, G.J. MacPherson, and L. Grossman, University of Chicago, Chicago, IL 60637.

Ion microprobe measurements have been made on GR-1, a second corundum-hibonite-bearing inclusion from the Murchison C2 chondrite (1). This inclusion differs from BB5 (2) in that it appears to contain two generations of hibonite. The hibonite within the core of the inclusion is associated with refractory rare-element nuggets and is less magnesium-rich than the hibonite at the rim (0.23 and 0.35 wt% MgO respectively (3)).

Preliminary magnesium isotope analyses have been made at low resolution (2) on the Chicago AEI IM20 ion microprobe. The hibonite crystals, unlike those of BB5, are isotopically normal and no ^{26}Mg excesses were observed in either the core or rim of the inclusion (Table 1). Corundum, with a magnesium content of 20-60 ppm, exhibits no ^{26}Mg excesses. Upper limits for the initial $^{26}Al/^{27}Al$ ratio of 2×10^{-7} and 7×10^{-7} are defined for the corundum and hibonite respectively.

^{26}Mg excesses indicating an initial $^{26}Al/^{27}Al$ ratio of 4.5×10^{-7} have been found to occur within a number of refractory inclusions within carbonaceous chondrites, especially inclusions bearing melilite and anorthite. In contrast, some of the most refractory inclusions, which may be expected to be formed in the solar nebula at an early stage, have been shown to contain little or no evidence for ^{26}Al presence. The variable nature of the initial $^{26}Al/^{27}Al$ ratios has previously been cited as possible evidence for the inhomogeneous distribution of ^{26}Al that had been produced in, and injected into, the ISM by a supernova. Nebula inhomogeneities are, however, less likely if ^{26}Al is continuously introduced into the ISM from novae, as has been suggested by Clayton (4). Assuming the ubiquitous initial presence of ^{26}Al, GR-1 would have to be formed, or its magnesium totally exchanged, more than 5 m.y. after the bulk of the Allende CAIs. Either mechanism would appear unlikely. Until the problem of the low ^{26}Al abundances within these presumed early condensates is satisfactorily explained, a supernovae origin for the ^{26}Al cannot be ruled out.

TABLE 1: Murchison GR-1

	$^{25}Mg/^{24}Mg$	$^{26}Mg/^{24}Mg$	^{26}Mg	Al/Mg
Hibonite (Core)	.12515 ± 37	.13596 ± 37	-2.6 (±5.2)	545
Hibonite (Rim)	.12683 ± 26	.13954 ± 36	-1.7 (±3.2)	306
Corundum	.12782 ± 320	.14145 ± 340	-2.8 (±35)	21870

References:
(1) MacPherson, G.J. et al. (1984) Lunar Plan. Sci. 15, 503-504.
(2) Bar-Matthews, M. et al. (1982) Geochim. Cosmochim. Acta 46, 31-41.
(3) MacPherson, G.J. et al. (1984) Submitted to Proc. Lunar Plan. Sci. Conf. 15th.
(4) Clayton, D.D. (1984) Lunar Plan. Sci. 15, 168-169.

Mg ISOTOPIC STUDIES OF LEOVILLE "COMPACT" TYPE A CAI; I.D. Hutcheon, J.T. Armstrong and G.J. Wasserburg, The Lunatic Asylum, Div. Geol. & Planet. Sci., California Institute of Technology, Pasadsena, CA 91125

One long-standing problem in the application of Al-Mg isotopic systematics to the chronology of CAI is the enigmatic Mg isotopic record of hibonite. Hibonite (ideally, $CaAl_{12}O_{19}$) is one of the first major element bearing phases to appear in the condensation sequence [1] and occurs as a major constituent only in CAI whose bulk composition is considerably more refractory than Allende Type B1 CAI. The Mg isotopic composition of hibonite, however, fails to reflect its presumed early origin with $^{26}Mg^*/^{27}Al$ ranging from $\sim 7\times10^{-5}$ to $< 2\times10^{-7}$ [2,3]. Hibonite is abundant in two "compact" Type A CAI (CTA) from Leoville and we have begun a petrographic and Mg isotopic study of coexisting phases to investigate the degree to which events of formation and metamorphism are reflected in the Mg isotopic record.

Leoville 575 (described in [4]) and 776 are both large elongated CTA's comprised predominantly of melilite (mel) (Åk ~ 3-30) enclosing abundant hibonite (hib) and spinel. Large (up to ~ 1 mm) mel laths in 575 are highly kink-banded and evidence of pervasive cataclastic deformation is extensive. Hib occurs as bladed and blocky crystals (up to ~ 100 μm) intimately intergrown with spinel. Minor polycrystalline plagioclase (plag) (up to ~20μm) is also present. Mel in 776 occurs as smaller (50-300μm) relatively strain free equant crystals with 120° triple grain boundaries. Hib is strongly pleochroic and occurs as clusters of 10-20μm crystals often bounded by spinel. The general fabric appears to reflect metamorphic recrystallization.

Both CAI have similar Mg isotopic patterns with hib containing much larger ^{26}Mg excesses (up to 75°/₀₀ in 575 and 16°/₀₀ in 776) than coexisting mel or plag. ^{26}Mg excesses in hib in both CAI are well correlated with $^{27}Al/^{24}Mg$ and all data lie along a correlation line with slope $^{26}Mg^*/^{27}Al = 5\times10^{-5}$, characteristic of Allende Type B1 CAI. Mel and plag in 575 also contain $^{26}Mg^*$ but these data fall well below the hib line and define a linear array with slope $^{26}Mg^*/^{27}Al = 3\times10^{-5}$. Mel in 776 contains no $^{26}Mg^*$ with $^{26}Mg^*/^{27}Al < 1.5\times10^{-5}$. The isotopic and petrologic data from these two CTA and a previously analyzed Allende CTA [2] suggest that CTA formed contemporaneously with Allende B1 CAI with uniform $^{26}Al/^{27}Al \sim 5\times10^{-5}$ in all phases. Subsequent metamorphism affected CTA to varying degrees and caused partial (in 575 and 3529-26 [2]) or complete (in 776) re-equilibration of the Al-Mg system. The petrologic evidence of greater recrystallization in 776 is consistent with the more extensive isotopic re-equilibration observed in 776. Hib in CTA appears to be more resistant to element redistribution than either plag or mel.

	Leoville 575		Leoville 776	
	$\delta^{26}Mg$(°/₀₀)	$^{27}Al/^{24}Mg$	$\delta^{26}Mg$(°/₀₀)	$^{27}Al/^{24}Mg$
Hb1	25 ± 4	56 ± 1	6 ± 3	18 ± 1
2	41 ± 4	100± 2	10 ± 2	30 ± 2
3A	56 ± 5	143± 5	16 ± 3	42 ± 2
3B	75 ± 7	201± 6	-	-
M11	10 ± 4	36 ± 2	0 ± 2	12 ± 1
2	20 ± 3	57 ± 3	0 ± 2	15 ± 1
Pg1	34 ± 12	173± 10	-	-

[1] GCA 36, 597 (1972); [2] ACS Symp. 176, 95 (1982); [3] Ap.J. 228, L93 (1979); [4] Kracher et al., sub. to GCA (1984).

ABSENCE OF EXCESS ^{26}Mg IN ANORTHITE FROM THE VACA MUERTA MESOSIDERITE

D.A. Papanastassiou[1], G.J. Wasserburg[1], and U.B. Marvin[2]; [1]The Lunatic Asylum, Div. Geol. & Planet. Sci., Calif. Inst. of Tech., Pasadena, CA 91125; [2]Center of Astrophysics, Cambridge, MA 02138.

The absence of ^{26}Mg excesses in Al-rich phases (feldspars) from basaltic achondrites, high petrographic grade chondrites and a K-feldspar from an iron meteorite was established by previous work[1]. After discovery of in situ decay of ^{26}Al in Ca-Al-rich inclusions in carbonaceous meteorites[2], of ^{107}Pd decay in iron meteorites[3], and of ^{129}I decay in silicate inclusions in iron meteorites[4], a re-examination of differentiated meteorites for ^{26}Mg appeared necessary. We selected a 30 g fragment of the Vaca Muerta mesosiderite with abundant silicates with crystals in the 50-1000μm range. One surface was polished for the electron microprobe. A 12 g piece was dissolved in dilute acetic acid and coarse anorthite grains were picked from the residue. The range of compositions was An 89-94.6, Ab 10.6-5.2, Or 0.4-0.2. Some anorthites were free of inclusions but many were cloudy with silica blebs (up to 10μm). Anorthite was also found as inclusions in tridymite, an accessory mineral in Vaca Muerta. Two anorthite crystals were analyzed for Mg by the direct loading technique. A composite of 10 crystals was checked for purity on the SEM and found to consist of anorthite with some SiO_2. The composite was dissolved. Aliquots were used to determine the Mg and Ca contents and the Mg isotopic composition. For the composite, using the Ca/Mg ratio and the assumption of anorthite stoichiometry we calculate a Mg content of 440 ppm and $^{27}Al/^{24}Mg = 5\times10^{2}$, both with an estimated uncertainty of less than 20% due to uncertainty in Ca/Al. The observed $^{26}Mg/^{24}Mg$ shows no significant excess ^{26}Mg. The data were adjusted by a 1.5‰ bias in $^{26}Mg/^{24}Mg$ for DLT analyses with high $^{27}Al^{+}/^{24}Mg^{+}$ (Table). By using an upper limit on $\delta^{26}Mg$ of 1.4‰ we obtain a limit on $^{26}Al/^{27}Al$ for Vaca Muerta plagioclase of 4×10^{-7}, which is in the range obtained by Schramm et al.[1] and indicates a minimum free-decay interval of ~5 m.y. between Ca-Al-rich inclusions and the Vaca Muerta anorthite. It is clear that effects in ^{26}Mg can be resolved only if differentiated meteorites formed on a fast timescale and have remained undisturbed. The absence of evidence of ^{26}Al in differentiated meteorites leaves open the question of whether ^{26}Al provided the heat source for differentiation of the parent planets. A report of excess ^{26}Mg in a hibonite clast from Dhajala (H3) shows that ^{26}Al was not limited to CAI's in carbonaceous meteorites[5].

[1]D.N. Schramm, F. Tera, G.J. Wasserburg (1970) EPSL 10,44; [2]T. Lee, D.A. Papanastassiou, G.J. Wasserburg (1977) Ap. J. Lett. 211, L107; [3]W.R. Kelly, G.J. Wasserburg (1979) GRL 5, 1079; [4]S. Niemeyer (1979) GCA 43, 843; [5]R.W. Hinton, A. Bischoff (1984) Nature 308, 169.

Table: Mg in Vaca Muerta Plagioclase

Sample	F_{Mg}[a] ‰ amu^{-1}	$\delta^{26}Mg$[b] ‰	$^{27}Al^{+}/^{24}Mg^{+}$[c]	DLT[d]
#3(250μm)	-1.5±4.4	0.5±1.7	10-45	Y
#4(200μm)	-1.7±2.6	0.6±0.8	20-50	Y
Composite[e]	-2.4±2.2	0.5±0.9	20-140	Y

[a]Isotope fractionation factor from the raw measured $^{25}Mg/^{24}Mg$ (2σ uncertainty); [b]Deviations in $^{26}Mg/^{24}Mg$ from normal, corrected for isotope fractionation ($2\sigma_{mean}$ uncertainty); [c]Range of ion beam intensity ratios during run; [d]Samples analyzed by the direct loading technique (DLT); [e]Composite of 10 crystals; analysis of 10% aliquot of dissolved sample.

A POSSIBLE ^{126}Sn CHRONOMETER FOR THE EARLY SOLAR SYSTEM

J.R. De Laeter and K.J.R. Rosman, Department of Applied Physics, Western Australian Institute of Technology, Australia. 6102.

The presence of the now extinct radionuclides ^{26}Al and ^{107}Pd in the early Solar System is now accepted. This implies that the nucleosynthetic event which produced these nuclides must have occurred no more than a few million years prior to the formation of solid bodies (1), although an alternative model based on grain carriers has also been proposed (2). Norman and Schramm (3) have recently proposed that the ^{182}Hf/^{182}W chronometer would provide another piece of evidence in the chronology of the formation of the Solar System and may help to determine the astrophysical sites of heavy element nucleosynthesis.

^{126}Sn is produced by the r-process and decays to ^{126}Sb with a half life of $\sim 10^5$y (4), and thence to the stable nuclide ^{126}Te. Any ^{126}Sn present at the time of solidification will have decayed to ^{126}Te in the very early history of the Solar System, and evidence for its presence would be an excess amount of ^{126}Te in meteoritic material. The excess ^{126}Te would be correlated with the Sn/Te elemental abundance ratio.

In order to maximise the probability of detecting a ^{126}Te excess, it is necessary to select meteoritic samples with a large Sn/Te ratio. Iron meteorites represent the best opportunity of searching for ^{126}Te excesses. De Laeter and Jeffery (5) have measured Sn concentrations in 14 irons and report a range from 0.1-7.6 ppm. Furthermore Shima (6) has shown that Sn is concentrated in the metal phase, and is depleted by $\sim$10X in the troilite phase of iron meteorites. Very few determinations of Te concentrations in iron meteorites have been made. Smith (7) has reported values from 0.005-0.156 ppm in 5 irons, while Goles and Anders (8) report a range of 0.017-0.09 ppm in 4 irons and 1.2-7.8 ppm in sulphide inclusions from a similar group of meteorites. Thus Sn/Te abundance ratios of $\sim$1500 could be obtained from selected iron meteorites, and this ratio could be increased by perhaps 10X if the samples were leached to remove troilite inclusions. It would therefore seem possible that Sn/Te ratios of $\sim 10^4$ could be obtained from selected meteoritic samples.

Preliminary mass spectrometric measurements of Te in selected iron meteorites will be reported.

Reference

1. Cameron, A.G.W. and Truran, J.W. (1977) Icarus, 30, 447-461.
2. Clayton, D.D. (1979) Space Sci. Rev., 24, 147-226.
3. Norman, E.B. and Schramm, D.N. (1983) Nature, 304, 515-517.
4. Dropesky, B.J. and Orth, C.J. (1962) J. Inorg. Nucl. Chem., 24, 1301-1316.
5. De Laeter, J.R. and Jeffery, P.M. (1967) Geochim. Cosmochim. Acta, 31, 969-985.
6. Shima, M. (1964) Geochim. Cosmochim. Acta, 28, 517-532.
7. Smith, C.L. (1977) Unpublished Thesis, Western Australian Institute of Technology.
8. Goles, G.G. and Anders, E. (1962) Geochim. Cosmochim. Acta, 26, 723-737.

ANOMALOUS SILVER IN SULFIDE NODULES; J.H. Chen and G.J. Wasserburg, The Lunatic Asylum, Division of Geological & Planetary Sciences, California Institute of Technology, Pasadena, CA 91125

Excesses of ^{107}Ag ($^{107}Ag^*$) correlated with Pd/Ag have been found in iron meteorites of IVA, IVB and IIIAB groups, and is inferred to be the daughter of extinct ^{107}Pd ($\bar{\tau}$ = 9.4 m.y.) (1-4). However the Pd/Ag systematics involving the coexisting metal and sulfide phases of Santa Clara (IVB) and Gibeon (IVA) do not show a good internal isochron. These meteorites have undergone shock melting and later heating and forging which may have redistributed Pd and Ag and confused the Pd-Ag systematics (5).

We have undertaken a detailed study of the sulfide inclusions and the adjacent metal in Gibeon in order to understand the Pd-Ag systematics in these phases. Three samples of Gibeon, ASU Lion River, USNM #3187, and USNM #679 were investigated. The metal phase shows a wide range of $^{107}Ag/^{109}Ag$ (1.54 to 9.23) and $^{108}Pd/^{109}Ag$ (1.8×10^4 to 3.2×10^5). These data plot close to a line with a slope corresponding to $^{107}Ag^*/^{108}Pd = 2.3\times10^{-5}$ and an initial $^{107}Ag/^{109}Ag$ = 1.13 which is greater than the normal value of 1.09. The Pd-Ag results on sulfides from USNM #3187 and ASU Lion River show greater $^{107}Ag/^{109}Ag$ values in the "interior" cores (1.19 to 1.28) than in the HCl leaches (1.10 to 1.12). The ^{108}Pd content in these sulfide nodules range from 4×10^{12} atoms/g (Lion River) to 1.6×10^{15} atoms/g (#3187) which are fully compatible with the proportion of metal taken up in the heavily shocked troilite-rich nodules (3). We report here on a new sulfide nodule from USNM #679 which consists of troilite-rich and metal-rich regions. The metal-rich parts of the nodule are fine grained material of eutectic texture which have flowed into the fine grained, more sulfide rich center. The results from the troilite-rich region are similar to those from the pure FeS sample of Lion River. The $^{107}Ag/^{109}Ag$ in the metal-rich region is 1.18 and the ^{108}Pd is 10^{15} atoms/g which is compatible with the presence of ~ 20% metal.

The sulfide nodules contain Ag which is isotopically very heterogeneous. The presence of $^{107}Ag^*$ in the nodules is interpreted to result from limited diffusion of $^{107}Ag^*$ from metal to the sulfide during rapid cooling (> 150° C/my) or due to admixtures of metal and sulfide during shock melting. To test for evidence that $^{107}Ag^*$ had diffused from the adjacent metal to the sulfide nodule we analyzed a piece of metal from the contact zone with the nodule. The metal sample represented ~ 1 cm thick region of the contact zone. The whole sample was first leached in hot aqua regia (leach-1) and then only the side which was in contact with the nodule was leached (leach-2). The interior core was then dissolved and analyzed. The $^{107}Ag/^{109}Ag$ ratios increase from 1.1 in leach-1 to 1.18 in leach-2 to 4.55 in the core, while $^{108}Pd/^{109}Ag$ ratios increase from 511 to 2000 and to 1.43×10^5. The $^{107}Ag^*$ content changes from 1.07×10^{11} to 2.27×10^{11} and to 1.35×10^{11} atoms/g. The Pd-Ag data for the core and total sample plot on the isochron for Gibeon and apparently did not show any preferential mobilities of Pd or Ag at the center of the contact zone on the sample scale. The Ag isotopic peculiarities of the "sulfide" phase for the IVAB meteorites and the transport of $^{107}Ag^*$ is apparently complex and not readily explained. However, the "metal" phase appears to be well behaved and shows a remarkably coherent behavior between $^{107}Ag^*$ and Pd.

Ref.: (1) Kelly, W.R. & Wasserburg, G.J., J. Geophys. Res. Lett. 5 1079-1082 (1978); (2) Kaiser, T. & Wasserburg, G.J., GCA 47 43-58 (1983); (3) Chen, J.H. & Wasserburg, G.J., GCA 47 1725-1737 (1983); (4) Chen, J.H. & Wasserburg, G.J., LPS XV, 144-145 (1984); (5) El Goresy, A. et al. LPS XV, 244-245 (1984).

PETROGRAPHY OF CAPE YORK AND GRANT: IRONS WITH SIMPLE Pd-Ag SYSTEMATICS; J.M. Teshima, G.J. Wasserburg & A. El Goresy, The Lunatic Asylum, Div. Geol. & Planet. Sci., California Inst. of Technology, Pasadena, CA 91125

The presence of excess ^{107}Ag from the decay of extinct $^{107}Pd(t_{1/2}=6.5$ my) has been determined in IVB, IVA and two anomalous irons (1). Excesses of ^{107}Ag in groups IIIAB and IIB meteorites, Cape York and Grant, and Derrick Peak, respectively, show the widespread presence of ^{107}Pd in the early solar system (2). Internal isochrons were established between metal and sulfide for the two IIIAB irons but similar data for Gibeon (IVA) and Santa Clara (IVB) reveal a complicated Pd-Ag evolution. Petrologic descriptions of the specific meteorites analyzed isotopically are needed to establish criteria which distinguish isotopically "well behaved" irons from those with more complicated Pd-Ag systematics. The petrography of Santa Clara and Gibeon have been presented (3). We will present the petrography of the "well behaved" meteorites Grant USNM #836 and Cape York (4). Grant consists of a 1.5 cmϕ sulfide nodule in metal matrix. The sulfide nodule is a single crystal of troilite, lenticularly twinned, indicating that Grant has been mechanically deformed. The nodule is mantled by a discontinuous band of kamacite and slightly fractured swathing schreibersite ~ 150μm wide. The surrounding metal exhibits a coherent, medium grained Widmanstätten pattern. Plessite fields have uninterrupted taenite borders supporting the premise that Grant has suffered only minor deformation and no plastic flow or remelting. Accessory minerals in the metal and sulfide were determined to locate possible Ag-bearing phase(s). The metal contains highly fractured Brezina lamellae with oblong (FeMn) phosphate inclusions (< 1 mm, length), idiomorphic chromite (as discrete crystals associated with troilite), schreibersite and anhedral native-Cu. Minerals in the sulfide nodule are schreibersite, pentlandite, mackinawite, chalcopyrite, ~ 50 μm idiomorphic chromite, (FeMn) phosphates and native-Cu. The sample of Cape York contains a large 3 cmϕ sulfide in metal matrix. The sulfide is essentially a single crystal of troilite which shows pervasive undulatory extinction due to deformation. It is rimmed by swathing schreibersite and taenite. The metal matrix displays an unaltered, medium-grained Widmanstätten pattern. Plessite fields adjacent to the sulfide nodule have kinked taenite borders reflecting minor deformation. These observations imply that Cape York suffered greater deformation than Grant but that sulfide and metal have retained primary textures. Accessory phases are described (4) but we note veinlets of native-Cu in idiomorphic chromite and swathing schreibersite. Late forming phases which may be Ag-bearing are Cu, chalcopyrrhotite, djerfisherite, and phosphates. Cape York and Grant are meteorites which have suffered slight shock deformation but lack textures which reflect melting of metal and sulfide. Santa Clara and Gibeon each have textures in which metal and sulfide have been intimately mixed by a post-formational melting episode which must have played a major role in producing confusing Pd-Ag isochrons. New data (6) shows an apparent depletion of Cu in iron meteorites relative to Cl-normalized Cu/Ni ratios. The presence of native-Cu in several IIIAB irons implies that these trends may be related. We believe that Cu-bearing minerals in sulfides in IIIAB irons may be more common than originally thought and may be an explanation for Cu depletions in the metal phase.

References: Kaiser, T. and Wasserburg, G.J. (1983) GCA, 47, 43. Chen, J.H. and Wasserburg, G.J. (1983) GCA, 47, 1725. El Goresy, Armstrong, J.T., Wasserburg, G.J. and Chen, J.H. (1984) LPS, XV, 244. Kracher, A., Kurat, G. and Buchwald, V.F. (1977) Geochem. J. 11, 207. Buchwald, V.F. (1975) Handbook of Iron Meteorites, U.C. Press, Berkeley. Malvin, D.J., Wang, D. and Wasson, J.T., (1984) GCA, 48, 785.

DISCOVERY OF NUCLEAR TRACKS IN INTERPLANETARY DUST. John P. Bradley, Walter C. McCrone Associates, Inc., 2820 S. Michigan Ave., Chicago, IL 60616; Donald E. Brownlee, Dept. of Astronomy FM-20, Univ. of Washington, Seattle, WA 98195.

Prior to capture by the Earth's atmosphere individual interplanetary dust particles (IDP's) have allegedly spent up to 10^5 years as discrete bodies within the interplanetary medium (1). If this is true then they should exhibit evidence of exposure to interplanetary space in the form of solar flare tracks. Observation of tracks in IDP's would provide hitherto unknown data about micrometeorites such as a) whether an IDP existed in space as an individual particle or as part of a larger meteroid; b) the degree to which a particle was heated during the trauma of atmospheric entry; c) residence time of an IDP within the interplanetary medium; d) possible hints as to the pre-accretional exposure of component mineral grains to solar or galactic irradiation.

Using transmission electron microscopy we have successfully identified tracks in several micrometeorites. All of the studied particles had been retrieved from the stratosphere by U-2 aircraft. The tracks were found by first examining a "standard" stratospheric micrometeorite (U2-14-6-9A) that had been irradiated with iron ions at the SuperHILAC Heavy-Ion Facility in Berkeley (2). This sample was prepared and irradiated by the R. Walker group at Washington University, St. Louis, and it provided the unprecedented opportunity to select a microscope operating configuration best suited to observe a known density of tracks in fine-grained micrometeoritic material. Examination of this "standard" IDP highlighted the practical difficulties that must be overcome to observe tracks in micrometeorites.

Three pristine IDP's (between 5 and 15 μm diameter) have so far been searched for solar flare tracks, and they have been found in the two smaller particles U2-20B11 (11 μm) and U2-20B37 (8 μm). The tracks are most easily observed in silicate grains that are relatively free of crystallographic imperfections and surface coatings. Both micrometeorites exhibit track densities between 1 and 5 x 10^{10} cm $^{-2}$, which implies space exposure times of 10^5 years (assuming each micrometeorite was irradiated as an approx. 10 μm diameter particle at 1 AU).

At present we are attempting to a) observe track density gradients in IDP's, and b) establish the presence of tracks in a wider range of IDP's. Identification of tracks also has implications in other areas of micrometeorite research. For example, because of the numerous dust rings recently discovered around nearby stars (e.g. Vega (3)), the ability to measure track densities in small IDP's enables determination of actual lifetimes of particles orbiting stars.

REFERENCES (1) D.E. Brownlee (1979), Rev. Geophys. Space Phys., 17, 1735-1743. (2) P. Fraundorf, G.J. Flynn, J. Shirck, R.M. Walker (1980), Proc. Lunar Planet. Sci. Conf. 11th, 1235-1249. (3) P.R. Weissman (1984), Science, 224, 987-989.

U-2 N85 15648

SPECULATIONS ON THE FORMATION OF METALLIC METEORITE PHASES

P.Z. Budka and F.F. Milillo, Dept. of Mechanical Engineering, Union College, Schenectady, New York 12308.

A new interpretation of the formation of metallic phases in pallasites and nickel-iron meteorites can be made using a non-equilibrium microgravity solidification hypothesis. This hypothesis implies that meteorites were initially large, weightless melts which solidified by radiative cooling.

Current theories do not satisfactorily explain the coexistence of equilibrium and metastable metallic phases. The proposed hypothesis accounts for the composition, morphology and coexistence of kamacite, plessite and pearlite within these same meteorites.

The solidification of metallic meteorite phases can be compared with that of low alloy steels. The relevant phase diagram for this process is approximated by the Ni-Fe phase diagram above 1400°C. Phase diagram boundaries can be significantly altered by minor elements in a melt. Solidification begins with the growth of delta ferrite dendrites, a BCC phase which can be retained at room temperature. The next expected transformation is a peritectic reaction in which $(\delta + L) \rightarrow \gamma$. It is not generally recognized that during cooling, the peritectic reaction stops after only a few atom layers of γ are formed on the solid δ phase (peritectic walling). The balance of the solute-enriched liquid solidifies as a remote alloy system of γ and $(\gamma + \alpha)$.

It is proposed that swathing kamacite and Widmanstatten kamacite are both derivative phases of retained delta ferrite. Swathing kamacite forms by heterogeneous nucleation on high temperature solids such as olivine in pallasites. Widmanstatten kamacite lamellae are delta ferrite dendrites. Their octahedral growth morphology is a response to non-equilibrium solidification, or oriented dendritic growth. Their relatively large size is due to enhanced crystal growth in microgravity. This phenomenon is documented by materials processing experiments conducted in space.

Solute elements rejected by the growing kamacite collect in liquid pools which solidify in a complex manner producing a wide variety of compounds and microstructural features commonly termed plessite. Since plessite is formed at lower temperatures from cubic system metals, it exhibits similar octahedral morphology but on a finer scale. This morphology is generically termed Widmanstatten structure.

It is shown that a broader and more consistent interpretation of microstructural features can be made by combining concepts from casting theory and the results of materials processing in space research.

BARNTRUP: LL-4 CHONDRITE, G.R.Levi-Donati (1), F.Brandstätter (2), and G.Kurat (2), (1) Istituto Tecnico Industriale di Stato, I-06100 Perugia, Italy; (2) Naturhistorisches Museum, Postfach 417, A-1014 Vienna, Austria.

Barntrup fell on May 28, 1886, and only 17 g were recovered (Häpke, 1889). No description or classification is available yet (Levi-Donati, 1983). In order to partly overcome this deficiency we did inspect the specimen preserved at the Naturhistorisches Museum in Vienna (Inv.no. D8334). The sample apparently is the smaller half of the recovered stone and weighs 6.3 g. It has one cut surface of about 2x2 cm. The rest is almost completely covered by a dark-brown fusion crust. The cut surface has a rough polish and shows a very distinct chondritic texture. Within a dense grey matrix there are embedded abundant chondrules (dark grey to light grey) of sizes up to 4 mm. Lithic fragments (up to 3 mm) are the most abundant component. Sulfide is abundant and partly concentrated in rounded or angular fragments. Metal has a low abundance and is evenly distributed in small grains over the total cut surface.

Electron microprobe analyses of different phases were done directly on the badly polished surface. The standard deviation therefore has to be expected to be considerably larger then for analyses made on perfectly polished surfaces. The following results were obtained :

Olivine fa 28.1 ($\pm$ 1.2)
Low-Ca pyroxene $\overline{fs}$ 23.7 ($\pm$ 0.8)
Plagioclase ab82 or5 $\overline{an13}$
Taenite Ni 25-33 weight-%

No kamacite was found. Glass-like matrices are abundant and show highly variable Na/K ratios(0.35-11)

In conclusion, the visual inspection and the phase analyses classify Barntrup as a member of the rather rare LL-4 chondrite class.

References: Häpke,L.(1889), Abhand.Naturwiss.Ver.Bremen II,323. Levi-Donati,G.R.(1983), Meteoritics 18, 4.

ON THE POTENTIAL IMPORTANCE OF CARBON DURING METAL CORE SEGREGATION IN PLANETOIDS; F. Ulff-Møller, Geologisk Museum, Øster Voldgade 5-7, DK-1350 København K, Denmark

Commonly accepted models for Earth-like planetoids assume agglomeration of carbonaceous chondrite material, adiabatic or radioactive heating, reduction and metal segregation. Despite the C-rich starting material, C is usually negelcted in core models due to the low C-content of magmatic irons while other light elements like H, O, S and Si are often used to account for density and degree of melting of the Earth's core.

Diffusion calculations indicate that C can migrate several metres between 500° and 400°C at cooling rates between 1 and 100°C/MA. C exsolved at higher temperature may thus have moved to distant nucleation sites (grain boundaries or major graphite bodies). Accordingly, a 2 metre-sized iron meteorite is not very likely to be a representative sample of metal with more than about 0.5% C.

The hypothetical presence of C would have a drastic influence on the physical and chemical conditions of liquid segregation in the planetoid. A study of the Disko iron (Ulff-Møller, submitted) shows that C-saturation in the Fe-C-S-O system may lead to immiscibility between metal, sulphide and oxide liquid around 1100°C and change minor and trace element distribution between liquids and solids considerably. In equilibrium with graphite, iron oxide liquid may form at 850°C (at 200-300 bars; Weidner, 1982) before sulphide and metal liquid are formed, thus providing a low-temperature mechanism for segregation in minor planetoids.

Ulff-Møller, F. (submitted) Solidification history of immiscible liquids in a troilite-iron lens from a basaltic dyke on Disko, central West Greenland. J. Petrol.

Weidner, J.R. 1982: Iron oxide magmas in the system Fe-C-O. Can. Mineralogist 20, 555-566.

AUTHOR INDEX

☆ U.S. GOVERNMENT PRINTING OFFICE: 1984—769-013/6738